The Role of High Molecular Weight Fibroblast Growth Factor-2 in Cardiac Response to Injury

By

Navid Koleini

A Thesis submitted to the Faculty of Graduate Studies of

The University of Manitoba

In partial fulfillment of the requirements of the degree of

Doctor of Philosophy

Department of Physiology and Pathophysiology

Max Rady College of Medicine

The University of Manitoba

Winnipeg, MB

Canada

Abstract:

Fibroblast growth factor-2 (FGF2) is a multifunctional protein expressed as 18 kDa, low molecular weight (Lo-FGF2), and >20 kDa, high molecular weight (Hi-FGF2) isoforms with potentially distinct biological functions. **In the current thesis we have investigated the general hypothesis that the FGF2 isoforms exert distinct long- term effects towards cardiac response to injurious stimuli.**

Administration of recombinant Lo- or Hi-FGF2 were equally effective in attenuating acute Doxorubicin (Dox)-induced cardiomyocyte damage and cell death *in vitro*, through the activation of mTOR/Nrf2/Heme oxygenase-1 pathway. Additionally, it was documented that a non-mitogenic, non-angiogenic mutant form of Lo-FGF2, carrying a serine-to-alanine, S117A, substitution, retained the cardioprotective properties against Dox.

A genetic mouse model lacking endogenous Hi-FGF2 (but not Lo-FGF2) expression, FGF2(Lo) was found to be protected from Dox-induced decline in contractile function, at 10 days post-Dox injection, as assessed by echocardiography, in both male and female mice. Wild type mice showed the expected decline in cardiac function post-Dox. Neutralizing anti-Hi-FGF2 antibodies, furthermore, were able to attenuate Dox-induced damage in cardiomyocytes co-cultured with wild type fibroblasts. Thus, elimination of endogenous Hi-FGF2, or neutralization of secreted, paracrine Hi-FGF2, increases cardiomyocyte resistance to Dox exposure.

Using transverse aortic constriction (TAC) surgery to induced pressure overload it was found that genetic elimination of Hi-FGF2 prevented the decline in systolic function, the increases in cardiac stress markers, and increases in cardiomyocyte size, present in FGF2 (WT) mice at 4-8 weeks post-TAC. In contrast, diastolic dysfunction, fibrosis, and cardiac mass

enlargement post-TAC were found to be independent of endogenous Hi-FGF2. Whole cardiac transcriptome analysis revealed increased expression of the cardioprotective heat shock 70 (HSP70) protein in the absence of endogenous Hi-FGF2. In addition, genes involved in modulation of the circadian rhythm, most prominently the nuclear receptor NR1D1, may also contribute to the protected phenotype of the FGF2(Lo) mice, as they were differentially regulated post-TAC depending on the presence or absence of endogenous Hi-FGF2.

Work presented here shows that endogenous Hi-FGF2 aggravates cardiac response to two major causes of heart failure, Dox-toxicity and pressure overload. Neutralization of paracrine Hi-FGF2 through an antibody-based approach is a possible therapeutic approach against these pathologies.

Acknowledgments:

I would like to sincerely thank my Ph.D. supervisor Dr. Elissavet (Vetta) Kardami. Vetta has been my mentor not only in my scientific journey, but also in all other aspects of my life. I am, indeed, very grateful to Vetta as her guidance and mentorship helped me thrive as a young scientist and taught me how to think critically. Thank you, Vetta! For not being tired of my endless questions and always, and eagerly, listening to my never-ending ideas and thoughts!

I would also like to give special thank you to my advisor committee members Dr. Ian Dixon, Dr. Lorrie Kirshenbaum, Dr. Jeffery Wigle, Dr. Michael Czubryt. Your advice and criticism have made my research more impactful and helped me to identify where I need to improve to become a better scientist. Thank you all for your support during my journey!

I would like to give special thanks to Dr. Peter Cattini for his unwavering support, encouragement and advice during my PhD.

I am very grateful to my friend, Mark Hnatowich, for always being supportive in my personal and scientific life. Thank you, Mark for everything!

I have had the opportunity to work with great people in Dr. Kardami's lab who are like my family members now. I would like to graciously thank Barbara Nickel and Robert Fandrich for their unwavering help, support, and encouragement! Thank you, Barb and Rob for always being helpful! I have learned almost every technique in the lab from you and will remain always grateful to you guys! I also would like to thank Wattamon Srisakuldee and Jon-Jon Santiago for their support and help in my PhD.

I would like to thank dr. Sanjiv Dhingra for his thoughtful guidance in my career development and life decisions. Thank you, Sanjiv for your support and help.

I am grateful to my friends, Natalie Landry and Sunil Rattan for their encouragement and support during my journey.

I am very grateful to Gail McIndless and Judith Olfert for their assistance during my PhD.

I would like to thank Shirley Mager for her service at the Institute of Cardiovascular Sciences and being a compassionate friend for me.

I am very grateful to have a very supportive and kind family and would like to thank my mother, my father, my brothers Peiman and Naeim, and my lovely niece Baran.

Last but not the least, I would like to give special thanks and love to my friend, love, and wife Farnaz for being always supportive, encouraging, and helpful. Thank you Farnaz!

I dedicate my thesis to

The love of my life, Farnaz

My Mother, Farkhondeh, and my Father, Ali

Table of Contents

List of Tables

List of Figures

Please note that the thesis contains part of a published review article, three published research manuscripts and one manuscript “in submission”. The figures are numbered sequentially as they appear in the thesis. The supplementary figures from all the manuscripts are placed in the Appendix (1-12), at the end of the thesis.

Contributions of Authors

The thesis contains three published research manuscripts and part of a review paper which are all used according to the Copyright and Permission terms of the publishers.

Manuscript 1: Koleini N. and Kardami E. Autophagy and mitophagy in the context of doxorubicin-induced cardiotoxicity. Oncotarget. 2017 Jul 11;8(28):46663-46680. doi: 10.18632/oncotarget.16944. Review.

I contributed 85% of the first draft of the manuscript including the revisions. I, made a major contribution to conception and preparation of idea; critically reviewing the literature; drawing the conclusion; drafting, editing, and revising the manuscript.

Manuscript 2: Koleini et al. Elimination or neutralization of endogenous high-molecular-weight FGF2 mitigates doxorubicin-induced cardiotoxicity. Am J Physiol Heart Circ Physiol. 2019 Feb 1;316(2):H279-H288. doi: 10.1152/ajpheart.00587.2018. Epub 2018 Nov 9.

I contributed work for 5 out of 6 figures and wrote 85% of the first draft, and of revisions.

Manuscript 3: Koleini et al. Fibroblast growth factor-2-mediated protection of cardiomyocytes from the toxic effects of doxorubicin requires the mTOR/Nrf-2/HO-1 pathway. Oncotarget. 2017 Aug 24;8(50):87415-87430. doi:10.18632/oncotarget.20558. eCollection 2017 Oct 20.

I contributed 10 out of 12 figures, wrote 85% of the first draft, and of revisions.

Manuscript 4: Koleini et al. Non-mitogenic FGF2 protects cardiomyocytes from acute doxorubicin-induced toxicity independently of the protein kinase CK2/heme oxygenase-1

pathway. Cell Tissue Res. 2018 Dec;374(3):607-617. doi: 10.1007/s00441-018-2905-z. Epub 2018 Aug 29.

I contributed 6 out of 8 figures, wrote 80% of the first draft , and of revisions.

Manuscript 5: Koleini et al. Genetic elimination of high molecular weight FGF2 prevents pressure overload-induced cardiac systolic dysfunction and implicates a beneficial effect of HSP70 and circadian rhythm modulation. (In preparation for submission)

I contributed 9 out of 11 figures, wrote 80% of the first draft, and expect to do the same for any revisions required.

List of Abbreviation:

FGF2	Fibroblast Growth Factor 2
Lo-FGF2	Low molecular weight Fibroblast Growth Factor 2
Hi-FGF2	High molecular weight Fibroblast Growth Factor 2
Dox	Doxorubicin
HO-1	Heme oxygenase 1
mTOR	Mammalian target of Rapamycin
TAC	transverse aortic constriction
NR1D1	Nuclear Receptor Subfamily 1 Group D Member 1
ARNTL	Aryl Hydrocarbon Receptor Nuclear Translocator Like
Dbp1	Albumin D site-binding protein
Sp1	Specificity protein 1
Egr-1	early growth response protein 1
TGF-β	Transforming growth factor beta 1
NF-κB	Nuclear factor kappa-light-chain-enhancer of activated B cells
EMV	Encephalomyocarditis virus
IRES	Internal ribosome entry site
NLS	Nuclear localization sequence
Kapβ2	Karyopherin-β2/Transportin
ATP1A1	ATPase Na+/K+ Transporting Subunit Alpha 1
FGFR	Fibroblast growth factor receptor
FGFBP1	Fibroblast Growth Factor Binding Protein 1
HSPG	Heparan Sulfate Proteoglycan

PLC	Phosphoinositide phospholipase C
PKC	Protein kinase C
MAPKKK	MAP kinase kinase kinase
MAPK	MAP kinase
PI3k	Phosphoinositide 3-kinase
STAT	Signal transducers and activators of transcription
AKT	Protein kinase B
GRB2	Growth factor receptor-bound protein 2
PDK1	Pyruvate Dehydrogenase Kinase 1
GAB1	GRB2-Associated Binding Protein 1
FOXO	Forkhead box
cAMP	Cyclic adenosine monophosphate
CREB	cAMP response element binding protein
GSK3	Glycogen synthase kinase 3
PIP2	Phosphatidylinositol 4,5-bisphosphate
DAG	Diacylglycerol
IP3	Inositol 1,4,5- trisphosphate
Bcl-2	B-cell lymphoma 2
Bad	Bcl-2 associated agonist of cell death
Bax	Bcl-2-associated X protein
4E-BP1	Eukaryotic translation initiation factor 4E-binding protein 1
S6K1	Ribosomal protein S6 kinase beta-1
FGF2-KO	FGF2 knockout

FGF2(WT)	Wild type mice
FGF2(Lo)	Hi-FGF2 knockout mice
I/R injury	Ischemia/reperfusion injury
αSMA	Alpha smooth muscle actin
HF	Heart failure
NYHA	New York Heart Association
HFrEF	Heart failure with reduced ejection fraction
HFpEF	Heart failure with preserved ejection fraction
ATP	Adenosine triphosphate
NOX	Nicotinamide adenine dinucleotide phosphate-oxidase
NOS	Nitric oxide synthase
eNOS	Endothelial NOS
iNOS	Inducible NOS
mPTP	Mitochondrial permeability transition pore
TOPIIα	Topoisomerase IIα
Bnip3	BH3-only protein Bcl-2-like 19 kDa-interacting protein-3
AMPK	AMP activated protein kinase
ATM	Ataxia telangiectasia mutated
ROS	Reactive oxygen species
RNS	Reactive nitrogen species
ER	endoplasmic reticulum
FHL1	four-and-half-LIM domain protein-1
MARP	muscle-specific ankyrin repeat protein

ECM	Extracellular matrix
AT	Angiotensin receptor
FDA	Food and Drug Association
DMEM	Dulbecco's modified Eagle's medium
iPSC	Induced pluripotent stem cells
PBMNC	Peripheral blood mononuclear cells
r-cardiomyocyte	Rat Cardiomyocyte
FBS	Fetal bovine serum
Hi-Ab	Polyclonal antibody against Hi-FGF2
IgG	Immunoglobulin
SDS	Sodium dodecyl sulphate
DSHB	Developmental Studies Hybridoma Bank
EF	Ejection fraction
LVEDD	Left ventricular end diastolic diameter
HW	Heart Weight
BW	Body weight
PWT	Posterior wall thickness
TUNEL	Terminal deoxynucleotidyl transferase dUTP nick end labeling
MEF	Mouse embryonic fibroblast
Fib^{iPSC}	Induced pluripotent stem cell derived fibroblasts
cTnT	Cardiac Troponin-T
LDH	Lactate dehydrogenase
Neu-Ab	Neutralizing antibodies against Hi-FGF2

LVESD	Left ventricular end systolic diameter
HR	Heart rate
ANOVA	Analysis of variance
LSD	Fishers Least Significant Difference
Nrf-2	Nuclear factor erythroid 2–related factor 2
p62/SQSTM1	Sequestosome 1
DCF-DA	2',7'-dichlorodihydrofluorescein diacetate
CQ	Chloroquine
TFEB	Transcription factor-EB
Tin-PP	Tin-Protoporphyrin
RP2	RNA polymerase II
LAMP1	Lysosomal-associated membrane protein 1
NQO1	NAD(P)H Quinone Dehydrogenase 1
CK2	Casein kinase 2
LC/MS/MS	Liquid Chromatography with tandem mass spectrometry
PAGE	Polyacrylamide gel electrophoresis
BCA	Bicinchoninic acid
PVDF	Polyvinylidene fluoride
OxPC	Oxidized phospholipids
PAPC	1-palmitoyl-2-arachidonoyl-sn-glycero-3-phosphocholine
PLPC	1-palmitoyl-2-linoleoyl-sn-glycero-3-phosphocholine
SLPC	1-stearoyl-2-linoleoyl-sn-glycero-3-phosphocholine
HODA-PPC	9-hydroxy-12-oxo-10-dodecenoic acid

HSP70	Heat shock protein 70
CXCL9	Chemokine (C-X-C motif) ligand 9
RAB6B	Ras-related protein Rab-6B
ANP	Atrial natriuretic peptide
BMAL1	Brain and Muscle ARNT-Like 1

Chapter I: Review of the Literature

FGF2. General Introduction

Fibroblast growth factor 2 (FGF2), or basic FGF2 as it used to be referred to, is a multifunctional protein which is ubiquitously expressed in variable amounts in cells and tissues and is implicated in multiple cellular pathways that affect proliferation, development, differentiation, and cell survival [1].

FGF2 belongs to the larger family of heparin-binding growth factors (FGF1 to 23) and is an extensively studied member of this group and was first purified in 1970 from bovine pituitary gland [2]. Cardiac tissue, especially cardiac atria, as well as highly vascularized organs are rich sources of FGF2 [3]. FGF2 consists of multiple isoforms which are made as a result of alternative translation. A number of studies have pointed to FGF2 as an important factor in cardiac response to injury; however, the majority of the literature refers to the 18-KDa isoform as "FGF2" neglecting the role of other isoforms. The latest information on FGF2 isoforms and the current knowledge on the role of FGF2 in cardiac physiology and pathophysiology will be reviewed.

FGF2: Gene expression and transcriptional regulation

The *FGF2* gene is located on chromosome 4, q26-27 region, of the human genome and consists of two introns (16kbp) and three exons [4]. The human and rat *FGF2* promoters lack the common TATA or CCAAT binding sites that are present in most promoters; instead the *FGF2* promoter contains multiple rich G/C sequences which could act as a binding site for the specificity protein 1 (Sp1) transcription factor. The promoter structure resembles that of constitutively active genes, the so-called housekeeping genes [5]. In addition, the *FGF2*

promoter contains early growth response protein 1 (Egr-1) binding elements. It has been shown that increase in Egr-1 activity stimulates *FGF2* mRNA transcription in rat cardiomyocytes. The overlap between the consensus sequences of Sp1 and Egr-1 results in a complex regulation of the promoter activity allowing the gene to be regulated in early and intermediate development as well as IN response to stress. Various stimuli and transcription factors have been reported to increase *FGF2* transcription including β-adrenergic agonist (isoproterenol), endothelin-1, TGF-β, angiotensin II, and transcription factor NF-κB [6].

In addition, the antisense strand of the FGF2 gene codes for nucleoside diphosphate-linked moiety X motif 6 gene. The transcribed mRNA, which is called FGF2 anti-sense, therefore would be complementary to the FGF2 mRNA and is proposed to regulate the stability of the FGF2 mRNA [7, 8].

FGF2: Translational regulation

Human, rodent and avian FGF2 mRNAs contain multiple translation initiation sites: CUG-initiated sites are located upstream of the more commonly used AUG-initiation consensus site, and produce high molecular weight (Hi, >20 kDa) FGF2 isoforms. Translation from the one AUG start site produces the low molecular weight (Lo, 17-18 kDa) FGF2 isoform. Human FGF2 mRNA contains 4x CUG start sites, corresponding to 22. 22.5, 24 and 34 kDa isoforms [5], while rodent FGF2 mRNA has 2 CUG start sites, corresponding to 21.2-23 kDa isoforms [5]. Most cell-extracted human Hi-FGF2 is composed of the 22-24 kDa isoforms [9].

The 34 kDa human FGF2 isoform is translated following the more common cap-dependent mechanism of translation initiation [10]; alternatively, internal ribosome entry sites (IRES) lead to cap-independent initiation of translation and therefore synthesis of the 24, 22.5,

22, and 18 kDa isoforms of human FGF2. IRES-mediated translation initiation can occur under conditions of cellular stress (heat shock, hypoxia, apoptosis) when cap-initiated translation is inhibited, and provides a strategy for "escaping the global decline in protein synthesis" [11].

The IRES is located in the first 176 nucleotides of the FGF2 mRNA leader forming two stem–loop regions and a G quartet motif structure [12]. Using transgenic mice expressing double luciferase bicistronic vectors with either the FGF2 or the encephalomyocarditis virus (EMV) IRES in the intercistronic region, Creancier et al. studied the FGF2 IRES regulation *in vivo* [13]. The FGF2 IRES activity was found to be high in the embryos at day 11 (E11) while inactive in the placental tissue. In contrast, at E16, FGF2 IRES activity decreases in most tissues but not in heart and brain. In adult mice, the FGF2 IRES activity was low in most tissues while remaining high in brain and testes [13]. IRES translation regulation of FGF2 is thought to play an important role in growth, development, and in response to injuries. For instance, in diabetic mice the activity of FGF2 IRES increases in the aorta in correlation with increased FGF2 expression resulting in an increased permeability of the vessels and stimulation of angiogenesis.

At least two IRES trans-acting factors have been shown to regulate FGF2 IRES: p53 can bind to the FGF2 mRNA leader region and block IRES as well as the cap dependent translation [14]; heterogeneous nuclear ribonucleoprotein A1 can directly bind to the FGF2 IRES facilitating 40S ribosomal binding and protein translation [15].

Limited information exists as to whether there is selective translational regulation of the AUG-initiated versus the CUG-initiated FGF2 isoforms. One study reported that stressed or transformed cells preferentially produce the CUG-initiated Hi-FGF2 isoforms, while 'normal cells' produce mainly the AUG-initiated Lo-FGF2 [16]; it was proposed that trans-acting factors

interacting preferentially with FGF-2 mRNA may promote translation initiation via CUG. The same group went on to identify a 'translational enhancer' sequence in the 3' untranslated sequence of human FGF2 mRNA [17]. These studies have not been confirmed by other laboratories, and merit re-examination.

FGF2: post-translational modifications and processing

FGF2 is subjected to post-translational modifications such as phosphorylation and methylation. The Tec tyrosine kinase phosphorylates FGF2 at tyrosine 82 which is required for its incorporation into the membrane phospholipids and secretion [18]. In addition, Pintucci et al. [19] demonstrated that Hi-FGF2 could be methylated and this modification was required for its nuclear accumulation; the same group also showed that the N-terminal extension of Hi-FGF2 isoforms contains multiple arginine residues which can be demethylated [20]. The 24 kDa isoform contains 8, while the 22 and 22.5 kDa isoforms contain five of these residues. These arginine residues are part of glycine-arginine-glycine repeats which resembles the methylated RGG box of the heterogeneous ribonucleoprotein particles where the sequence serves as a RNA-binding site [19].

The N-terminus of Hi- FGF2, and to some extent of Lo-FGF2 as well, contains cleavage sites for serine proteases; these proteases often bind to heparin-sepharose affinity columns (used for FGF2 purification) and, unless inhibited by proteolytic inhibitors, are capable of converting the >20 kDa Hi-FGF2 isoforms to 16-18 kDa Lo-FGF2-like proteins. Inadequate prevention of endogenous proteolysis is likely responsible for the underestimation of the actual levels of Hi-FGF2 present in various tissues and cells [21]. The limited proteolysis of the N-terminal extension of Hi-FGF2 by thrombin is likely of physiological significance as it would be expected to convert an anti-angiogenic FGF2 isoform (Hi-FGF2) to a pro-angiogenic Lo-FGF2 [22].

Santiago et al have demonstrated that thrombin can cleave fibroblast-secreted and pro-hypertrophic Hi-FGF2 to an 18 kDa, non-hypertrophic, Lo-FGF2 [9].

FGF2: Tissue, cellular and subcellular localization

Tissue, cellular and subcellular localization of proteins provides clues as to their potential function. In the case of FGF2, it is abundantly expressed in the brain, smooth muscles, adipose tissue, kidneys and cardiac atrial tissue. The Kardami group has shown that cardiac atrial tissues contain greater amounts of FGF2 as compared to the ventricular tissues in various species, including chicken, bovine, sheep, and rats [3]. The large amounts of FGF2 found in the atria implicates its importance of this growth factor in the normal physiology of tissue and may be related to the higher proliferative capacity of atrial fibroblast [23]. FGF2 is also highly expressed in vascularized tissues implicating its role in angiogenesis [24]. Although FGF2 is ubiquitously expressed, its expression is much greater in mesenchymal-derived cells, like fibroblasts [9, 25].

FGF2 isoforms have been localized in both the extracellular and intracellular spaces, including the nucleus and cytosol [9, 25]. The traditional belief, based mainly on overexpression studies in a limited number of cell types [26] has been that Hi-FGF2 isoforms localize only to the nucleus, and thus they were called nuclear FGF2, while Lo-FGF2 could accumulate in the nucleus and cytosol as well as be secreted to the extracellular space [26].

Kardami and colleagues have shown that Hi-FGF2 is also exported to the extracellular space, and can be localized in the cytosol, as well as the nucleus of cells [9]. Rat cardiac ventricular, as well as human atrial and ventricular fibroblasts were shown to export Hi-FGF2, in addition to Lo-FGF2, to the extracellular milieu; extracellular Hi-FGF2 could be found in both

the soluble phase, and also in association with the cell surface, due to its affinity to heparan sulfate proteoglycans [25].

Importantly, the Kardami group has shown that Hi-FGF2 is present in human biological fluids, such as pericardial fluid [25]. Overall, and in contrast to the prevailing knowledge [26], both Hi and Lo-FGF2 are capable of paracrine and autocrine activities, and can therefore be targeted by reagents, such as monoclonal antibodies, that can reach the extracellular space.

A nuclear localization sequence (NLS), residues 116-129 (RSRKYTSWYVALKR) is common to both Lo- and Hi-FGF2 isoforms [27]. This sequence is critical for nuclear localization of endogenous FGF2 and also internalization/nuclear accumulation of the exogenously imported FGF2 [27] . Additional NLS are located at the N-terminal extension of the Hi-FGF2 isoforms, which contribute to the sequestration of a substantial amount of produced Hi-FGF2 in the nucleus. These NLS are rich in arginine residues in multiple arginine-glycine sequences; conjugation of the N-terminal extension of Hi-FGF2 is sufficient to direct chloramphenicol acetyltransferase and β-Galactosidase to the nucleus [28, 29]. Hi-FGF2 directly interacts with nuclear transport protein Karyopherin-β2/Transportin (Kapβ2) which facilitates its nuclear import; knock-down of Kapβ2, or Ran GTPase, involved in nuclear transportation of proteins, can prevent nuclear accumulation of Hi-FGF2 [30]. These data strongly suggest that the NLS in the N-terminal extension of Hi-FGF2 are important for the biological function of Hi-FGF2.

Overall it is not yet understood what determines the subcellular localization of Hi-FGF2; it is possible that interaction with other factors mask nuclear localization signals, and/or direct Hi-FGF2 export from the cell.

FGF2 export to the extracellular space

Secreted proteins, including hormones and cytokines, are capable of paracrine, autocrine, as well as systemic modes of action. It has long been established that FGF2 is present at the extracellular space, in support of the notion that it is exported from cells. Unlike most secreted proteins, however, FGF2 does not have a signal peptide for secretion via vesicle sorting at the endoplasmic membrane or Golgi apparatus. Several studies over the years have proposed various mechanisms controlling FGF2 release from cells. Minor and reversible plasma membrane injury, as might occur during cellular contraction, results in FGF2 release to the extracellular space [25]. Involvement of the plasma membrane Na+/K+ ATPase was inferred in earlier studies, where it was shown that FGF2 export was inhibited by ouabain [31]; Functional genomics based on RNAi screening studies identified the ATPase Na+/K+ Transporting Subunit Alpha 1 (ATP1A1) and Tec kinase as two major proteins involved in FGF2 secretion [32]. Tec kinase phosphorylates FGF2 at tyrosine 82 which is required for its polymerization and subsequent secretion. ATP1A1 physically interacts with FGF2 and is thought to bring FGF2 in close proximity to the Tec kinase at the inner leaflet of the plasma membrane.

Studies by the Nickel group [32, 33] revealed that Lo-FGF2 secretion is contingent on its interaction with phosphoinositide PI(4,5)P2, a membrane lipid abundant at the inner leaflet of the plasma membrane. The head group of PI(4,5)P2 interacts with a highly specific pocket of the FGF2 molecule which triggers FGF2 polymerization and insertion into the plasma membrane. Polymerized FGF2 in the plasma membrane forms pore like structures which allow transit of FGF2 through the membrane. Heparan sulphate proteoglycans (HSPG) on the extracellular surface are required for the final stage of FGF2 secretion. FGF2 contains a pocket which strongly interacts with HSPs with binding to HSPs or PI(4,5)P2 being mutually exclusive meaning that

FGF2 can either be bound to PI(4,5)P2 or HSPs [34]. Importantly, the binding affinity of FGF2 to HSPGs (K_D ~5 μM) is greater than that of PI(4,5)P2 (K_D ~100 nM) resulting in release of the membrane incorporated PI(4,5)P2-bound FGF2 to the extracellular space.

FGF2 secretion was also shown to occur by a mechanism similar to that of interleukin-1 and other proteins that lack a conventional signal peptide for secretion; the mechanism requires the activity of caspase-1, a major enzyme involved with the inflammasome and innate inflammation [35, 36]. Recently, Javidi-Sharifi and colleagues showed that stromal bone marrow cells can release FGF2 after packaging it within small entities (exosomes) [37]. In reviewing articles on the topic of FGF2 export/secretion, it became evident that there may exist species, cell type, and developmental-stage-specificity in the mode by which FGF2 exits cells. Methodologies used in some studies, such as overexpression of FGF2, or expression of "tagged"-FGF2, may also have affected findings and raise issues about physiological significance. A systematic study of the topic has not yet been done.

It should be emphasized that the studies reviewed in the preceding paragraph reflect findings on Lo-FGF2, which has long been assumed to be the only isoform that is capable of exiting the cell and exerting paracrine activities, while Hi-FGF2 is often referred to as "the nuclear" FGF2. The Kardami lab has, however, demonstrated that Hi-FGF2 (rodent, human) is indeed exported to the extracellular space, and represents the majority of exported FGF2 ; secreted Hi-FGF2 is fully capable of paracrine activities such as stimulation of myocyte hypertrophy [9], and is dependent on caspase-1 activity for secretion implicating this isoform with innate inflammation [25]. Failure to detect Hi-FGF2 in conditioned media or body fluids likely reflects inadequate prevention of its degradation by co-existing proteases, and lack of isoform-selective antibodies [21].

FGF2 signal transduction

The biological effects of extracellular FGF2 are initiated by binding and activating plasma membrane tyrosine kinase FGF receptors, FGFR1-4 [38]. Most of the information from now on reflects signaling mediated by FGFR1, the most abundant receptor in the heart and other tissues. FGFR belongs to the larger family of receptors containing immunoglobulin-like domain in their ligand binding region; FGFR1 has 2 or 3 immunoglobulin-like domains, a transmembrane domain and a cytosolic (catalytic) domain. In addition to FGFR, HSPGs such as syndecans at the plasma membrane are an integral part of the canonical FGF signaling [39].

HSPGs can independently bind both FGFs and FGFR1 and are thought to stabilize the FGF/FGFR1 complexes [39]. In addition, HSPGs at the extracellular space can act as 'sinks' or storage pools for FGF2 [39]. Following FGF2 ligand binding FGFR dimerizes, an event that facilitates trans-phosphorylation of its tyrosine kinase domain. Firstly, tyrosine 653 becomes phosphorylated resulting in significant activation of the tyrosine kinase activity; this is followed by the phosphorylation of tyrosines 583, 463, 585, and 766. Phosphorylation of tyrosine 654 further increases tyrosine kinase activity of the receptor [39]. Activated FGFR1 phosphorylates adaptor proteins resulting in activation of major signaling pathways in the cells, including the PLCγ/PKC-, MAPK (ERK, p38, JNK)- , PI3k-AKT, SRC-, signal transducer and activator of transcription (STAT)- pathways. A schematic illustrating the FGF2 mediated signal transduction is shown in Figure 1.

Figure 1. Schematic of FGF2 signal transduction

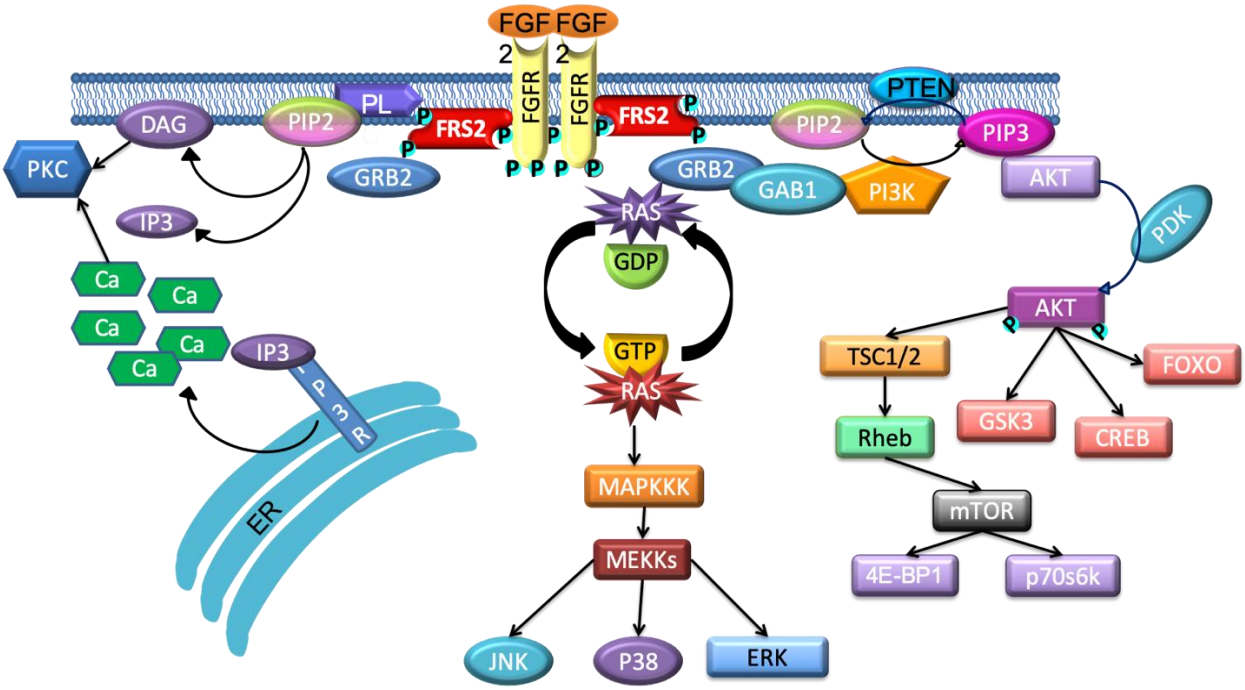

Figure 1. Schematic showing signal transduction pathways triggered by extracellular-acting FGF2 via plasma membrane FGFR1. Extracellular FGF2 signaling starts by its binding to the FGFR1 at the plasma membrane. FGFR1 dimerizes and transphosphorylates itself at tyrosine sites, resulting in activation of major pathways in the cells including AKT, ERK, PKC, JNK, and p38. FRS2 (Fibroblast Growth Factor Receptor) and GRB2 (Growth factor receptor-bound protein 2) are adaptor proteins docking to the active receptor. PI3K (Phosphoinositide 3-kinase) which is activated via GAB1 (GRB2-associated-binding protein 1) catalyzes the conversion of PIP2 (Phosphatidylinositol 4,5-bisphosphate) into PIP3 (Phosphatidylinositol (3,4,5)-trisphosphate). PIP3 acts as a binding site for AKT (via its pleckstrin homology domain) resulting in Akt phsophorylation by PDK1 (phosphoinositide-dependent kinase 1). Phosphatase and tensin homolog (PTEN) catalyze the conversion of PIP3 to PIP2 halting the AKT activation. AKT activation results in activation of Forkhead box (FOXO), cAMP response element binding (CREB), mTOR activation and phosphorylation deactivation of glycogen synthase kinase3 (GSK3). GRB2 catalyzes Ras GTP/GDP exchange activating RAS, which, in turn, results in sequential activation of MAPKKK (mitogen activator kinase kinase kinase), MAPKK (mitogen activator kinase kinase), and MAPK (mitogen activator kinases), including (ERK) extracellular signal-regulated kinases, p38, and c-Jun N-terminal kinases (JNK). Phospholipase C is also activated downstream of FGFR1 culminating in the activation of the various members of the PKC (protein kinase C) family.

Activation of FGFR1 results in sequential recruitment of substrates, adaptors and kinases resulting in the recruitment of the RAS-GTPase; activated RAS uses its effector RAF to then activate mitogen-activated protein kinases (MAPKs) in different downstream branches of the pathway, including the ERK1/ERK2 pathway, the p38 pathway, and the JNK pathway. Of these, the ERK pathway has been studied extensively regarding FGF2/FGFR signaling, and is considered to mediate FGF2-induced cell proliferation, cytoprotection, and even hypertrophy [40-42]. It should be noted that different FGF2 isoforms may engage the ERK pathway to achieve different end-points; Ma et al. demonstrated that both Hi- and Lo-FGF2 can activate the ERK pathway with equal potency, but in the case of Hi-FGF2, the ERK pathway mediated apoptosis caused by increased nuclear accumulation of Hi-FGF2.[43].

PI3k-AKT/mTOR pathway

Phosphoinositide 3-kinase (PI3K)-AKT is another major signaling pathway activated downstream of FGFR1. It regulates proliferation, cell cycle, survival, metabolism, and cancer development; in the heart, AKT is considered essential for preconditioning and cardio-protection [44].

Following FRS2α-GRB2 docking to FGFR1, GRB2 associated binding protein-1 (GAB1) is recruited by GRB2 resulting in activation of PI3K [24]. GAB1 phosphorylation creates binding sites for the p85 subunit of PI3K, thus, activating this enzyme [45]. PI3k enzymes are divided into four classes [46]. Among them, class I PI3K catalyzes formation of phosphatidylinositol (3,4,5)-trisphosphate (PIP3) from PI 4,5-bisphosphate (PIP2). PIP3 acts as a docking site for protein kinase B (AKT) and phosphoinositide-dependent protein kinase (PDK). PDK1 and PDK2 mediate phosphorylation of AKT at tyrosine 308 and 473, respectively [46]. These phosphorylation events are important for activation of AKT. As long as PIP3 persists, the

phosphorylation of AKT continues; phosphatases and tensin homolog (PTEN) dephosphorylates PIP3 to PIP2 blocking AKT phosphorylation. Phosphorylated AKT has a wide range of effects in cells which include [46]: stimulation of cAMP response element binding protein altering gene transcription; inhibition of glycogen synthase kinase (GSK) which in turn increases glucose metabolism, cell proliferation, and migration; activation of pro-survival/anti-apoptotic pathways via upregulation of B-cell lymphoma 2 (Bcl-2) [47] and inhibition of Bcl-2-associated death promoter (Bad) and bcl-2-like protein 4 (Bax) [46].

FGF2-induced cytoprotection, migration, and mitochondrial function, are mediated through AKT activation. For example, FGF2 secreted from vascular smooth muscle cells in response to hypoxia/reoxygenation protected co-cultured H9C2 cells via the AKT pathway [48]. The FGF2 stimulated migration of Sca1+ cardiac stem cells was attenuated by the PI3K-AKT inhibitor, deguelin [49]. The FGF2- protection from hydrogen peroxide induced necrosis and mitochondrial dysfunction in H9C2 cells required the AKT pathway [50]. Additional examples of FGF2 cytoprotection via the AKT pathway can be found in references [51-53].

FGF2 and mTOR signaling

Through a series of steps, activated AKT results in the phosphorylation (activation) of the mammalian target of Rapamycin (mTOR) on serine 2448. mTOR signaling is activated downstream of growth factor activation and is generally associated with anabolic processes. mTOR is an atypical serine/threonine kinase which forms two complexes, mTORC1 and mTORC2, through assembly of different adaptors. mTOR complexes are master regulators of protein synthesis, autophagy, homeostasis and lipid synthesis as well as mitochondrial and lysosomal biogenesis. mTORC1 is sensitive to rapamycin through its Raptor subunit; in contrast mTORC2 contains Rictor which makes this complex insensitive to rapamycin. mTOR complexes

play differential role in cardiac cells. While mTORC1 is implicated in metabolism, homeostasis, and cell proliferation, mTORC2 is involved in cancer cell maintenance [54]. Complete knockout of mTOR results in dilated cardiomyopathies and severe maladaptive response to cardiac stimuli. The most well-known substrates of mTORC1 are S6 kinase 1 (S6K1) and 4E (eIF4E)-binding protein 1 (4E-BP1). mTORC1 phosphorylates S6K1 which in turn stimulates mRNA biogenesis and protein translation; while, it inhibits 4E-BP1 allowing formation of eIF4F complex and, therefore, Cap-dependent protein translation. mTORC1, also promotes ribosomal biogenesis as well as lipid membrane formation through sterol regulatory element-binding protein dependent lipid synthesis [55]. Active mTOR signaling is important for lysosomal biogenesis and completion of autophagy through the lysosomal degradation of autophagic cargo [56]. Ischemia/reperfusion (I/R) injury inhibits mTOR in the myocardium resulting in dysregulated autophagy, but FGF2 was able to counteract these effects [57].

Phospholipase C/ protein kinase C pathway

Findings summarized in this section reflect activities of Lo-FGF2. FGF2-triggered activation/phosphorylation of FGFR1 results in phosphorylation/activation of phospholipase C (PLC). In addition, FGF2 is capable of activating PLC β in adult cardiomyocytes [58]. PLCs are membrane associated enzymes hydrolyzing PIP2 to inositol triphosphate (IP3) and diacylglycerol (DAG). DAG and IP3 are important second messengers controlling various cellular processes in response to receptor tyrosine kinases and G protein coupled receptors. DAG is anchored to the inner leaflet of the plasma membrane and interacts with several targets. In contrast, IP3 which is soluble and cytosolic can activate IP3 receptors at the rough endoplasmic reticulum triggering calcium gated channels and calcium release into the cytosol. FGF2 activates the protein kinase C, PKC, family of enzymes downstream of PLC. The so-called “canonical”

PKC enzymes require DAG and increase calcium for activation, while non-canonical PKCs only require DAG, while atypical PKCs require neither.

PLC/PKC activation is an integral part of FGF2 stimulated cardiomyocyte proliferation, as well as increased cardiac resistance against various injuries. The Kardami group has conducted several studies on the role of FGF2 mediated PKC activation in the heart. In 1998, Padua et al. showed that FGF2 mediates transient negative inotropism in perfused adult rat hearts and also protects them from reperfusion injury which coincided with increased association of PKCε and PKCδ with the sarcolemma membrane, indicative of activation. These effects were prevented by chelerythrine, a PKC inhibitor [59]. Using mutant FGF2, with diminished affinity for FGFR1, Jiang et al. demonstrated that intact FGF2/FGFR1 binding followed by PKC activation are required for FGF2 mediated protection in perfused rat hearts post-ischemia [60]. In addition, it was shown that the FGF2 mediated phosphorylation of Connexin-43 through PKCε at the intercalated disks and mitochondria was essential for FGF2 mediated protection [61-63]. Finally, the 18 kDa FGF2 ability to exert cardiomyocyte protection against genotoxic stress by Doxorubicin was also found to require PKC activity [64].

The effect of endogenous FGF2 and FGF2 isoforms in physiology and pathophysiology

Several laboratories have created mouse models lacking FGF2 gene expression (FGF2 knockouts) to examine the role of FGF2 in normal development and physiology. Overall, FGF2 knockout (FGF2-KO) mice, lacking both Hi- and Lo-FGF2, are viable, display broadly normal development, pregnancy, and are fertile. Zhou and colleagues reported that lack of endogenous FGF2 gene expression results in decreased vascular smooth muscle contractility and hypotension but does not affect the hyperplastic response of the vessel cells [65]. Another team reported that the development of the cerebral cortex is impaired in FGF2-defficient mice; they also documented reduced blood pressure in FGF2-deficient mice (most notably in females) caused by impaired neural reflex control [66]. Yet another team reported delayed wound (skin) healing in FGF2-defficient mice, and also documented neuronal defects [67]. Regarding pressure-overload-induced cardiac hypertrophy, the Doetschman group reported that FGF2 null mice were incapable of a hypertrophic response after transverse aortic coarctation [68]. Similar findings regarding the requirement for FGF2 gene expression for cardiac hypertrophy to develop were reported by Pellieux et al [69]. We have some concerns about the method used by the Doetschman group and Pellieux et al., which might have introduced unaccounted for variables. The authors mentioned that the FGF gene was knocked out by replacing most of the second exon by homologous recombination which resulted in deletion of sequences encoding amino acids 82-93. Their approach, however, may still have produced a protein product with similarities to FGF2 (but lacking amino acids 82-93), or a protein product composed of the N-terminal extension of Hi-FGF2 in addition to amino acids 1 to 82 of the Lo-FGF2. No information was provided as to whether such protein products were produced and what their contribution to the observed phenotype might be.

Echocardiographic measurements of heart function revealed that there were no baseline differences between wild type, FGF2(WT) and FGF2-KO mice [70, 71]. Differences became apparent when some form of stress was applied: cardiac injury was exacerbated in FGF2-KO mice. Stress conditions (left anterior descending coronary artery ligation) that did not affect left ventricular contractility of FGF2(WT) mice, elicited a significant functional decline in FGF2-KO mice [70]. The FGF2(WT) mice developed increased cardiomyocyte size and collagen deposition as well as higher density of vessels in the myocardium, implicating FGF2 in adaptive cardiac remodeling (hypertrophy, fibrosis, neovascularization) after hemodynamic overload [70].

Isoproterenol infusion induced cardiac hypertrophy in FGF2(WT) and to a lesser extent in FGF2-KO mice [41]. At the same time, cardiac-specific overexpression of FGF2 (human cDNA coding for both Hi- and Lo- FGF2 isoforms) resulted in an exacerbated hypertrophic response to isoproterenol [41]. FGFR1- mediated ERK activation was shown to be the downstream signaling responsible for the hypertrophy; the ERK pathway inhibitor, UO126, attenuated hypertrophy in FGF2(WT) and FGF2 transgenic mice [41].

Exogenous administration of the 18 kDa FGF2 caused transient hypotension, as well as negative inotropic effect [72]; these findings suggested that lack of FGF2 in vivo would have the opposite effect, but this was not the case. FGF2 knockout mice presented with lower blood pressure, decreased vascular tone, and decreased vascular smooth muscle contractility compared to their wild type counterparts [65].

All of these studies strongly suggested an important role for FGF2 in cardiac as well as vascular response to stress stimuli, but they provided limited information as to isoform-specific contributions. To address this question, Doetschman and Arnal groups created genetically engineered mice that expressed only Hi-FGF2 [73], or only Lo-FGF2 (Hi-FGF2 knock-outs) [74]

at endogenous levels. Using mice expressing only the Hi-FGF2 isoforms, the estrogen-mediated endothelial cell migration was shown to require Hi-FGF2 expression [73]. Comparisons of the baseline cardiac structure and function between mice expressing only Hi-FGF2, or only Lo-FGF2, all bred on a mixed Black Swiss background; the authors reported a complex series of small difference in a number of parameters, indicative of isoform-specific, and sex-dependent fine modulation of cardiac physiology by FGF2. For example, only female mice lacking Lo-FGF2 presented features suggestive of dilated cardiomyopathy [75]. Whether these differences are species or mouse strain-specific remains to be determined.

The Hurley group has extensively studied the role of FGF2 isoforms in bone homeostasis and osteoarthritis. They have shown that transgenic mice harbouring overexpression of (human) Hi-FGF2 (under type I collagen regulatory sequences) manifest with symptoms similar to that of hypophosphatemia rickets: dwarfism, reduced bone mineral density, osteomalacia, and decreased plasma phosphate levels [76]. Supplementation with phosphate [76] or treatment with a FGFR1 inhibitor [77] partially ameliorated the symptoms. They have shown that knocking out Hi-FGF2 increased bone mineral density in the femur and lumbar vertebrae and promoted formation of trabeculated bone [76]. Furthermore, they demonstrated that Hi-FGF2 transgenic mice (mice overexpressing human Hi-FGF2) develop osteoarthritis [78]. Finally, they found Hi-FGF-induced bone effects are mediated through upregulation of another member of the FGF family, FGF23, where neutralizing antibodies against FGF23 attenuated Hi-FGF2 effects [79].

Florkiewicz et al. demonstrated that in normal gastric mucosa Lo-FGF2 is almost the exclusive FGF2 isoform, whereas inducing mucosal injury results in significant upregulation of Hi-FGF2 isoforms which may be implicated in maladaptive inflammation [80].

Importantly, Hi-FGF2 has been linked to increased aggressiveness of endocrine-resistance breast cancers [81]. Sahores et al. have recently shown that overexpression of Hi-FGF2 resulted in induction of breast tumor growth, lung metastasis, and development of resistance to anti-progestin treatments [81].

The effects of FGF2 isoforms in the heart

There is a large body of evidence showing that treatment with Lo-FGF2 protects cardiac cells against various types of stresses including ischemia-reperfusion [57, 59, 82-84], oxidative stress [50, 51], and Doxorubicin toxicity [64, 85]. Relatively limited information exists regarding Hi-FGF2 activity in this context. A series of studies by the Kardami team pointed to some differences between Lo- and Hi-FGF2: overexpression of Hi- or Lo-FGF2 in immature chicken or rat cardiomyocytes in culture via transient cDNA transfection showed that while exported FGF2 (Lo- as well as Hi-) increase myocyte DNA synthesis and proliferation, endogenous, nuclear Hi-FGF2 (but not Lo-FGF2) promoted chromatin condensation indicative of apoptosis. In addition, intracellular Hi-FGF2 increased the incidence of cardiomyocyte bi-nucleation [86, 87]. Subsequent studies, using adenovirally mediated gene transferred which ensured high transfection efficiency, showed that overexpressed Hi-FGF2 decreased DNA synthesis [88] and promoted apoptotic cell death mediated by mitochondrial damage [43].

It is of interest that, although both Hi- and Lo-FGF2 can localize to the nucleus, they have been detected in distinct nuclear sites, at least in the mouse. Lo-FGF2 shows localization into Cajal bodies [89], protein-RNA enriched areas in the nucleus which are involved in RNA processing [90], while Hi-FGF2 is found instead in the nucleoplasm [89].

The Kardami team was the first to document that administration of Lo-FGF2 to the heart *ex vivo* by perfusion, or *in vivo* by intracardiac injection protected from I/R pathologies [59, 82, 91]. Intracardiac injection of FGF2 isoforms during the development of myocardial infarction due to irreversible left coronary artery occlusion revealed common as well as distinct effects of the isoforms: in the acute phase (within 24 of ligation) both Hi- and Lo-FGF2 exerted a similar

degree of cardioprotection, by reducing infarct size, troponin release, and decline in contractile function. The ability of exogenous Hi-FGF2 to be cardioprotective in the short-term was further documented by Jiang et al [91]: Hi-FGF2 administered to the ischemic ex vivo heart during reperfusion was as potent as Lo-FGF2 in protecting from I/R loss of function and mitochondria-mediated cell death [91]. Long-term studies, on the other hand, showed that only Lo-FGF2 treatment elicited sustained cardioprotection from functional decline assessed up to 8 weeks post-MI, in vivo. Only Hi-FGF2 injection promoted cardiac enlargement and cardiomyocyte hypertrophy, and reduced vascularization in the peri-infarct area at 4-8 weeks post MI. Furthermore, only Hi-FGF2 (but not Lo-FGF2) injection caused accumulation of cardiotrophin-1 in the hearts post MI. Jiang et al., further documented that Hi-FGF2 (but not Lo-FGF2) stimulates cardiomyocyte hypertrophy *in vitro* [91]. The work by Jiang et al was the first report showing that FGF2 isoforms could have distinct functions in the pathophysiology of cardiac disease. Subsequent studies showed that cardiac specific overexpression of Hi-FGF2 exacerbated cardiac injury compared to wild type hearts [92], which suggested that genetic deletion of Hi-FGF2 might be protective from I/R injury. Indeed, Liao et al. in 2010 demonstrated that knockout of Hi-FGF2 increases resistance to I/R in working perfused hearts [92].

Hi-FGF2 is mainly produced and exported from non-myocytes in the adult heart ventricles. Santiago et al. have shown that Hi-FGF2 content of either neonatal or adult rat fibroblasts is substantially higher than their corresponding cardiomyocytes [25]. In addition, neurohormonal factors that become elevated during cardiac hemodynamic stress (catecholamines, angiotensin II) stimulate Hi-FGF2 upregulation in cardiac fibroblasts, and myofibroblasts [25]. Hi-FGF2, acting in an autocrine fashion, likely promotes the pro-fibrotic, activated fibroblast phenotype, a least *in vitro*. Santiago et al. have demonstrated that

neutralizing secreted Hi-FGF2 significantly reduced expression of myofibroblast activation markers including αSMA, procollagen, embryonic smooth muscle myosin heavy chain, and ED-A fibronectin in human fibroblasts [9]. Activated fibroblast-exported Hi-FGF2 can promote cardiomyocyte hypertrophy in a paracrine fashion [25]. Thus, one might envisage a potential therapeutic application *in vivo*, such as neutralizing secreted Hi-FGF2 through antibody recognition, to reduce undesirable autocrine and paracrine effects

A study conducted by Sun et al. suggested a positive correlation between plasma levels of Hi-FGF2 and occurrence of heart failure (HF) in patients with atrial fibrillation (AF) [93]. In addition, patient with AF have a higher plasma concentration of Hi-FGF2 compared to the healthy control population [93]. These results should be regarded with caution at this point, as the authors did not clearly state the method of Hi-FGF2 quantification. If validated, this report would link Hi-FGF2 to development of HF in humans [93].

Heart failure and FGF2

Heart failure (HF) is defined as the inability of the heart to sufficiently pump blood to match the metabolic needs of the body [94]. It is estimated that about 670,000 Canadians and 23 million individuals worldwide are living with diagnosed heart failure. Regardless of the underlying pathologies the incidence of HF increases with age. Signs and symptoms associated with HF include those related to fluid retention (edema and dyspnea) and those related to low cardiac output (fatigue and weakness) which are exacerbated with exercise. HF is largely a clinical diagnosis based on the patient's history, including assessment of New York Heart Association (NYHA) functional class, and physical examination. Based on left ventricular ejection fraction, HF is divided in two categories: ***(1) heart failure with reduced ejection fraction (HFrEF)*** where EF drops below 40% and is also called systolic heart failure. The most common causes of systolic dysfunction are ischemic heart disease, idiopathic cardiomyopathy, hypertension, and valvular disease. Among patients presenting with initially unexplained HF, myocarditis, ischemic heart disease, hypertension and pressure overload, and Doxorubicin toxicity were among the most common causes [95].

(2) heart failure with preserved ejection fraction (HFpEF) where EF is greater than 50%. Patients with EF between 41 and 49% may be categorized as HFpEF, borderline. Diastolic dysfunction can be caused due to the same common conditions that lead to systolic dysfunction. Ischemic heart disease, hypertension, diabetes mellitus, and hypertrophic obstructive cardiomyopathies are the common causes of diastolic dysfunction.

A comprehensive review on the clinical manifestations, etiology, diagnosis, and treatment of HF can be found in [96].

Despite advancements in treatment there is still a high morbidity and mortality associated with HF, and there is a need for additional understanding of underlying cell and molecular mechanisms to generate approaches for prevention, management and even reversal of this disease. As reviewed here, there is ample evidence that FGF2, an endogenous factor, can influence cardiac response to injury. FGF2 isoforms may have multiple effects, both beneficial and detrimental, on cardiac pathophysiology. However, the role of FGF2 isoforms in pathologies leading to HF is not understood.

In addition to ischemic heart disease, and genetic cardiomyopathies, major causes of HF include **cancer-drug-induced toxicity**, and **pressure-overload**-induced maladaptive functional and structural changes. **The focus of my project is to understand the role of FGF2 isoforms in Doxorubicin-induced cardiotoxicity, and in pressure-overload cardiac pathology.**

The following sections will provide an overview of the mechanism underlying cancer-drug cardiotoxicity, using Doxorubicin drug as an example; and an overview of pressure overload-induced heart remodeling.

Doxorubicin induced cardiotoxicity

This section is part of a published review article "Navid Koleini, Elissavet Kardami. Autophagy and mitophagy in the context of doxorubicin-induced cardiotoxicity. Oncotarget. 2017 Aug 24;8(50):87415-87430. doi: 10.18632/oncotarget.20558. eCollection 2017 Oct 20." and used according to the Creative Commons Attribution 3.0 License (CC BY 3.0) which permits using whole or parts of the published work.

The full text of article can be found in this link:

http://www.oncotarget.com/index.php?journal=oncotarget&page=article&op=view&path%5B%5D=16944&path%5B%5D=54219

Doxorubicin (Dox), a non-selective class I anthracycline antibiotic, is a potent chemotherapeutic agent which is used for the treatment of numerous cancers [97]. The use of Dox is limited, however, due to serious side effects; the most prominent is cardiotoxicity which can manifest acutely as well as years after treatment has been discontinued leading to left ventricular dysfunction, dilated cardiomyopathy and heart failure [98-100]. Toxic effects of Dox include cardiomyocyte damage and apoptotic and necrotic cell death [101]. The severity of Dox induced heart disease is linked to accumulated Dox dosage during the course of the anticancer therapy ranging from 3-5% in patients that received a cumulative dose of 400mg/m2 to 18-48% in patients receiving 700mg/m2 (and 100% of mice receiving 71mg/ m2) [97, 102, 103].

Dox is a mitochondrial toxin, and mitochondrial damage is central to Dox-induced cardiac dysfunction and cell death [104]. Cardiomyocytes require large numbers of healthy-functioning mitochondria to ensure sufficient ATP production for contractile function and cell

survival. Dox-induced over-production of reactive oxygen and nitrogen species (ROS and RNS) such as superoxide, hydrogen peroxide, hydroxyl radical and peroxynitrite has been proposed to be the main cause of Dox-induced acute cardiomyocyte toxicity and cell death by damaging various molecular constituents and organelles [105-108]. A detailed description of the pathways by which Dox induces production of ROS and RNS can be found in references [109, 110]. Nitric oxide synthase (NOS) and nicotinamide adenine dinucleotide phosphate-oxidase (NOX) enzymes play an important role in Dox-induced production of ROS [111]. Dox can be reduced to a semiquinone by NOX and/or NOS leading to the production of superoxide and hydrogen peroxide, and subsequently the highly reactive hydroxyl radical [110]. NOS enzymes catalyze the production of nitric oxide from N-arginine; superoxide can react with nitric oxide producing peroxynitrite which is highly reactive oxidizing DNA, proteins, and peroxidizing lipids. Both endothelial NOS (eNOS) and inducible NOS (iNOS) isoforms have been implicated in mediating Dox toxicity via the production of RNS [112]. Deletion or overproduction of eNOS in mice was shown, respectively, to improve or worsen cardiac outcome post-Dox compared to wild type groups [113]. There is also some evidence that iNOS, which is increased by Dox administration, contributes to the production of RNS; iNOS-knockout mice showed protection from Dox-induced toxicity [114]. Dox also interacts with iron and Dox-iron complexes contribute to further hydroxyl radical production. Hydroxyl radical damages DNA and proteins and extensively peroxidizes lipids which contribute to major cellular damage and death [115].

Dox has a robust attraction to negatively charged membranes such as the inner mitochondrial membrane causing lipid peroxidation [106, 116]. Dox-induced peroxidation of cardiolipin uncouples respiratory chain complexes at mitochondria, resulting in reduced ATP and increased ROS production [117-120], and promoting formation of the mitochondrial

permeability transition pore, mPTP. Formation of the mPTP causes cytochrome C release and induction of the intrinsic pathway of apoptosis; it is also an important feature of necrotic cell death [121]. Despite multiple studies and strong evidence from many pre-clinical experimental models that anti-oxidant therapies can decrease or prevent Dox-induced cardiotoxicity, results have not been as promising in the clinical setting [122-124]. Additional mechanisms of Dox-toxicity need to be considered and targeted.

Dox kills rapidly proliferating cancer cells by intercalating their DNA and forming covalent adducts which lead to the inhibition of DNA polymerase and nucleic acid synthesis. Additionally, Dox cross-links Topoisomerase IIα (TOPIIα) to the DNA, forming a TOPIIα-Dox-DNA complex resulting in DNA breakage and cell death, a major mechanism for killing cancer cells which express high levels of TOPIIα [125-129]. Unlike tumor cells, cardiomyocytes do not express TOPIIα, rather they express topoisomerase IIβ (TOPIIβ) which can also form DNA-TOPIIβ-Dox complexes, cause double-strand breaks and cell death [130, 131]. Dox-induced DNA damage, mediated by TOPIIβ significantly alters the nuclear and mitochondrial transcriptome and markedly decreases mitochondrial biogenesis [132, 133]. There is strong evidence that TOPIIβ is a major contributor to Dox-induced cardiotoxicity; transgenic mice lacking TOPIIβ were not susceptible to Dox cardiotoxicity in an acute as well as chronic setting [133]. Interestingly, the compound dexrazoxane which is in clinical use for preventing Dox-induced cardiomyopathy due to its iron-chelating and anti-oxidant properties[134], belongs to the molecular category of TOPII poisons. It has been suggested that the TOPIIβ inhibitory activity, rather than the iron-chelating action, of dexrazoxane confers protection of cardiomyocytes from Dox [135].

Dox induced DNA damage leads to the activation of the Ataxia-Telangiectasia Mutated kinase (ATM) which binds to DNA break sites and upregulates and activates the tumor suppressor protein p53 [136]. Upregulation of p53 by Dox has been linked to increased ROS and double strand DNA damage, and there is considerable support to the notion that p53 protein is mediating Dox-induced apoptotic cell death of cardiomyocytes in vitro and in vivo [137-139]. Anthracycline-induced p53 up-regulation is reported to suppress transcription of GATA-4, a cardioprotective transcription factor [140]. Nevertheless, p53-independent pathways to Dox-induced deleterious effects in cardiomyocytes, such as apoptotic cell death, oxidative and nitrosative stress, and cardiac fibrosis have also been documented, in a mouse model of cardiomyocyte-specific p53 knockout [141]. In addition, using a juvenile model of Dox toxicity, Zhu and colleagues reported antithetical roles for p53 in the acute versus chronic response to Dox: the expression of dominant-interfering p53 in the heart resulted in short-term (1 week) protection against Dox, but worse outcome, compared to wild type mice at 13 weeks post -Dox [142]. Overall, it would appear that the role of p53 in mediating the multiple Dox-induced deleterious effects is context dependent, and likely depends on the model used and the timing of the assessment.

An important effector of Dox-induced cell death is Bnip3 (BH3-only protein Bcl-2-like 19 kDa-interacting protein-3), a member of the Bcl-2 family of proteins. There is evidence that Dox-induced cardiotoxicity is mediated by upregulation of Bnip3 and induction of necrosis in cardiomyocytes [143]. A similar protein, Bnip3L/NIX, an effector of apoptosis, was also found to be upregulated in the heart and myocytes by Dox, in vivo and in vitro, in response to Dox-induced downregulation of miR-30 [144]. To show the crucial role of Bnip3, transgenic mice were created expressing a mutant form of Bnip3 which is unable to insert into mitochondrial

membranes; these mice were resistant to Dox induced cardiotoxicity [143]. Bnip3 causes depolarization of mitochondria by promoting mPTP formation which leads to cell death [143]. Both p53 and Bnip3 als regulate autophagy [143], as will be discussed in the following section. Dox treatment promotes premature ageing of cardiomyocytes, *in vitro* (long-term cultures) and *in vivo* [145, 146]. It is of interest that ageing is characterized by decreased potential for autophagy and mitophagy, and this in turn contributes to the pathology of ageing [147]. One might therefore surmise that Dox-induced chronic changes would, as in ageing, also include reduced ability for autophagy. This was shown to be the case by Hoshino and colleagues [148], who reported decreased autophagic elimination of damaged mitochondria (mitophagy) in models of ageing as well as during Dox-induced cardiotoxicity in vitro and in vivo. Figure 2 shows a broad overview of the mechanisms implicated in Dox-cardiotoxicity.

Figure 2, Subcellular events associated with Doxorubicin-induced cardiotoxicity.

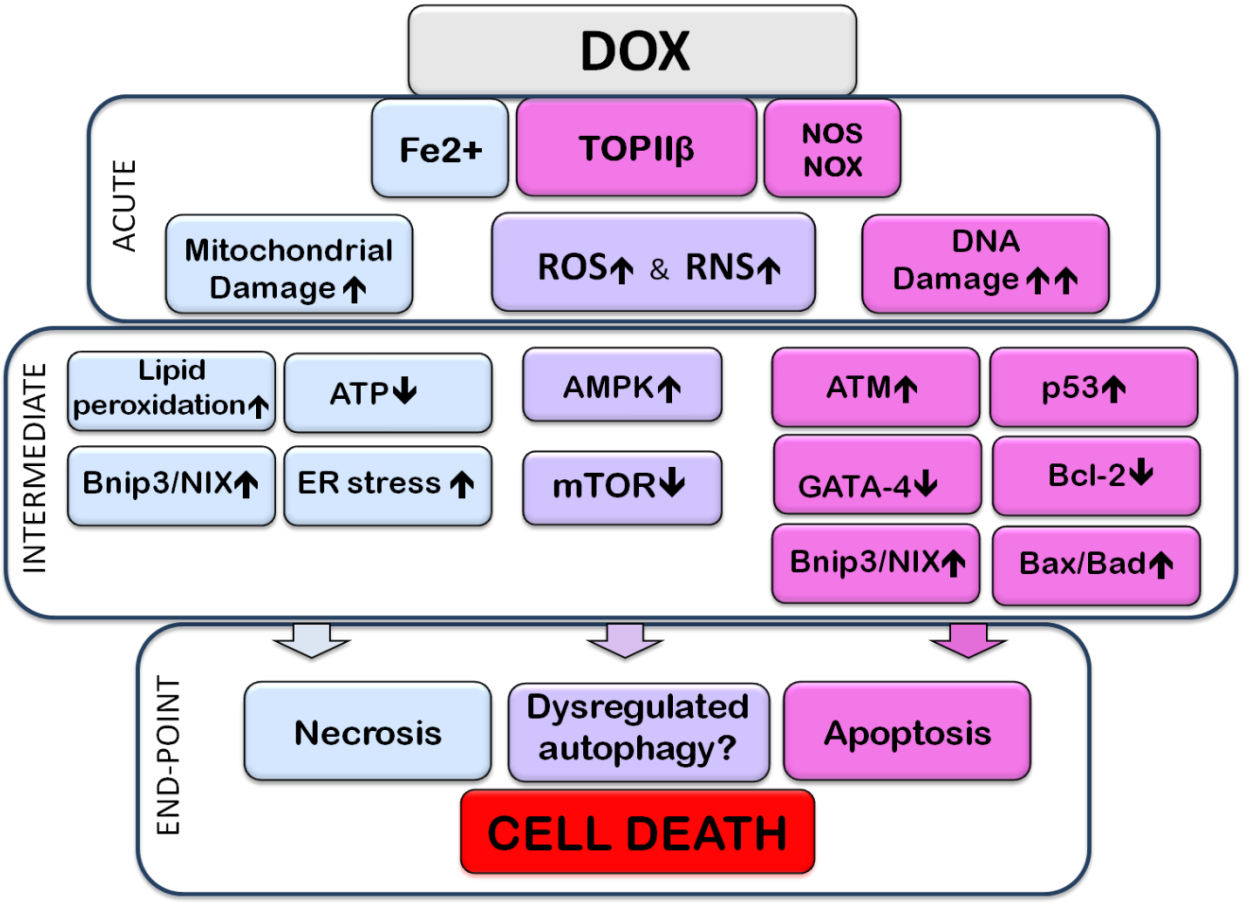

Figure 2. Subcellular events associated with Doxorubicin-induced cardiotoxicity.

The image highlights acute, intermediate, and end-point (cell death) events resulting from exposure to Doxorubicin (Dox). The acute section illustrates the direct interaction of Dox with subcellular entities; the intermediate section illustrates direct consequences of these interactions. Events within the acute, or intermediate sections are likely to occur simultaneously and cross-talk with each other. The end-point section is meant to show that the preceding events lead to apoptotic, necrotic, and/or dysregulated autophagy-associated cell death. Acute Events: Dox, upon entering the cell, interacts directly with molecules and organelles: interaction with topoisomerase-IIβ (TOPIIβ) leads to DNA damage. Interaction with nitric oxide synthase (NOS), nicotinamide adenine dinucleotide phosphate-oxidase (NOX) and Fe2+, promotes reactive oxygen or nitrogen species stress (ROS or RNS, respectively), contributing to further DNA damage, oxidation and nitrosylation of proteins and peroxidation of lipids. Dox binds to mitochondrial DNA and impairs the electron transport chain resulting in production of ROS and decreased ATP. Fe2+-Dox complexes are toxic to mitochondria and the endoplasmic reticulum (ER), by causing, for example, lipid (including cardiolipin) peroxidation. The DNA damage response activates the ataxia telangiectasia mutated (ATM) protein which upregulates and activates the tumor suppressor p53. P53 upregulates expression of pro-apoptotic members of the Bcl-2 family such as Bax and Bad; it also increases expression of Bcl2/adenovirus E1B 19 kDa protein-interacting protein 3 (Bnip3), which can cause mitochondrial damage and necrotic cell death, as well as initiate mitophagy. DNA damage and increased levels of ROS lead to downregulation of the transcription factor GATA-4 which decreases expression of the anti-apoptotic, and anti-autophagy-initiation protein, Bcl-2. P53 can also inhibit the activity of mTOR signaling, thus dis-inhibiting autophagy initiation. Dox can elicit AMP activated protein kinase

(AMPK) activation, although there is controversy regarding this. Activation of AMPK, resulting from reduced ATP levels, can inactivate mammalian target of Rapamycin (mTOR) and initiate autophagy. Dox-induced effects on ROS and RNS production, mitochondrial and ER damage, DNA and gene expression, culminate in the promotion of apoptotic and necrotic cell death. Dysregulation of the autophagy/mitophagy processes are also linked to Dox-induced cell death. Signals/events associated mostly, although not exclusively, with apoptotic or necrotic cell death is included, respectively, in pink or pale-blue boxes. Pale-purple boxes contain signals/pathways associated with various types of subcellular dysfunction, including autophagic dysregulation.

Pressure overload

Pressure overload is a state in which ventricular muscles contract against excessive afterload and is associated with conditions such as chronic hypertension and aortic stenosis [149]. A persistent increase in intraventricular pressure elicits a compensatory increase in cardiac mass (hypertrophy) which is beneficial by increasing contractile units and reducing wall tension, according to the law of Laplace. In the long-term, compensatory hypertrophy transitions to pathologic hypertrophy, cardiac contractile dysfunction, extracellular matrix remodeling, continuous collagen deposition (fibrosis) and eventually heart failure [94]. Cardiomyocyte dysfunction and loss (due to apoptosis and necrosis) and their replacement with myofibroblasts significantly decreases contractility contributing to systolic dysfunction; while myocardial stiffness due to extracellular matrix and fibrosis disrupt ventricular relaxation during diastole leading to diastolic dysfunction [94].

Molecular mechanisms underlying cardiac remodeling following pressure overload have been extensively discussed in the literature [150]. Mechanical stress, neuro-hormonal overstimulation, and myocardial inflammation are the primary stimuli for myocardial remodeling.

With regard to mechanical stress, sarcomeres, intercalated disks, and integrins are the key sites for mechanotransduction. Sarcomeres are the basic units in cardiomyocytes generating force of contraction. Sarcomeres' link to the cytoskeleton and sarcolemma enable them to sense the mechanical stress in myocytes which has been shown to be mediated through Titin. Titin is a large protein spanning from the Z-disk to the M-line providing passive tension in the sarcomeres which transduce mechanical force to biochemical signaling through recruitment of cardiac LIM protein, titin-Cap, calsarcin-1, four-and-a half-LIM domain protein-1 (FHL1) and muscle-

specific ankyrin repeat protein (MARP). Fascia adherens, a form of cell-cell junction, is another site for mechanotransduction transferring the tension to the sarcomeres. The transmembrane protein N-Cadherin, located in the fascia adherens, transfers the mechanical force generated in the adjacent cell to α-Catenin via physical interaction of β-Catenin to α-Catenin and N-Cadherin resulting in a force-dependent conformational change in α-Catenin unmasking its vinculin binding sites. Recruitment of vinculin by α-Catenin interconnects the complex to fibrillar actin which is, on the other hand, linked to the sarcomeres, thus, transmitting the tension to the sarcomere complex. Integrins, key mechanoreceptors in cardiomyocytes and fibroblasts, are a family of cell surface receptors consisting of a large extracellular, single transmembrane, and a small cytosolic domain [151]. The extracellular domain is linked to ECM proteins and is capable of sensing mechanical stress. The cytosolic domain is associated with the cytoskeleton, through α-actinin, talin, vinculin, paxillin, and tensin [152]. On the other hand, the intracellular domain can be engaged with focal adhesion kinase (a non-receptor tyrosine kinase) through Src which could, then, recruit signal transduction intermediates, such as Grb2, Sos, Ras, PLCγ, and MAPKs, transducing mechanical force to biochemical signaling.

The principal neurohormonal systems involved in cardiac remodeling are adrenergic stimulation and activation of the renin-angiotensin system. Adrenergic stimulation can increase heart rate and contractility but can have damaging effects on the myocardium in the long-term [153]. Adrenergic receptors are class of G protein coupled receptors eliciting inotropism and chronotropism in the heart consisting of different types such as α_1, α_2, β_1, β_2, and β_3 [153]. While the same ligands (epinephrine and norepinephrine) can engage these receptors, they show significantly different effects [154]. It has been shown that the failing heart displays a significant decrease in β_1 receptor; thus, heart contractility would be mainly dependent on the activity of β_2

receptors [155, 156]. Activation of β_1 receptor has been shown to induce myocyte apoptosis and necrosis via calcium overload and mPTP opening, while the β_2 activation counteracts β_1 effect by exerting anti-apoptotic effects [157, 158]. Therapies aimed at exclusive blockage of β_1 receptors while leaving β_2 receptors active have been shown to ameliorate cardiac remodeling, although long-term mortality was not changed in the patients [159, 160].

In contrast, blocking the renin-angiotensin system is associated with a significant improvement in HF patients' mortality and cardiac remodeling [161]. The renin-angiotensin system is activated in response to hemodynamic changes as well as local factors. Angiotensin II binds to angiotensin receptors (AT), AT_1 and AT_2 which are a class of G coupled protein receptors with wide variety of effects in cardiomyocytes and non-myocytes [162]. Both receptors are expressed in the adult myocardium, nonetheless, the expression of AT_2 significantly decreases after birth [163]. Activation of AT_1 induces vasoconstriction, cardiac hypertrophy, fibrosis, and ECM remodeling where specific inhibitors block these actions. However, the AT_2 effects are shown to counteract those of AT_1, causing vasodilation and mitigating hypertrophy and fibrosis [164]. Overstimulation of adrenergic (through mainly β_1 receptors) and angiotensin (through AT_1) result in fetal gene reprogramming, increase ROS accumulation, calcium overload, and mitochondrial damage in cardiomyocytes leading to myocyte dysfunction and loss [165]; while inducing epithelial mesenchymal transition, fibroblast-to-myofibroblast phenoconversion, and ECM remodeling in non-myocytes.

The role of endogenous FGF2 isoforms in the development of heart failure following chronic pressure overload is not known. It was hypothesized that genetic elimination of Hi-FGF2 increases resistance to pressure overload induced adverse cardiac responses (Chapter III).

Chapter II: FGF2 and Doxorubicin Cardiotoxicity

Rationale and Hypothesis

As reviewed, Doxorubicin has well documented damaging effects in the heart, limiting its use in the clinic. In addition, there is evidence that of the two types of FGF2 isoforms, Lo-FGF2 is clearly cytoprotective/cardioprotective while Hi-FGF2 may exert adverse effects in the context of cardiac response to injury. In this chapter we have addressed a number of issues revolving around the role of administered or endogenous FGF2 isoforms in mitigating Dox-cardiotoxicity. The following hypotheses were investigated:

(1) Genetic elimination of Hi-FGF2 mitigates Dox cardiotoxicity *in vivo*, in mice (Chapter II, Section 1)

(2) Neutralization of paracrine Hi-FGF2 increases resistance to Dox-induced cardiomyocyte damage *in vitro* (Chapter II, Section 1)

(3) Exogenously added Hi- or Lo-FGF2 exert an acute protective effect against multiple aspects of Dox-induced cardiomyocyte damage, *in vitro* (Chapter II, Section 2)

(4) A mutant form of Lo-FGF2, lacking mitogenic and angiogenic activity, retains the ability to protect cardiomyocytes against Dox damage (Chapter II, Section 3).

Section 1. Elimination or neutralization of endogenous high molecular weight FGF2 mitigates Doxorubicin induced cardiotoxicity

Published in: Am J Physiol Heart Circ Physiol. 2019 Feb 1;316(2):H279-H288. doi: 10.1152/ajpheart.00587.2018. Epub 2018 Nov 9.

Navid Koleini[*1,2], Jon Jon Santiago[*2], Barbara E Nickel[2], Glen Lester Sequiera[1,2], Jie Wang[1], Robert R Fandrich[2,3], Davinder S Jassal[1,2,4], Sanjiv Dhingra[1,2], Lorrie A Kirshenbaum[1,2,5], Peter A Cattini[1], Elissavet Kardami[1,2,3]

*: co-first authors

1: Department of Physiology & Pathophysiology, Max Rady College of Medicine, Rady Faculty of Health Sciences, University of Manitoba, Winnipeg, MB, Canada

2: Institute of Cardiovascular Sciences, St. Boniface Hospital Albrechtsen Research Centre, Winnipeg, MB, Canada

3: Department of Human Anatomy & Cell Sciences, Max Rady College of Medicine, Rady Faculty of Health Sciences, University of Manitoba, Winnipeg, MB, Canada

4: Section of Cardiology, Department of Internal Medicine, Max Rady College of Medicine, Rady Faculty of Health Sciences, University of Manitoba, Winnipeg, MB, Canada

5: Department of Pharmacology & Therapeutics, Max Rady College of Medicine, Rady Faculty of Health Sciences, University of Manitoba, Winnipeg, MB, Canada

Running Head

FGF2 isoforms and cardiac resistance to Doxorubicin

Corresponding Author

Elissavet Kardami, PhD

Rady Faculty of Health Sciences, University of Manitoba and Institute of Cardiovascular Sciences,

R3008, St.Boniface Albrechtsen Research Centre, 351 Taché Ave,Winnipeg, Manitoba, Canada, R2H 2A6

Email: ekardami@sbrc.ca, Tel: +1 (204) 235 3519, Fax: +1 (204) 233 6723

Abstract

Cardiac FGF2 exerts multiple paracrine activities related to cardiac response to injury. Endogenous FGF2 is composed of a mixture of 70% high (Hi-) and 30% low (Lo-) molecular weight isoforms; while exogenously added Lo-FGF2 is cardioprotective, the role of endogenous Hi- or Lo- FGF2 is not well defined. Therefore, we investigated the effect of eliminating Hi-FGF2 expression on susceptibility to acute cardiac damage *in vivo*, caused by an injection of the genotoxic drug Doxorubicin (Dox). Mice genetically depleted of endogenous Hi-FGF2 and expressing only Lo-FGF2 (FGF2(Lo) mice), were protected from the Dox-induced decline in ejection fraction displayed by their wild type FGF2(WT) mouse counterparts, regardless of sex, as assessed by echocardiography for up to 10 days post-Dox treatment. Because cardiac FGF2 is produced mainly by non-myocytes, we next addressed potential contribution of fibroblast-produced FGF2 on myocyte vulnerability to Dox. In co-cultures of neonatal rat cardiomyocytes (r-cardiomyocytes) with mouse fibroblasts from FGF2(WT) or FGF2(Lo) mice only the FGF2(Lo)-fibroblast co-cultures protected r-cardiomyocytes from Dox-induced mitochondrial and cellular damage. When r-cardiomyocytes were co-cultured with or exposed to conditioned medium from human fibroblasts, neutralizing antibodies for human Hi-FGF-2, but not total FGF2, mitigated Dox-induced injury of cardiomyocytes. We conclude that endogenous Hi-FGF2 reduces cardioprotection by endogenous Lo-FGF2. Antibody-based neutralization of endogenous Hi-FGF2 may offer a prophylactic treatment against agents causing acute cardiac damage.

Key words:

FGF2 isoforms; Drug-induced cardiotoxicity; neutralizing antibody treatment; High molecular weight FGF2

Introduction

Fibroblast growth factor 2 (FGF2) is an endogenous heparin-binding multifunctional growth factor expressed and secreted predominantly by cardiac non-myocytes (fibroblasts) in the heart (12). Administered or overexpressed FGF2 is reported to be cardioprotective in different injury models including ischemia- as well as genotoxic drug- induced damage (8, 12, 28). Thus, it is reasonable to surmise that endogenous FGF2 would regulate cardiac vulnerability to stress stimuli; however, it should be noted that the majority of studies on FGF2 cardioprotection rely on exogenous supplementation with, or over-expression of, the 18 kDa FGF2 isoform (12). Activation of plasma membrane FGF2 tyrosine kinase receptor (s), FGFR1, downstream activities of protein kinase C (PKC), extracellular signal–regulated kinase (ERK) and protein kinase B (AKT) pathways and phosphorylation of the cellular and mitochondrial channel protein connexin-43 are implicated in the mechanism of FGF2 cardioprotection (8, 26, 28). In addition, a recent study showed that administered FGF2 is protective by activating endogenous anti-oxidant and detoxification pathways (Nuclear factor (erythroid-derived 2)-like 2 (Nrf2)/ hemoxygenase-1(HO-1)) during acute Doxorubicin (Dox) treatment (15). Endogenous FGF2 is expressed as >20 kiloDalton (kDa) leucine (CUG)- initiated isoforms, collectively referred to as high molecular weight FGF2 (Hi-FGF2) and constituting 70-80% of total expressed and 'secreted' FGF2, in addition to the methionine (AUG)-initiated low molecular weight FGF2 (18 kDa; Lo-FGF2)(12, 23, 24). The role of endogenous FGF2 in the context of cardiac response to genotoxic agents such as Dox *in vivo* is not known. Here, we provide evidence that wild type mice, expressing

both Hi and Lo-FGF-2 isoforms, are more vulnerable to Dox-induced cardiac damage when compared to mice expressing only Lo-FGF2. Furthermore, elimination or neutralization of endogenous Hi-FGF2 reduces cardiac vulnerability to Dox treatment.

Materials and Methods

Animals. This study was done according to the NIH Guide for the Care and Use of Laboratory Animals (NIH Publication, 8th Edition. Revised 2011). Approval was given by the Protocol Management and Review Committee of the University of Manitoba. Generation and characterization of mice genetically engineered by Doetschman and colleagues to lack endogenous Hi-FGF2 expression and express only Lo-FGF2, $Fgf2^{tm3Doe}$ has been described previously (1). These mice were bred onto a C57BL/6J genetic background and are referred to here as FGF2(Lo) mice. Both FGF2(Lo) and wild type C57BL/6J (FGF2(WT)) mice were purchased from Jackson Laboratories.

***In vivo* model for acute cardiotoxic effects.** To induce acute cardiac injury a single intraperitoneal injection of the anthracycline Doxorubicin (Dox) was used at 20 mg/kg. This model is meant for proof-of principle studies of acute Dox cardiotoxicity and not intended to simulate the chronic effects of repeated Dox injections as would occur in anti-cancer treatments of different types of cancer patients. Eight-week-old groups of male or female FGF2(WT) and FGF2(Lo) mice were each randomly divided into saline- and Dox-treated groups; sample size was n=10 unless stated otherwise. At day 10 post-Dox treatment, mice were killed humanely by administering ketamine (150 mg/kg) and xylazine (10 mg/kg) intraperitoneally for induction of deep terminal anesthesia. Hearts were then collected for biochemical analyses.

Echocardiography. Serial murine echocardiography was performed at baseline and daily for up to 10 days post-Dox treatment, as described previously in detail (2, 11).

***In vitro* experiments.** Neonatal rat ventricular cardiomyocytes (referred to as r-cardiomyocytes) were isolated from 1-2-day old rat pups as previously described (23).

Primary mouse embryonic fibroblasts (MEFs)-r-cardiomyocyte co-cultures. MEFs were isolated as described (18). R-cardiomyocytes were plated at a density of 5×10^4 cells/cm^2 on collagen (Corning, #354236) coated glass coverslips in the presence of 20% fetal bovine serum (FBS) in Hams F-10 culture medium; 24 hours later the media was changed and MEFS from FGF2(WT) and FGF2(Lo) strains ($2x10^4$/cm^2) were added to the cultures in low-serum medium (0.5% FBS, 1% insulin, 1% transferrin/selenium, and 1% ascorbic acid) in Dulbecco's modified Eagle's medium (DMEM). After 48 hours, co-cultures were incubated with low serum medium supplemented or not with Dox, 0.5 µM. Conditioned media were collected 24 h later, and stored at -80°C. Cells attached on coverslips were used for the Calcein-AM/Cobalt chloride mPTP assay.

Human induced pluripotent stem cells (iPSC)- derived fibroblasts. As described in our recent study, iPSC were derived from peripheral blood mononuclear cells (PBMNC) (25). All the protocols were approved by the Research Ethics Board, University of Manitoba. Briefly, blood samples were derived from healthy individuals, and PBMNC were isolated using the Lympholyte H kit (Cedarlane). PBMNC were reprogrammed to iPSCs using CytoTuneTM-iPS 2.0 Sendai Reprogramming Kit (ThermoFisher Scientific). The pluripotency of the established iPSC line (SGC 005.2) was checked through immunostaining with anti- -Oct4, -Sox2, -Nanog, -Tra-1-60, -Tra-1-81 and -SSEA4 and tri-lineage differentiation. The iPSC were differentiated into fibroblasts (iPSC-Fibs) using a previously described protocol (3). The iPSC colonies were cultured in low attachment 6 well dishes (ThermoFisher Scientific) to form embryoid bodies (EBs). The EBs were then cultured in DMEM-High Glucose (ThermoFisher Scientific)

supplemented with 10% FBS, 1X non-essential amino acid and 0.1 mM β-mercaptoethanol. The EBs were then plated onto 0.1% gelatin-coated dishes in the EB medium on day 8 at 1-2 EBs per 6-cm plate. After 12 days of culture, only the outgrowing cells were collected, trypsinized and plated onto non-gelatin coated dishes. These were passaged twice and then immunostained for fibroblast-specific markers (vimentin, fibroblast-surface protein and heat shock protein 47). Only those culture plates which showed >99% staining for all the three markers were used for further experiments.

Fib^{iPSC}-r-cardiomyocyte co-cultures. R-cardiomyocytes were plated at a density of 5 × 10^4 cells/cm^2 on collagen coated plates in the presence of 20% (FBS) in Hams F-10 culture medium. After 24 hours, the media was changed to low serum medium (LSM, 0.5% FBS, 1% insulin, 1% transferrin/selenium, 1% ascorbic acid, and 1% bovine serum albumin) in Dulbecco's modified Eagle's medium (DMEM). Fib^{iPSC} were added to the cultures at a density of 3x10^4/cm^2. Anti-human Hi-FGF2 antibody (Hi-Ab, 20µg/ml) or non-immune rabbit IgG (20 µg/ml) were added to the cultures after 6 hours. Another 'dose' of Hi-Ab or rabbit IgG were added to the co-cultures after 24 hours. At 48 hours of co-culturing cardiomyocytes with Fibs^{iPSC} the media was refreshed, Hi-Ab or rabbit IgG supplemented, and Dox (0.5 µM) or saline was added to the cultures for 24 hours. Subsequently, the media was collected and stored at -80°C.

Fib^{iPSC}-r-cardiomyocyte Transwell co-cultures. After seeding r-cardiomyocytes at 5 × 10^4 cells/cm^2 on collagen coated plates in the presence of 20% (FBS) in Hams F-10 medium for 24 hours, the media was changed to LSM. Transwell permeable inserts (1 µm pore size) were used to grow Fibs^{iPSC} (5 × 10^4 cells/cm^2) in co-culture with r-cardiomyocytes. The co-cultures were supplemented with 20 µg/ml Hi-Ab or rabbit IgG every 24 hours. After 48 hours Dox (0.5

μM) or saline was added to the cultures for 24 hours before the media was collected and stored at -80°C.

R-cardiomyocytes cultured with Fib^{iPSC} conditioned media. Fib^{iPSC} were grown in 100 mm dishes in 10% FBS in DMEM until 80% confluent. Media were then replaced with 5 ml of LSM per plate. One day later 2.5 ml conditioned medium was removed/100 mm dish, and used as Fib^{iPSC} conditioned medium for experiments. R-cardiomyocytes were plated on collagen-coated plates at 5×10^4 cells/cm^2 in the presence of 20% (FBS) in Hams F-10 culture medium for 24 hours. Then the media was replaced with 1 ml of fresh Fib^{iPSC} conditioned-medium supplemented with 20 μg/ml of: Hi-Ab, or rabbit IgG, or mouse monoclonal anti-total-FGF2 antibody (Millipore #05-117), or mouse IgG. One day later, another 1 ml of conditioned media containing the various neutralizing antibodies or IgGs were added to the cultures. Subsequently, myocytes were exposed, or not, to Dox, for 24h, at which point the media were collected and stored at -80°C until further analysis.

Hi-FGF2 antibody. Rabbit anti-Hi-FGF2 antibodies (Hi-Ab) were made against a sequence unique to the amino-terminal extension of human Hi-FGF2 and affinity purified by Genscript. Characterization and validation were done as described previously(24).

Protein extraction and immunoblotting (western blot). At the end of the in vivo study, hearts were collected, snap frozen in liquid nitrogen, and stored at -80°C. For total protein extraction, hearts were powdered in liquid nitrogen using a mortar and pestle prior to being homogenized in 10 mM Tris-HCl pH 7.4, 100 mM NaCl, 300 mM sucrose, 2 mM $MgCl_2$, 1 % thiodiglycol, 60 mM B glycerophosphate, 10 mM NaF and an equal volume of 20% glycerol, 100mM Tris/HCl PH=6.8, and 2% sodium dodecyl sulphate (SDS). All buffers were supplemented (1:100) with protease inhibitor cocktail (Sigma-Aldrich, #8304) and phosphatase

inhibitor cocktail set II and IV (Calbiochem, #524625 and #524628). Samples were boiled, sonicated, and centrifuged for 15 min at 21,000xg to remove residual debris. Protein concentration was measured using the bicinchoninic acid assay from Sigma. Following SDS-polyacrylamide gel electrophoresis and protein transfer to polyvinylidene fluoride (PVDF) membranes, total protein was stained using 2% Ponceau S (Sigma-Aldrich, P3504) (w/v) in 30% trichloroacetic acid to assess overall protein transfer. Non-specific binding sites were blocked by incubation in 10% milk/TBS-T for 1 hour at room temperature. The following antibodies were used: mouse monoclonal Bnip3 (1:1000), as previously described (22) and cTroponin-T (RV-C2, Developmental Studies Hybridoma Bank (DSHB), 1:200). The original densitometry values from the Western blots were adjusted based on corresponding Ponceau S staining of the whole lane.

Immunoprecipitation. A clarified (150 μg) protein solution, extracted from Fib^{iPSC} cultures directly into radioimmunoprecipitation, RIPA, buffer (150 mM NaCl, 1% (v/v) NP-40, 0.25% (w/v) deoxycholate, 0.1% (w/v) SDS, 50 mM Tris-HCl pH 8.0, 1 mM EGTA, 1 mM EDTA, 1 mM Na_3VO_4) supplemented with protease inhibitors, was mixed with 3 μg of purified Hi-Ab, followed by the addition of protein-A conjugated to Dynabeads™ (Thermofisher Scientific #10001D) to isolate antigen-antibody complexes, as per manufacturer's instructions. Immunoblotting was performed as described (24).

Mitochondrial permeability transition pore (mPTP) assay. Formation of mPTP was visualized as a reduction in the intensity of mitochondrial calcein staining using the Image-iT ™ LIVE Mitochondrial Transition Pore Assay Kit (I35103; Thermofisher), according to the manufacturer instructions. Image J software was used to measure individual cell fluorescence

intensity of Calcein-AM (green). Mitochondria were counterstained (red) with the Mitotracker reagent in the kit.

Statistical analysis: Two-way ANOVA with Sidak and Fisher's Least Significant Difference (LSD) *post-hoc* tests; one-way ANOVA with Tukey *post-hoc* test; or Student's t-test were used, as required, using GraphPad Prism 6 software. A $p<0.05$ was considered as statistically significant. For the *in vivo* echocardiography experiments, data were obtained from 9-10 mice per group, unless otherwise indicated.

Results:

Endogenous FGF2 expression and vulnerability to Dox. Baseline characteristics of the FGF2(Lo) mouse model have been reported previously (1). Echocardiographic measurements indicated that systolic function and left ventricular cavity dimensions were within the normal range for all groups of male and female mice.

Dox had minimal effects on mortality in both FGF2(Lo) and FGF2(WT) mice models. In males, Dox administration was associated with one death in ten animals, in either the FGF2(WT) or the FGF2(Lo) groups. No death occurred in any of the female groups. The effect of Dox- or saline-injection on ejection fraction (EF) for up to 10 days post-Dox treatment in FGF2(WT) and FGF2(Lo) mice is shown for males (Fig.3A) and females (Fig.3B). In Fig. 3A or B, panels (i) and (ii), comparisons are made between the Dox- and corresponding saline-treated (sham) animals at each time point. In males, the wild type FGF2(WT) mouse group, Fig 3A, panel (i), displayed a gradual decrease in EF, compared to sham, reaching 10% decrease by day 10. The Dox-treated FGF2(Lo) group did not show a decline in EF, as compared to sham, Fig.3A, panel (ii). As shown in Fig.3B (panels (i) and (ii)) the female groups had similar patterns of EF changes post-Dox as their male counterparts. EF was also compared between FGF2(WT) and FGF2(Lo) mice at baseline and 10 days post-Dox treatment, shown in Fig.3A or B, panel (iii). While no significant differences were seen at baseline, at 10 days post Dox treatment the EF values of male as well as female FGF2(WT) groups were significantly lower (by 12% and 11%, respectively) compared to corresponding FGF2(Lo) mouse groups.

Measurements of left ventricular end diastolic dimension, LVEDD at baseline, one day- and 10 days post-Dox treatment, in FGF2(WT) versus FGF2(Lo) mice, in males and females, are shown in Fig. 4. There were no differences between FGF2(WT) versus FGF2(Lo) mouse groups

at baseline or at one day post-Dox treatment in either males or females. At 10 days post-Dox, LVEDD in the FGF2(WT) mice was higher, by 14% in males or by 16% in females, compared to the corresponding FGF2(Lo) mouse groups (Fig.4).

Overall, the FGF2(WT) mouse groups showed Dox-induced deterioration of cardiac parameters (based on EF and LVEDD measurements) which were not observed in the FGF2(Lo) mouse groups. Additional data, from echocardiography and heart weight/body weight (HW/BW) parameters, at day 10 post-Dox or post-saline administration, are summarized in Table 1. The FGF(WT) but not the FGF(Lo) groups displayed a significant increase in left ventricular end systolic diameter, LVESD, compared to the corresponding saline group, but no changes in posterior wall thickness, PWT, or heart rate, HR, post-Dox in either males or females. In addition, no significant differences in HW/BW were observed between groups. No sex-related differences were evident in any of these measurements. Pilot studies using frozen cardiac ventricular sections from the various groups, obtained at 10 days post-saline or post-Dox, did not show evidence for apoptosis, myocardial damage or fibrosis, assessed, respectively, by: TUNEL staining; eosin / hematoxylin staining; Picrosirius Red staining, and were not pursued further. Based on previous work (6) in a similar model, it is assumed that any Dox-induced cell death and tissue damage might have been detectable at earlier time points, such as days 3-7 post-Dox, but not necessarily later on.

Accumulation of the pro-cell death protein Bnip3. Increases in the pro-cell death protein Bnip3 (BCL2/adenovirus E1B 19 kDa protein-interacting protein) are implicated in Dox-induced mitochondrial damage and dysfunction, leading to cell death and cardiac deterioration (5). Therefore, Bnip3 protein expression was examined to determine whether it would parallel the functional differences observed between the FGF2(WT) versus FGF2(Lo) groups post Dox

treatment (Fig. 5A, B). Baseline Bnip3 protein levels were similar between all groups (Fig. 5C). Please note that the anti-Bnip3 antibodies recognized several immunoreactive bands at 21 to 30 kDa, as reported by others for MEFs, or rat cardiac ventricles (27, 29). The anti-Bnip3 21-30 kDa immunoreactive bands were used for relative quantification of Bnip3 at day 10 post-treatment. The western blot data suggested that, in males, Dox upregulated cardiac Bnip3 protein in FGF2(WT) by 1.5-fold versus the saline-treated group (Fig.5A). No significant Bnip3 increase was observed in the FGF2(Lo) mice compared to their corresponding sham groups. In females, Dox did not seem to increase cardiac Bnip3 significantly in either FGF2(WT) or FGF2(Lo) mice compared to their corresponding sham controls, Fig.5B, suggesting the possibility of sex-related differences in Dox-induced Bnip3 response in wild type mice. Further studies are required to investigate this issue.

The effects of FGF2 expression by MEFs on r-cardiomyocyte resistance to Dox. To examine the role of FGF2 produced by non-myocytes on cardiomyocyte resistance to injury, r-cardiomyocytes were co-cultured with MEFs derived from FGF2(WT) and FGF2(Lo) mice for two days and then they were treated with Dox. Note, r-cardiomyocytes express negligible levels of FGF2 protein relative to non-myocytes, as reported for both neonatal and adult cell lysates analyzed by protein (western) immunoblotting, as well as by immunostaining of adult hearts (23). Thus, it is expected that the total secreted/extracellular FGF2 in the co-cultures would largely reflect contribution from MEFs. R-cardiomyocyte-specific damage was detected by probing for cardiac cTnT in the culture medium. Dox-induced cTnT release was observed in co-cultures with FGF2(WT) but not with FGF2(Lo) MEFs (Fig. 6A-B). Dox triggers formation of mPTPs leading to cell death (14). A Calcein AM-cobalt chloride assay kit was used on live cells (in co-cultures) to visualize healthy mitochondria and viable cells post-Dox treatment. As

mitochondria are more abundant in cardiomyocytes than in fibroblasts, myocyte mitochondria are the main contributors to the calcein fluorescence signal. The relative intensity of calcein fluorescence of r-cardiomyocytes exposed to Dox was significantly higher in co-cultures with FGF2(Lo)-MEFs, compared to co-cultures with FGF2(WT)-MEFs (Fig. 6C-D). Thus, the MEF co-culture findings are in broad agreement with the *in vivo* mouse data presented here (Figs. 3 and 4). Furthermore, these observations are consistent with the notion that the isoform composition of FGF2 expressed by non-myocytes is playing a crucial role in determining cardiomyocyte vulnerability to Dox injury. These findings also suggest that the simultaneous presence of Hi- and Lo- FGF2 in the extracellular milieu, at the 7:3 ratio determined by our previous studies (23, 24), is not, compared to secretion of Lo-FGF2 alone, protective from Dox injury. If so, selective neutralization of paracrine Hi-FGF2 is predicted to be beneficial to cardiomyocytes with a wild type FGF-2 background, by allowing the 'unopposed' protective action by Lo-FGF2.

The effects of (human) Hi-FGF2-specific antibodies on Dox-induced r-cardiomyocyte injury *in vitro*. Hi-FGF2 isoforms possess an extra amino-terminal extension which is absent from Lo-FGF2 (7). To selectively target Hi-FGF2, and discriminate between the isoforms, affinity-purified antibodies (Hi-Ab) were generated against a sequence in the amino-terminal extension of human Hi-FGF2 (21, 24). Hi-Ab was shown in our previous studies to selectively neutralize the activity of extracellular-acting human Hi-FGF2 produced by adult human fibroblasts *in vitro* (24). The human fibroblasts used here as a source of paracrine-acting Hi-FGF2 were derived from induced pluripotent stem cells (h-Fib^{iPSC}). Both types of isoforms are expressed by and are exported to the extracellular space by, h-Fib^{iPSC}, Fig.7. As shown in Fig.7 (lanes 1-3), Hi-Ab interacts with and immunoprecipitated native human Hi- but not human

Lo-FGF2 from h-Fib^{iPSC}. In the example shown in Fig.7, Hi-Ab immunoprecipitated about 40% of the soluble Hi-FGF2; similar findings have been reproduced twice using lysates from different batches of cells. It is surmised that, by interacting with extracellular human Hi-FGF, Hi-Ab decrease the relative levels of free human Hi-FGF2 available to interact with r-cardiomyocyte cell surface receptors in our co-cultures. In addition, because Hi-Ab does not recognize and cannot neutralize rat Hi-FGF2, as demonstrated in previous studies (24), any observed effect by Hi-Ab can be attributed to the neutralization of human Hi-FGF2 produced by h-Fib^{iPSC}.

R-cardiomyocytes were co-cultured with h-Fibs^{iPSC} followed by exposure to Dox in the presence of Hi-Ab or, as a control, non-immune rabbit immunoglobulin (IgG). Dox promoted robust cardiomyocyte damage as measured by cTnT release in control co-cultures (Fig. 8A). These findings are qualitatively very similar to those obtained when r-cardiomyocytes were co-cultured with FGF2(WT)-MEFs (Fig.6A), demonstrating that both mouse and human fibroblasts exert similar effects in co-culture with r-cardiomyocytes. Addition of Hi-Ab nearly eliminated Dox-induced damage (Fig.8A), indicating that neutralization of paracrine human Hi-FGF2 was protective.

In a parallel experiment, r-cardiomyocytes were separated from h-Fib^{iPSC} by plating the latter in Transwell permeable inserts in the presence of Hi-Ab or control IgG; Dox-induced damage (cTnT) was reduced by 50% in the presence of Hi-Ab (Fig. 8B). In a third approach, r-cardiomyocytes were cultured with conditioned medium from h-Fibs^{iPSC} in the presence of Hi-Ab or control IgG. Hi-Ab reduced Dox-induced damage (LDH release) significantly by 25% (Fig. 8C).

A different preparation of neutralizing antibodies (Neu-Ab) raised against the core Lo-FGF2 sequence present in both types of isoforms) is capable of recognizing, and neutralizing Lo- as well as Hi-FGF2, as demonstrated in our previous studies: Neu-Ab was capable of neutralizing the paracrine activity of Hi- or Lo-FGF2, individually overexpressed in r-cardiomyocytes (19) ; Neu-Ab could also detect human Hi- as well as Lo-FGF-2 overexpressed in human embryonic kidney 293 cells (24). It is therefore expected that Neu-Ab is capable of neutralizing extracellular/paracrine Hi- and Lo- FGF2 in our co-cultures. R-cardiomyocytes were incubated with h-Fib^{iPSC} conditioned medium in the presence of Neu-Ab or control IgG. No protection was observed in the presence of Neu-Ab; in contrast to the protection seen with Hi-Ab, Neu-Ab elicited a small but significant increase in Dox-induced damage compared to control IgG (Fig. 8D).

Table 1, Echocardiography and heart weight/body weight parameters.

Mouse Strain	FGF2(WT)		FGF2(Lo)	
	Saline	Dox	Saline	Dox
Male mice				
LVESD, mm	1.58 ± 0.06	1.95 ± 0.05*†	1.51 ± 0.11	1.53 ± 0.07
PWT, mm	0.94 ± 0.07	0.97 ± 0.05	0.90 ± 0.09	0.93 ± 0.04
HR, beats/min	712 ± 39	665 ± 27	700 ± 41	658 ± 85
Heart weight/body weight, $\times 10^{-2}$	0.46 ± 0.03	0.44 ± 0.06	0.45 ± 0.03	0.43 ± 0.04
Female mice				
LVESD, mm	1.54 ± 0.04	1.83 ± 0.08*†	1.41 ± 0.05	1.42 ± 0.08
PWT, mm	0.95 ± 0.06	0.89 ± 0.05	0.89 ± 0.06	0.84 ± 0.04
HR, beats/min	723 ± 34	645 ± 73	683 ± 30	670 ± 33
Heart weight/body weight, $\times 10^{-2}$	0.44 ± 0.03	0.43 ± 0.02	0.48 ± 0.05	0.44 ± 0.03

Data are means ± SD. Echocardiography and heart weight/body weight parameters from the wild-type fibroblast growth factor 2 [FGF2(WT)] and low-molecular-weight FGF2 [FGF2(Lo)] groups at *day 10* post-doxorubicin (Dox) or postsaline administration are shown. Comparisons between groups were made using two-way ANOVA (variables are strain and treatment). LVESD, left ventricular end-systolic diameter; PWT, posterior wall thickness; HR, heart rate. *Significant differences between saline- and Dox-treated groups within the same strain; †significant differences between FGF(WT) versus FGF(Lo) either after saline or after Dox treatment.

Table 1. Echocardiography and Heart Weight/Body Weight parameters.

Echocardiography and Heart Weight/Body Weight (HW/BW) parameters from the FGF2(WT) and FGF2(Lo) groups at day 10 post-Doxorubicin (Dox)- or -saline administration, as indicated. Comparisons between groups were made using 2-way ANOVA (variables are strain and treatment). Data shown are means ±SD. LVESD=Left Ventricular End Systolic Diameter, PWT=Posterior Wall Thickness, HR= Heart Rate. *points at significant differences between Saline and Dox groups within the same strain, $^{\#}$points to differences between FGF(WT) versus FGF(Lo) either after saline-; or after Dox-treatment. Sections A, B, show values from male and female groups, respectively.

Figure 3, Elimination of endogenous Hi-FGF2 prevents the doxorubicin (Dox)-induced decrease in ejection fraction.

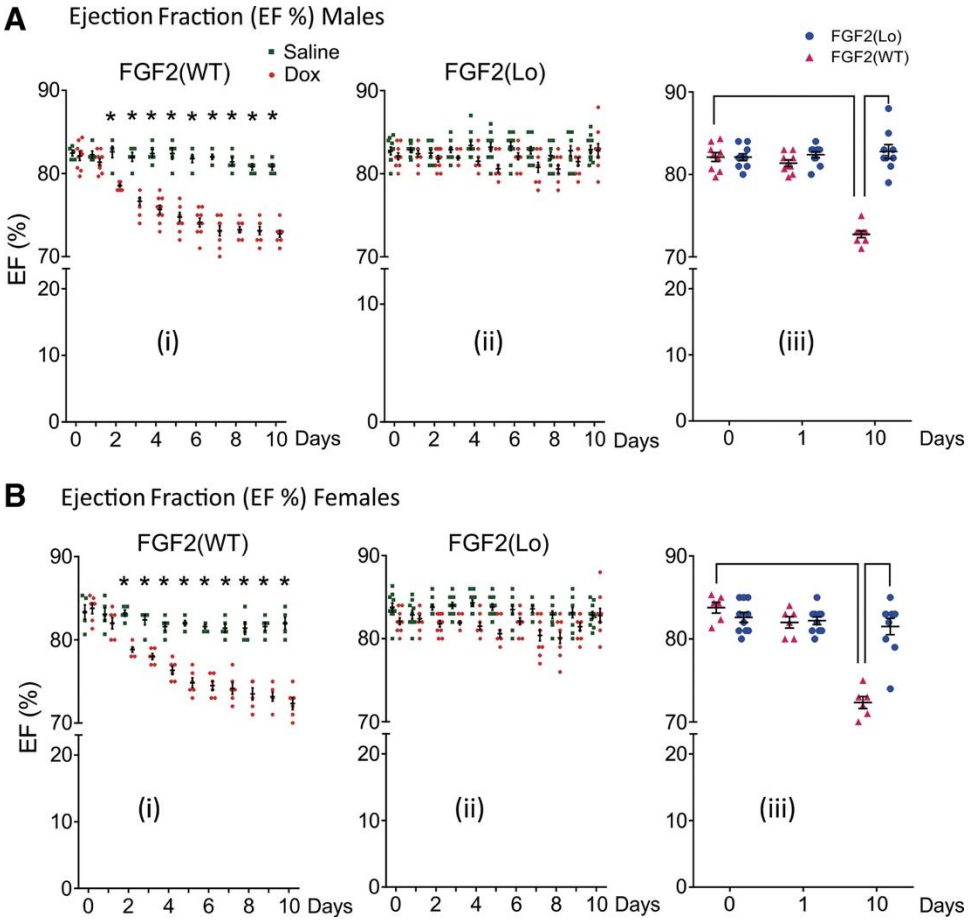

Figure 3. Sections A and B show Ejection Fraction (%EF) post-Dox injection, in male and female groups including wild type FGF2(WT) and Hi-FGF2-depleted FGF2(Lo) mice, as indicated. Panels (i) and (ii) show %EF at baseline and up to 10 days post-Dox in sham, saline-injected (green squares) versus Dox-injected (red circles) animals. Asterisks point to significant differences between the Dox-treated group and its corresponding sham group at the same time point ($p<0.05$). Panel (iii) shows EF of the FGF2(WT) mice, purple triangle, and the FGF2(Lo) mice, blue circle, groups before Dox (baseline), and at 1 day and 10 days post-Dox treatment. Brackets mark groups with statistically significant differences from each other. Sample sizes in (A) are n=9-10 for Dox- and n=10 for saline- treated groups for both FGF2(WT) and FGF2(Lo) mice; and in B, n=5 or 6 for the FGF2(WT) saline- and Dox- treated groups, respectively; n=10 for the FGF2(Lo) groups. Two-way ANOVA and Sidak *post hoc* tests were used to analyze the data.

Figure 4, Elimination of endogenous Hi-FGF2 prevents the doxorubicin (Dox)-induced increase in left ventricular end diastolic dimension (LVEDD).

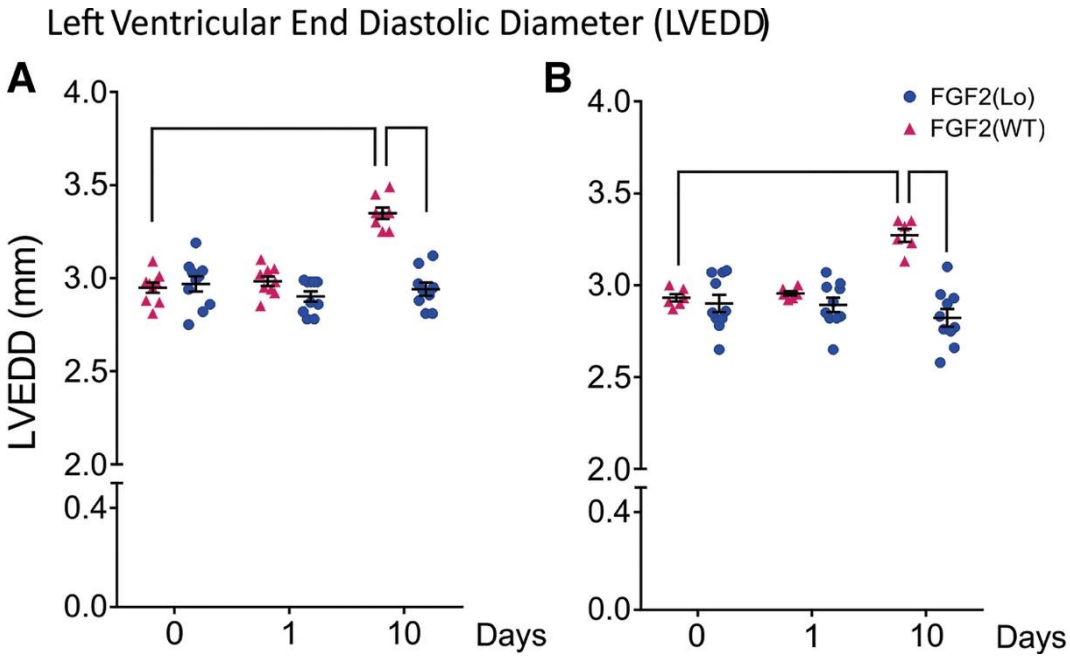

Figure 4. Panels A and B show LVEDD values at baseline, and at 1 and 10 days post-Dox in FGF2(WT) (purple triangles) and FGF2(Lo) (blue circles) in male and female mouse groups, respectively. Values for the FGF2(WT) mouse groups are compared to those of the FGF2(Lo) mouse group at each time point; comparisons were also made within each group, comparing values at baseline to those at 10 days post-Dox treatment. Significant differences between groups are marked by brackets, $p<0.05$. Sample sizes in (A) are n=10 for both FGF2(WT) and FGF2(Lo) mice at baseline and at 1 day post-Dox; n=9 for both groups at 10 days post Dox. In B, n=6 or 10 for the FGF2(WT) or the FGF2(lo) mouse groups, respectively. Two-way ANOVA and Sidak *post hoc* tests were used to analyze the data.

Figure 5, Relative Bnip3 protein levels post-Dox.

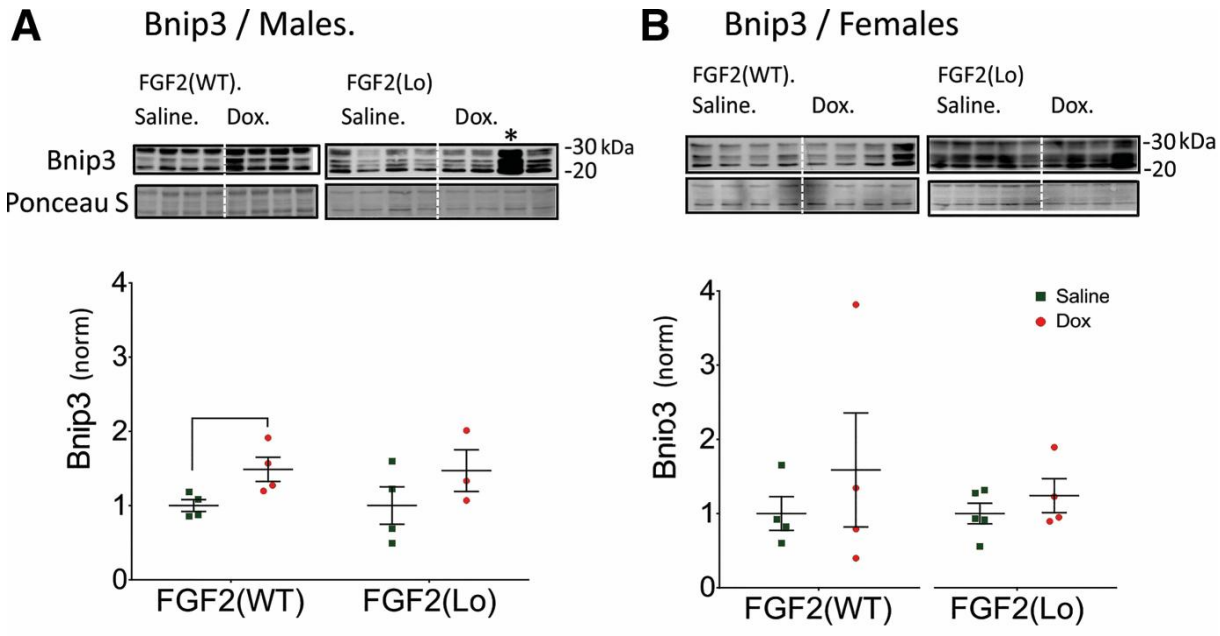

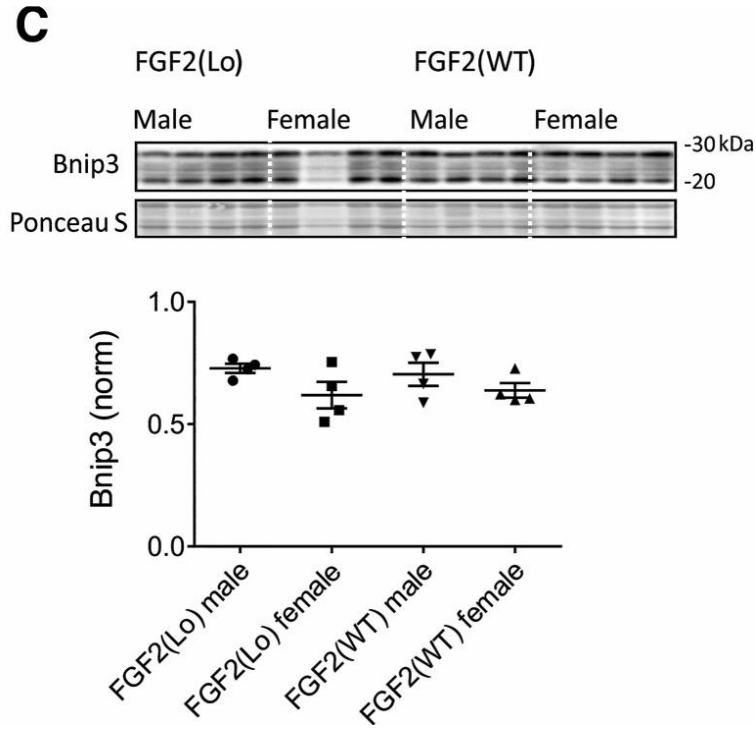

Figure 5. Protein immunoblot-based analyses of the anti-Bnip3 signal (21-30 kDa) in cardiac extracts from: panels (A) male and (B) female FGF2(WT) or FGF2(Lo) mouse groups, at 10 days after Dox- or saline- injection, as indicated; panel (C) shows relative Bnip3 signal at baseline for all groups, as indicated. In (A) the measurement from the lane marked with an asterisk was excluded because it was a significant outlier. Densitometry values from each saline-injected group were arbitrarily assigned a value of 1, and values from the Dox-injected groups were adjusted accordingly. Sample size n=4 for all groups except male FGF2(Lo) where n=3. Brackets denote significant differences between groups, at $P<0.05$, Student's t-test. Please note that for panels (A) and (B) four different protein immunoblots were used (and shown) to allow simultaneous analysis of the Bnip3 signal between the Dox- and its corresponding saline-treated group. As conditions of Bnip3 detection/exposure may differ slightly, these blots are not suitable for comparing signals between different blots. Panel (C) shows Bnip3 signal at baseline for all groups, all analyzed in the same 32-lane 'wide' gel: 20 μg protein/lane. Ponceau S staining was used to adjust for loading variations. No significant differences were found between the baseline groups when compared using one-way ANOVA.

Figure 6, Elimination of Hi-FGF2 from mouse embryonic fibroblasts (MEFs) protects r-cardiomyocytes (in co-culture) from doxorubicin (Dox)-induced injury and death.

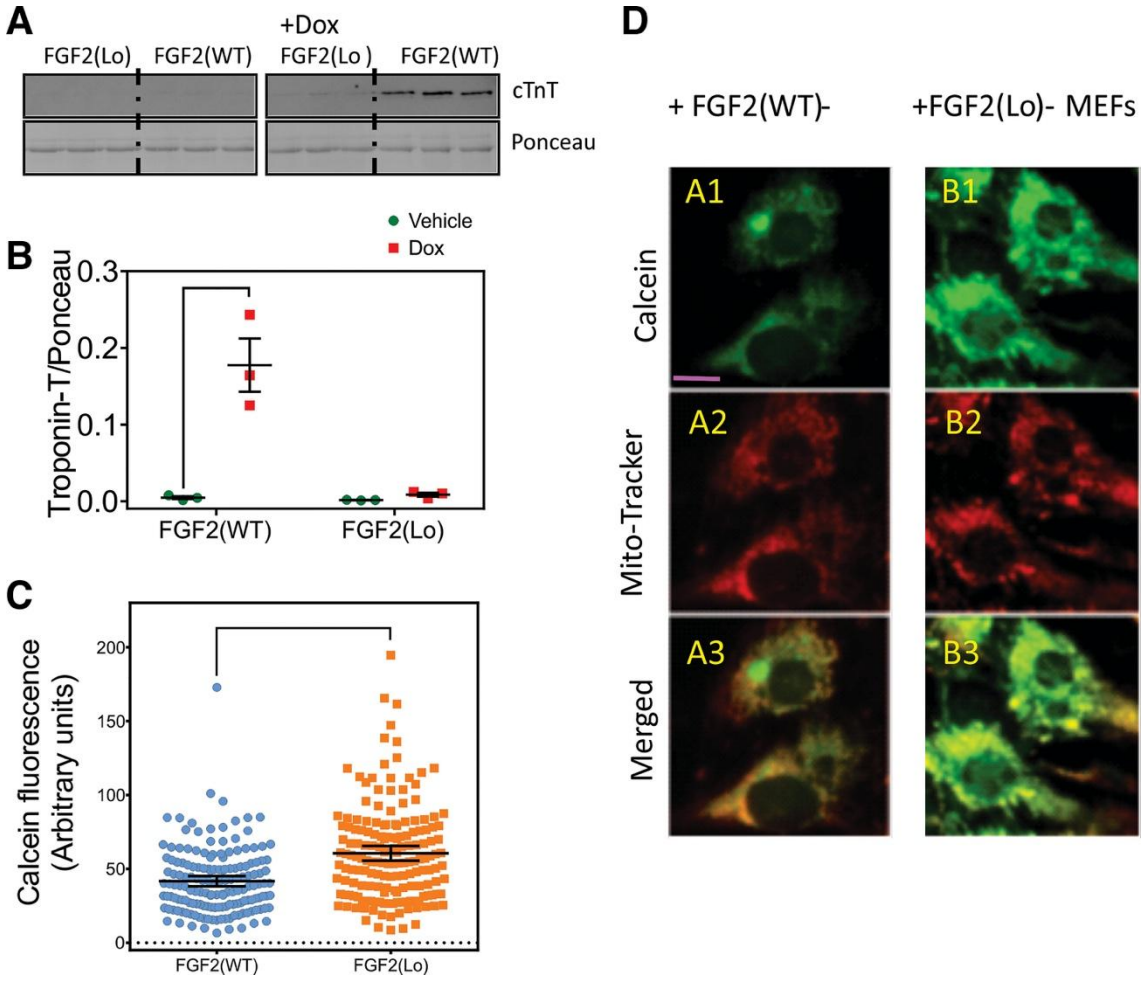

Figure 6. **Panel A** shows a protein immunoblot of supernatants obtained from r-cardiomyocyte-MEF co-cultures and probed for cTnT; Ponceau S staining of the same membrane is also shown. Myocytes were co-cultured with FGF2(WT) or FGF2(Lo) mouse-derived MEFs and exposed (red squares) or not (green circles) to Dox, as indicated. All lanes shown were obtained from the same gel and immunoblot. **Panel B** shows quantitation of the cTnT signal shown in Panel A, normalized for Ponceau staining. Brackets show significant differences ($P<0.05$) between groups, compared using Two-way ANOVA (Fisher's LSD *post hoc*), n=4. **Panel C** shows relative calcein fluorescence intensity of cells in co-cultures, stained using the Calcein-Cobalt assay to visualize mitochondrial permeability pore formation, seen as a loss of 'green' signal. Fluorescence was measured using Image J (n=160 in r-myocyte-MEF-FGF2(WT), orange circles), and n=168 in r-myocyte-MEF-FGF2(Lo) co-cultures (blue circles), as indicated. A Student's t-test was used to compare the groups, and brackets denote significant differences, $P<0.05$. **Panel D** shows representative fluorescence images of the co-culture groups, stained for calcein (green) and counterstained with Mito-tracker (Red), to visualize mitochondria. Images A1,2,3 show the same field from r-myocyte-MEF- FGF2(WT) mouse co-cultures stained for Calcein, Mitotracker, as well a merge of both stains. Images B1,2,3 show the same field from r-myocyte-MEF- FGF2(Lo) mouse co-cultures stained for Calcein, Mitotracker, as well a merge of both stains. Purple sizing bar in A1 corresponds to 20 μm.

Figure 7, Antibodies to human Hi-FGF2 (Hi-Ab) interact selectively with 21-24 Hi-FGF2.

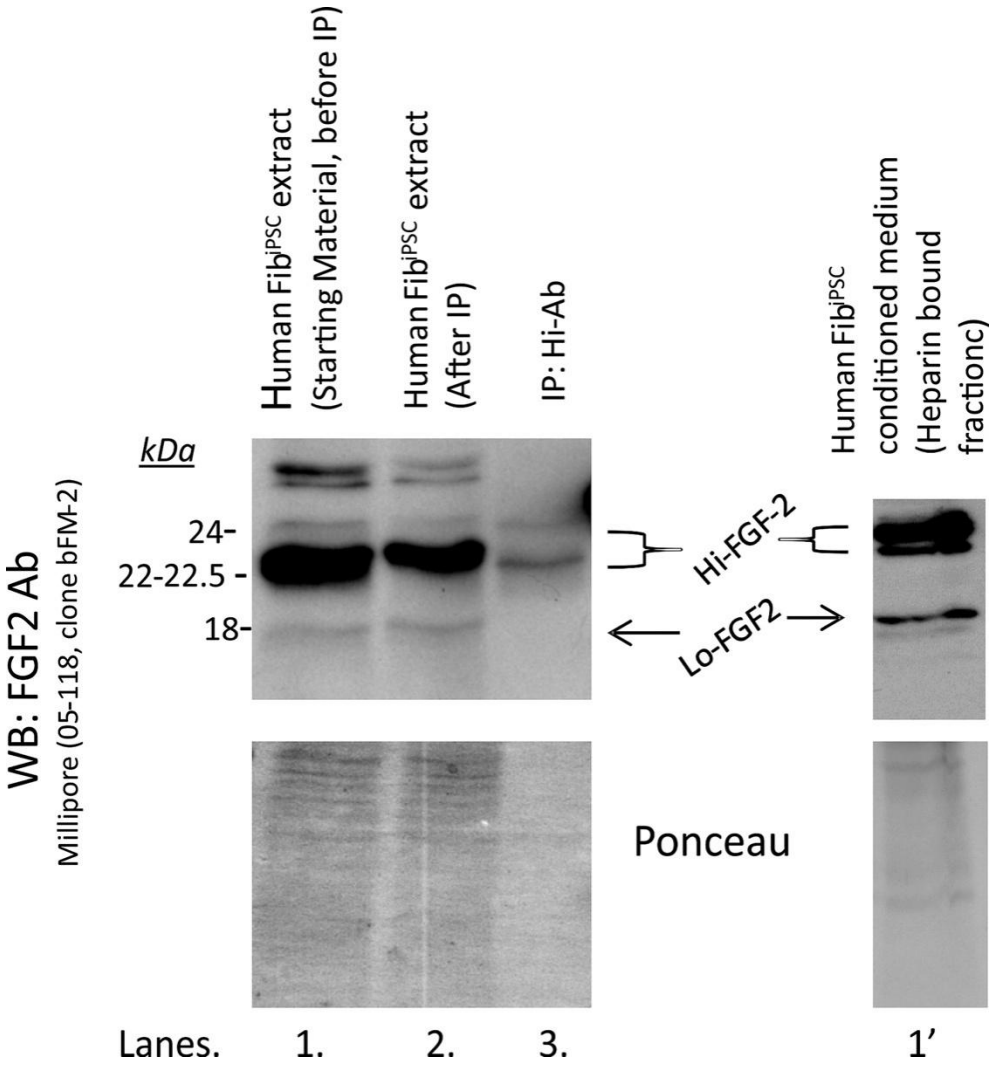

Figure 7. Immunoblot analysis of FGF2 isoforms present in h-Fib^{iPSC} cell extracts, before and after immunoprecipitation with Hi-Ab (rabbit polyclonal), using a mouse monoclonal antibody recognizing all FGF2 isoforms. Lane 1, extracts from h-Fib^{iPSC} are seen to contain Lo-FGF2 (18 kDa) and Hi-FGF2 (>20 kDa). Lane 2 contains anti-FGF2 immunoreactive proteins remaining in the extract after removal of the Hi-Ab immunoprecipitated material. Lane 3 contains material immunoprecipitated with Hi-Ab from a total of 150 μg protein extracted from human Fib^{iPSC} and presenting a signal for only 22-24 kDa Hi-FGF2. Lane 1' was obtained from a different immunoblot and shows the presence of Hi- and Lo-FGF2 as concentrated from 40 ml of h-Fib^{iPSC} -conditioned medium using heparin-sepharose beads. Ponceau Red staining of the corresponding immunoblots is included.

Figure 8, Neutralization of paracrine-acting human fibroblasts (FibIPSC)-produced Hi-FGF2 attenuates doxorubicin (Dox)-induced cardiomyocyte damage.

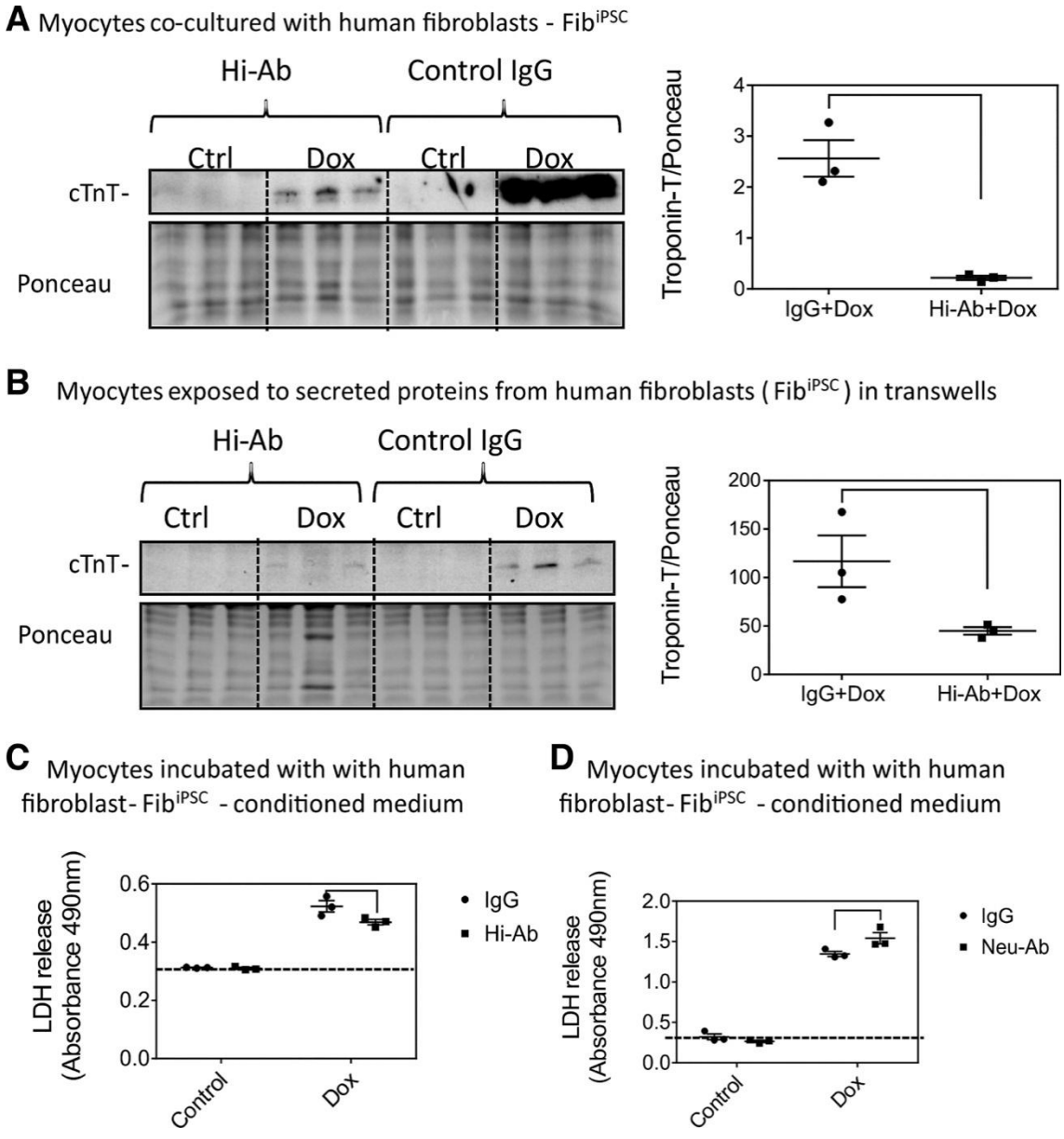

Figure 8. **Panel A** shows protein immunoblot detection and quantification of cTnT signal in the supernatant from co-cultures of cardiomyocytes with human Fib^{iPSC}, exposed or not to Dox, in the presence of control IgG or anti-Hi-FGF2 antibodies (Hi-Ab), as indicated. The corresponding Ponceau S staining is also shown. Cumulative data from densitometry of the two Dox-treated groups, normalized for Ponceau staining, are shown in the included graph. The bracket denotes statistically significant differences between the two groups, n=3. Two-tailed Student's t-test was used to analyze data, $P<0.05$. **Panel B** shows immunoblot detection and quantification of cTnT signal in the supernatant of cardiomyocytes exposed to secreted materials from human Fib^{iPSC} grown in inserts in a Transwell set-up. Corresponding Ponceau S staining is also shown Myocytes were insulted, or not, with Dox, in the presence of Hi-Ab, or control IgG, as indicated. Cumulative data from densitometry of the two Dox-treated groups, adjusted for Ponceau S staining, are shown in the included graph. The bracket denotes statistically significant differences between the two groups, n=3. Two-tailed Student's t-test was used to analyze data, $P<0.05$. **Panel C** shows LDH in the supernatant of cardiomyocytes exposed to human Fib^{iPSC} conditioned medium, in the presence of control IgG or Hi-Ab and treated or not with Dox, as indicated (n=3). Brackets show significant difference between the Dox-treated groups; Hi-Ab reduced Dox-induced damage. **Panel D** shows LDH in the supernatant of cardiomyocytes exposed to human Fib^{iPSC} conditioned medium, in the presence of control IgG or Neu-Ab (neutralizing both Hi- and Lo-FGF2) and treated or not with Dox, as indicated (n=3). Brackets show significant difference between the Dox-treated groups; Neu-Ab increases Dox-induced damage. Two-way ANOVA (Sidak *post hoc*) was used to analyze data in panels C and D.

Discussion

The focus of this study was to investigate the consequences of eliminating endogenous Hi-FGF2 but not Lo-FGF2 on cardiac resistance to a genotoxic insult, using an *in vivo* murine model of acute Dox-induced damage. Major novel findings presented here are: (1) exclusive endogenous Lo-FGF2 expression, either chronically *in vivo* or only by fibroblasts in short-term co-cultures, raised cardiac resistance to Dox-induced loss of cardiac function or cardiomyocyte injury, respectively; (2) the wild type FGF2 phenotype, which consists of expression of both Hi- and Lo-FGF2 isoforms in a 7:3 ratio in hearts *in vivo*, is more vulnerable to Dox-induced deleterious effects compared to the exclusive expression of Lo-FGF2; (3) in a wild type genetic background, blocking non-myocyte Hi-FGF2 but not Lo-FGF2 with a specific antibody protected cardiomyocytes from Dox-induced injury.

Endogenous Lo-FGF2 expression increases cardiac resistance to Dox. Our studies demonstrated that the FGF2(Lo) mice, male or female, were clearly protected from Dox-induced effects leading to heart failure such as declining systolic function; and increasing LVEDD which is indicative of maladaptive remodeling. Although the hearts of adult female animals are generally considered to be more resistant to injurious stimuli compared to males, no sex-related differences were identified regarding vulnerability to Dox and FGF2 isoform expression, at least within the 'acute' time frame of our studies and based on the parameters measured.

Dox is a known mitochondrial toxin forming mitochondrial permeability transition pores leading to apoptosis and necrosis (16, 31). There is evidence that Bnip3, which is localized to cardiac mitochondria via its transmembrane domain, is central in Dox-induced mitochondrial perturbation and eventual cell death (5). Several *in vivo* studies have reported that Dox upregulated cardiac Bnip3 in male mice. In agreement, in our male groups, Dox upregulated

Bnip3 protein only in the FGF2(WT), while no changes were seen in the FGF2(Lo) group. These findings suggested that Dox-induced cardiotoxicity may be mitigated in FGF2(Lo) mice by prevention of Bnip3 upregulation. Our recent *in vitro* studies support this notion: pre-exposure of cardiomyocytes to Lo-FGF2 prevented the Dox-induced upregulation of p53 as well as its downstream target Bnip3, by an mTOR/Nrf2/HO-1 dependent pathway (15).

As selective elimination of Hi-FGF2 isoforms in the FGF2(Lo) mice was protective, we suggest that the concomitant expression of Hi-FGF2 in excess of Lo-FGF2 in FGF2(WT) mice antagonizes or prevents protection by Lo-FGF2, by an as yet undetermined mechanism. Acute as well as sustained cardioprotection by extracellular-acting Lo-FGF2 is known to require FGF receptor 1 (FGFR1) (8) as well as the downstream activation of PKC-epsilon and protein kinase CK2 (9, 10). Extracellular-acting Hi-FGF2 is believed to activate plasma membrane FGFR1 and downstream pathways in a manner broadly similar to Lo-FGF2(13, 15). we speculate that Hi-FGF2/FGFR1-triggered signaling pathways may not be identical to those triggered by Lo-FGF2/FGFR1, especially in the long-term. Binding of FGF2 isoforms to FGFR1 could elicit different receptor conformations culminating in some differences in downstream signaling. It is of relevance that Hi-FGF2 but not Lo-FGF2 prevents cell migration, a property requiring its unique amino-terminal extension which differentiates it from Lo-FGF2; in addition, Levin and colleagues have shown that the amino-terminal domain of Hi-FGF2 depends on an interaction with the co-receptor neuropilin 1 in order to inhibit cell migration (30). Thus, we suggest that different outcomes by paracrine/autocrine acting FGF2 isoforms may be caused by interaction with isoform-selective co-receptors, in addition to the isoform-non-selective FGFR1. Hi-FGF2 which exists in excess of Lo-FGF2 *in vivo* would be expected to occupy most of the plasma membrane FGF2 ligand binding sites, thereby favoring Hi-FGF2-driven signal transduction

pathways, while reducing the contribution of Lo-FGF2/FGFR1-triggered signaling. Furthermore, FGF2 isoforms can become internalized and can also signal in an intracrine manner. We have shown that intracrine Hi-FGF2 can exert distinct, often deleterious effects, regardless of cell surface receptor occupancy; ectopic expression of Hi-FGF2 but not Lo-FGF2 caused myocyte binucleation (19), as well as mitochondrial damage, chromatin compaction, and myocyte cell death *in vitr*o, and these effects were reversed by the pro-survival member of the Bcl-family, Bcl-2 (17). It is of interest that the ERK pathway, which is equally activated downstream of FGFR1 by Hi- and Lo-FGF2 (4), and which is considered cytoprotective and cardioprotective, can also mediate pro-apoptotic effects of intracellular Hi-FGF2 (17).

FGF2 expressed by non-myocytes can determine cardiomyocyte susceptibility to Dox. Cardiac fibroblasts are a major cell population in the heart and, through their paracrine action, integrate various pathological stimuli to cause adaptive and maladaptive heart remodeling after various types of injury. Cardiac fibroblasts represent a major source of FGF2 produced in the heart (23, 24); previous studies have shown that lack of FGF2 expression in fibroblasts is responsible for the excessive dilatation in the hearts of mice depleted of all FGF2 after infarction or in response to angiotensin II (20). It was therefore reasonable to hypothesize that FGF2 expression by fibroblasts, in co-culture or fibroblast-conditioned medium experiments, could modulate the vulnerability of cardiomyocytes to a toxic agent, a hypothesis proven to be correct. We have previously shown that both Lo-FGF2 and Hi-FGF2 are secreted from normal rat or human fibroblasts and are present in conditioned media, in association with the extracellular matrix, as well as pericardial fluid (24). MEFs from FGF2(WT) and FGF2(Lo) mouse strains co-cultured with r-cardiomyocytes elicited distinct effects on cardiomyocyte vulnerability to Dox and, to some degree, recapitulated the *in vivo* phenotype as incubation with FGF2(Lo)-MEFs

was protective. More specifically, this protection was measured by reduced cTnT release and increased mitochondrial calcein fluorescence in the attached cells, indicative of mitochondrial functionality and cell viability. At the same time, incubation with FGF2(WT) MEFs allowed Dox-induced toxicity to manifest, in agreement with our *in vivo* findings.

In the wild type background, blocking secreted (human) Hi-FGF2 with a neutralizing antibody mitigates Dox toxicity on cardiac myocytes. We have provided evidence that 'native' expression of FGF2 isoforms *in vivo* and *in vitro* (by fibroblasts) renders cardiomyocytes more vulnerable to Dox, compared to sole expression of Lo-FGF2. Hence, we postulated that targeting Hi-FGF2 selectively by a neutralizing antibody could protect cardiomyocytes. A neutralizing antibody specific for human Hi-FGF2 (Hi-Ab) was indeed able to attenuate Dox-induced damage in r-cardiomyocytes in three different scenarios: (1) r-cardiomyocytes cultured with human fibroblasts plated on permeable Transwell membranes, (2) co-cultures of r-cardiomyocytes with human fibroblasts, or (3) application of conditioned media from human fibroblasts on r-cardiomyocyte monolayers. Importantly, in the last scenario, use of neutralizing antibodies for total FGF2 did not exert protection but rather an increase in vulnerability to Dox, presumably by blocking the action of Lo-FGF2, in addition to Hi-FGF2.

It was noted that when using conditioned medium from $Fibs^{iPSC}$, relative damage by Dox, as well as protection by Hi-Ab, appeared less pronounced than when $Fibs^{iPSC}$ are co-plated with myocytes. It is reasoned that in direct co-cultures the relative levels of paracrine human FGF2 (dominated by Hi-FGF2) are higher than those in conditioned medium alone, because they include not only FGF2 present in the soluble phase (conditioned medium) but also cell-released human FGF2 that is sequestered by the extracellular matrix. Our previous studies have demonstrated that human fibroblast-secreted FGF2 is detected in both conditioned medium and

also amongst proteins bound to the cell surface/extracellular matrix (24). Higher relative levels of paracrine Hi-FGF2 (in solution and in association with the matrix) would be expected to be more deleterious to Dox-treated myocytes, and at the same time allow a larger range against which to measure protection by Hi-Ab. Variations in culture medium volume may also contribute to dilution of signal for Dox-induced cTnT release in the Transwell set-up. Regardless however of the magnitude of damage and protection, all *in vitro* experiments show qualitatively similar results namely that paracrine-acting FGF2 produced by fibroblasts influences r-cardiomyocyte vulnerability to Dox and that, in a wild type environment, neutralization of paracrine Hi-FGF2 raises cardiomyocyte resistance to Dox, likely by allowing unopposed action of Lo-FGF2.

Conclusion. We have documented that exclusive expression of Lo-FGF2 *in vivo* at endogenous levels is cardioprotective, preventing Dox-induced cardiac deterioration. Our *in vitro* studies support the *in vivo* observations and produced the novel and important finding that cardiomyocyte protection from Dox can be promoted via selectively neutralizing Hi-FGF2 in a wild type paracrine environment. Antibody-based approaches are widely used in humans to neutralize the activity of ligands or receptors via systemic administration. Thus, an antibody-based approach to target paracrine Hi-FGF2 in the extracellular matrix *in vivo* would be expected to confer cardioprotection against genotoxic damage as well as other injurious stimuli.

Limitations. The genetically engineered mouse model used here does not allow for cell-specific or time-specific events to be separated; the FGF2(Lo) mouse model may have adaptations favoring survival and these adaptations could influence the response to Dox. Regardless, our findings using relatively short-term wild type myocyte cultures and co-cultures with mouse and human fibroblasts support our findings from the *in vivo* studies. In the future, it would be

important to apply cardiac fibroblast-restricted and conditional FGF2 isoform silencing, to understand their function with precision. Longer term studies in chronic cardiac drug toxicity or disease models would also be required to fully appreciate the potential of anti-Hi-FGF2 therapies in a clinically applicable setting.

Funding

This work was funded (EK, PAC, DSJ) by the Canadian Institutes of Health Research (FRN-74733). NK is the recipient of the Bank of Montreal and Alfred E. Deacon studentships.

Disclosures

EK and NK obtained a provisional patent for the design and application of neutralizing antibodies or other Hi-FGF2 targeting approaches against Hi-FGF-2 for prevention of Dox induced cardiotoxicity.

References:

1. Azhar M, Yin M, Zhou M, Li H, Mustafa M, Nusayr E, Keenan JB, Chen H, Pawlosky S, Gard C, Grisham C, Sanford LP, and Doetschman T. Gene targeted ablation of high molecular weight fibroblast growth factor-2. Developmental dynamics : an official publication of the American Association of Anatomists 238: 351-357, 2009.

2. Bordun KA, Premecz S, daSilva M, Mandal S, Goyal V, Glavinovic T, Cheung M, Cheung D, White CW, Chaudhary R, Freed DH, Villarraga HR, Herrmann J, Kohli M, Ravandi A, Thliveris J, Pitz M, Singal PK, Mulvagh S, and Jassal DS. The utility of cardiac biomarkers and echocardiography for the early detection of bevacizumab- and sunitinib-mediated cardiotoxicity. American journal of physiology Heart and circulatory physiology 309: H692-701, 2015.

3. Chen HF, Chuang CY, Shieh YK, Chang HW, Ho HN, and Kuo HC. Novel autogenic feeders derived from human embryonic stem cells (hESCs) support an undifferentiated status of hESCs in xeno-free culture conditions. Human reproduction (Oxford, England) 24: 1114-1125, 2009.

4. Cheng Y, Li Z, Kardami E, and Loh YP. Neuroprotective effects of LMW and HMW FGF2 against amyloid beta toxicity in primary cultured hippocampal neurons. Neuroscience letters 632: 109-113, 2016.

5. Dhingra R, Margulets V, Chowdhury SR, Thliveris J, Jassal D, Fernyhough P, Dorn GW, 2nd, and Kirshenbaum LA. Bnip3 mediates doxorubicin-induced cardiac myocyte necrosis and mortality through changes in mitochondrial signaling. Proceedings of the National Academy of Sciences of the United States of America 111: E5537-5544, 2014.

6. Feridooni T, Hotchkiss A, Remley-Carr S, Saga Y, and Pasumarthi KB. Cardiomyocyte specific ablation of p53 is not sufficient to block doxorubicin induced cardiac fibrosis and associated cytoskeletal changes. PloS one 6: e22801, 2011.

7. Florkiewicz RZ, and Sommer A. Human basic fibroblast growth factor gene encodes four polypeptides: three initiate translation from non-AUG codons. Proceedings of the National Academy of Sciences of the United States of America 86: 3978-3981, 1989.

8. Jiang ZS, Padua RR, Ju H, Doble BW, Jin Y, Hao J, Cattini PA, Dixon IM, and Kardami E. Acute protection of ischemic heart by FGF-2: involvement of FGF-2 receptors and protein kinase C. American journal of physiology Heart and circulatory physiology 282: H1071-1080, 2002.

9. Jiang ZS, Srisakuldee W, Soulet F, Bouche G, and Kardami E. Non-angiogenic FGF-2 protects the ischemic heart from injury, in the presence or absence of reperfusion. Cardiovascular research 62: 154-166, 2004.

10. Jiang ZS, Wen GB, Tang ZH, Srisakuldee W, Fandrich RR, and Kardami E. High molecular weight FGF-2 promotes postconditioning-like cardioprotection linked to activation of protein kinase C isoforms, as well as Akt and p70 S6 kinases. [corrected]. Canadian journal of physiology and pharmacology 87: 798-804, 2009.

11. Jimenez SK, Jassal DS, Kardami E, and Cattini PA. A single bout of exercise promotes sustained left ventricular function improvement after isoproterenol-induced injury in mice. The journal of physiological sciences : JPS 61: 331-336, 2011.

12. Kardami E, Detillieux K, Ma X, Jiang Z, Santiago JJ, Jimenez SK, and Cattini PA. Fibroblast growth factor-2 and cardioprotection. Heart failure reviews 12: 267-277, 2007.

13. Kole D, Grella A, Dolivo D, Shumaker L, Hermans W, and Dominko T. High molecular weight FGF2 isoforms demonstrate canonical receptor-mediated activity and support human embryonic stem cell self-renewal. Stem cell research 21: 106-116, 2017.

14. Koleini N, and Kardami E. Autophagy and mitophagy in the context of doxorubicin-induced cardiotoxicity. Oncotarget 8: 46663-46680, 2017.

15. Koleini N, Nickel BE, Wang J, Roveimiab Z, Fandrich RR, Kirshenbaum LA, Cattini PA, and Kardami E. Fibroblast growth factor-2-mediated protection of cardiomyocytes from the toxic effects of doxorubicin requires the mTOR/Nrf-2/HO-1 pathway. Oncotarget 8: 87415-87430, 2017.

16. Lebrecht D, Setzer B, Ketelsen UP, Haberstroh J, and Walker UA. Time-dependent and tissue-specific accumulation of mtDNA and respiratory chain defects in chronic doxorubicin cardiomyopathy. Circulation 108: 2423-2429, 2003.

17. Ma X, Dang X, Claus P, Hirst C, Fandrich RR, Jin Y, Grothe C, Kirshenbaum LA, Cattini PA, and Kardami E. Chromatin compaction and cell death by high molecular weight FGF-2 depend on its nuclear localization, intracrine ERK activation, and engagement of mitochondria. Journal of cellular physiology 213: 690-698, 2007.

18. Mesaeli N, and Phillipson C. Impaired p53 expression, function, and nuclear localization in calreticulin-deficient cells. Mol Biol Cell 15: 1862-1870, 2004.

19. Pasumarthi KB, Kardami E, and Cattini PA. High and low molecular weight fibroblast growth factor-2 increase proliferation of neonatal rat cardiac myocytes but have differential effects on binucleation and nuclear morphology. Evidence for both paracrine and intracrine actions of fibroblast growth factor-2. Circulation research 78: 126-136, 1996.

20. Pellieux C, Foletti A, Peduto G, Aubert JF, Nussberger J, Beermann F, Brunner HR, and Pedrazzini T. Dilated cardiomyopathy and impaired cardiac hypertrophic response to angiotensin II in mice lacking FGF-2. J Clin Invest 108: 1843-1851, 2001.

21. Piotrowicz RS, Maher PA, and Levin EG. Dual activities of 22-24 kDA basic fibroblast growth factor: inhibition of migration and stimulation of proliferation. J Cell Physiol 178: 144-153, 1999.

22. Ray R, Chen G, Vande Velde C, Cizeau J, Park JH, Reed JC, Gietz RD, and Greenberg AH. BNIP3 heterodimerizes with Bcl-2/Bcl-X(L) and induces cell death independent of a Bcl-2 homology 3 (BH3) domain at both mitochondrial and nonmitochondrial sites. The Journal of biological chemistry 275: 1439-1448, 2000.

23. Santiago JJ, Ma X, McNaughton LJ, Nickel BE, Bestvater BP, Yu L, Fandrich RR, Netticadan T, and Kardami E. Preferential accumulation and export of high molecular weight FGF-2 by rat cardiac non-myocytes. Cardiovasc Res 89: 139-147, 2011.

24. Santiago JJ, McNaughton LJ, Koleini N, Ma X, Bestvater B, Nickel BE, Fandrich RR, Wigle JT, Freed DH, Arora RC, and Kardami E. High molecular weight fibroblast growth factor-2 in the human heart is a potential target for prevention of cardiac remodeling. PloS one 9: e97281, 2014.

25. Sequiera GL, Saravanan S, and Dhingra S. Human-Induced Pluripotent Stem Cell-Derived Mesenchymal Stem Cells as an Individual-Specific and Renewable Source of Adult Stem Cells. Methods in molecular biology (Clifton, NJ) 1553: 183-190, 2017.

26. Srisakuldee W, Jeyaraman MM, Nickel BE, Tanguy S, Jiang ZS, and Kardami E. Phosphorylation of connexin-43 at serine 262 promotes a cardiac injury-resistant state. Cardiovascular research 83: 672-681, 2009.

27. Vengellur A, and LaPres JJ. The role of hypoxia inducible factor 1alpha in cobalt chloride induced cell death in mouse embryonic fibroblasts. Toxicological sciences : an official journal of the Society of Toxicology 82: 638-646, 2004.

28. Wang J, Nachtigal MW, Kardami E, and Cattini PA. FGF-2 protects cardiomyocytes from doxorubicin damage via protein kinase C-dependent effects on efflux transporters. Cardiovascular research 98: 56-63, 2013.

29. Zhang J, Ye J, Altafaj A, Cardona M, Bahi N, Llovera M, Canas X, Cook SA, Comella JX, and Sanchis D. EndoG links Bnip3-induced mitochondrial damage and caspase-independent DNA fragmentation in ischemic cardiomyocytes. PloS one 6: e17998, 2011.

30. Zhang L, Parry GC, and Levin EG. Inhibition of tumor cell migration by LD22-4, an N-terminal fragment of 24-kDa FGF2, is mediated by Neuropilin 1. Cancer research 73: 3316-3325, 2013.

31. Zhang S, Liu X, Bawa-Khalfe T, Lu LS, Lyu YL, Liu LF, and Yeh ET. Identification of the molecular basis of doxorubicin-induced cardiotoxicity. Nature medicine 18: 1639-1642, 2012.

Section 2. Fibroblast growth factor-2- mediated protection of cardiomyocytes from the toxic effects of doxorubicin requires the mTOR/Nrf-2/HO-1 pathway

Published in: Oncotarget. 2017 Aug 24;8(50):87415-87430. doi: 10.18632/oncotarget.20558.

The full-text can be found in:

http://www.oncotarget.com/index.php?journal=oncotarget&page=article&op=view&path%5B%5D=20558&path%5B%5D=65528

Navid Koleini[1, 2], Barbara E. Nickel[1], Jie Wang[2], Zeinab Roveimiab[1], Robert R. Fandrich[1, 3], Lorrie A Kirshenbaum[1,2], Peter A. Cattini[2], Elissavet Kardami[1, 2, 3]

1: Institute of Cardiovascular Sciences, Albrechtsen Research Centre, Winnipeg, Manitoba

2: Department of Physiology and Pathophysiology, University of Manitoba

3: Department of Human Anatomy and Cell Sciences, University of Manitoba

Contact information of the corresponding author:

Dr. Elissavet Kardami

Institute of Cardiovascular Sciences , St.Boniface hospital Albretsen research center, University of Manitoba

R3008, 351 Tache Ave, Winnipeg, MB, R2H 2A6

Email: ekardami@sbrc.ca, Tell: +1 (204) 235 3411, Fax: +1 (204) 233 6723

Key words: Fibroblast Growth Factor 2 isoforms, Doxorubicin cardiotoxicity, Heme oxygenase 1 cardioprotection, Nrf-2 activation, mTOR signaling

Abstract:

Background. Cardiotoxic side effects impose limits to the use of anti-tumour chemotherapeutic drugs such as doxorubicin (Dox). There is a need for cardioprotective strategies to prevent the multiple deleterious effects of Dox. Here, we examined the ability of administered fibroblast growth factor-2 (FGF-2), a cardioprotective protein that is synthesized as high and low molecular weight (Hi-, Lo-FGF-2) isoforms, to prevent Dox-induced: oxidative stress; cell death; lysosome dysregulation; and inactivation of potent endogenous protective pathways, such as the anti-oxidant/detoxification nuclear factor erythroid-2-related factor (Nrf-2), heme oxygenase-1 (HO-1) axis.

Methods and Results. Brief pre-incubation of neonatal rat cardiomyocyte cultures with either Hi- or Lo-FGF-2 reduced the Dox-induced: oxidative stress; apoptotic/necrotic cell death; lysosomal dysregulation; decrease in active mammalian target of Rapamycin (mTOR). FGF-2 isoforms prevented the Dox-induced downregulation of Nrf-2 and promoted robust increases in the Nrf-2-downstream targets including the cardioprotective protein HO-1, and p62/SQSTM1, a multifunctional scaffold protein involved in autophagy. Chloroquine, an autophagic flux inhibitor, caused a further increase in p62/SQSTM1, indicating intact autophagic flux in the FGF-2-treated groups. A selective inhibitor for HO-1, Tin-Protoporphyrin, prevented the FGF-2 protection against cell death. The mTOR inhibitor Rapamycin prevented FGF-2 protection and blocked the FGF-2 effects on Nrf-2, HO-1 and p62/SQSTM1.

Conclusions. In an acute setting**,** Hi- or Lo-FGF-2 protect cardiomyocytes against multiple Dox-induced deleterious effects, by a mechanism dependent on preservation of mTOR activity, Nrf-2 levels, and the upregulation of HO-1. Preservation/activation of endogenous anti-oxidant/detoxification defences by FGF-2 is a desirable property in the setting of Dox-cardiotoxicity.

Introduction:

Doxorubicin (Dox) is a potent chemotherapeutic drug used against many types of cancers, but is associated with numerous side effects, including an increased risk for acute and chronic cardiotoxicity leading to cardiomyopathy and heart failure [1]. Dox toxicity has been studied extensively, and multiple mechanisms are implicated including: excessive production of reactive oxygen and nitrogen species, interference with iron metabolism, mitochondrial damage, intercalation with nuclear DNA and binding to Topoisomerase II (Top-II), activation of pro-cell death pathways involving increased expression of p53 and BCL2/adenovirus E1B 19 kDa protein-interacting protein 3 (Bnip-3). In addition, dysregulation of autophagy, mitophagy and lysosomal biogenesis all contribute to Dox toxicity, causing dysfunction and loss of cardiomyocytes [1-3]. While various types of anti-oxidant therapies have been effective in preventing or attenuating Dox-cardiotoxicity in animal models, clinical trials have not provided conclusive evidence [4]. Dox-induced heart disease may be managed by using drugs such as dexrazoxane, which is believed to act by chelating iron and/or by preventing Dox-Top-II interaction, and by drugs traditionally used in the treatment for heart failure [1, 5]. There is a need for additional strategies aimed at prevention or treatment of Dox-cardiotoxicity. Endogenously expressed cardioprotective factors, such as fibroblast growth factor-2 (FGF-2), as well as endogenous cytoprotective pathways merit consideration in this context.

FGF-2 is a multifunctional protein which is expressed as high (>20 kDa, Hi-FGF-2) and low molecular weight (18 kDa, Lo-FGF-2) isoforms, products, respectively, of leucine (CUG)- or methionine (AUG)-initiated translation of the same messenger (m) RNA [6]. Hi-FGF-2 is the predominant isoform found in the human, rat and mouse heart, and like Lo-FGF-2 is detected in the intracellular as well as extracellular environment [7, 8]. Lo-FGF-2 is well documented to be

cardioprotective, preventing myocardial loss and contractile dysfunction during myocardial infarction and in ischemia-reperfusion scenarios [9, 10]. Lo-FGF-2 was also shown to protect neonatal rat cardiomyocytes from Dox-induced cell death *in vitro* [11]. A non-mitogenic mutant Lo-FGF-2 has also been shown to protect isolated mouse hearts against acute Dox-induced decrease in contractility [12]. Less is known regarding the role of the Hi-FGF-2 isoform in the heart. Extracellular-acting, cell-released Hi-FGF-2 induces cardiomyocyte hypertrophy and may contribute to maladaptive chronic remodeling [7, 8]. Overexpression of Hi-, but not Lo-, FGF-2 promoted apoptosis in cardiomyocytes via an intracrine pathway [13]. There is, however, no information on the effect of exogenously administered Hi-FGF-2, compared to Lo-FGF-2, on Dox-induced cardiomyocyte damage and cell death.

Here we present evidence that Hi- or Lo- FGF-2 are equally protective against multiple aspects of acute Dox-induced toxicity in neonatal rat cardiomyocytes *in vitro*. Furthermore, the FGF-2 isoform-induced protection requires activation of endogenous cytoprotective antioxidant pathways such as the Nrf-2/HO-1axis.

Results

(i). Effect of FGF-2 isoforms on Dox-induced cardiomyocyte toxicity *in vitro*. Dox is known to induce apoptotic and necrotic death in cardiomyocytes in *in vitro* models, and *in vivo*. To recapitulate the effects of Dox in vitro, cardiomyocytes were exposed to 0.5 μM Dox, as used in our previous study [11].

Pre-incubation with recombinant Lo- or Hi-FGF-2 (10 ng/ml) for 30 minutes protected cardiomyocytes from Dox toxicity by a number of measures, assessed at 24 hours post-Dox (Fig. 9). Pilot dose-response studies indicated that both FGF-2 isoforms displayed the same level of protection in the 1-100 ng/ml range, so we used the 10 ng/ml concentration for all further experiments. Based on the Live-Dead assay (Fig. 9, A-B), Dox caused a significant, over 3-fold, increase in the percentage of dead cells when compared to control cultures. This effect was prevented by either Lo- or Hi-FGF-2 pre-treatment. Relative levels of LDH in the culture medium were measured, as an indicator of disruption of cardiomyocyte plasma membrane integrity. Released LDH was increased by Dox treatment, while pre-treatment with either FGF-2 isoform attenuated this increase (Fig. 9C). Also, FGF-2 isoform pre-treatment abolished the Dox-induced upregulation in active (17 kDa) caspase-3, the tumour suppressor p53, and Bnip-3 protein levels (Fig. 9, D-G), consistent with prevention of Dox-induced apoptotic and necrotic cell death. Bnip-3 immunoreactive bands migrated at 20-30 kDa, likely representing different degrees of post-translational modifications, similar to previous reports [14]; all anti-Bnip3 bands were included in our calculations. Dox caused formation of mitochondrial permeability transition pores (mPTP), as observed by the Calcein-Cobalt mPTP assay, and both FGF-2 isoforms prevented mPTP formation. Representative images are shown in Appendix 1. In addition, both FGF-2 isoforms were able to limit the Dox-induced decrease in ATP, and increase in ADP levels

(Fig.9, H), consistent with protective effects at the mitochondrial level. Lysates from attached cells were used for western blot-based determinations of Dox toxicities (p53, caspase 3, Bnip-3 upregulation) and the effect of both FGF-2 isoforms. We have not included detached cells which were occasionally observed in the Dox-treated samples only. As a consequence, measurements of Dox toxicities by western blotting may be an underestimate of the magnitude of damage to the whole cell population; however, this does not change the central observation that the FGF-2 isoforms are protective.

Dox at 0.5 μM was also found to be toxic for MCF-7 cells (a human breast cancer cell-line), as measured by Calcein-AM assay. However, unlike primary cardiomyocytes, the MCF-7 cells were not protected against Dox toxicity by either FGF-2 isoforms under the conditions tested (Appendix 2).

Overall, these observations show that both Hi- and Lo- FGF-2 can exert acute cardiomyocyte protection from Dox-induced cell death with apoptotic and necrotic features.

(ii) Effect of FGF-2 on cardiomyocyte antioxidant/detoxification responses (Nrf-2 and downstream targets). As anticipated, Dox increased levels of reactive oxygen species (ROS) in cardiomyocytes as measured by fluorescence intensity of DCF-DA (Fig. 10A). This effect was attenuated by either Hi- or Lo-FGF-2 (Fig. 10A). The transcription factor Nrf-2 is a master regulator of the endogenous antioxidant response [15]. Dox caused a reduction in the RNA and protein levels of Nrf-2; either FGF-2 isoform not only prevented this Dox-induced reduction, but also resulted in a 2-fold increase in Nrf-2 transcripts compared to controls in the presence of Dox (Fig. 10, C). The Dox-induced decrease in total Nrf-2 protein was prevented by either FGF-2 isoform. Relative levels of Nrf-2 protein in the presence of Hi-FGF-2 (but not Lo-

FGF-2) in the Dox-treated groups were significantly higher than those of the control group; this represents the only difference between Hi- and Lo- FGF-2 activities in the present study. Please note that data shown for Nrf-2 protein represent measurements from the 100 kDa immunoreactive band, corresponding to the previously published electrophoretic migration for Nrf-2 [16]. An immunoreactive, faster migrating band was also present and may represent a truncated or modified Nrf-2. The faster band displayed the same pattern of response as the 100 kDa band but was not included in our measurements.

Nrf-2 binds to the antioxidant response element in the promoter region of numerous target genes, including HO-1 and p62/SQSTM1. In the presence of Dox both FGF-2 isoforms significantly increased mRNA and protein levels for HO-1 relative to control cells (Fig. 10, B, C). Dox alone had no significant effect on HO-1 protein levels. In the absence of Dox the FGF-2 isoforms had no effect on relative Nrf-2 and HO-1 protein levels (Appendix 3). HO-1 is a 32 kDa protein; the antibodies to HO-1detected faint immunoreactive bands at 32-34 kDa in control samples, and a 32 kDa band in the Dox/FGF-2 - exposed samples. It is possible that the 34 kDa band represents a modified HO-1. Both immunoreactive bands were included in our densitometric measurements.

The FGF-2 isoforms elicited significant increases in p62/SQSTM1 mRNA and protein over controls, in the presence of Dox (Fig. 11, A-C). The p62/SQSTM1 is an autophagy adaptor that binds ubiquitinated items destined to be eliminated by autophagy and mitophagy [17], and represents another target of Nrf-2[18]. Increased accumulation of p62/SQSTM1 is often interpreted as defective/blocked autophagic flux [19]. To determine if autophagic flux was blocked we examined the effect of a lysosomal/autophagy flux inhibitor, Chloroquine (CQ) on p62/SQSTM1 accumulation in the FGF-2/Dox groups. As shown in Fig.11, A-B, CQ caused

additional accumulation of p62/SQSTM1 in control and FGF-2/Dox-treated groups, indicative of functional autophagic flux in these groups. CQ had no effect on p62/SQSTM1 accumulation in the presence of Dox, consistent with reports of impaired flux in this group [2, 20].

Figure 9, FGF2 isoforms prevent doxorubicin-induced toxicity in cardiomyocytes.

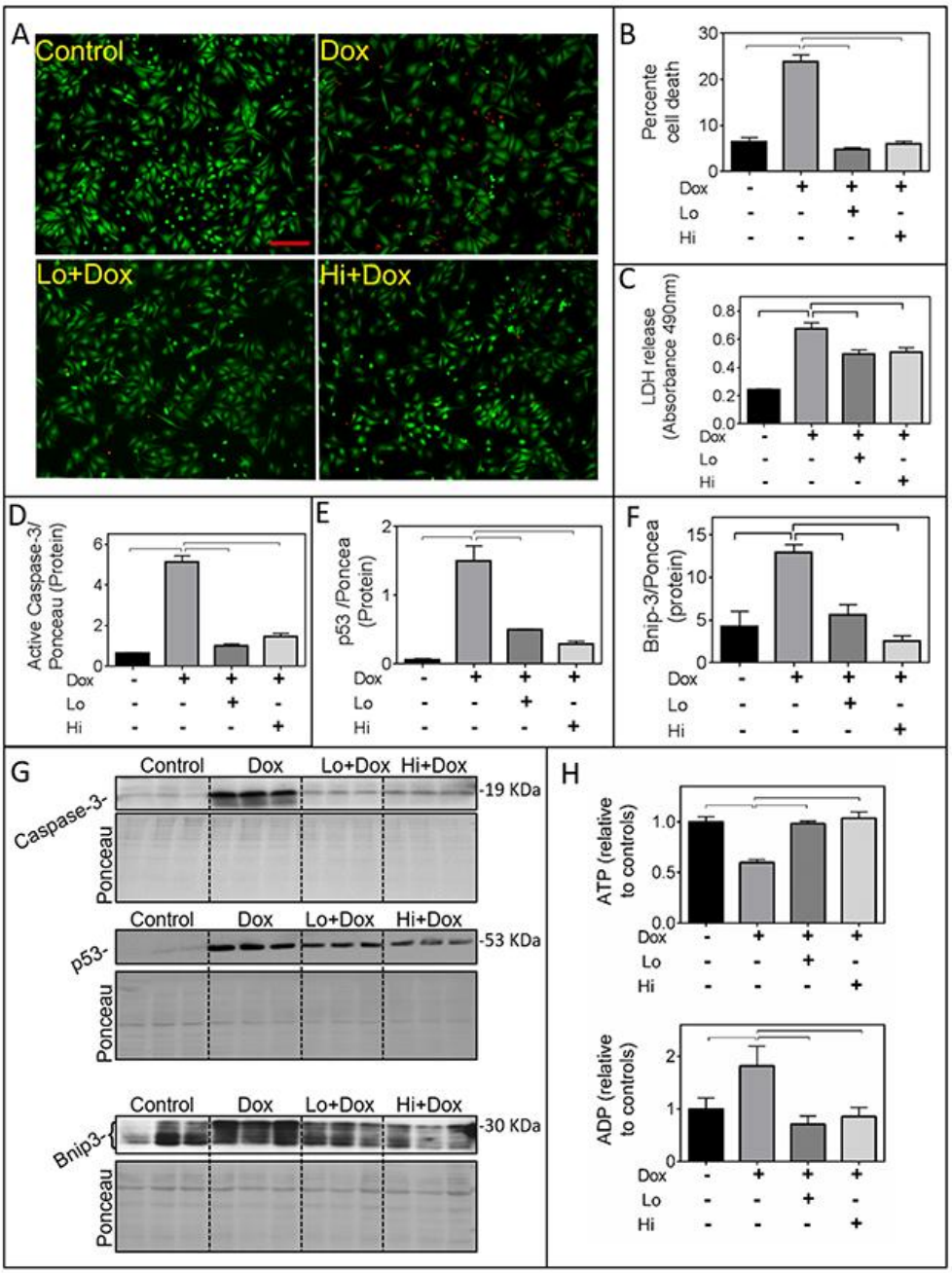

Figure 9. **Panels A-H** show the effects of Doxorubicin (Dox) exposure for 24 hours in the presence and absence of Lo- or Hi-FGF-2 pre-incubation, as indicated. **(A)** and **(B)** show, respectively, representative images of myocytes stained with the Live-Dead assay: Calcein-AM (green, live cells) / Ethidium homodimer (red, dead cells), and the corresponding graph with the percentage of cell death in attached cells. **(C)**, LDH released in culture medium, assessed by absorbance at 490 nm (n=6). **(D), (E), (F),** show, respectively, relative protein levels of cleaved (active) caspase-3 (19 kDa), p53 (53 kDa), and Bnip-3 (~30 kDa). Data for the graphs were obtained from the corresponding western blots shown in panel **(G);** images of the same membranes stained for Ponceau S are also included, and served to adjust for minor variations in protein loading. **(H),** ATP and ADP levels relative to controls, as indicated (n=6). Data is plotted as mean ± SEM and statistically significant differences are shown by brackets between groups; a $P<0.05$ was considered significant.

Impaired autophagic flux can be due to defects in lysosomal biogenesis and/or function [2]. To further document an effect of Dox on lysosomes, relative levels of the mRNA for the transcription factor-EB (TFEB, a master transcription factor for lysosomal biogenesis) and of the lysosomal protein LAMP1 were assessed. Dox significantly reduced relative levels of TFEB mRNA and LAMP1 protein, and these effects were prevented by FGF-2 isoforms (Fig. 12, A & B).

(iii) The role of mTOR and HO-1 in the FGF-2-induced protection from Dox.

Exposure of cardiomyocytes to Dox resulted in a significant decrease in the active (p-Ser2448)-mTORC1/total mTORC1 ratio, an effect that was limited by either Lo- or Hi-FGF-2 pre-treatments (Fig.13, A and appendix 4, A). A selective inhibitor for mTORC1, Rapamycin, was used to examine whether mTOR activity mediated the protective effects of Hi- and/or Lo-FGF-2. Cells were treated with Rapamycin for 30 min prior to stimulation by FGF-2 for an additional 30 min, and then exposed to Dox for 24 hours. Rapamycin alone had no effect on cell survival in the absence or presence of Dox, but abrogated both Hi- and Lo-FGF-2 induced protection, as measured by the Calcein-AM viability assay (Fig. 13, B). Rapamycin prevented the FGF-2-induced restoration of relative Nrf-2 protein levels (Fig. 13, C and E). In addition, Rapamycin prevented the robust upregulation of HO-1 protein in the FGF-2/Dox groups (Fig. 13, D and E). Finally, Rapamycin prevented the protective effect of FGF-2 isoforms against Dox-induced upregulation of Caspase 3/7 activity, LDH release, and Dox-mediated upregulation of p53 as well as cleaved (active) caspase-3 (Fig. 14, A & B, and Appendix 4, C). Another inhibitor of the mTOR pathway, Torin-1, was also able to prevent cardiomyocyte protection, and HO-1 upregulation by FGF-2 isoforms in the presence of Dox (Appendix 5). Thus, mTOR

activity is required for protection from Dox-induced apoptotic and necrotic cell death, and HO-1 upregulation, by FGF-2.

A selective inhibitor of HO-1, Tin-Protoporphyrin (Tin-PP) was then used to determine if the protective effects of FGF-2 isoforms were mediated by HO-1. Tin-PP blocked FGF-2 protection from Dox-induced increase in caspase 3/7 activity, LDH release, p53 upregulation, and active caspase 3 (Fig. 14, A, B, and Appendix 4, C).

Figure 10, FGF-2 isoforms attenuate the effects of doxorubicin on reactive oxygen species (ROS), Nrf-2 and its downstream target heme oxygenase 1 (HO-1

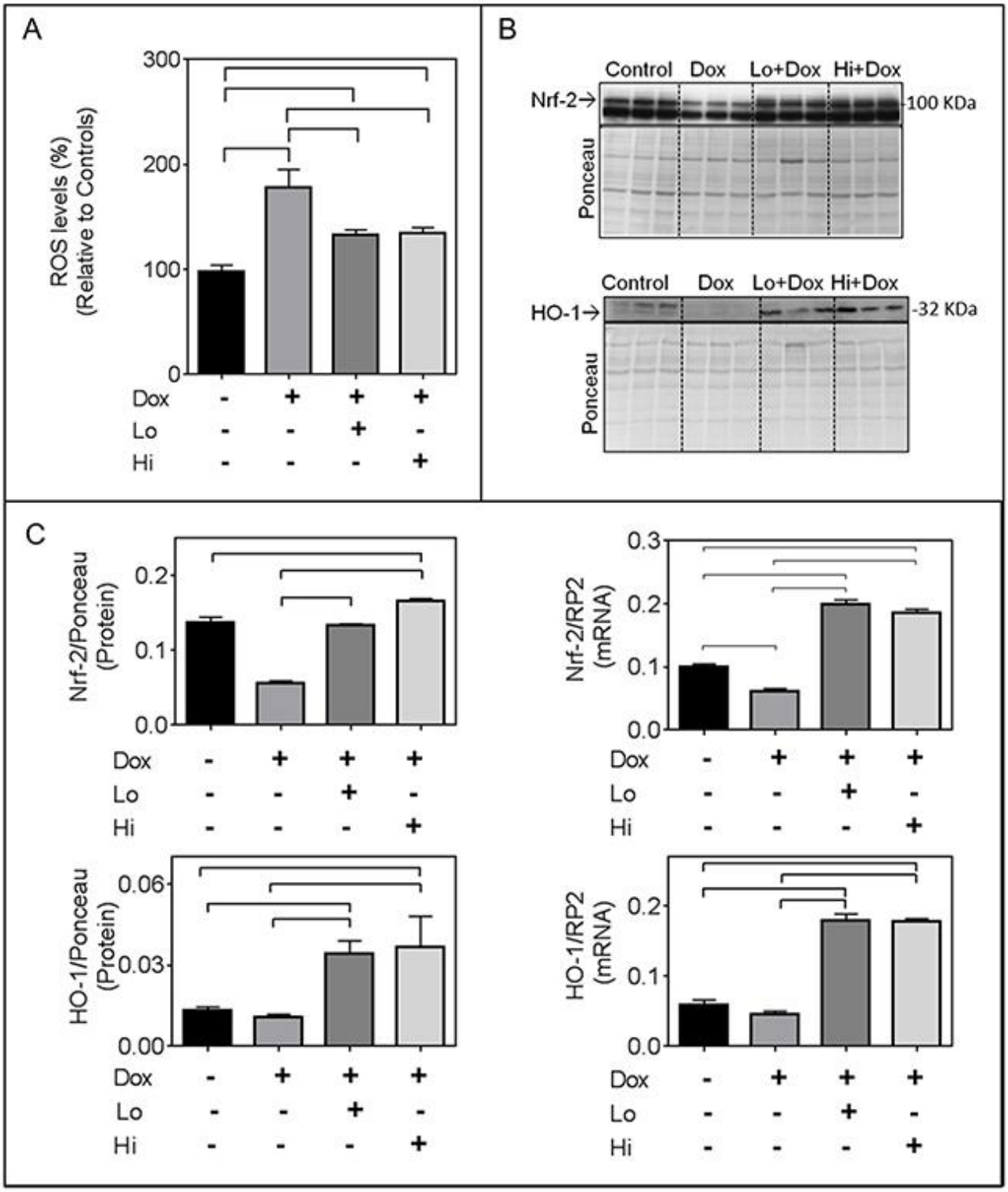

Figure 10. **Panel (A).** Relative ROS as measured by the fluorescence intensity of 2',7' – dichlorofluorescin diacetate (DCFDA), n=8, in the absence or presence of Dox and FGF-2 isoform pre-treatment, as indicated. **(B),** Western blots for Nrf-2, and HO-1, as indicated. Nrf-2 migrates as a 100 kDa band, while HO-1 is at 32 kDa. Quantitative assessments of immunoreactive bands are included in panel C. **Panel (C)** relative Nrf-2 and HO-1 protein (n=3) as well as corresponding mRNA levels, assessed by q-PCR, (n=4), as indicated. For the mRNA or protein determinations, cardiomyocytes were exposed to Dox for, respectively, 8 or 24 hours, in the presence and absence of Lo- or Hi-FGF-2 pre-treatment. For western blot analysis, the densitometry values of the probed proteins were corrected using the densitometry values of the whole lane Ponceau S stain of the same membrane. For qPCR analysis, all target RNA levels were normalized to rat RNA polymerase II (RP2) levels. Data is plotted as mean ± SEM. Bracket indicate groups whose values are show statistically significant differences, $P<0.05$).

Figure 11, In the presence of doxorubicin, FGF-2 isoforms promote p62/SQSTM1 upregulation which is further increased by Chloroquine (CQ).

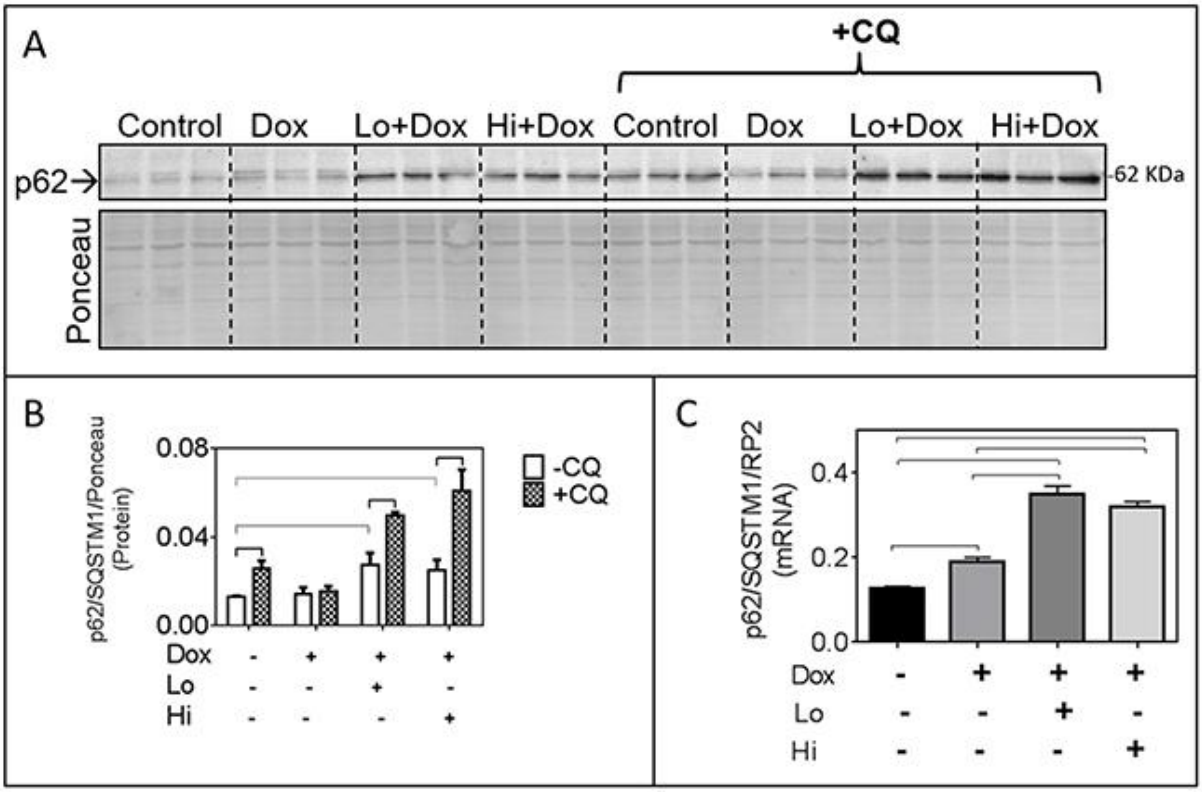

Figure 11. **Panel A**. Western blot showing p62/SQSTM1 immunoreactivity, in the absence and presence of the lysosomal/autophagy flux inhibitor CQ, in cardiomyocytes exposed or not to Dox and FGF-2 pre-treatment, as indicated. Corresponding densitometric data are shown in panel B. **Panel B**, relative protein levels of p62/SQSTM1, in response to CQ. Densitometry of the Ponceau S (scan of the whole lane) was used to adjust for minor loading variations. **Panel C**, relative levels of p62/SQSTM1 mRNA in cardiomyocytes exposed, or not, to Dox and FGF-2 isoforms, as indicated; n=4. Data is plotted as mean ± SEM. For the mRNA or protein determinations, cardiomyocytes were exposed to Dox for, respectively, 8 or 24 hours, in the presence and absence of Lo- or Hi-FGF-2 pre-treatment. Rat RNA polymerase II (RP2) levels were used to normalize the target mRNA. Statistically significant differences ($P<0.05$) between groups are indicated by brackets.

Figure 12, FGF-2 isoforms prevent the Dox-induced downregulation of transcription factor EB (TFEB) and lysosomal associated membrane protein-1 (LAMP-1).

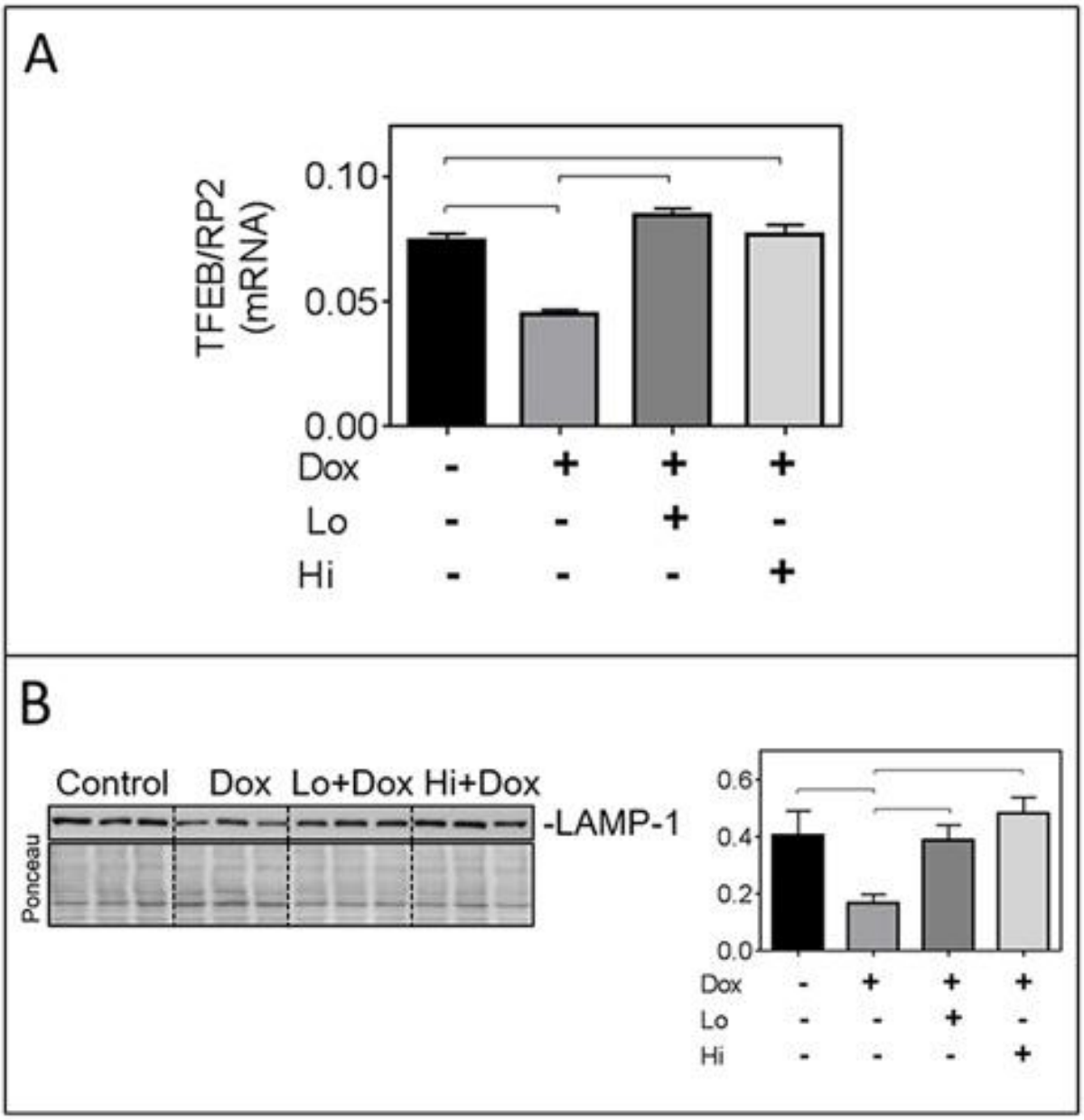

Figure 12. **Panel (A).** Relative mRNA levels of TFEB in cardiomyocytes exposed to Dox for 8 hours in the presence and absence of pre-incubation with FGF-2 isoforms. Rat RNA polymerase II (RP2) levels were used to normalize the target mRNA. **(B)** Western blot for LAMP-1, and corresponding graph after 24-hour exposure to Dox in the presence and absence of Lo- or Hi-FGF-2 pre-incubation. Ponceau S stain of the same membrane used to correct for variations in loading. Brackets indicate groups displaying statistically significant differences ($P<0.05$).

Figure 13, The mTOR pathway mediates the FGF-2 induced effects on Nrf-2 and HO-1.

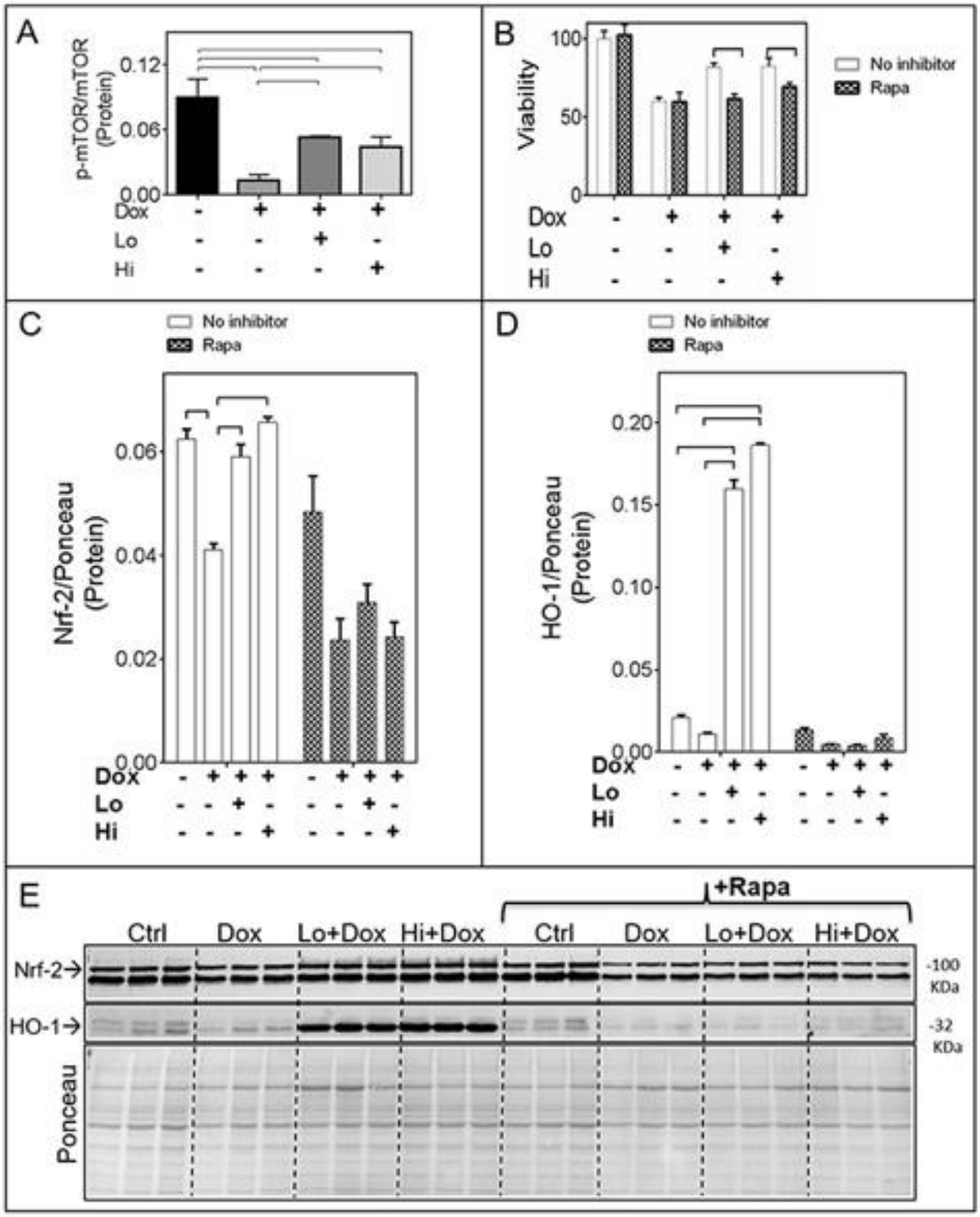

Figure 13. **Panel (A).** Relative levels of active (phospho-Ser2448 mTOR)/total mTOR (n=4). The corresponding western blot is shown in Appendix 4, A. **(B).** Cardiomyocyte viability as estimated by the Calcein-AM (fluorescence intensity) assay, in the absence (empty columns) or presence (shaded columns) of Rapamycin (100nM), Dox, and FGF-2 isoforms (n=8), as indicated. **(C)** and **(D)**. Relative protein levels for, respectively, Nrf-2 and HO-1 in the absence (empty columns) or presence (shaded columns) of Rapamycin (n=3). Data is plotted as mean ± SEM and statistical differences are shown by brackets where significant $P<0.05$. The corresponding western blot is shown in **Panel E.**

Figure 14, The mTOR and heme oxygenase-1 (HO-1) activities mediate the pro-cell survival effects of FGF-2 isoforms.

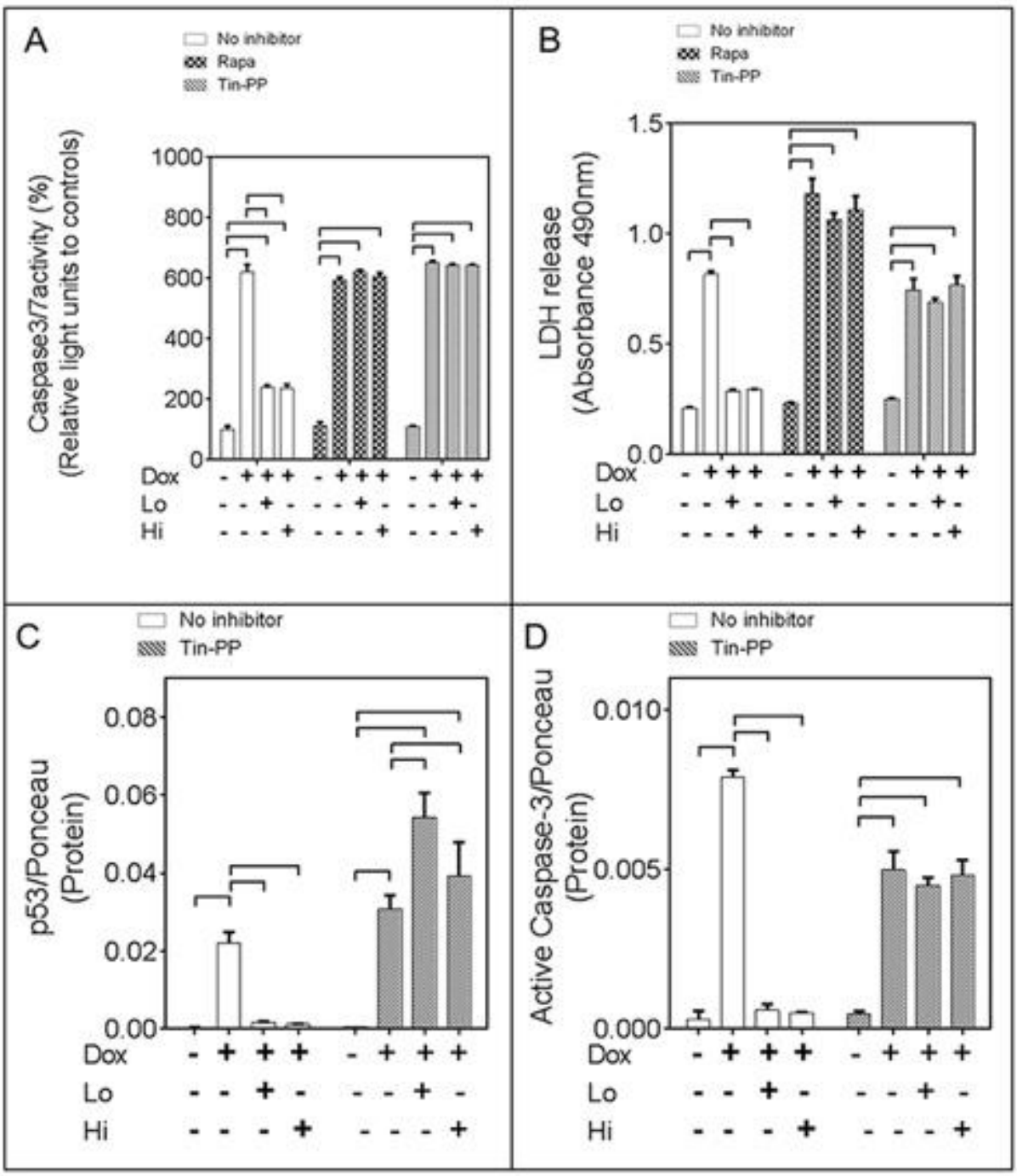

Figure 14. **Panels (A) and (B).** Relative caspase 3/7 activity, and LDH release, respectively, in cardiomyocytes exposed to Dox, and FGF-2 isoform pre-treatment, in the absence or presence of Rapamycin (mTOR inhibitor, 100nM) and Tin-Protorphyrin (Tin-PP, 10 μM), as indicated; n=4. **Panels (C) and (D).** p53, or cleaved 19 kDa caspase-3 levels, respectively, in cardiomyocytes exposed to Dox, and FGF-2 isoform pre-treatment, in the absence or presence of Rapamycin and Tin-PP, as indicated, n=3. Corresponding western blots are included in Appendix 4, C. Ponceau S stain of the same membrane, used to adjust for minor variations in loading. Data is plotted as mean ± SEM and brackets denote groups presenting statistically significant ($P<0.05$) differences.

Figure 15, The proposed mechanism of cardioprotection against doxorubicin by FGF-2 isoforms.

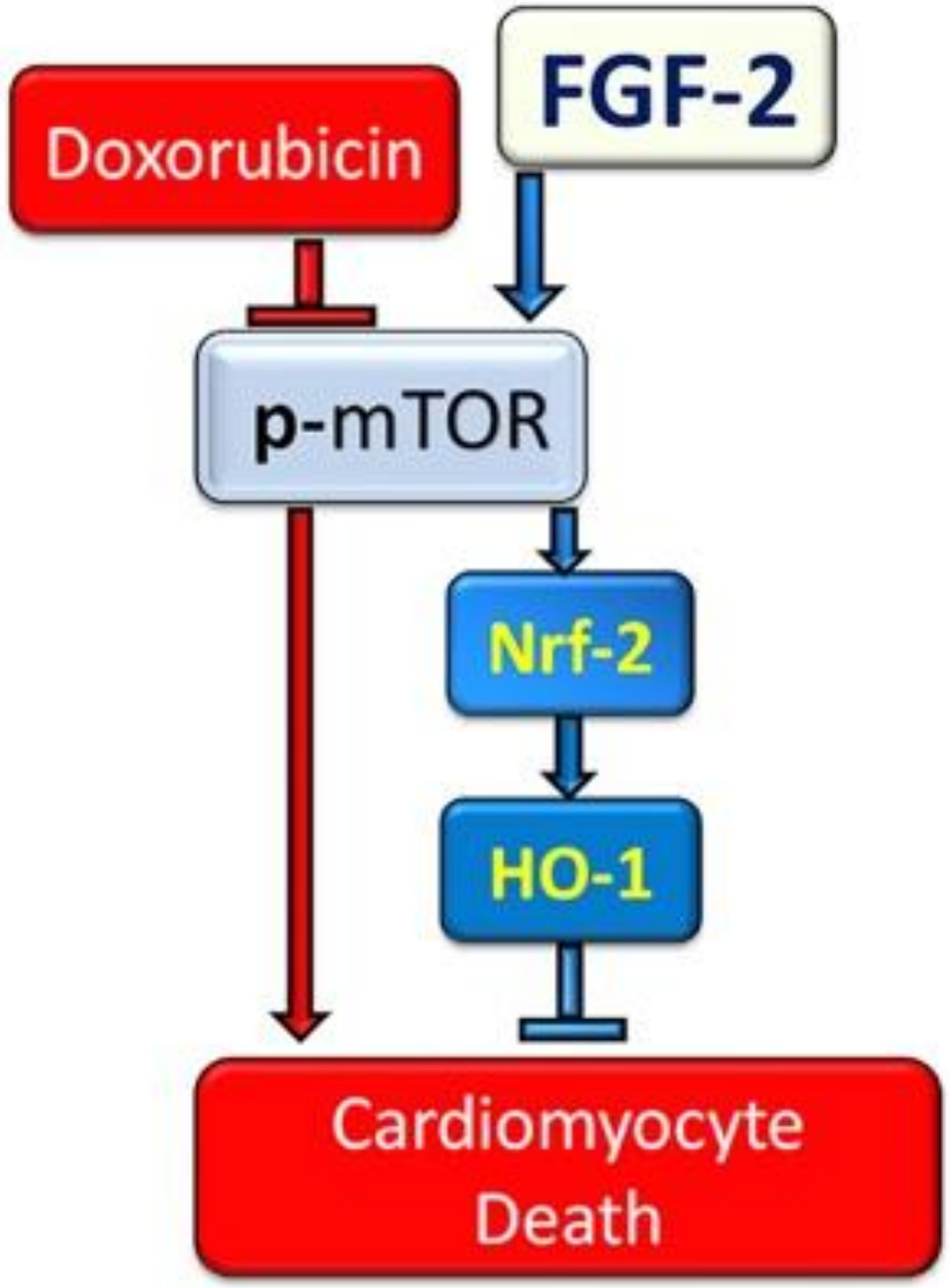

Figure 15. FGF-2 mediated protection against Dox is shown to be via restoration of Nrf-2 and robust upregulation of its target HO-1 in cardiomyocytes. mTOR re-activation is essential for FGF-2 mediated protection and restoration/upregulation of Nrf-2/HO-1.

Discussion

Novel findings presented in this work are: (1) Hi-FGF-2 increases the resistance of cardiomyocytes to (acute) Dox-induced cell death and lysosomal dysregulation in a similar manner to Lo-FGF-2; (2) FGF-2 isoforms stimulate upregulation of Nrf-2 and its downstream targets HO-1 and p62/SQSTM1 in the presence, but not absence, of Dox; (3) mTOR activity is required for FGF-2 induced protection and Nrf-2, HO-1, and p62/SQSTM1 upregulation; and (4) HO-1 mediates FGF-2 protection (Fig. 15).

(i) Hi-FGF-2 protects from Dox-toxicity in an acute setting. It is well established that Dox cardiotoxicity includes mitochondrial damage, apoptotic and necrotic cell death as well as lysosomal and autophagic dysregulation [21]. In our *in vitro* model, Dox upregulated ROS, decreased cellular ATP, promoted LDH release, upregulated pro-cell death markers such as p53, Bnip-3 and active caspase 3 and caused formation of mPTP. Dox also downregulated active mTOR, which is a master regulator of growth and an inhibitor of autophagy initiation; its downregulation is expected to trigger autophagy initiation [2]. At the same time Dox caused lysosome-associated changes indicative of dysregulation, by decreasing expression of TFEB the master transcription factor for lysosomal biogenesis, and of LAMP1 protein, consistent with decreases in lysosomal numbers. Lysosomal dysregulation contributes to blocked autophagic clearance/flux in the presence of Dox resulting in proteotoxicity according to previous reports [20, 22], and confirmed in our system. Overall our model recapitulated multiple components of Dox-induced cardiotoxicity, supporting its validity in examining potential protective manipulations and associated mechanisms. It is of interest that FGF-2 isoforms did not protect a breast cancer cell line (MCF-7) from Dox toxicity, suggesting the possibility, in need of further investigation, that an FGF-2-based therapy may not affect the toxicity of anthracyclines against

at least some types of cancer cells. It is not clear why MCF-7 cells were not protected by FGF-2, although others have reported broadly similar findings [23]. One may speculate that although MCF-7 cells do express FGF-2 receptor 1 (FGFR1), [24] the receptor may be already fully activated by MCF-7-produced endogenous FGFs, or that it may display an aberrant pattern of activation as has been reported [25].

Both FGF-2 isoforms were found to prevent or attenuate all of the deleterious effects of Dox on cardiomyocytes. In the case of Lo-FGF-2, our results are broadly consistent with previous studies showing the protective effect of Lo-FGF in multiple scenarios of cardiomyocyte injury, as reviewed [9], including Dox toxicity [11]. Although less information exists regarding the effects of extracellular-acting Hi-FGF-2, our previous *in vivo* studies documented that direct administration of Hi-FGF to the heart exerts short-term (one day) protection from cardiac ischemic injury and cell death. Interestingly, the protective effects of Hi-FGF-2, unlike those of Lo-FGF-2, were not sustained at longer time points post-ischemia [26]. Another study showed that administered Hi-FGF-2 exerts acute post-conditioning-like cardioprotection against ischemia-reperfusion cardiac dysfunction and cell death [27]. Our present study reinforces the notion of acute cardiomyocyte protection by administered Hi-FGF-2, this time in the context of Dox-induced cardiotoxicity *in vitro*. It remains to be determined whether Hi- and/or Lo-FGF-2, can exert sustained protection from Dox cardiotoxicity.

(ii) The Nrf-2/HO-1 pathway is a major endogenous cytoprotective mechanism activated under conditions of oxidative stress. Under non-stressed conditions, Nrf-2 is sequestered in the cytosol via its interaction with Keap-1 which also facilitates proteasomal degradation of Nrf-2. In response to oxidative stress, Nrf-2 dissociates from Keap1, translocates to the nucleus, and stimulates expression of HO-1 as well as multiple genes belonging to several

antioxidant cell detoxification pathways [15, 28-30]. While exposure of neonatal cardiomyocytes to moderate, non-toxic, oxidative stress was reported to upregulate Nrf-2 and Nrf-2-target genes including HO-1 [31], excessive oxidative stress induced by Dox likely overwhelms the antioxidant defenses of cardiomyocytes. Indeed, we found that Dox downregulated Nrf-2 and failed to upregulate HO-1. Previous studies have shown that dysregulation of the Nrf-2/HO-1 axis contributes to Dox-induced cardiotoxicity: a lack of Nrf-2 exacerbated Dox-induced cardiotoxicity, while induction of increased expression of Nrf-2 was protective *in vivo* [32-34]. FGF-2 isoforms, as shown here, prevented the Dox-induced effects on Nrf-2, and promoted robust upregulation of Nrf-2 targets such as HO-1 (and p62/SQSTM1), often used to demonstrate Nrf-2 activity. Our data indicate that FGF-2 protection from Dox toxicity is mediated by restoring or boosting the Nrf-2/HO-1 axis.

The competitive HO-1 inhibitor, Tin-PP, prevented the FGF-2 induced beneficial effects against cell death and damage, offering further support to this notion. The cardioprotective effect of HO-1 has been documented by multiple groups, as reviewed recently [35]. Lack of HO-1 sensitizes cardiac cells to various types of stress stimuli, including Dox and ischemia/reperfusion injury [36-38], while enhancing cardiac HO-1 expression is sufficient to blunt Dox and reperfusion damage [36, 39-43]. In view of its potent protective effects, there is strong interest in identifying drugs capable of boosting endogenous HO-1 and its downstream metabolites, such as carbon monoxide (CO) to enhance cardiac resistance to toxic conditions [35, 39, 44, 45]. In this context, FGF-2 administration to the heart may be considered as a means to upregulate HO-1 under conditions of oxidative stress.

In contrast to other cytoprotective agents like sulphoraphane [32, 33] and even FGF-1 in astrocytes [46], FGF-2 isoforms did not upregulate Nrf-2 / HO-1 protein levels under normal

non-stressed conditions in cardiomyocytes, but only did so in the presence of Dox. Thus, the ability of FGF-2 pre-treatment to prevent the Dox-induced Nrf-2 loss (mRNA and protein), and to even upregulate HO-1 protein accumulation substantially above control levels likely requires additional, Dox-induced signal(s). One can speculate that since we found that FGF-2 decreased but did not eliminate ROS production by Dox, residual ROS was able to activate the Nrf-2/HO-1 antioxidant line of defense.

(iii). p62/SQSTM1 is a multifunctional scaffold protein and another well-known target of Nrf-2. We found that it was robustly upregulated by FGF-2 in the presence but not absence of Dox [47]. The p62/SQSTM1 accumulates at sites of autophagosome formation and facilitates tethering of ubiquitinated cargo at the autophagosome [17]. As p62/SQSTM1 is expected to become degraded upon completion of autophagy (fusion of autophagosome with the lysosome, and degradation of cargo), its accumulation above control levels, as observed in the FGF-2/Dox groups, could be interpreted as the result of blocked autophagic flux. However, this does not appear to be the case. Firstly, we observed significant increases in p62 mRNA, consistent with Nrf-2-mediated transcription, indicative of increased de novo synthesis. Secondly, the autophagy flux inhibitor CQ elicited further, significant, increases in p62 protein accumulation, showing that autophagic flux was not blocked in the FGF-2/Dox groups. By the same criteria, autophagic flux was found to be blocked in the Dox-groups, consistent with previous reports [20]. Therefore, our work indicates that FGF-2 pre-treatment corrected autophagic dysregulation, and possibly proteotoxic cell death, caused by Dox. It is possible that increased p62 levels, in an environment of functional autophagic flux, might better facilitate elimination of damaged cargo through autophagic clearance. In general agreement with our findings, it has been reported that

Lo-FGF-2 protects cardiac cells against ischemia/reperfusion injury by p62/SQSTM1-mediated enhancement of ubiquitinated protein clearance [48].

(iv) The mTOR pathway is activated downstream of growth factor signaling [2]. mTOR is the master regulator of protein, nucleotide, and lipid synthesis and turnover and controls cell growth, differentiation, autophagy and metabolism of the cell [49]. Transgenic mice expressing a constitutively active form of mTOR are resistant to Dox cardiotoxicity, highlighting the crucial role of mTOR signaling in cardioprotection [50]. A serine/threonine protein kinase, mTOR is the active subunit of two different complexes: complex 1 (mTORC1) and complex 2 (mTORC2).

The mTORC1 complex, which is inhibited by Rapamycin, promotes anabolic processes, and suppresses autophagy, while the mTORC2 complex is activated primarily downstream of PI3 kinase and is associated with cell proliferation and survival [49].

Dox-induced inhibition of mTOR in cardiomyocytes contributes to Dox toxicity [50-52]. We showed that FGF-2 attenuated the Dox-induced decrease in activated mTOR, and in turn Rapamycin (mTORC1 inhibitor), and Torin 1 (mTORC1 and mTORC2 inhibitor), prevented the FGF-2-triggered protective effects. Rapamycin abrogated the FGF-2-induced effects on Nrf-2 and its downstream targets HO-1 and p62/SQSTM1; while FGF-2 isoforms prevented the Dox-induced downregulation of active mTOR. Taken together our data indicate that the mTORC1 pathway is required for the FGF-2-induced effects on Nrf-2, HO-1, and p62/SQSTM1. A direct link may exist between mTOR and the FGF/FGFR1 axis. It is possible that mTOR may become phosphorylated/activated by direct interaction with FGFR1 and associated signals: in vascular smooth muscle cells mTOR was shown to interact directly with FGFR1 via Fibroblast Growth Factor Receptor Substrate 2 [53]. Further studies are required to address this issue.

Prolonged inhibition of mTOR by Rapamycin is reported to be protective against Dox-toxicity, by upregulating autophagy [54]. Rapamycin, as used in our system, was not protective by itself, likely because of the brevity of pre-treatment.

It is of interest that p62/SQSTM1 can also promote Nrf-2 activation by a positive feedback mechanism. It was demonstrated that mTOR phosphorylates p62/SQSTM1, thus strengthening the interaction of the latter with Keap-1. This results in dissociation and stabilization of Nrf-2, which can then translocate to the nucleus and activate expression of target genes such as HO-1 [55]. It will be important to determine whether the increased expression/accumulation of p62/SQSTM1 reported here contributed to Nrf-2 stabilization and activity.

In Conclusion. Dox-induced cardiotoxicity remains a major concern for patients receiving chemotherapy. There is strong interest in identifying compounds and developing drugs aimed at stimulating Nrf-2 and HO-1 upregulation, as a means to elicit tissue protection from toxic stimuli including Dox [35, 56]. In this context, FGF-2 isoforms, capable of activating/boosting endogenous cardioprotective (anti-oxidant/detoxification) pathways through the mTOR-Nrf-2-HO-1 signal transduction pathway, as shown here, could be considered as naturally occurring proteins to be harnessed in strategies to elicit cardioprotection from Dox.

Materials and Methods

This study was done according to the NIH Guide for the Care and Use of Laboratory Animals (NIH Publication, 8th Edition. Revised 2011). Approval was given by the Protocol Management and Review Committee of the University of Manitoba.

Cultures. Hearts obtained from one day-old sprague dawley rat pups were used to isolate ventricular cardiomyocytes, which were plated at a density of 5×10^4 cells/cm^2 on collagen (Corning, #354236) coated dishes in the presence of 20% fetal bovine serum (FBS) in Hams F-10 culture medium, and allowed to attach overnight as described [57, 58]. The next day cells were incubated with low-serum medium (0.5% FBS, 1% insulin, 1% transferrin/selenium, 1% ascorbic acid, and 1% bovine serum albumin) in Dulbecco's modified Eagle's medium (DMEM) for 24 hours. Subsequently, cardiomyocyte cultures were treated, or not, with FGF-2 isoforms (10 ng/ml) for 30 minutes, followed by administration of doxorubicin (Dox; 0.5 μM). Cells were exposed to Dox for 8 or 24 hours, for extraction of RNA or protein, respectively. Inhibitors were added to the cells 30 minutes prior to FGF-2 exposure. Myocyte purity was assessed by immunofluorescence, staining myocytes for alpha-actinin which highlights the striated nature of these cells. Cultures consisted of 95 % alpha-actinin-positive cells (cardiomyocytes), and this relative composition did not change with treatments for the duration of our experiments.

Reagents. Recombinant rat Hi- or Lo-FGF-2 were produced in-house using plasmids described in [59]. Briefly, Lo- or Hi-FGF-2 sequence was inserted into the EcoR1 site of pET19b resulting in a histidine tag at the N-terminal of the fusion protein. The pET vector was transformed into the expression host, Escherichia coli (BL21(DE3)pLysS), by heat shock. The cultures were grown in the presence of 50 ug/ml carbenicillin and 34 ug/ml chloramphenicol. Overnight ExpressTM Autoinduction system (Novagen) was used according to manufacturer's instructions to induce protein expression without the need to monitor cell growth. Immobilized metal affinity chromatography (IMAC) using Nickel- sepharose (Ni-sepharose, High Performance from GE Healthcare, # 17-5268-01) was used according to the manufacturer's instructions to purify proteins containing a histidine tag. To reduce non-specific binding to beads

all buffers contained 5 mM 2-mercaptoethanol and 10% glycerol. NP-40 (0.1%) was added to the binding buffer and the first wash buffer. Immidazole was removed from purified eluates by dialysis against PBS or 0.1 M $NaHCO_3$/0.5 M NaCl. Protein concentration of the recombinant protein was calculated from the absorbance at 280 nm wavelength and the coefficient for absorbance 0.1% (rat Lo-FGF-2 Coef for Abs = 0.86, Hi-FGF-2 = 00.735). Dox was purchased from Pfizer. Chloroquine (Sigma-Aldrich, c6628) was used at a final concentration of 5 μM. Rapamycin (Cayman, CAS 53123-88-9),Tin-PP (SantaCruz, CAS 14325-05-4), and Torin1 (APExBIO, A8312) were used at concentrations of 100 nM, 10 μM, and 100 nM respectively. The following antibodies were purchased from Cell Signaling: Cleaved Caspase-3 (1:1000, #9661), p53 (1:1000, #2524), Bnip3 (1:1000, #3769), p62/SQSTM1 (1:1000, #5114), p-Ser2448-mTOR(1:1000, #2971), mTOR (1:1000, #2972). Antibodies to Nrf-2 and HO-1 were, respectively, from Proteintec (1:2000, 16396-1-AP), and Abcam: HO-1 (1:7500, ab68477). Donkey anti-rabbit (1:5,000, Jackson Immunoresearch, #711-035-152) and anti-mouse (1:5,000, Jackson Immunoresearch, #715-035-150) antibodies conjugated to horseradish peroxidase were used as secondary antibodies. Antigen-antibody complexes were detected by Pierce™ ECL Plus Western Blotting Substrate (Thermofisher, #80196).

Calcein-AM/Ethidium homodimer viability assay. To measure cardiomyocyte viability, cells were rinsed twice with phosphate buffered saline (PBS) at 37 °C, then incubated with Calcein-AM (2 μM, C3100, Thermofisher) and ethidium homodimer (2.5 μM, E1169, Thermofisher) in PBS for 30 minutes. Images were obtained with an LSM 5 PASCAL fluorescence microscope. The fluorescence intensity of Calcein-AM (485/535 nm) and ethidium homodimer (530/620 nm) were also measured using a Microplate Fluorometer (SPECTRAMAX, GEMINI XS).

Protein (western) immunoblotting. Cells were snap-frozen using liquid nitrogen and stored at -80 °C. Cells were scraped, lysed, boiled and sonicated (Vibra cell) in sodium dodecyl sulphate (SDS)/polyacrylamide gel electrophoresis (PAGE) sample buffer (1%(w/v) SDS) supplemented (1:100) with protease inhibitor cocktail (Sigma-Aldrich, #8304) and phosphatase inhibitor cocktail set II and IV (Calbiochem, #524625 and #524628). Cell homogenates were then centrifuged briefly at 21,000 g to remove cellular debris. A bicinchoninic acid assay was used to measure protein concentration in the supernatants. Following SDS-PAGE, proteins were transferred to polyvinylidene fluoride (PVDF) membranes. The PVDF membranes were stained for 5 min by 0.01% (w/v) Ponceau S (Sigma-Aldrich, P3504) in 0.15% trichloroacetic acid to assess overall protein transfer. Non-specific binding was blocked by incubation in 10% milk/TBS-T or 5% BSA/TBS-T for 1 hour at room temperature. Ponceau S (total protein estimate) was used to correct for loading variations. Densitometry values (arbitrary density units) for a particular band were divided by the corresponding densitometry values (arbitrary units) of the Ponceau S staining of the whole lane.

ATP/ADP assay. Luminescent ATP Detection Assay Kit (Abcam, ab113849) was used to measure the levels of ATP, ADP, and ATP/ADP ratio according to the manufacturer's protocol.

Real-time reverse transcriptase polymerase chain reaction (qPCR). Cardiomyocyte RNA extraction followed by qPCR was done as previously described [60]. All target RNA levels were normalized to rat RNA polymerase II (RP2) levels and shown as relative ratios (delta delta C_T). Specific primers used for amplification are listed below:

Primer	Forward (5'→3')	Reverse (5'→3')
HO-1	CAGGGAAGGCTTTAAGCTGGT	GGGTTCTGCTTGTTTCGCTC
Nfe2l2 (Nrf-2)	CATTTGTAGATGACCATGAGTCGC	GCCAAACTTGCTCCATGTCC
NQO1	ACATCACAGGGGAGCCGAAG	GGCCTTCCTTATACGCCAGAG
p62/SQSTM1	AGAATGTGGGGGAGAGCGTGGC	GGGTGTCAGGCGGCTTCTCTT
RNA Polymerase-II	GGCTCTCCAGATTGCGATGTG	GCAGGTAACGGCGAATGATGATG
TFEB	CGACAACATTATGCGCCTGG	GACAGGGGTAGCGTGTTAGG

Commercial kit-based assays. Kits were used according to the manufacturers' instructions. Image-iT™ LIVE Mitochondrial Transition Pore Assay Kit (I35103) was used to study mitochondrial permeability transition pore opening (mPTP). DCF-DA (2'7'-dichlorodihydrofluorescein diacetate (Thermofisher, D399)) was used to measure levels of ROS in cardiomyocytes. The Pierce™ LDH Cytotoxicity Assay Kit (Thermofisher, 88953) was used to measure relative levels of LDH released by the cells, as an indicator of plasma membrane damage. Caspase-Glo® 3/7 Assay kit (Promega, G8090) was used to assess activation of caspases 3 and 7, as indicators of apoptosis.

Data analysis and statistics. Each experiment used one preparation of primary cardiomyocytes, isolated from the hearts of 36 rat pups, and distributed into several plates (either 96-well plates, or 6-well-plates of 35 mm diameter/well), that were subsequently grouped based on treatment. Group size (N=number of individual wells/plates per group) varied between 3-8, unless otherwise stated. Each experiment was repeated in its entirety at least 3 times, with independently generated cardiomyocyte cultures, again with N=3-5. Data were reproducible between experiments using different myocyte isolations. The results shown in figures represent one complete representative experimental series. GraphPad Prism 6 was used to analyze data in each experimental series. One-way or two-way ANOVA (Fisher's LSD test as post-hoc) were used as appropriate. P value <0.05 was considered significant. Data is shown as mean plus or minus standard error mean (SEM).

Author Contributions

NK contributed to study conception and design, acquisition of data, analysis and interpretation of data, and drafting/revising the manuscript. BEN and RRF contributed to acquisition of data, analysis and interpretation of data, and critical revision of the manuscript. JW and ZR contributed to acquisition of data. LAK and PAC contributed to portions of study conception and design, analysis and interpretation of data, and critical revision of the manuscript. EK contributed to study conception and design, analysis and interpretation of data, and drafting/revising the manuscript.

Conflict of interest:

None declared.

Funding

This work was funded by the Canadian Institutes for Health Research (FRN-74733). NK is the recipient of the Alfred E. Deacon doctoral scholarship, Institute of Cardiovascular Sciences, *St. Boniface* Hospital *Albrechtsen Research Centre*. JW is the recipient of a Research Manitoba Ph.D. Graduate Studentship.

References:

1. Mitry, M.A. and J.G. Edwards, Doxorubicin induced heart failure: Phenotype and molecular mechanisms. Int J Cardiol Heart Vasc, 2016. 10: p. 17-24.
2. Koleini, N. and E. Kardami, Autophagy and mitophagy in the context of doxorubicin-induced cardiotoxicity. Oncotarget, 2017.
3. Dhingra, R., et al., Bnip3 mediates doxorubicin-induced cardiac myocyte necrosis and mortality through changes in mitochondrial signaling. Proc Natl Acad Sci U S A, 2014. 111(51): p. E5537-44.
4. Simunek, T., et al., Anthracycline-induced cardiotoxicity: overview of studies examining the roles of oxidative stress and free cellular iron. Pharmacol Rep, 2009. 61(1): p. 154-71.
5. Hamo, C.E., et al., Cancer Therapy-Related Cardiac Dysfunction and Heart Failure: Part 2: Prevention, Treatment, Guidelines, and Future Directions. Circ Heart Fail, 2016. 9(2): p. e002843.
6. Liao, S., et al., Biological functions of the low and high molecular weight protein isoforms of fibroblast growth factor-2 in cardiovascular development and disease. Dev Dyn, 2009. 238(2): p. 249-64.
7. Santiago, J.J., et al., High molecular weight fibroblast growth factor-2 in the human heart is a potential target for prevention of cardiac remodeling. PLoS One, 2014. 9(5): p. e97281.
8. Santiago, J.J., et al., Preferential accumulation and export of high molecular weight FGF-2 by rat cardiac non-myocytes. Cardiovasc Res, 2011. 89(1): p. 139-47.
9. Kardami, E., et al., Fibroblast growth factor-2 and cardioprotection. Heart Fail Rev, 2007. 12(3-4): p. 267-77.

10. Liao, S., et al., The cardioprotective effect of the low molecular weight isoform of fibroblast growth factor-2: the role of JNK signaling. J Mol Cell Cardiol, 2007. 42(1): p. 106-20.
11. Wang, J., et al., FGF-2 protects cardiomyocytes from doxorubicin damage via protein kinase C-dependent effects on efflux transporters. Cardiovasc Res, 2013. 98(1): p. 56-63.
12. Sontag, D.P., et al., FGF-2 and FGF-16 protect isolated perfused mouse hearts from acute doxorubicin-induced contractile dysfunction. Cardiovasc Toxicol, 2013. 13(3): p. 244-53.
13. Ma, X., et al., Chromatin compaction and cell death by high molecular weight FGF-2 depend on its nuclear localization, intracrine ERK activation, and engagement of mitochondria. J Cell Physiol, 2007. 213(3): p. 690-8.
14. Shi, R.Y., et al., BNIP3 interacting with LC3 triggers excessive mitophagy in delayed neuronal death in stroke. CNS Neurosci Ther, 2014. 20(12): p. 1045-55.
15. Zhou, S., et al., The role of Nrf2-mediated pathway in cardiac remodeling and heart failure. Oxid Med Cell Longev, 2014. 2014: p. 260429.
16. Lau, A., et al., The predicted molecular weight of Nrf2: it is what it is not. Antioxid Redox Signal, 2013. 18(1): p. 91-3.
17. Katsuragi, Y., Y. Ichimura, and M. Komatsu, p62/SQSTM1 functions as a signaling hub and an autophagy adaptor. Febs j, 2015. 282(24): p. 4672-8.
18. Jain, A., et al., p62/SQSTM1 is a target gene for transcription factor NRF2 and creates a positive feedback loop by inducing antioxidant response element-driven gene transcription. J Biol Chem, 2010. 285(29): p. 22576-91.
19. Klionsky, D.J., et al., Guidelines for the use and interpretation of assays for monitoring autophagy (3rd edition). Autophagy, 2016. 12(1): p. 1-222.

20. Li, D.L., et al., Doxorubicin Blocks Cardiomyocyte Autophagic Flux by Inhibiting Lysosome Acidification. Circulation, 2016. 133(17): p. 1668-87.

21. Bartlett, J.J., P.C. Trivedi, and T. Pulinilkunnil, Autophagic dysregulation in doxorubicin cardiomyopathy. J Mol Cell Cardiol, 2017. 104: p. 1-8.

22. Bartlett, J.J., et al., Doxorubicin impairs cardiomyocyte viability by suppressing transcription factor EB expression and disrupting autophagy. Biochem J, 2016. 473(21): p. 3769-3789.

23. Coleman, A.B., et al., Chemosensitization by fibroblast growth factor-2 is not dependent upon proliferation, S-phase accumulation, or p53 status. Biochem Pharmacol, 2002. 64(7): p. 1111-23.

24. Lehtola, L., et al., Analysis of tyrosine kinase mRNAs including four FGF receptor mRNAs expressed in MCF-7 breast-cancer cells. Int J Cancer, 1992. 50(4): p. 598-603.

25. Luqmani, Y.A., M. Graham, and R.C. Coombes, Expression of basic fibroblast growth factor, FGFR1 and FGFR2 in normal and malignant human breast, and comparison with other normal tissues. Br J Cancer, 1992. 66(2): p. 273-80.

26. Jiang, Z.S., et al., High- but not low-molecular weight FGF-2 causes cardiac hypertrophy in vivo; possible involvement of cardiotrophin-1. J Mol Cell Cardiol, 2007. 42(1): p. 222-33.

27. Jiang, Z.S., et al., High molecular weight FGF-2 promotes postconditioning-like cardioprotection linked to activation of protein kinase C isoforms, as well as Akt and p70 S6 kinases. [corrected]. Can J Physiol Pharmacol, 2009. 87(10): p. 798-804.

28. Fourquet, S., et al., Activation of NRF2 by nitrosative agents and H2O2 involves KEAP1 disulfide formation. J Biol Chem, 2010. 285(11): p. 8463-71.

29. Zhang, D.D. and M. Hannink, Distinct cysteine residues in Keap1 are required for Keap1-dependent ubiquitination of Nrf2 and for stabilization of Nrf2 by chemopreventive agents and oxidative stress. Mol Cell Biol, 2003. 23(22): p. 8137-51.

30. Gorrini, C., I.S. Harris, and T.W. Mak, Modulation of oxidative stress as an anticancer strategy. Nat Rev Drug Discov, 2013. 12(12): p. 931-47.

31. Purdom-Dickinson, S.E., et al., Induction of antioxidant and detoxification response by oxidants in cardiomyocytes: evidence from gene expression profiling and activation of Nrf2 transcription factor. J Mol Cell Cardiol, 2007. 42(1): p. 159-76.

32. Li, B., et al., Sulforaphane prevents doxorubicin-induced oxidative stress and cell death in rat H9c2 cells. Int J Mol Med, 2015. 36(1): p. 53-64.

33. Singh, P., et al., Sulforaphane protects the heart from doxorubicin-induced toxicity. Free Radic Biol Med, 2015. 86: p. 90-101.

34. Wang, L.F., et al., Tert-butylhydroquinone ameliorates doxorubicin-induced cardiotoxicity by activating Nrf2 and inducing the expression of its target genes. Am J Transl Res, 2015. 7(10): p. 1724-35.

35. Otterbein, L.E., R. Foresti, and R. Motterlini, Heme Oxygenase-1 and Carbon Monoxide in the Heart: The Balancing Act Between Danger Signaling and Pro-Survival. Circ Res, 2016. 118(12): p. 1940-59.

36. Hull, T.D., et al., Heme oxygenase-1 regulates mitochondrial quality control in the heart. JCI Insight, 2016. 1(2): p. e85817.

37. Juhasz, B., et al., Postischemic cardiac recovery in heme oxygenase-1 transgenic ischemic/reperfused mouse myocardium. J Cell Mol Med, 2011. 15(9): p. 1973-82.

38. Yoshida, T., et al., H(mox-1) constitutes an adaptive response to effect antioxidant cardioprotection: A study with transgenic mice heterozygous for targeted disruption of the Heme oxygenase-1 gene. Circulation, 2001. 103(12): p. 1695-701.

39. Kim, D.S., et al., CO and bilirubin inhibit doxorubicin-induced cardiac cell death. Immunopharmacol Immunotoxicol, 2009. 31(1): p. 64-70.

40. Liu, L., et al., Over-expression of heat shock protein 27 attenuates doxorubicin-induced cardiac dysfunction in mice. Eur J Heart Fail, 2007. 9(8): p. 762-9.

41. Piantadosi, C.A., et al., Heme oxygenase-1 regulates cardiac mitochondrial biogenesis via Nrf2-mediated transcriptional control of nuclear respiratory factor-1. Circ Res, 2008. 103(11): p. 1232-40.

42. Bak, I., et al., Reduction of reperfusion-induced ventricular fibrillation and infarct size via heme oxygenase-1 overexpression in isolated mouse hearts. J Cell Mol Med, 2010. 14(9): p. 2268-72.

43. Hinkel, R., et al., Heme Oxygenase-1 Gene Therapy Provides Cardioprotection Via Control of Post-Ischemic Inflammation: An Experimental Study in a Pre-Clinical Pig Model. J Am Coll Cardiol, 2015. 66(2): p. 154-65.

44. Wang, G., et al., Cardioprotective and antiapoptotic effects of heme oxygenase-1 in the failing heart. Circulation, 2010. 121(17): p. 1912-25.

45. Suliman, H.B., et al., The CO/HO system reverses inhibition of mitochondrial biogenesis and prevents murine doxorubicin cardiomyopathy. J Clin Invest, 2007. 117(12): p. 3730-41.

46. Vargas, M.R., et al., Fibroblast growth factor-1 induces heme oxygenase-1 via nuclear factor erythroid 2-related factor 2 (Nrf2) in spinal cord astrocytes: consequences for motor neuron survival. J Biol Chem, 2005. 280(27): p. 25571-9.

47. Jain, A., et al., p62/Sequestosome-1, Autophagy-related Gene 8, and Autophagy in Drosophila Are Regulated by Nuclear Factor Erythroid 2-related Factor 2 (NRF2), Independent of Transcription Factor TFEB. J Biol Chem, 2015. 290(24): p. 14945-62.

48. Wang, Z.G., et al., bFGF regulates autophagy and ubiquitinated protein accumulation induced by myocardial ischemia/reperfusion via the activation of the PI3K/Akt/mTOR pathway. Sci Rep, 2015. 5: p. 9287.

49. Saxton, R.A. and D.M. Sabatini, mTOR Signaling in Growth, Metabolism, and Disease. Cell, 2017. 169(2): p. 361-371.

50. Zhu, W., et al., Acute doxorubicin cardiotoxicity is associated with p53-induced inhibition of the mammalian target of rapamycin pathway. Circulation, 2009. 119(1): p. 99-106.

51. Wu, Y., et al., Sevoflurane ameliorates doxorubicin-induced myocardial injury by affecting the phosphorylation states of proteins in PI3K/Akt/mTOR signaling pathway. Cardiol J, 2017.

52. Cao, Y., et al., Astragalus polysaccharide restores autophagic flux and improves cardiomyocyte function in doxorubicin-induced cardiotoxicity. Oncotarget, 2017. 8(3): p. 4837-4848.

53. Chen, P.Y. and R. Friesel, FGFR1 forms an FRS2-dependent complex with mTOR to regulate smooth muscle marker gene expression. Biochem Biophys Res Commun, 2009. 382(2): p. 424-9.

54. Xu, X., R. Bucala, and J. Ren, Macrophage migration inhibitory factor deficiency augments doxorubicin-induced cardiomyopathy. J Am Heart Assoc, 2013. 2(6): p. e000439.

55. Ichimura, Y., et al., Phosphorylation of p62 activates the Keap1-Nrf2 pathway during selective autophagy. Mol Cell, 2013. 51(5): p. 618-31.

56. Nikam, A., et al., Diverse Nrf2 Activators Coordinated to Cobalt Carbonyls Induce Heme Oxygenase-1 and Release Carbon Monoxide in Vitro and in Vivo. J Med Chem, 2016. 59(2): p. 756-62.

57. Doble, B.W. and E. Kardami, Basic fibroblast growth factor stimulates connexin-43 expression and intercellular communication of cardiac fibroblasts. Mol Cell Biochem, 1995. 143(1): p. 81-7.

58. Doble, B.W., et al., Fibroblast growth factor-2 decreases metabolic coupling and stimulates phosphorylation as well as masking of connexin43 epitopes in cardiac myocytes. Circ Res, 1996. 79(4): p. 647-58.

59. Pasumarthi, K.B., E. Kardami, and P.A. Cattini, High and low molecular weight fibroblast growth factor-2 increase proliferation of neonatal rat cardiac myocytes but have differential effects on binucleation and nuclear morphology. Evidence for both paracrine and intracrine actions of fibroblast growth factor-2. Circ Res, 1996. 78(1): p. 126-36.

60. Sofronescu, A.G., K.A. Detillieux, and P.A. Cattini, FGF-16 is a target for adrenergic stimulation through NF-kappaB activation in postnatal cardiac cells and adult mouse heart. Cardiovasc Res, 2010. 87(1): p. 102-10.

Section 3. Non-mitogenic FGF2 protects cardiomyocytes from acute Doxorubicin induced toxicity via a protein kinase CK2/ heme oxygenase 1 (HO-1) independent pathway

Published in Cell Tissue Res. 2018 Dec;374(3):607-617. doi: 10.1007/s00441-018-2905-z. Epub 2018 Aug 29.

The full-text can be found in: https://link.springer.com/article/10.1007%2Fs00441-018-2905-z

Navid Koleini[1,2], Barbara E Nickel[1], Andrea L Edel[1], Robert R Fandrich[3], Amir Ravandi[1,2,4], Elissavet Kardami[1,2,3]

1: Institute of Cardiovascular Sciences, St. Boniface Hospital Albrechtsen Research Centre. 351 Tache Ave, Winnipeg, Manitoba, Canada, R2H2A6

2: Department of Physiology & Pathophysiology, University of Manitoba, Winnipeg, Canada

3: Department of Human Anatomy and Cell Sciences, University of Manitoba, Winnipeg, Canada

4: Interventional Cardiology, Section of Cardiology, Max Rady College of Medicine, University of Manitoba

Corresponding author:

Dr. Elissavet Kardami

St. Boniface Hospital Albrechtsen Research Centre

351 Tache Ave,Winnipeg, Manitoba, R2H 2A6

Email: ekardami@sbrc.ca, Tel: +1 (204) 235 3519, Fax:+1 (204) 233 6723

Key words: Non-mitogenic FGF2, acute Doxorubicin cardiotoxicity, CK2-HO-1 signaling, oxidized phospholipids, rat cardiomyocytes

Funding

EK is funded by the Canadian Institutes for Health Research (FRN-74733). AR is funded by Heart and Stroke Foundation G-14-0006050 and Research Manitoba 983. NK is the recipient of a Bank of Montreal studentship award via the St. Boniface Hospital Albrechtsen Research Centre.

Abstract.

Doxorubicin (Dox)-induced cardiotoxicity, a limiting factor in the use of Dox to treat cancer, can be mitigated by the mitogenic factor FGF2 in vitro, via a heme oxygenase 1 (HO-1)-dependent pathway. HO-1 upregulation was reported to require protein kinase CK2 activity. We have shown that a mutant non-mitogenic FGF2 (S117A-FGF2), which does not activate CK2, is cardioprotective against acute cardiac ischemic injury. We have now investigated the potential of S117A-FGF2 to protect cardiomyocytes against acute Dox injury and decrease Dox-induced upregulation of oxidized phospholipids. The roles of CK2 and HO-1 in cardiomyocyte protection were also addressed.

Rat neonatal cardiomyocyte cultures were used as an established in vitro model of acute Dox toxicity. Pretreatment with S117A-FGF2 protected against Dox-induced: oxidative stress; upregulation of fragmented and non-fragmented oxidized phosphatidylcholine species, measured by LC/MS/MS; and cardiomyocyte injury and cell death measured by LDH release and a live-dead assay. CK2 inhibitors (TBB and Ellagic acid), did not affect protection by S117A-FGF2, but prevented protection by mitogenic FGF2. Furthermore, protection by S117A-FGF2, unlike that of FGF2, was not prevented by HO-1 inhibitors, and S117A-FGF2 did not upregulate HO-1. Protection by S117A-FGF2 required the activity of FGF receptor 1 and ERK.

We conclude that mitogenic and non-mitogenic FGF2 protect from acute Dox toxicity by common (FGFR1) and distinct, CK2/HO-1- dependent or -independent (respectively), pathways. Non-mitogenic FGF2 merits further consideration as a preventative treatment against Dox cardiotoxicity.

Introduction

Doxorubicin (Dox) is a chemotherapy drug which is widely used to treat many types of malignancies including breast cancer, lymphoma, and acute lymphoblastic leukemia in patients of all ages; cardiotoxicity which can manifest acutely, sub-acutely, or late-onset, has posed limitation to the use of Dox [1]. Dox-cardiotoxicity is attributed to elevated oxidative stress, DNA and mitochondrial damage, and deleterious changes in gene expression, culminating in the dysregulation of multiple signal transduction pathways leading to cardiac cell death [2]. Currently, the only FDA approved drug to mitigate Dox-induced cardiotoxicity is Dexrazoxane which has been of restricted use due to the concern for cancer outcomes [3].There is clearly a need for new approaches to protect the heart from Dox, without compromising the efficacy of Dox. Fibroblast growth factor 2 (FGF2) is a heparin binding growth factor ubiquitously expressed in all tissues as high (>20 kDa) and low (18 kDa) molecular weight isoforms [4-6]. Please note that for the rest of this work the term FGF2 will refer to the 18 kDa FGF2 isoform.

We have recently published that FGF2 protects neonatal rat cardiomyocytes against acute Dox-induced damage and cell death by a mammalian target of rapamycin/ Nuclear factor (erythroid-derived 2)-like (Nrf2) / Heme Oxygenase -1 (HO-1)-dependent pathway *in vitro* [7]. A concern with using FGF2 as a cardioprotective strategy against Dox is the possibility of undesirable effects on cancer cell proliferation and survival. FGF2 is a potent mitogen and angiogenic agent and may increase tumor proliferation and blood vessel formation [8, 9]. Previous studies have demonstrated that a mutated form of FGF2, carrying a serine-to-alanine (S117A) substitution (S117A-FGF2) retains acute cardioprotective potential against cardiac ischemic injury, but lacks mitogenic and angiogenic activity [9-11]. It is postulated that if the S117A-FGF2 retains

cardioprotective properties against Dox-induced cardiomyocyte oxidative stress and injury/death, it would merit further consideration as a prophylactic treatment against Dox.

The S117A-FGF2 has lost the ability to interact with and activate the ubiquitous protein kinase CK2 which promotes cell proliferation and angiogenesis [10, 12]. Furthermore, CK2 is required for the upregulation of HO-1 in chondrocytes [13], which would suggest that S117A-FGF2 may be incapable of upregulating HO-1 in cardiomyocytes. Since HO-1 was required for the protective effect of FGF2 [7], the possibility arose that S117A-FGF2 may not protect against Dox-induced cardiomyocyte damage, or, if it did, a non-CK2/HO-1 pathway would be involved.

Here we will report on our findings regarding the ability of S117A-FGF2 to protect cardiomyocytes against Dox damage, increased oxidative stress, increased oxidized-phosphatidylcholines, and the role of CK2/HO-1 and ERK in cardioprotection by S117A-FGF2.

Materials and Methods

This study was done according to the NIH Guide for the Care and Use of Laboratory Animals (NIH Publication, 8th Edition. Revised 2011). Approval was received from the Protocol Management and Review Committee of the University of Manitoba.

Cultures. Hearts were collected from 1-2 day old rat pups and ventricular cardiomyocytes were isolated as previously described [7]. After isolation, cardiomyocytes were plated at a density of 5 $\times 10^4$ cells/cm^2 on collagen-coated culture plates in 20% fetal bovine serum (FBS) F10 media and allowed to attach over-night. The next day culture medium was changed to 0.5% FBS, 1% insulin, 1% transferrin/selenium, 0.5% ascorbic acid, and 1% bovine serum albumin and cells were incubated for 48 hours. S117A-FGF2 (10 ng/ml) was added to the cultures 30 min before Dox addition. Myocytes were then exposed to Dox (0.5 μM) for up to 24 hours. Inhibitors were added 30 min before the addition of S117A-FGF2. Culture media was collected and stored at -80°C for LDH assays. The cells were snap frozen in liquid nitrogen and stored at -80°C for extraction and western blotting.

Reagents. Recombinant rat FGF2 and S117A-FGF2 were produced in-house using plasmids described in [7, 10]. Histidine Tag at the N-terminal of the fusion proteins was used to purify the recombinant proteins using Nickel- sepharose (Ni-sepharose, High Performance from GE healthcare, # 17-5268-01), according to the manufacturer protocols. FGFR1 antibody (anti-pY766-FGFR1) was purchased from SantaCruz (#sc-16309). The phospho (P) ERK (#9101),ERK (#9102), AKT (#9272),P- AKT (#9271), p38 (#9212), and P-p38 (#9211S) antibodies were purchased from Cell Signaling Technology. Optima LC/MS grade solvents were obtained from Fisher Scientific (Ottawa, Ontario, Canada). 1,2-Dinonanoyl-sn-glycero-3-phosphocholine (09:0 PC), was purchased from Avanti Polar Lipids (Alabaster, AL, USA).

Butylated hydroxytoluene (BHT) was purchased from Sigma Aldrich (Oakville, Ontario, Canada).

Calcein-AM/Ethidium homodimer viability assay. Cells were rinsed two times with phosphate buffered saline (PBS) at 37°C, then incubated with Calcein-AM (2 μM, C3100, Thermofisher) and ethidium homodimer (2.5 μM, E1169, Thermofisher) in PBS for 30 minutes. Images were taken using an LSM 5 PASCAL fluorescence microscope.

MTT assay. MTT (3-(4,5-Dimethylthiazol-2-yl)-2,5-Diphenyltetrazolium Bromide (Sigmaaldrich, # M2128) assay was used to measure cell number. MCF-7 cells were grown in 24 well plates (in 1 ml of to 0.5% FBS, 1% insulin, 1% transferrin/selenium, 0.5% ascorbic acid, and 1% bovine serum in DEM) until 50% confluence. FGF2 or S117A-FGF2 (10 ng/ml) were added to the cultures for 24 hours. The next day 100 μl of 5 mg/ml MTT in PBS was added to the cultures for 1 hour. The media was discarded and cells were washed gently in phosphate buffered saline (PBS) twice. 150 μl of 1:1 ethanol-DMSO was added to each well and mixed for 10 min. The absorbance of formazen was read at 570 nm; the absorbance at 630 nm was used as the reference.

Protein (western) immunoblotting. Cells were scraped in sodium dodecyl sulphate (SDS)/polyacrylamide gel electrophoresis (PAGE) sample buffer (1%(w/v) SDS) supplemented (1:100) with protease inhibitor cocktail (Sigma-Aldrich, #8304) and phosphatase inhibitor cocktail set II and IV (Calbiochem, #524625 and #524628). The lysates were boiled, sonicated, and centrifuged (14,000g for 15 min) to remove debris. Bicinchoninic acid (BCA) assay was used to determine protein concentration in the samples. Following SDS-PAGE, proteins were transferred to polyvinylidene fluoride (PVDF) membranes. 0.01% (w/v) Ponceau S (Sigma-

Aldrich, P3504) in 0.15% trichloroacetic acid was used to stain the membrane to assess protein transfer and used to correct for protein loading. The membranes were incubated in 5% BSA/TBS-T for 1 hour at room temperature to block non-specific binding.

Commercial kit-based assays. The Pierce™ LDH Cytotoxicity Assay Kit (Thermofisher, 88953) was used to measure LDH in supernatants, as an indicator of plasma membrane damage. To measure the levels of ROS, DCF-DA (2′7′-dichlorodihydrofluorescein diacetate). (ThermoFisher, D399) was used. The assay was done according to the manufacturer protocols.

Phospholipid extraction from cardiomyocytes. Cardiomyocytes were grown on 60 mm dishes. After the cells were treated, they were scraped into 200 µl PBS-EDTA. The lysates were quickly frozen and kept at -80°C. Thawed cardiomyocytes were lysed using sonication. One hundred and fifty microliters of cell mixture was extracted with 2:1 (vol/vol) chloroform:methanol containing 0.01% BHT using the method described by Folch et al [14]. One hundred microliters of 1,2-dinonanoyl-*sn*-glycero-3-phosphocholine (09:0 PC; 0.1 µg/ml) was added as internal standard prior to lipid extraction. 20 µl of the lysates were used to determine protein concentration. To solubilize the proteins, 5 µl of the 5X SDS buffer was added to the lysates. The mixtures were briefly boiled and sonicated. Protein concentration was measured using the BCA method.

OxPC Analysis by LC/MS/MS. Reverse phase-high performance liquid chromatography (RP-HPLC) was used to separate OxPC species, as previously described [15]. Cardiomyocyte lipid extracts were reconstituted in 100 µl of mobile phase A. Thirty microliters were injected onto an Ascentis Express C18 HPLC column (15 cm × 2.1 mm, 2.7 µm; Supelco Analytical, Bellefonte, Pennsylvania, USA) using a Prominence HPLC system (Shimadzu Corporation, Canby, Oregon, USA). Analyte separation was accomplished using a linear gradient of solvents A

(acetonitrile/water, 60:40 vol/vol) and B (isopropanol/acetonitrile, 90:10, vol/vol), each containing 10 mM ammonium formate and 0.1% formic acid. The elution profile was as follows: initial solvent B at 32%, increased to 45% B until 4.00 min; 5.00 min 52% B; 8.00 min 58% B; 11.00 min 66% B; 14.00 min 70% B; 18.00 min 75% B; 21.00 min 97% B; 25.00 min 97% B; 25.10 min 32% B with an overall run time of 30.10 min. Separation was performed using a flow rate of 0.26 ml/min. while the temperature of the sample tray and column oven were maintained at 4 and 45 ˚C, respectively.

Analyte detection was accomplished using a 4000 QTRAP® triple quadrupole mass spectrometer (MS) (AB Sciex, Framingham, Massachusetts, USA) as has been fully described [15, 16]. OxPC were calculated relative to the amount of internal standard with final results represented as amount (ng) of OxPC per μg protein.

Data analysis and statistics. Each experiment was repeated at least 3 times using different cardiomyocyte cultures. In each repeat, the group size was 3-5. GraphPad Prism 6 was used for statistical analysis. One-way (Tukey post hoc or LSD) or two-way ANOVA (Sidak post hoc or LSD) was used (as appropriate). P value was set at $P<0.05$. The data is shown as mean ± standard error of the mean (SEM).

Results

The effect of S117A-FGF2 against Dox-induced cardiomyocyte damage. We have recently reported that primary cultures of neonatal rat cardiomyocytes represent a good *in vitro* model to study multiple aspects of acute Dox-induced toxicity [7]. This model was used to examine the effect of pre-treatment with S117A-FGF2, and FGF2 (used as positive control), on Dox-induced LDH release, and cell death. As shown in Fig.16 a, S117A-FGF2 was equally potent as FGF2 in reducing cardiomyocyte plasma membrane damage induced by Dox, estimated by decreased LDH release. Using a Calcein-AM/Ethidium homodimer assay, where live cells stain green (Calcein-AM) and dead cells are stained red (Ethidium homodimer), S117A-FGF2 was found to decrease the relative abundance of dead cells significantly, Fig.16 b-and c-c'".

We next examined the effect of S117A-FGF2 on a breast cancer cell line, MCF-7 cells. MCF-7 exposed to Dox for 24 hour had increased LDH release, an effect that was not prevented by S117A-FGF pre-incubation (Appendix 6). Using an MTT assay as an estimate of cell number, we found that S117A-FGF2 had no effect on proliferation, unlike FGF2 which elicited a small but statistically significant increase in cell number (Appendix 6).

The role of FGFR1 and ERK in S117A protection against Dox-induced cardiomyocyte damage

Fibroblast growth factor receptor-1 (FGFR1) is the main cardiomyocyte FGF2 receptor [17, 18]. Upon ligand binding, FGFR1 dimerizes and becomes trans-phosphorylated on tyrosine (Y) 766 [19]. As shown in Fig.17a and a', S117A-FGF2 stimulation for 30 min significantly upregulated relative levels of pY766-FGFR1 compared to unstimulated cells. Increased pY766-FGFR1 levels in S117A-FGF2 treated cells persisted even after Dox exposure, Fig.17a and a'. Pre-

incubation of cardiomyocytes with the specific FGFR1 inhibitor PD173074 abolished the S117A-FGF2-induced protection from Dox-induced LDH release, Fig.17b.

Several kinases associated with regulation of cardioprotection are known to be activated downstream of the FGF2/FGFR1 axis. These include ERK (or p44/42 MAPK), p38 and AKT [20]. Exposure of cardiomyocytes to S117A-FGF2 for 30 min upregulated P-ERK, compared to unstimulated cells (Fig.18a-a'). Phospho-ERK remained elevated in S117A-FGF2 treated cells even after incubation with Dox for 30 min, Fig.18 a-a'. The specific ERK inhibitor U0261 abolished S117A-FGF mediated cardiomyocyte protection against Dox, Fig.18b. In addition, as shown in Appendix 7, both mitogenic FGF2 and S117-FGF2 upregulated cardiomyocyte P-p38 as well as P-AKT, after 60 min.

The role of HO-1 and CK2 in S117A-FGF2 protection against Dox-induced cardiomyocyte damage. We have recently shown that FGF2 upregulated HO-1 in Dox-treated cardiomyocytes, and that FGF2-induced cardiomyocyte protection from Dox was blocked by the HO-1 inhibitor Tin-protoporphyrin (Tin-PP) [7]. We have now examined the ability of S117A-FGF2 to upregulate HO-1, and the ability of Tin-PP to prevent S117A-FGF2 protection from Dox. As shown in Fig.19 a-a', while FGF2 elicited significant upregulation of the HO-1 protein, compared to control or Dox-treated myocytes, S117A-FGF2 had no effect. Furthermore, Tin-PP did not block S117A-FGF protection against Dox-induced LDH release (Fig 19 b), indicating that HO-1 was not required for S117A-FGF2 protection.

We also examined the role of CK2, a likely upstream activator of HO-1 upregulation [13], in mediating protection by S117A-FGF2, in comparison to FGF2, from Dox-induced

cardiomyocyte damage. Two CK2 inhibitors were used, TBB and Ellagic acid. These inhibitors blocked cardiomyocyte protection by FGF2, but not S117A-FGF2, Fig.19c.

Effects of S117A on accumulation of reactive oxygen species (ROS) and oxidized phospholipids. Excessive ROS production is a major contributor to Dox-induced cardiomyocyte toxicity [21]. As shown in Figure 20a, S117A-FGF2 attenuated the Dox-induced accumulation of ROS in cardiomyocytes, measured by the fluorescence intensity of 2',7'dichlorodihydrofluorescein diacetate (DCF-DA). Inhibition of ERK blocked the S117A-FGF2- mediated decreases in ROS production, but did not decrease Dox-induced ROS, Fig.20a.

Increased ROS causes oxidation of DNA, proteins, and peroxidation of lipids. It has been shown previously that oxidized phospholipid (OxPC) molecules are increased in cardiac tissue in response to Dox treatment and correlate with left ventricular dysfunction [22]. We hypothesized that a cardioprotective agent should decrease relative levels of Dox-induced oxidized phospholipids. We measured the most abundant oxidation products of polyunsaturated phospholipid species present in cardiomyocytes: oxidized forms of three phosphatidylcholines (a class of phospholipids): 1-palmitoyl-2-arachidonoyl-*sn*-glycero-3-phosphocholine (PAPC), 1-palmitoyl-2-linoleoyl-sn-glycero-3-phosphocholine (PLPC), and 1-stearoyl-2-linoleoyl-*sn*-glycero-3-phosphocholine (SLPC).

As shown in Fig.20b, Dox induced formation of a fragmented PLPC (HODA-PPC, 9-hydroxy-12-oxo-10-dodecenoic acid), which was not detectable in controls, an effect that was significantly attenuated by S117A-FGF2. Dox also increased relative levels of PAPC (-OOH), and SLPC (-OH, -OOH); S117A-FGF2 significantly attenuated the Dox-induced increase in the former, Fig.20b, but not the latter oxidized phosphatidylcholine, Fig.20c-d.

In additional analyses, shown in the Supplement (Appendix 8), Dox was found to significantly upregulate PAPC (-OH) and SLPC (-epoxy, -keto), but these changes remained unaffected by S117A-FGF2A. Dox, with or without S117A-FGF2, had no statistically significant effect on PLPC (-keto), PLPC (-OOH), KODA-PPC (PLPC) and SONPC (SLPC).

Figure 16, Non mitogenic (S117A) FGF2 protects cardiomyocytes from Dox toxicity.

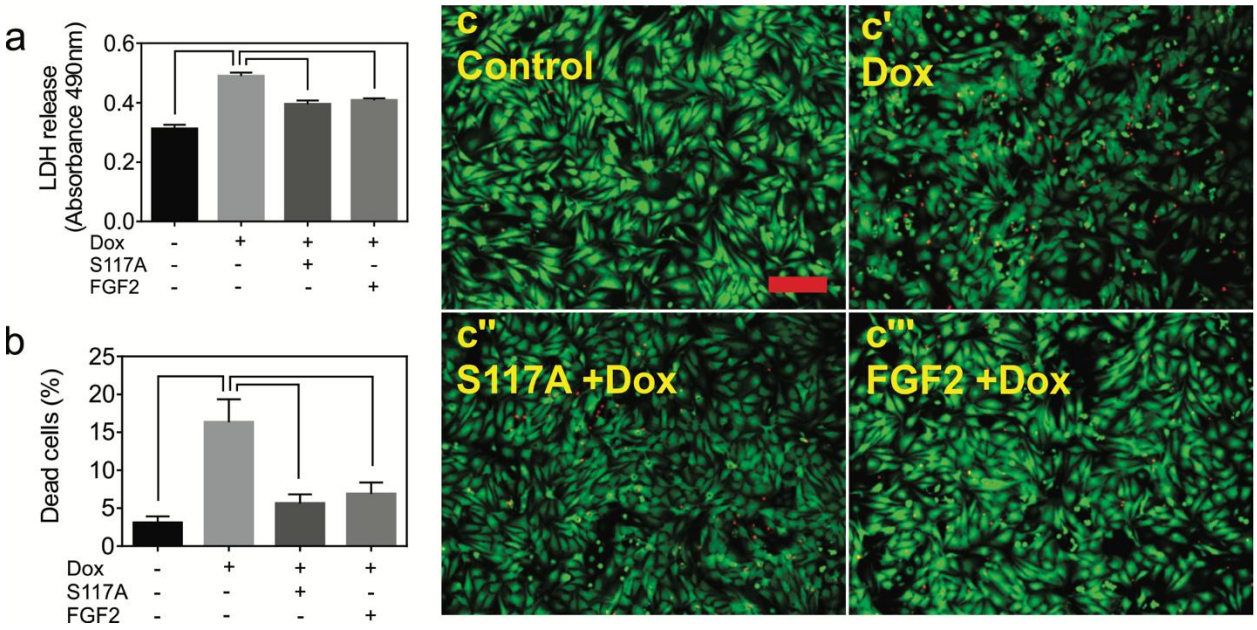

Figure 16. Panel a shows the effect of Doxorubicin (Dox) on LDH released to the medium by cardiomyocytes, as well as the effect of pre-treatment with S117A-FGF2, versus FGF2, on Dox-induced LDH release, as indicated. Panel b shows the effect of Dox on the percentage of dead cells, as measured by the Calcein-AM/Ethidium Homodimer assay; the effect of pretreatment with S117A-FGF2, or FGF2, on Dox-induced cell death is also shown. Representative fluorescence images are included in Panels c-c''', where green or red stain live or dead cells, respectively. Brackets mark groups that differ significantly from each other (n=4), $p < 0.05$.

Figure 17, S117A-FGF2 requires FGFR1 to protect cardiomyocytes against Dox damage.

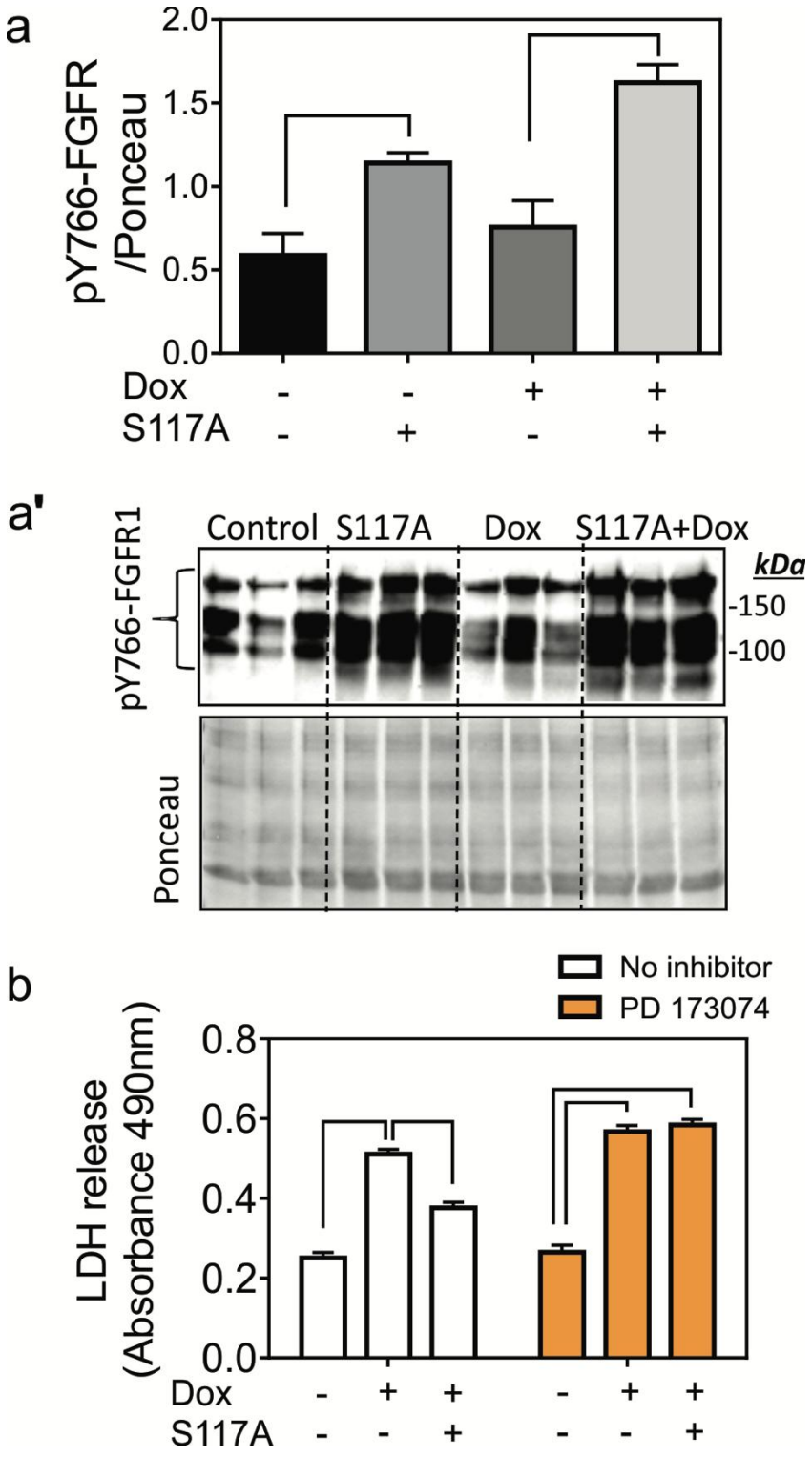

Figure 17. Panel a, shows the effect of S117A-FGF2 on relative pY766-FGFR1 after 30 min cardiomyocyte stimulation, and after Dox exposure for another 30 min. Brackets show groups significantly different from each other (n=3). Images of the corresponding western blot probed for anti-pY766-FGFR1, or stained with Ponceau S are also included (panel a'). Panel b, the effect of PD173074 (FGFR1 inhibitor, 50nM) on S117A-FGF2 protection from Dox-induced LDH release. Brackets point to groups that are significantly different from each other ($p<0.05$). In the presence of PD173074, S117A-FGF2 is unable to reduce Dox-induced LDH release.

Figure 18, The S117A-FGF2 protection from Dox requires ERK activity.

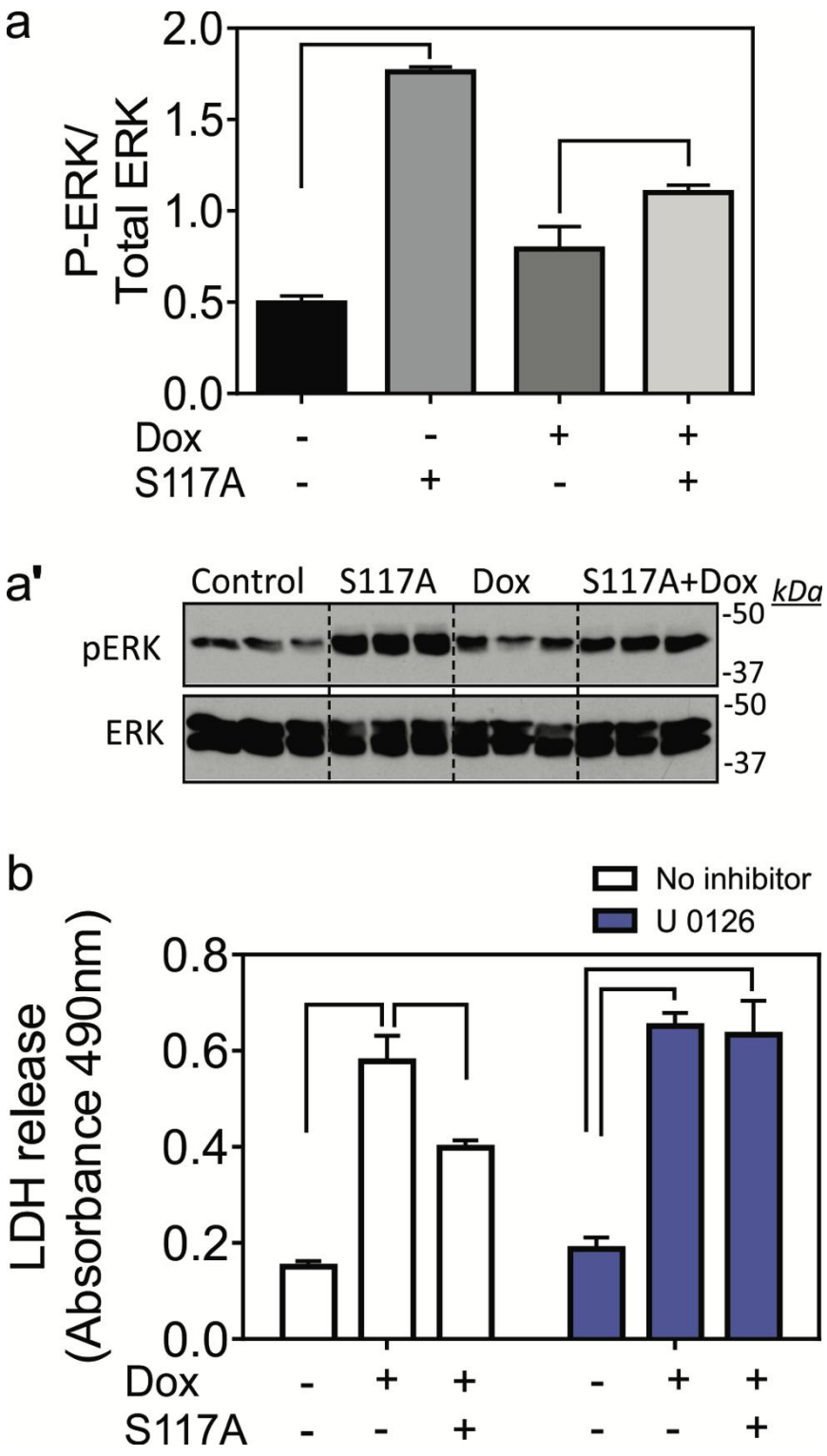

Figure 18. Panel a shows the effect of S117A-FGF2 on pERK/ERK ratio after 30 min cardiomyocyte stimulation, and after Dox exposure for another 30 min. Images of the corresponding western blots probed for anti-pERK or anti-ERK are also included (a', n=3). Panel b. The effect of UO126 (inhibitor of ERK activation, 100nM) on S117A-FGF2 protection from Dox-induced LDH release. Brackets point to groups that are significantly different from each other. In the presence of UO126, S117A-FGF2 is unable to reduce Dox-induced LDH release.

Figure 19, The S117A-FGF2 protection from Dox does not require HO-1 or CK2 activity.

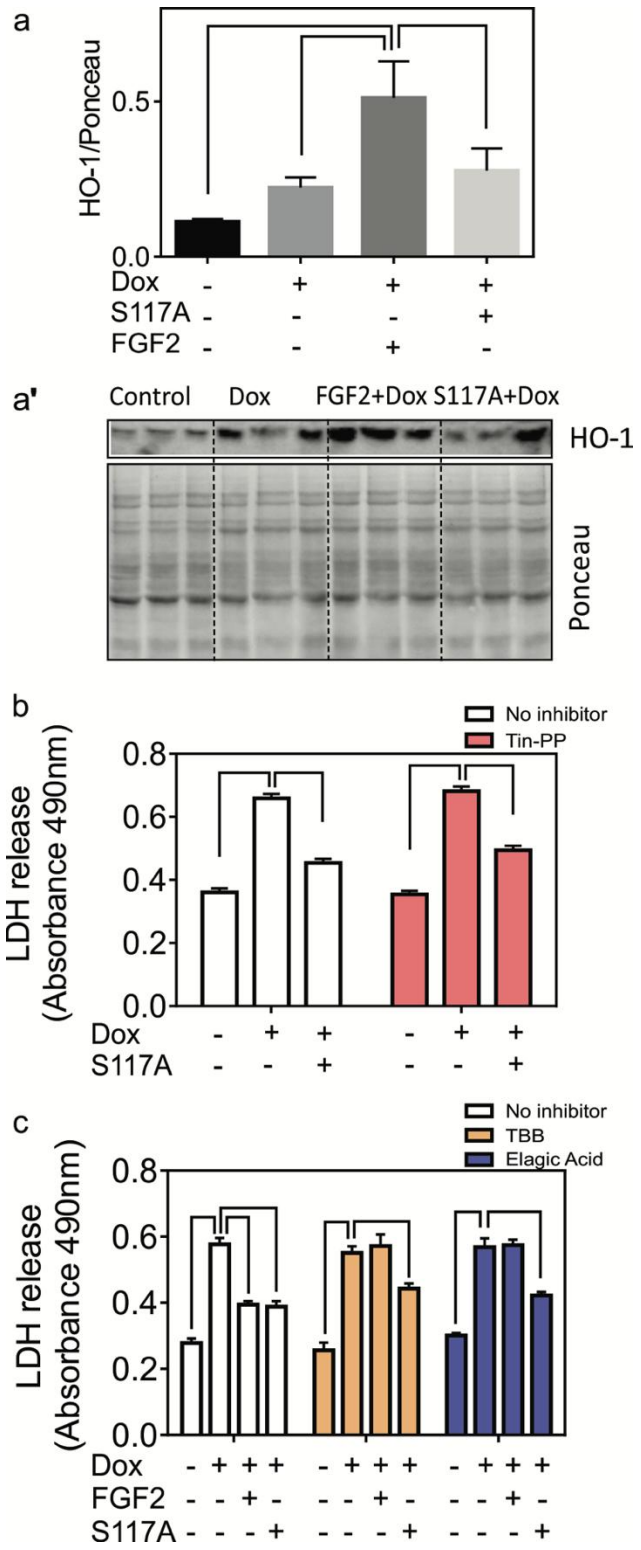

Figure 19. Panel a shows the effect of S117A-FGF2, versus FGF2, on relative HO-1 levels in cardiomyocytes treated with Dox, as estimated by western blotting. Images from the corresponding blot probed for HO-1, or stained with Ponceau S, are also included (a'). Panel b shows the effect of Tin-PP (HO-1 inhibitor, 100 nM) on S117A-FGF2 protection from Dox-induced LDH release, as indicated. Inhibition of HO-1 does not prevent S117A-FGF2 protection. Panel c shows the effect of two CK2 inhibitors, TBB (1μM) or Elagic acid (100nM) , on the protective effect of S117A-FGF2, or FGF2, against Dox-induced LDH release. In the absence of inhibitors, both S117A-FGF2 and FGF2, significantly reduce Dox-induced LDH release. In the presence of either inhibitor, FGF2 is no longer protective, while S117A-FGF2 retains significant protective ability. In all panels, brackets denote groups significantly different from each other ($p<0.05$).

Figure 20, S117A-FGF2 prevents Dox-induced ROS accumulation and oxidation of phosphatidylcholines.

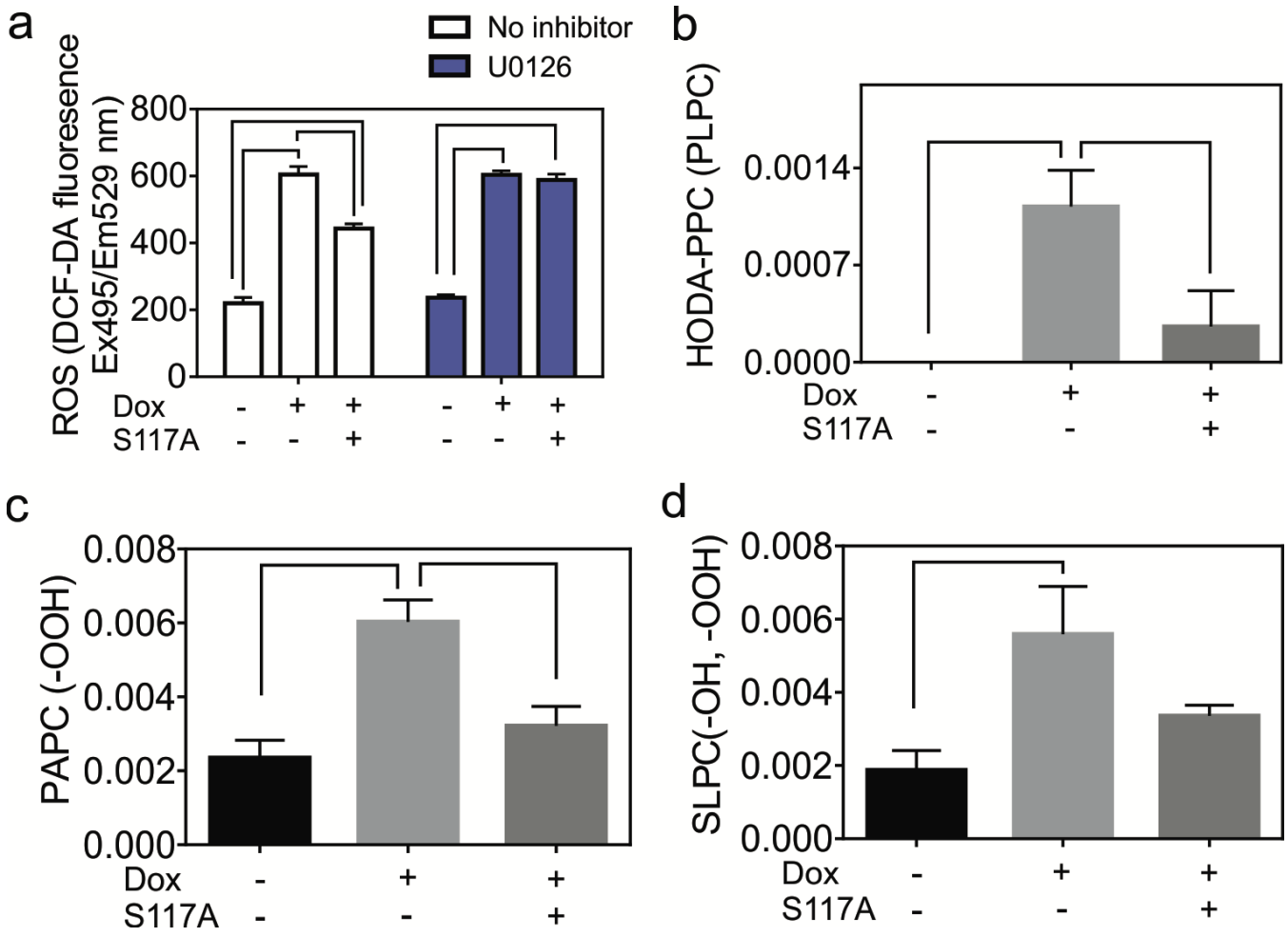

Figure 20. Neonatal rat cardiomyocytes were treated with Dox in the presence and absence of S117A-FGF-2 pre-treatment. Panel a shows the effect of S117A-FGF2 on Dox-induced ROS upregulation as measured by the DCF-DA assay. Panels b-d show levels of oxidized phosphatidylcholine species (HODA-PPC (PLPC); PAPC (-OOH); SLPC (-OH, -OOH)) measured by LC/MS/MS and normalized for protein concentration. The Y-axis in panels b-d shows the amount (ng) of OxPC per μg cardiomyocyte protein. In all panels, brackets denote groups significantly different from each other (n=3 independent analyses, $p<0.05$).

Figure 21, Diagrammatic representation of the proposed signaling mechanisms mediating FGF2 versus S117A-FGF2 protection from dox-induced damage.

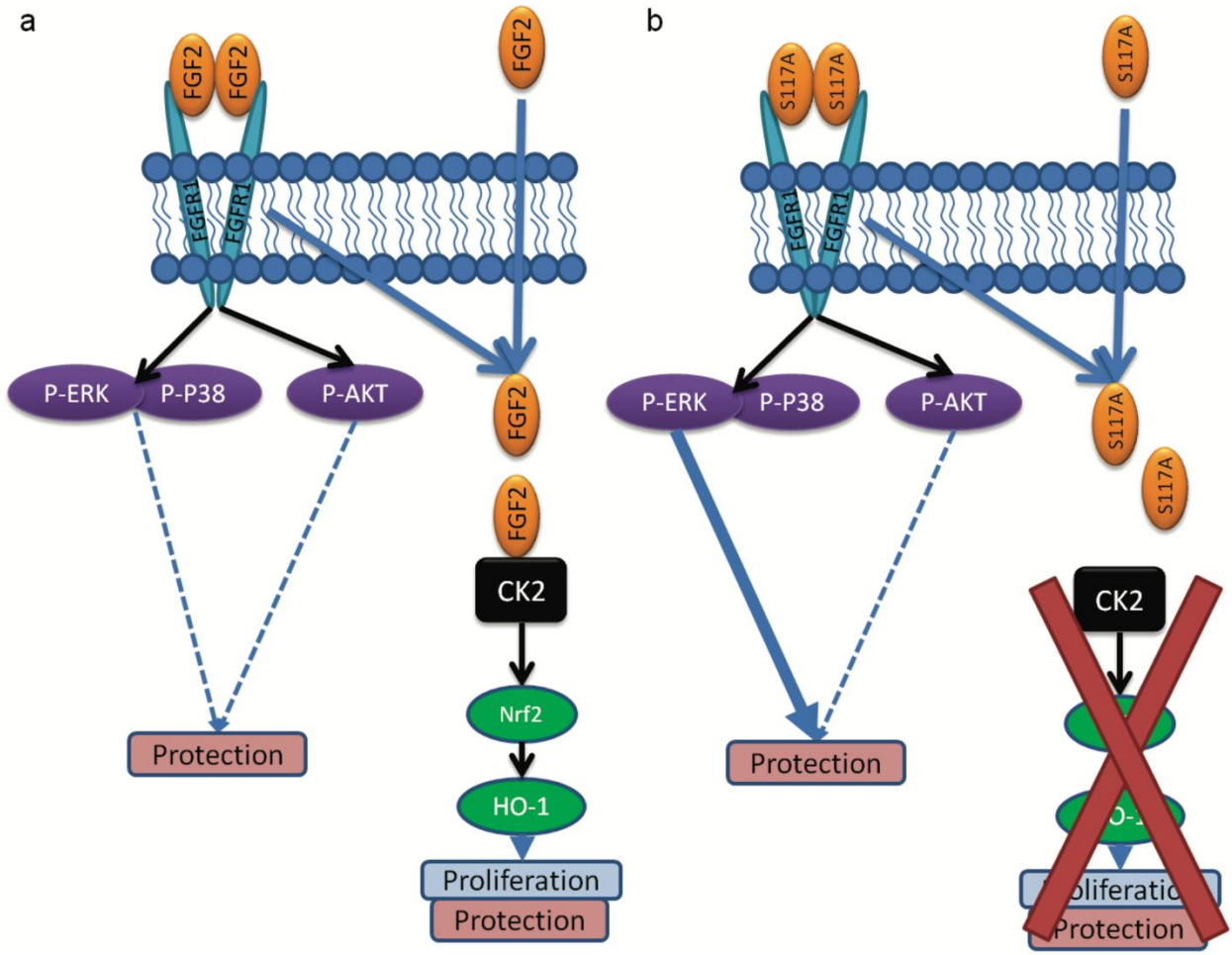

Figure 21. Panel a illustrates signaling by mitogenic FGF2, which activates FGFR1, and downstream kinases implicated in the modulation of cytoprotection, including ERK, p38 and AKT; the dotted lines indicate potential effects based on general literature but not studied here. Internalized FGF2 (via FGFR1-dependent or independent mechanism), interacts with and activates CK2 and CK2-dependent pathways (Nrf2, HO-1) that promote proliferation, and proliferation-linked cytoprotection. Panel b illustrates signaling by S117A-FGF2, which lacks the ability to activate CK2 and the CK2-dependet effects on proliferation. S117A-FGF2 retains the ability to activate FGFR1 and downstream kinases (ERK, p38 and ERK); of these, ERK was shown here to be required for S117A-FGF2 protection in Dox-treated cardiomyocytes.

Discussion

The main findings of this study are: (1) a mutated non-mitogenic form of FGF2, S117A-FGF2, protects cardiomyocytes against acute Dox-induced toxicity, (2) S117A-FGF2 protection is contingent on FGFR1/ERK activation, (3) CK2 and HO-1 are not required for S117A-FGF2 protection, and (4) S117A-FGF2 protects against Dox-induced upregulation of certain oxidized phosphatidylcholines.

Non-mitogenic FGF2 protects cardiomyocytes from Dox-induced toxicity. Our previous studies, documenting the protective potential of FGF2 isoforms against Dox-induced cardiomyocyte injury and cell death, validated the use of LDH release as an overall indicator of cellular damage; the pattern from the LDH release data was paralleled by measurement of % dead cells (live-dead assay) and by the overall reduction in ROS, as well as several other markers associated with cell death [7]. The present study used LDH release as a representative end-point to assess and document protection by non-mitogenic S117A-FGF2 from Dox-induced damage. Results from the LDH release assay were paralleled by the relative reduction in: percentage of dead cells; overall ROS production; reduction in specific OxPC species. Taken together our results demonstrated, for the first time, that S117A-FGF2 protected cardiomyocytes from Dox-induced cellular damage and death, to a similar extent as FGF2, at least in the acute setting (24 h) of our experiment. In a previous study, S117A-FGF2 was found to attenuate the Dox-induced decline in developed pressure of isolated perfused mouse hearts, although no evidence of Dox-induced cellular injury/death was detectable during the two hours of perfusion [23].

Regarding the corresponding mechanism of protection, and as shown previously in different cardiac injury models [11], protection by S117A-FGF2, as by FGF2, required the activation of FGFR1; indeed, as shown here, S117A-FGF2 promoted significant Y766-FGFR1

phosphorylation, and a specific FGFR1 inhibitor blocked S117A-FGF2 protection. ERK is activated downstream of FGFR1, and is considered a cardiac pro-survival kinase [24]. Our results show that non-mitogenic FGF2 depends on FGFR1/ERK signaling for protection against acute Dox toxicity.

A class of chemotherapeutic drugs (for instance Sunitinib) relies on the inhibition of tyrosine kinase receptors such as FGFR1 [25]; S117A-FGF2 which depends on FGFR1 activity for cardioprotection, would therefore not be expected to be cardioprotective in patients receiving these categories of drugs, but would still be useful in anthracycline-based treatments. Localized administration, or gene-therapy based approaches, such as, for example, systemic administration of AAV9-expressing S117A-FGF2, could potentially deliver S117A-FGF2 to the heart and induce protection.

CK2 has been associated with the proliferation and survival of normal, as well as rapidly proliferating cancer cells [26]. FGF2 activates nuclear CK2 which then targets nucleolin; this sequence of events is important to the mitogenic effect of FGF2 [10]. FGF2 triggered activation of CK2 requires internalization of FGF2. In addition, it has been shown that FGF2 can be internalized via FGFR1 dependent and independent (Syndecan-4) pathways [27]. However, it is not as yet determined if FGFR1 activation is needed for FGF2 internalization/CK2 activation in cardiomyocytes. It would appear that CK2 activity is also required for the pro-survival effect of mitogenic FGF2 in our model, since two CK2 inhibitors, TBB and Ellagic acid, eliminated FGF2 protection, as shown here. It is therefore intriguing that S117A-FGF2, which cannot activate CK2, retains pro-survival effects against Dox. This was further validated by our findings that CK2 inhibitors did not block S117A-FGF2 protection. Thus, a CK2-independent pathway, activated in parallel to, or downstream of FGFR1/ERK, mediated protection by the non-

mitogenic S117A-FGF2. Detailed description of the FGF2 versus S117A-FGF2-triggered pathways awaits further studies using systems biology approaches. It would seem, however, that neither AKT nor p38 kinases are responsible for the differences between mitogenic and non-mitogenic FGF2, since they were similarly activated by both.

CK2 can activate the Nrf2 transcription factor and upregulate its downstream target HO-1 in chondrocytes [13]. It is likely that CK2 is also required for the FGF2-induced HO-1 upregulation in Dox-treated cardiomyocytes [7]. Catabolic end-products elicited by the action of HO-1 exert "antioxidant, anti-apoptotic, and immune-modulating effects, leading to overall cytoprotective and beneficial functions" [28] for non-malignant tissues. On the other hand, in the case of cancer, HO-1 is pro-tumorigenic, and causes resistance to anti-cancer drug treatments; inhibition or modulation of HO-1-generating pathways is beneficial in the treatment of leukemias [28]. As we showed here, S117A-FGF2 did not upregulate HO-1, and its ability for acute cardiomyocyte protection against Dox was not blocked by HO-1 inhibition. This reinforces the notion that S117A-FGF2 is an attractive candidate to provide acute cardiac protection from Dox-treatment, as it would not affect cancer cell proliferation and survival via the CK2/HO-1 axis. Our study which showed that S117A-FGF2 did not promote survival or proliferation of the breast cancer cell line MCF-7 supports the therapeutic potential of S117A-FGF2. In addition, our previous studies have demonstrated that S117A-FGF2, unlike FGF2, is incapable of stimulating cardiomyocyte DNA synthesis, measured by the incorporation of bromodeoxyuridine in the genomic DNA [9].

S117A prevents Dox induced upregulation of ROS and OxPC. One of the main mechanisms contributing to Dox cardiotoxicity is increased ROS accumulation which causes DNA and mitochondrial damage, iron toxicity and lipid peroxidation [2]. We found that ERK inhibition

prevented S117A-FGF2- mediated downregulation of Dox-induced ROS accumulation and thus conclude that activation of ERK by S117A-FGF2 (via FGFR1) is a critical step toward its protective antioxidant effects.

Hydroxy radical $OH^{\bullet}$ formed during Dox-induced oxidative and nitrosative stress can cause severe oxidative damage to proteins and DNA and can promote lipid peroxidation. Lipid peroxidation is a chain reaction, mediated by free radicals (mainly $OH^{\bullet}$), leading to structural damages to unsaturated fatty acids of the phospholipids [21]. There is increasing understanding of the importance of oxidized phospholipids in the development of cardiovascular disease [29, 30]. It has been shown that oxidized phospholipids can alter signaling pathways in the cells, induce formation of mitochondrial permeability transition pores leading to cytochrome C release and apoptosis, and act as a signal on the plasma membrane to promote binding of leukocytes [29]. Oxidation can cause a vast number of changes in the structure of fatty acids forming various types of structurally and functionally different biomolecules. In chemotherapy-induced cardiomyopathy OxPC have been shown to correlate with myocardial toxicity, left ventricular dysfunction and cell death [22, 31, 32]. Given the biological activity of OxPC they are not only bystanders of cellular ROS production but also have toxic effects towards cardiomyocytes in a different scenario, reperfusion injury [15, 33, 34].

To our knowledge, the present study shows for the first time that Dox increased several OxPC -containing phospholipids in cardiomyocytes, including PAPC(-OOH), SLPC (-OH, -OOH), and HODAPPC. Protection by S117A-FGF2 was associated with attenuation or prevention of Dox-induced upregulation of these oxidized phosphatidylcholines. It is reasonable to expect that the S117A-FGF2- induced decreases in overall ROS production contributed to decreased production of the OxPC measured, and that decreased ox-phospholipid levels contributed to protection. It is

intriguing that S117A-FGF2 appeared to be selective in protecting against increases of only some of the OxPC species that were upregulated by Dox. The reason for this selectivity is unclear at present but could be explained by hypothesizing that several different signaling pathways, and/or different subcellular sites are involved in the oxidation of the various PC species, and only some of them are accessible to S117A-FGF2 signal transduction.

We have evaluated the protective effects of non-mitogenic FGF2 in an in vitro model of Dox cardiotoxicity. Further experiments are required to validate the protective effects of S117A-FGF2 against Dox in vivo. In addition, short versus long-term effects of S117A-FGF2 treatment in vivo need to be investigated.

In conclusion, we have shown non-mitogenic FGF2 maintains the ability for acute cardioprotection from Dox cardiomyocyte toxicity while lacking characteristics that are undesirable in a cancer environment, such as the potential for CK2 activation and upregulation of HO-1. Our findings reinforce the notion that non-mitogenic FGF2 should be considered as an acute cardioprotective or prophylactic therapy against Dox cardiotoxicity.

Conflict of interest: none declared

References

1. Zamorano, J.L., et al., 2016 ESC Position Paper on cancer treatments and cardiovascular toxicity developed under the auspices of the ESC Committee for Practice Guidelines: The Task Force for cancer treatments and cardiovascular toxicity of the European Society of Cardiology (ESC). Eur Heart J, 2016. 37(36): p. 2768-2801.
2. Koleini, N. and E. Kardami, Autophagy and mitophagy in the context of doxorubicin-induced cardiotoxicity. Oncotarget, 2017. 8(28): p. 46663-46680.
3. van Dalen, E.C., et al., Cardioprotective interventions for cancer patients receiving anthracyclines. Cochrane Database Syst Rev, 2011(6): p. Cd003917.
4. Santiago, J.J., et al., Preferential accumulation and export of high molecular weight FGF-2 by rat cardiac non-myocytes. Cardiovasc Res, 2011. 89(1): p. 139-47.
5. Santiago, J.J., et al., High molecular weight fibroblast growth factor-2 in the human heart is a potential target for prevention of cardiac remodeling. PLoS One, 2014. 9(5): p. e97281.
6. Kardami, E., et al., Fibroblast growth factor-2 and cardioprotection. Heart Fail Rev, 2007. 12(3-4): p. 267-77.
7. Koleini, N., et al., Fibroblast growth factor-2-mediated protection of cardiomyocytes from the toxic effects of doxorubicin requires the mTOR/Nrf-2/HO-1 pathway. Oncotarget, 2017. 8(50): p. 87415-87430.
8. Li, D., et al., Dual blockade of vascular endothelial growth factor (VEGF) and basic fibroblast growth factor (FGF-2) exhibits potent anti-angiogenic effects. Cancer Lett, 2016. 377(2): p. 164-73.

9. Jiang, Z.S., et al., Non-angiogenic FGF-2 protects the ischemic heart from injury, in the presence or absence of reperfusion. Cardiovasc Res, 2004. 62(1): p. 154-66.
10. Bailly, K., et al., Uncoupling of cell proliferation and differentiation activities of basic fibroblast growth factor. Faseb j, 2000. 14(2): p. 333-44.
11. Jiang, Z.S., et al., Acute protection of ischemic heart by FGF-2: involvement of FGF-2 receptors and protein kinase C. Am J Physiol Heart Circ Physiol, 2002. 282(3): p. H1071-80.
12. Feng, D., et al., Protein kinase CK2 is a regulator of angiogenesis in endometriotic lesions. Angiogenesis, 2012. 15(2): p. 243-52.
13. Kim, K.M., et al., Protein kinase CK2 mediates peroxynitrite-induced heme oxygenase-1 expression in articular chondrocytes. Int J Mol Med, 2012. 29(6): p. 1039-44.
14. Folch, J., M. Lees, and G.H. Sloane Stanley, A simple method for the isolation and purification of total lipides from animal tissues. J Biol Chem, 1957. 226(1): p. 497-509.
15. Ganguly, R., et al., Alpha linolenic acid decreases apoptosis and oxidized phospholipids in cardiomyocytes during ischemia/reperfusion. Mol Cell Biochem, 2018. 437(1-2): p. 163-175.
16. Torzewski, M., et al., Lipoprotein (a)-Associated Molecules Are Prominent Components in Plasma and Valve Leaflets in Calcific Aortic Valve Stenosis. JACC: Basic to Translational Science, 2017. 2(3): p. 229-240.
17. Liu, L., et al., Adult cardiomyocytes express functional high-affinity receptors for basic fibroblast growth factor. Am J Physiol, 1995. 268(5 Pt 2): p. H1927-38.
18. Kardami, E., et al., Regulation of basic fibroblast growth factor (bFGF) and FGF receptors in the heart. Ann N Y Acad Sci, 1995. 752: p. 353-69.

19. Ornitz, D.M. and N. Itoh, The Fibroblast Growth Factor signaling pathway. Wiley Interdiscip Rev Dev Biol, 2015. 4(3): p. 215-66.
20. Katoh, M., FGFR inhibitors: Effects on cancer cells, tumor microenvironment and whole-body homeostasis (Review). Int J Mol Med, 2016. 38(1): p. 3-15.
21. Damiani, R.M., et al., Pathways of cardiac toxicity: comparison between chemotherapeutic drugs doxorubicin and mitoxantrone. Arch Toxicol, 2016. 90(9): p. 2063-76.
22. Zeglinski, M., et al., Congenital absence of nitric oxide synthase 3 potentiates cardiac dysfunction and reduces survival in doxorubicin- and trastuzumab-mediated cardiomyopathy. Can J Cardiol, 2014. 30(3): p. 359-67.
23. Sontag, D.P., et al., FGF-2 and FGF-16 protect isolated perfused mouse hearts from acute doxorubicin-induced contractile dysfunction. Cardiovasc Toxicol, 2013. 13(3): p. 244-53.
24. Hausenloy, D.J., et al., Ischemic preconditioning protects by activating prosurvival kinases at reperfusion. Am J Physiol Heart Circ Physiol, 2005. 288(2): p. H971-6.
25. Chu, T.F., et al., Cardiotoxicity associated with tyrosine kinase inhibitor sunitinib. Lancet, 2007. 370(9604): p. 2011-9.
26. Trembley, J.H., et al., Protein kinase CK2 in health and disease: CK2: a key player in cancer biology. Cell Mol Life Sci, 2009. 66(11-12): p. 1858-67.
27. Tkachenko, E., et al., Fibroblast growth factor 2 endocytosis in endothelial cells proceed via syndecan-4-dependent activation of Rac1 and a Cdc42-dependent macropinocytic pathway. J Cell Sci, 2004. 117(Pt 15): p. 3189-99.
28. Salerno, L., et al., Heme oxygenase-1: A new druggable target in the management of chronic and acute myeloid leukemia. Eur J Med Chem, 2017. 142: p. 163-178.

29. Salomon, R.G., Structural identification and cardiovascular activities of oxidized phospholipids. Circ Res, 2012. 111(7): p. 930-46.

30. Allen, D., D. Hasanally, and A. Ravandi, Role of oxidized phospholipids in cardiovascular pathology. Clinical Lipidology, 2013. 8(2): p. 205-215.

31. Bordun, K.A., et al., The utility of cardiac biomarkers and echocardiography for the early detection of bevacizumab- and sunitinib-mediated cardiotoxicity. Am J Physiol Heart Circ Physiol, 2015. 309(4): p. H692-701.

32. Goyal, V., et al., The Cardioprotective Role of N-Acetyl Cysteine Amide in the Prevention of Doxorubicin and Trastuzumab-Mediated Cardiac Dysfunction. Can J Cardiol, 2016. 32(12): p. 1513-1519.

33. White, C.W., et al., A whole blood-based perfusate provides superior preservation of myocardial function during ex vivo heart perfusion. J Heart Lung Transplant, 2015. 34(1): p. 113-21.

34. White, C.W., et al., A cardioprotective preservation strategy employing ex vivo heart perfusion facilitates successful transplant of donor hearts after cardiocirculatory death. J Heart Lung Transplant, 2013. 32(7): p. 734-43.

Chapter III: The effect of FGF2 isoforms on cardiac pressure overload-induced changes

Rationale and Hypothesis

In the previous sections we provided evidence that Hi-FGF2 plays a pathological role in the development of systolic dysfunction in response to a genotoxic drug. Next, we examined whether Hi-FGF2 could contribute to other cardiac pathologies, such as pressure overload-associated cardiac functional and structural changes (remodeling), using the Hi-FGF2 knockout mice. Cardiac remodeling in response to pressure overload results in debilitating heart failure. Despite improvement in the morbidity and mortality by current treatments, pressure overload induced heart failure is still a global concern

Hypothesis.

Hi-FGF2 promotes maladaptive cardiac changes in response to pressure overload.

Genetic elimination of high molecular weight FGF2 prevents pressure overload-induced cardiac systolic dysfunction and implicates a beneficial effect of HSP70 and circadian rhythm modulation

Navid Koleini[1,2], Barbara E Nickel[1], Raghu S Nagalingam[1,2], Natalie M Landry[1,2], Robert R Fandrich[1], Ian M Dixon[1,2], Michael Czubryt[1,2], Davinder Jassal[1,3], Peter A Cattini[2], Elissavet Kardami[1,2,4]

1: Institute of Cardiovascular Sciences, St. Boniface Hospital Albrechtsen Research Centre. 351 Tache Ave, Winnipeg, Manitoba, Canada, R2H2A6

2: Department of Physiology & Pathophysiology, University of Manitoba, Winnipeg, Canada

3: Interventional Cardiology, Section of Cardiology, Max Rady College of Medicine, University of Manitoba

4: Department of Human Anatomy and Cell Sciences, University of Manitoba, Winnipeg, Canada

Corresponding author:

Dr. Elissavet Kardami

St. Boniface Hospital Albrechtsen Research Centre

351 Tache Ave,Winnipeg, Manitoba, R2H 2A6

Email: ekardami@sbrc.ca, Tel: +1 (204) 235 3519, Fax:+1 (204) 233 6723

Abstract

Fibroblast growth factor 2 (FGF2) is produced as high and low molecular weight isoforms in the heart. While endogenous low molecular weight FGF2 (Lo-FGF2) is cardioprotective, the more abundant high molecular weight FGF2 (Hi-FGF2) is proposed, based on *in vitro* studies, to promote maladaptive cardiac remodeling. To investigate the *in vivo* role of endogenous Hi-FGF2, the effect of transverse aortic constriction (TAC) surgery was compared in Hi-FGF2 knock-out mice [FGF2(Lo)], expressing only Lo-FGF2 and wild type mice [FGF2(WT)] expressing both Hi-FGF2 and Lo-FGF2. By echocardiography, TAC surgery induced a decline in systolic function in FGF2(WT) but not in FGF2(Lo) mice at 4- and 8-weeks post-TAC, when compared to corresponding sham-operated animals. TAC surgery increased levels of markers of myocardial stress/damage such as B-type natriuretic peptide and the pro-cell death protein BCL2/adenovirus E1B 19 kDa protein-interacting protein-3 in FGF2(WT) but not FGF2(Lo) mice. TAC induced a Hi-FGF2-independent increase in cardiac mass (heart weight/tibia length) and fibrosis (relative picrosirius red staining of tissue sections). Increased cardiomyocyte size, however, was only observed in FGF2(WT) but not FGF2(Lo) hearts post-TAC; increased expression of cyclin D2 in FGF2(Lo) hearts suggested that absence of Hi-FGF2 favors cell cycle stimulation. Based on microarray analysis and subsequent validation, the absence of Hi-FGF2 was also associated with upregulation of cardioprotective heat shock protein 70 (HSP70) as well as, post-TAC surgery, the circadian rhythm modulator Nuclear Receptor Subfamily 1 Group D Member 1 (NR1D1) mRNA and protein in FGF2(Lo) mice. Thus, a role for increased HSP70 and NR1D1 levels is proposed in the improved post-TAC outcome in mice expressing only Lo-FGF2.

Key words: Endogenous high molecular weight fibroblast growth factor 2; pressure overload remodeling; cardioprotection; HSP70; circadian rhythm modulation; NR1D1

Introduction

Heart failure is associated with significant morbidity and mortality and presents a substantial socio-economic burden in the Western world, especially in an aging population [1]. Pressure overload, in addition to ischemic heart disease and diabetes, are the most common causes of heart failure [2, 3]. Pressure overload is a state in which ventricular wall tension increases where compensatory mechanisms result in increased wall thickness (hypertrophy) to overcome the excess tension, according to the law of Laplace [4]. Mechanical stress, neurohormonal stimulation, as well as upregulation of local and systemic growth factors and vasoactive agents lead to pressure overload-induced cardiac remodeling and eventually, heart failure [5]. Overstimulation of adrenergic and renin-angiotensin-aldosterone pathways leads to increased tension, which is sensed by mechanoreceptors, causing downstream activation of fetal gene reprogramming and cardiac/cardiomyocyte hypertrophy; this initially adaptive response eventually becomes maladaptive, and leads to heart failure [6]. In chronic pressure overload, extracellular matrix remodeling and ongoing fibrosis contribute to diastolic dysfunction [7]. Despite extensive use of renin-angiotensin system inhibitors for preventing the progression to heart failure, morbidity and mortality rates are still high [8]. It is important to identify additional factors involved in cardiac remodeling to potentially augment the efficacy of current treatments, and Fibroblast Growth Factor 2 (FGF2) may be one such factor.

FGF2 is expressed as high molecular weight (>22KDa, Hi-FGF2) and low molecular weight (18kDa) isoforms (Lo-FGF2) [9], representing 70% and 30% of total cardiac FGF2, respectively [10]. Lo-FGF2, has been established as a cardioprotective agent [11, 12]. Conversely, Hi-FGF may oppose some of the beneficial effects of Lo-FGF2; we have recently reported that endogenous Hi-FGF2 contributes to chemotherapy induced cardiotoxicity in a

mouse model, and that genetic elimination or antibody-based neutralization of Hi-FGF2 might confer cardioprotection against genotoxic agents [13]. *In vitro* studies suggested that paracrine-acting Hi-FGF2, but not Lo-FGF2, induces cardiomyocyte hypertrophy [10] and a pro-fibrotic phenotype in cardiac fibroblasts [10]. Because cardiac hypertrophy and fibrosis are characteristics of pressure overload-induced maladaptive remodeling, we investigated the effect of Hi-FGF2 knockout on cardiac response to transverse aortic constriction (TAC) surgery-induced pressure overload, as well as on the cardiac transcriptome. Here, we provide evidence that genetic elimination of Hi-FGF protected mice from TAC-induced systolic dysfunction and myocardial damage but did not prevent the development of cardiac fibrosis or cardiac mass increase. It did, however, prevent increases in cardiomyocyte size. Analysis of select markers, as well as of the whole transcriptome, suggested that elimination of Hi-FGF2 is beneficial by allowing the upregulation of HSP70, and the post-TAC increase in the circadian rhythm modulator, NR1D1.

Materials and Methods

Animals. This study was conducted according to the NIH Guide for the Care and Use of Laboratory Animals (NIH Publication, 8th Edition. Revised 2011). Approval was obtained from the Protocol Management and Review Committee of the University of Manitoba (#15-050). Mice, genetically engineered as to lack expression of Hi-FGF2 thus only expressing endogenous Lo-FGF2, ($Fgf2^{tm3Doe}$), referred to as FGF2(Lo), as well as wild type C57BL/6J mice, [FGF2(WT)], were purchased from Jackson laboratories. The $Fgf2^{tm3Doe}$ mice were originally generated and characterized by Doetschman and colleagues [14] and bred into the C57BL/6J genetic background at Jackson Laboratories. The two groups are referred to as FGF(Lo) and FGF2(WT) mice. Our studies were conducted on male mice, since our previous work indicated lack of sex-related differences in cardiac response to another type of stress, doxorubicin toxicity [13].

Transverse aortic constriction (TAC) surgery: Eight-week-old male mice were subjected to TAC or sham surgery in the R.O. Burrel Lab, St. Boniface Hospital Research Centre. A midline incision was made from the salivary gland region extending to the 3rd rib. The manubrium was cut following the sternum as closely as possible and the first and second ribs were cut. The chest was opened 1 cm using a retractor. Thymus was moved gently to expose the transverse aorta. A blunted 27-gauge needle was placed next to the aorta and 7/0 silk was used to ligate the needle and aorta. The needle was then carefully removed. The chest was closed using a simple interrupted suture pattern aligning the ribs using 5-0 absorbable suture.

After 4- or 8-weeks of TAC or sham surgery, mice were euthanized humanely by administering ketamine (150 mg/kg) and xylazine (10 mg/kg) intraperitoneally for induction of deep terminal anesthesia. Hearts were then collected for weighing and biochemical analyses. Heart weight

(WT), body weight (BW), and tibia length (TL) were determined for sham and TAC groups at all time points.

Echocardiography. Murine echocardiography was performed at baseline, 4- and 8-weeks post-surgery, as described previously in detail [13, 15, 16].

RNA extraction: RNA was extracted from frozen heart tissues using the Monarch Total RNA Miniprep Kit (New England Biolabs, T2010S) as per manufacturer's instructions. Briefly, frozen hearts were crushed into pieces (5-10 mg). One piece per heart was submerged in the RNA protection buffer and then homogenized using Bel-Art™ SP Scienceware™ disposable polypropylene pestles. Protein digestion was done using proteinase K at 56°C for 10 minutes. Genomic DNA was removed by centrifuging over columns provided in the kit. The flow-through was spun to bind RNAs to the columns and further washed using the RNA wash buffer. Further genomic DNA removal was done by enzymatic digestion using DNAase for 15 minutes at room temperature. Columns were further washed using "RNA prime" and "RNA wash" buffers to eliminate contaminants. Nucleotide free water (100 µL) was used to elute RNA. RNA concentration was measured using a Nanodrop Spectrophotometer Lite spectrophotometer (Thermo Scientific).

cDNA synthesis: First strand cDNA was synthesized using qScript™ cDNA SuperMix, QuantaBio (#95048) as per manufacturer's instructions.

qPCR: Quantitative PCR**:** Sample messenger RNA levels were measured using QuantStudio™ 3 thermocycler (Applied Biosciences), using the fast cycling mode. Luna® Universal qPCR Master Mix (New England Biolabs, M3003L) and specific primers at a final concentration of 200 nM were used to amplify the targets. A complete list of primers can be found in the appendix 9.

Microarray analysis: The GeneChip™ Mouse Gene 2.0 ST Array (Affymetrix, 902119) was used to evaluate the whole-transcriptome profile of messenger and long non-coding RNA in samples. RNA samples of FGF2(WT) and FGF2(Lo) mouse hearts taken at 8 weeks post-TAC or -sham surgery (n=3/ per group). Samples were sent to The Centre for Applied Genomics (Hospital for Sick Children, Toronto ON, Canada) for microarray analysis. Transcriptome Analysis Console software (Thermofisher version 4.0.1) was used to analyze the data.

Protein extraction and immunoblotting (western blot): Hearts were collected, snap frozen in liquid nitrogen, and stored at -80°C at the end of the *in vivo* study. Protein was extracted as previously described [13]. The protein lysates were subjected to sodium dodecyl sulphate polyacrylamide gel electrophoresis for separation (20 μg/lane). The gels were transferred to polyvinylidene difluoride membranes. Antibodies for NR1D1 (#13418), rodent Bnip3 (#3769), and HSP70 (#4872) were purchased from Cell Signaling Technology. Densitometry values from bands on the western blots were corrected for loading variations based on the corresponding Ponceau S staining of the whole lane on the transfer membrane.

Picrosirius Red Staining of Cardiac Tissue Sections: Hearts were frozen in Optimal cutting temperature compound (Fisher Healthcare™ Tissue-Plus™ O.C.T. Compound, #4585) according to the manufacturer protocols. Tissue blocks were sectioned (7μm thickness) using Cryostat Microm HM550 - 388114 - Thermo Fisher Scientific and mounted on glass slides. Direct Red 80 (#365548 Sigma-Aldrich) was used according to the manufacturer protocols to stain collagen fibers in the sections.

Statistical analysis: Grouped analyses were performed using two-way ANOVA with Fisher's Least Significant Difference (LSD) *post-hoc* test or one-way ANOVA with Tukey *post-hoc* test.

Student's T-test was used in pairwise comparisons, as required. All statistical analyses were performed using GraphPad Prism 7 software, and $P < 0.05$ was considered as statistically significant. For *in vivo* echocardiography recordings, data were obtained from 10-20 mice per group, unless otherwise indicated.

Results

The effect of endogenous Hi-FGF2 on post-TAC cardiac function and damage

TAC surgery was used to induce pressure overload injury in FGF2(Lo) mice lacking Hi-FGF2 and expressing only the Lo-FGF2 isoform and compared to the effect seen in wild type FGF2(WT) mice. These wild type mice express endogenous levels of Hi- and Lo-FGF2, representing 70% and 30% of total endogenous FGF2, respectively [10]. Sham surgery was used in parallel to provide TAC-independent values (sham controls) for each group. No mortality was observed in any of the groups. Echocardiographic assessment of cardiac function was obtained at baseline and at 4- and 8-weeks post-surgery. No difference in the echocardiographic parameters measured was observed between the FGF2(WT) and FGF2(Lo) groups under baseline, non-stress conditions, in agreement with our previous study [13].

For each mouse strain comparisons were made between animals subjected to TAC versus those subjected to sham surgery. Left ventricular ejection fraction (LVEF) showed a statistically significant decrease in the FGF2(WT) mice at 4- and 8-weeks post-TAC; no decline in LVEF was observed for the FGF2(Lo) mice at any time point (Fig 22a). Left ventricular end systolic diameter (LVESD) increased in FGF2(WT) but not FGF2(Lo) mice at 8 weeks post-TAC (Fig 22b). Thus, systolic function was preserved in the FGF2(Lo) mice up to 8 weeks post-TAC. In addition, heart rate decreased in FGF2(WT) at 8 weeks post-TAC, by 46 beats/min (Fig 22c), suggesting eventual transition to uncompensated heart failure. Heart rate did not change in FGF2(Lo) mice.

Diastolic function parameters such as Tissue Doppler Index (TDI) and Strain Rate (SR) declined after 4- and 8-weeks post-TAC in both FGF2(WT) and FGF2(Lo) mice (Fig 23a and b).

Posterior wall thickness (PWT) increased in the FGF2(WT) mice at 4 and 8 weeks as well as in the FGF2(Lo) mice at 8 weeks (Fig 23c).

Increased brain natriuretic peptide (BNP) levels due to pressure overload represent an indicator of severity of myocardial stress [17]. Cardiac BNP mRNA was increased in FGF2(WT), but not FGF2(Lo) post-TAC compared to corresponding sham surgery control mice (Fig 24a, c). The pro-cell death protein BCL2/adenovirus E1B 19 kDa protein-interacting protein 3 (Bnip3), which can be considered as an indicator of mitochondrial and cardiac damage leading to cell death, was upregulated in FGF2(WT) but not FGF2(Lo) post-TAC hearts (Fig 24b). Overall, these results indicate that elimination of Hi-FGF2 confers protection from a TAC-induced decline in systolic function and heart rate and attenuates stress-induced myocardial responses as estimated by relative BNP (mRNA) and Bnip3 (protein) levels.

Effects of endogenous Hi-FGF2 on cardiac fibrosis, mass, and myocyte size

TAC surgery promotes matrix remodeling and fibrosis as well as cardiomyocyte and cardiac hypertrophy [18]. The effect of eliminating Hi-FGF2 on the presence and/or extent of fibrosis post-TAC was examined. Picrosirius red staining of heart sections was used to detect fibrotic tissue. Relative extent of picrosirius red staining increased to a similar degree in both FGF2(WT) and FGF2(Lo) mice compared to their sham surgery littermate controls at 8-weeks post-TAC (Fig 25). Perivascular as well as interstitial fibrosis were detected in both FGF2(WT) and FGF2(Lo) hearts post-TAC.

The PWT echocardiography data indicated increased myocardial thickness regardless of the presence of Hi-FGF2 at 8 weeks post-TAC (Fig 23). To assess cardiac hypertrophy, heart weight normalized to tibial length (HW/TL) or to body weight (HW/BW) were measured.

HW/TL as well as HW/BW increased to a similar extent in both FGF2(WT) and FGF2(Lo) mice at 4- and 8-weeks post-TAC (Fig 26a and b) suggesting increased myocardial mass. Cardiomyocyte surface area in cross-sections from hearts at 8-weeks post-TAC were examined as an indication of whether increased cardiac mass was reflective of increased cardiomyocyte size (hypertrophy). Myocyte cross-sectional surface area showed a statistically significant increase in FGF2(WT) but not FGF2(Lo) mice post-TAC (Fig 26c). Together these findings indicate that the increased heart mass in FGF(WT) mice is reflective of hypertrophy at the cellular, cardiomyocyte, level.

In the absence of measurable cardiomyocyte hypertrophy post-TAC in Hi-FGF2-depleted hearts, the possibility that the increase in cardiac mass is a result of increased cardiomyocyte number was pursued. An increase in cell number may result from elevated proliferation and/or protection from cell death. Thus, differential expression of genes associated with stimulation and inhibition of the cardiomyocyte cell cycle was assessed in FGF(WT) versus FGF2(Lo) mice post-TAC. It has been proposed that the interplay between cell cycle stimulators (such as cyclins) and inhibitors (such as p21 $^{WAF1/CIP1}$) could determine the balance between a hypertrophic or hyperplastic cardiomyocyte response to a common stimulus [19, 20]. Relative cardiac mRNA levels of the cell cycle activator cyclin D2 increased 3.8-fold ($p=0.03$) in the FGF2(Lo) but not the FGF2(WT) hearts at 8 weeks post-TAC (Fig 27a). Relative cardiac mRNA levels for the cell cycle inhibitor p21 $^{WAF1/CIP1}$ increased 2.9-fold ($p=0.02$) in FGF2(WT) mice (Fig 27b). A statistically significant change in p21 was not observed in FGF2(Lo) hearts post-TAC; however, variability between values was substantial in this group (Fig 27b).

Effects of Hi-FGF2 and TAC on the cardiac transcriptome

Whole-transcriptome analysis of FGF2(WT) and FGF2(Lo) mice was conducted at 8 weeks post TAC or sham surgery (n=3). Gene expression analysis was conducted using a mouse gene 2.0 ST microarray. Firstly, to detect differences unrelated to TAC, comparisons were made between sham operated FGF2(WT) and FGF2(Lo) mice. Amongst 34,472 transcript probes, 118 genes were differentially expressed in total, of which 67 genes were upregulated and 51 downregulated in FGF2(Lo) compared to the FGF2(WT) mice.

Table 2 shows a list of genes expressed at different levels depending on the presence or absence of endogenous Hi-FGF2, in non-stressed (sham surgery) animals; the Table contains differences greater than 2.5-fold (±) with a p-value <0.05. The most upregulated mRNAs in the absence of endogenous Hi-FGF2 include: the heat shock protein 1B and 1A (otherwise known as HSP70), which is implicated in cardioprotection [21]; the membrane solute carrier family 6, member 16, involved in the transport of amino-acids or amino-acid like substances [22]; the aryl hydrocarbon receptor nuclear translocator-like (*ARNTL*), a core component of the circadian clock [23]; and the natriuretic peptide type A (*NppA*, or ANP), considered beneficial against heart failure due to its vasodilatory and anti-cardiomyocyte hypertrophy properties [24]. In addition, nuclear receptor, *NR4A1* (or Nur77) showed a 2-fold upregulation (p=0.003) in the absence of Hi-FGF2. Studies have shown that increased expression of Nur77 in cardiomyocytes is protective against apoptosis [25]. The mRNAs expressed at higher levels in the presence of Hi-FGF2 include those coding for the Ras-like small G-protein *RAB6b* (a protein proposed to regulate intracellular trafficking of adrenergic receptors [26]), the chemokine (C-X-C motif) ligand 9, *CXCL9*, involved in tissue inflammation [27], and the nuclear receptor subfamily 1 group D member 1 (*NR1D1*), a transcriptional suppressor and a modulator of the circadian clock [28]. Gene set enrichment analysis by Enrichr using KEGG 2019 Mouse database (taking into

consideration the fold change(log10)) predicted the circadian rhythm-associated pathway (*NR1D1* and *ARNTL*) as the main difference between FGF2(WT) and FGF2(Lo) mice.

Table 2, list of genes expressed at different levels depending on the presence or absence of endogenous Hi-FGF2, in non-stressed (sham surgery) animals.

Fold Change FGF2(Lo) vs FGF2(WT)	P-value	Gene Symbol	Description
6.37	2.00E-04	Hspa1b; Hspa1a	heat shock protein 1B; heat shock protein 1A
5.59	1.28E-06	Slc6a16	solute carrier family 6, member 16
4.13	4.00E-04	Hspa1a	heat shock protein 1A
3.92	6.61E-06	Arntl	aryl hydrocarbon receptor nuclear translocator-like
3.84	9.36E-05	Abhd1	abhydrolase domain containing 1
3.39	1.34E-02	Bex1	brain expressed gene 1
2.99	0.0019	Nppa	natriuretic peptide type A
2.93	0.0021	Atp10d	ATPase, class V, type 10D
2.6	0.0005	Spon2	spondin 2, extracellular matrix protein
2.57	0.0311	Nrn1	neuritin 1
2.55	0.0232	Snord45b; Rabggtb	small nucleolar RNA, C/D box 45B; Rab geranylgeranyl transferase, b subunit
2.54	0.0002	Mboat2	membrane bound O-acyltransferase domain containing 2
2.54	0.0249	Fam188b2-ps	family with sequence similarity 188, member B2, pseudogene
2.52	0.0449	Cyp4b1-ps2	cytochrome P450, family 4, subfamily b, polypeptide 1, pseudogene 2
2.52	0.0125	Hsph1	heat shock 105kDa/110kDa protein 1
-2.51	0.0039	Tcap	titin-cap
-2.58	0.0028	Traj16; Trav4d-4	T cell receptor alpha joining 16; T cell receptor alpha variable 4D-4
-2.59	0.0001	Bst2	bone marrow stromal cell antigen 2
-2.73	0.0343	Rpl12-ps1	ribosomal protein L12, pseudogene 1
-2.8	0.0024	Ptges3l	prostaglandin E synthase 3 (cytosolic)-like
-3.15	8.36E-05	Dbp	D site albumin promoter binding protein
-3.52	2.00E-04	Nr1d1	nuclear receptor subfamily 1, group D, member 1
-3.76	2.84E-05	Zbtb16	zinc finger and BTB domain containing 16
-3.99	3.50E-03	Cxcl9	chemokine (C-X-C motif) ligand 9
-4.56	2.53E-07	Rab6b	RAB6B, member RAS oncogene family

To validate selected microarray results, relative levels of *HSP70*, *Nur77*, *ANP*, *RAB6b*, and *CXCL9* mRNA were assessed by qPCR. Relative cardiac protein levels for HSP70 and NR1D1 were also assessed by western blotting of cardiac lysates. Increases in HSP70 mRNA and protein in the absence of Hi-FGF2 were confirmed, as seen by comparing FGF2(Lo)-sham to FGF2(WT)-sham surgery values (Fig.28a,b); the HSP70 protein is upregulated after TAC in both groups but significantly more so in the absence of Hi-FGF2 (Fig 28b; see also appendix 10). The mRNA for *Nur77* was also significantly upregulated 6-fold in the absence of Hi-FGF2 (Fig 28c). An increase in ANP mRNA is also suggested but did not reach significance (p=0.06), Fig.28d. The mRNA levels for *RAB6B* and *CXCL9* were found to be higher in FGF2(WT) compared to FGF2(Lo) mice (Fig 28e and f). Relative levels of cardiac *NR1D1* mRNA and protein were both expressed at lower levels in non-stressed FGF2(Lo) compared to FGF2(WT) mice (Fig.29a). In addition, observed differences in *RAB6B*, and *NR1D1* mRNA levels were maintained *in vitro*: FGF2(WT)-derived embryonic fibroblasts expressed higher levels of levels of *RAB6B*, and NR1D1 mRNA compared to those from FGF2(Lo) mice (Appendix 11).

Transcriptome comparisons were made between sham and TAC mice within each mouse strain; several transcripts were changed by TAC in a similar manner regardless of the expression of Hi-FGF2. These included TAC-induced upregulation of connective tissue growth factor (*CTGF*), beta myosin heavy chain (*MHY7*), *NppA* (or BNP) and downregulation of G protein coupling receptor 22 (*GPCR-22*), which is reported to be downregulated following pressure overload injury [29]. These changes were validated by qPCR (Appendix 12). Thus, TAC surgery was effective in eliciting several pressure overload-linked changes regardless of Hi-FGF2 expression.

To obtain a better understanding of genes that may participate in the preservation of systolic function in FGF2(Lo) mice post-TAC, "differences of the differences" in gene expression post-TAC between FGF2(WT) and FGF2(Lo) mice were examined. An interaction algorithm was applied using transcriptome analysis software. Genes with more than a 3-fold change based on this analysis were identified (Table 3). Hierarchical clustering of the genes in the heart samples and scatter of differentially transcribed genes were also assessed (Appendix 13). This analysis pointed to the expression of circadian-rhythm associated genes such as *NR1D1* (or Rev-ERBa) and its target gene *ARNTL* (or *BMAL1*) and *Dbp1* as genes differentially modulated post-TAC between FGF2(WT) and FGF2(Lo) mice. *NR1D1* mRNA levels were the most differentially affected (5.41-fold) post TAC between FGF2(WT) and FGF2(Lo) mice. These results were further evaluated by qPCR (n=6) and showed that *NR1D1* mRNA levels are upregulated in the FGF2(Lo) but not in FGF2(WT) mice post-TAC (Fig 29); at the protein level, *NR1D1* was downregulated by TAC in FGF2(WT) mice but upregulated in FGF2(Lo) mice (Fig 29a). NR1D1 is known to negatively regulate the expression of ARNTL involved in circadian rhythm regulation [30, 31]. As shown, the decrease in *NR1D1* protein post-TAC seen in FGF2(WT) mice was accompanied with increased *ARNTL* and decreased *Dbp1* mRNAs (Fig. 29b), presumably maintaining the relationship between the circadian genes [32]. In the absence of endogenous Hi-FGF2, no significant changes were observed in *ARNTL* and *Dbp1* mRNA levels post-TAC.

Table 3, Comparison of differentially modulated genes post-TAC between FGF(Lo) and FGF(WT)

Fold Change FGF2(Lo) vs FGF2(WT): TAC vs Sham	P-value	Gene Symbol	Description
5.41	0.0001	Nr1d1	nuclear receptor subfamily 1, group D, member 1
3.67	0.0007	Dbp	D site albumin promoter binding protein
3.48	0.0483	Cox5b	cytochrome c oxidase subunit Vb
3.29	0.0139	Snora69	small nucleolar RNA, H/ACA box 69
3.26	0.0006	H2-M10.3	histocompatibility 2, M region locus 10.3
-3.02	0.0395	Mboat2	membrane bound O-acyltransferase domain containing 2
-3.08	0.0326	Spon2	spondin 2, extracellular matrix protein
-3.11	0.0388	Scd4	stearoyl-coenzyme A desaturase 4
-3.13	0.0348	Ms4a14	membrane-spanning 4-domains, subfamily A, member 14
-3.19	0.01	Ap3s1-ps2	adaptor-related protein complex 3, sigma 1 subunit, pseudogene 2 [Source:MGI Symbol;Acc:MGI:1929217]
-3.33	0.0447	Abra	actin-binding Rho activating protein
-3.34	0.0014	Lrrcc1	leucine rich repeat and coiled-coil domain containing 1
-3.37	0.0005	Tmem171	transmembrane protein 171
-3.43	0.001	Magea3	melanoma antigen, family A, 3
-3.5	0.0026	Gm13238	carnitine deficiency-associated gene expressed in ventricle 3 pseudogene
-3.64	0.0022	Arntl	aryl hydrocarbon receptor nuclear translocator-like
-4.4	0.0178	Cyp4b1-ps2	cytochrome P450, family 4, subfamily b, polypeptide 1, pseudogene 2

Figure 22, Elimination of Hi-FGF2 prevents pressure overload induced decline in systolic function.

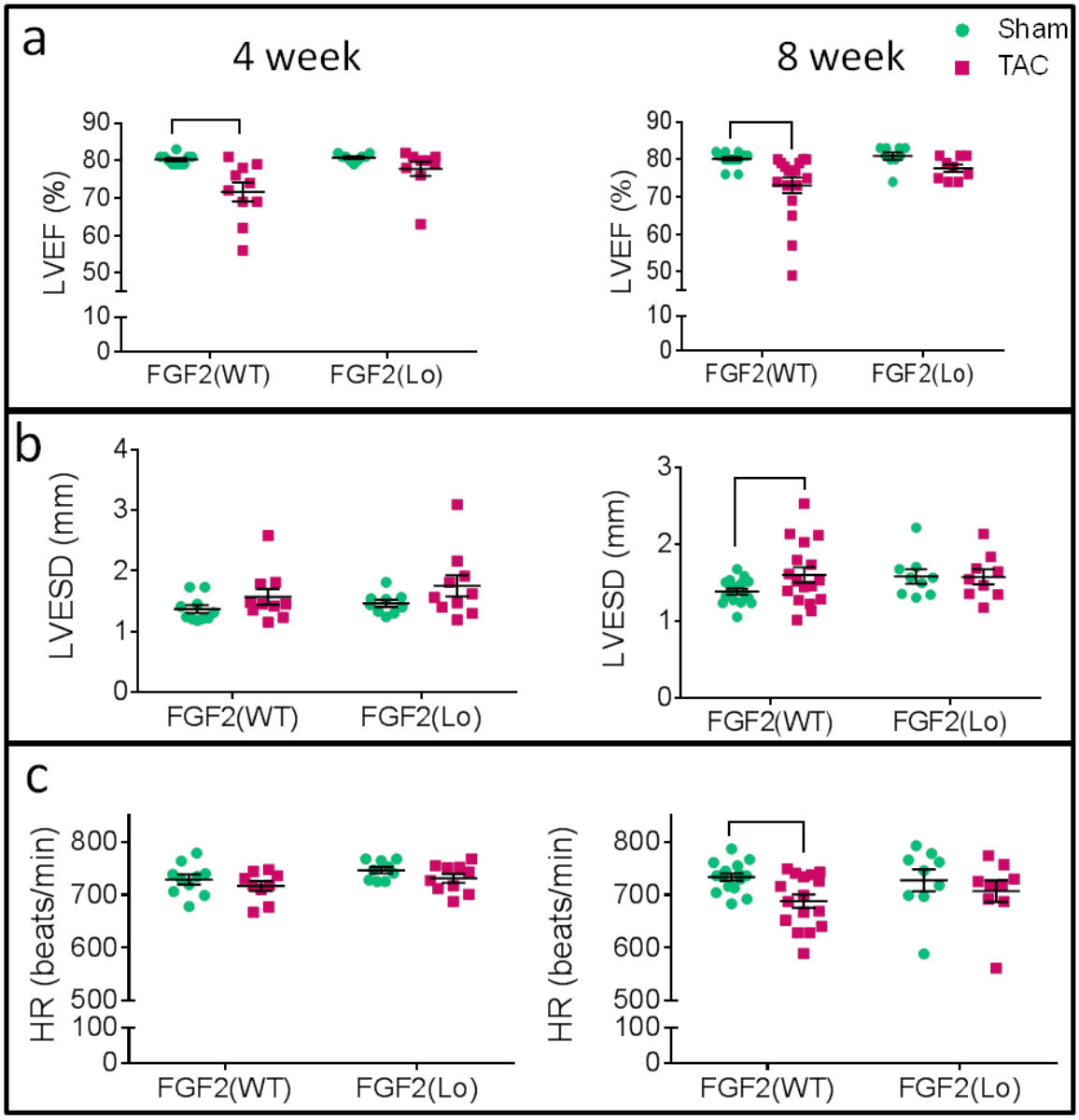

Figure 22. Elimination of Hi-FGF2 prevents pressure overload induced decline in systolic function. Panels a, b and c show respectively measurements of left ventricular ejection fraction (LVEF), left ventricular end systolic diameter (LVESD), heart rate (HR) at 4 and 8 weeks post-sham (green) or TAC- (magenta) surgery. in FGF2(WT) and FGF2(Lo) mice, as indicated. Brackets point to significant difference between the sham and TAC animals ($p<0.05$) by 2-way-ANOVA LSD post-hoc. Sample sizes are n=9-17.

Figure 23, Pressure overload induces decline in diastolic function and increases posterior wall thickening (PWT) regardless of Hi-FGF2 expression

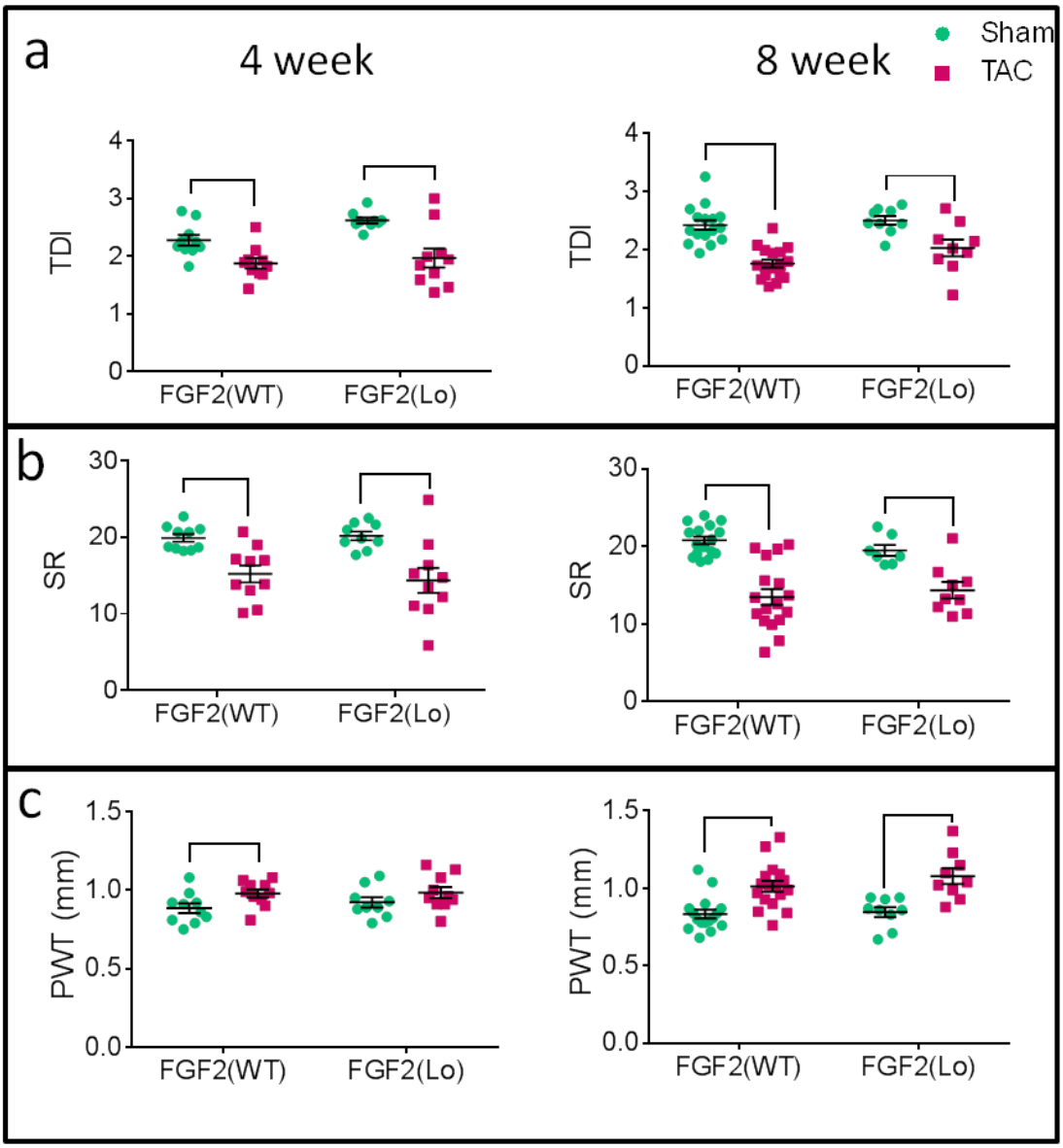

Figure 23. Pressure overload induces decline in diastolic function and increases posterior wall thickening (PWT) regardless of Hi-FGF2 expression. Panels a, b and c show respectively measurements of tissue doppler index (TDI), strain rate (SR), and PWT in FGF2(WT) and FGF2(Lo) mice, at 4 weeks and 8 weeks following TAC (magenta) or sham (green) surgery, as indicated. Brackets points to significant differences between the sham and TAC animals ($p<0.05$), by 2-way-ANOVA LSD post-hoc. Sample sizes are n=9-17.

Figure 24, Elimination of Hi-FGF2 prevents upregulation of cardiovascular pathology indicators.

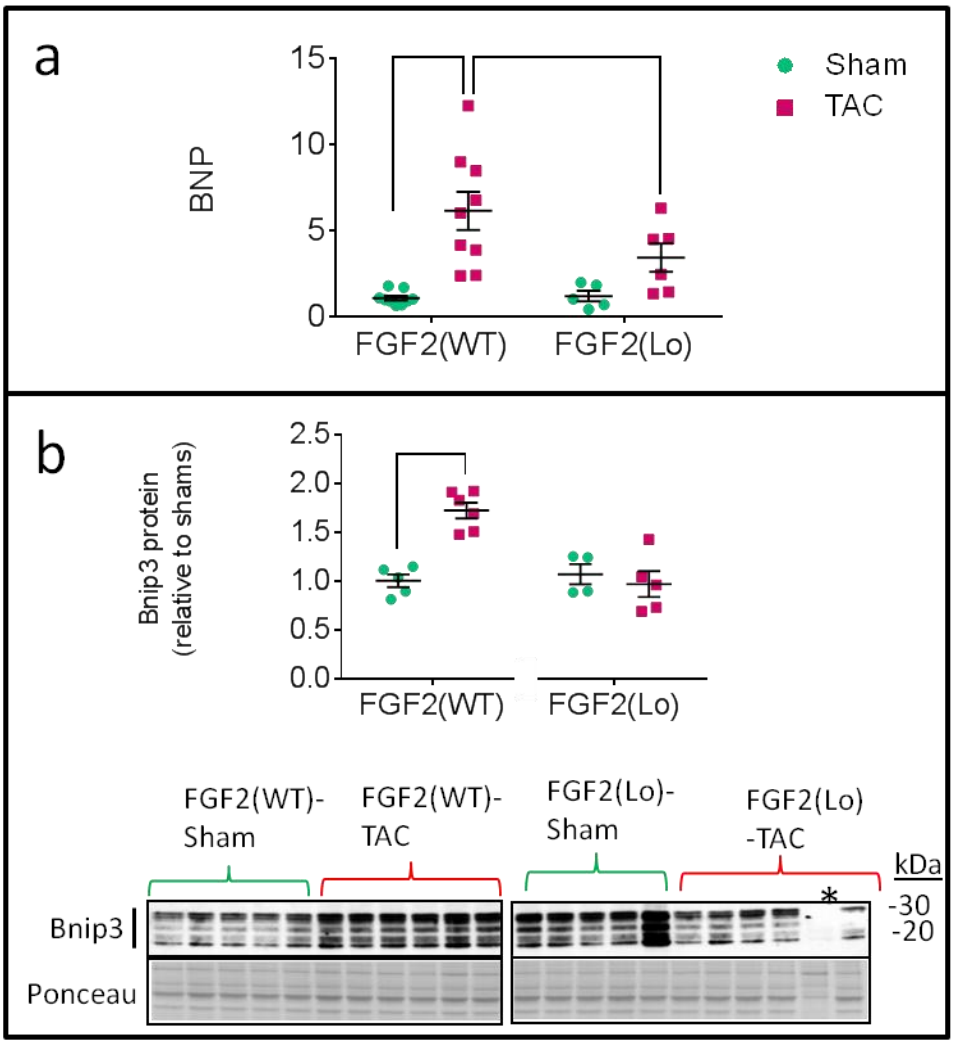

Figure 24. Elimination of Hi-FGF2 prevents upregulation of cardiovascular pathology indicators. Panel (a) shows relative mRNA levels (qPCR) of brain natriuretic peptide (BNP), in FGF2(WT) and FGF2(Lo) mouse hearts at 8 weeks post-TAC (magenta) or sham (green) surgery as indicated. Sample sizes are n=8 and 9 for FGF2(WT) sham and TAC, respectively, and n=5 and 6 for FGF2(Lo) sham and TAC, respectively. Brackets indicate significant differences between groups by 2-way-ANOVA LSD post hoc. Panel (b) shows relative Bnip3 protein levels of FGF2(WT) and FGF2(Lo) heart lysates at 8 weeks post-TAC (magenta) or sham (green) surgery, as indicated. The western blot used to detect Bnip3 (20-30 kDa), and corresponding Ponceau S stained membrane, is also included. Bnip3 densitometry values were adjusted for protein loading variations based on corresponding Ponceau S values reflective of total protein per lane. For each mouse strain, TAC-values are normalized relative to sham-values, to illustrate fold change. The bracket points to significant differences between the sham and TAC group, by student T-test, $P<0.5$, n=5-6. The asterisk point to a western blot lane excluded from the analysis as a statistical outlier.

Figure 25, Pressure overload induced fibrosis is independent of Hi-FGF2 expression.

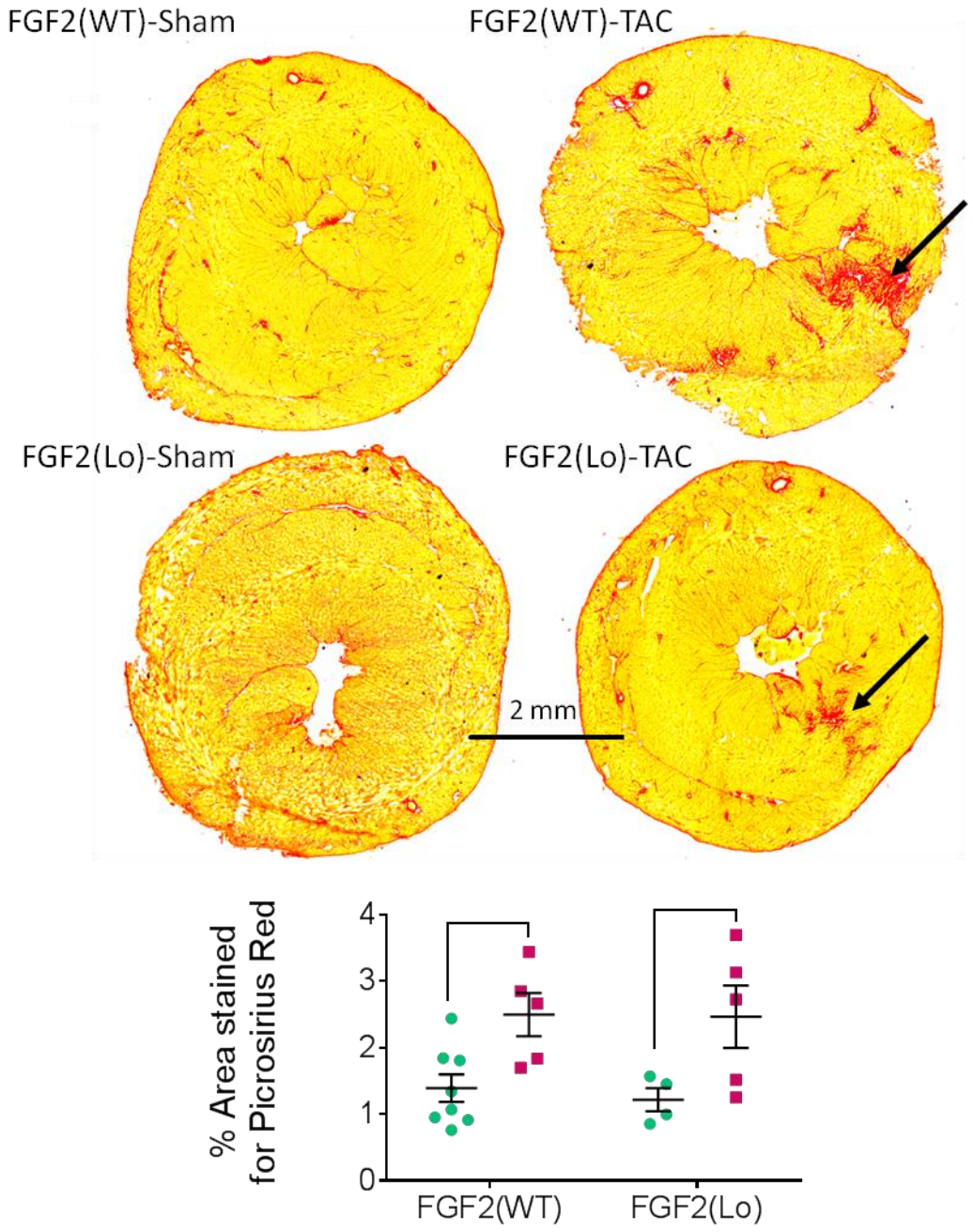

Figure 25. Pressure overload induced fibrosis is independent of Hi-FGF2 expression. Selected images of picrosirius red- stained mouse heart transverse sections at 8 weeks post-TAC or –sham surgery, showing the presence of fibrotic lesions (stained red, arrows) post-TAC, using a 4X magnification lens. The accompanying graph represents the percentage of cross-sectional area stained for picrosirius red in FGF2(WT) and FGF2(Lo) mice heart post-TAC (magenta) or sham (green). The brackets point to significant difference between the sham and TAC animals ($p<0.05$) by 2-way-ANOVA LSD post-hoc. Sample sizes are n=4-8.

Figure 26, Elimination of Hi-FGF2 does not prevent the increase in cardiac mass post-TAC, but prevents the increase in cardiomyocyte size.

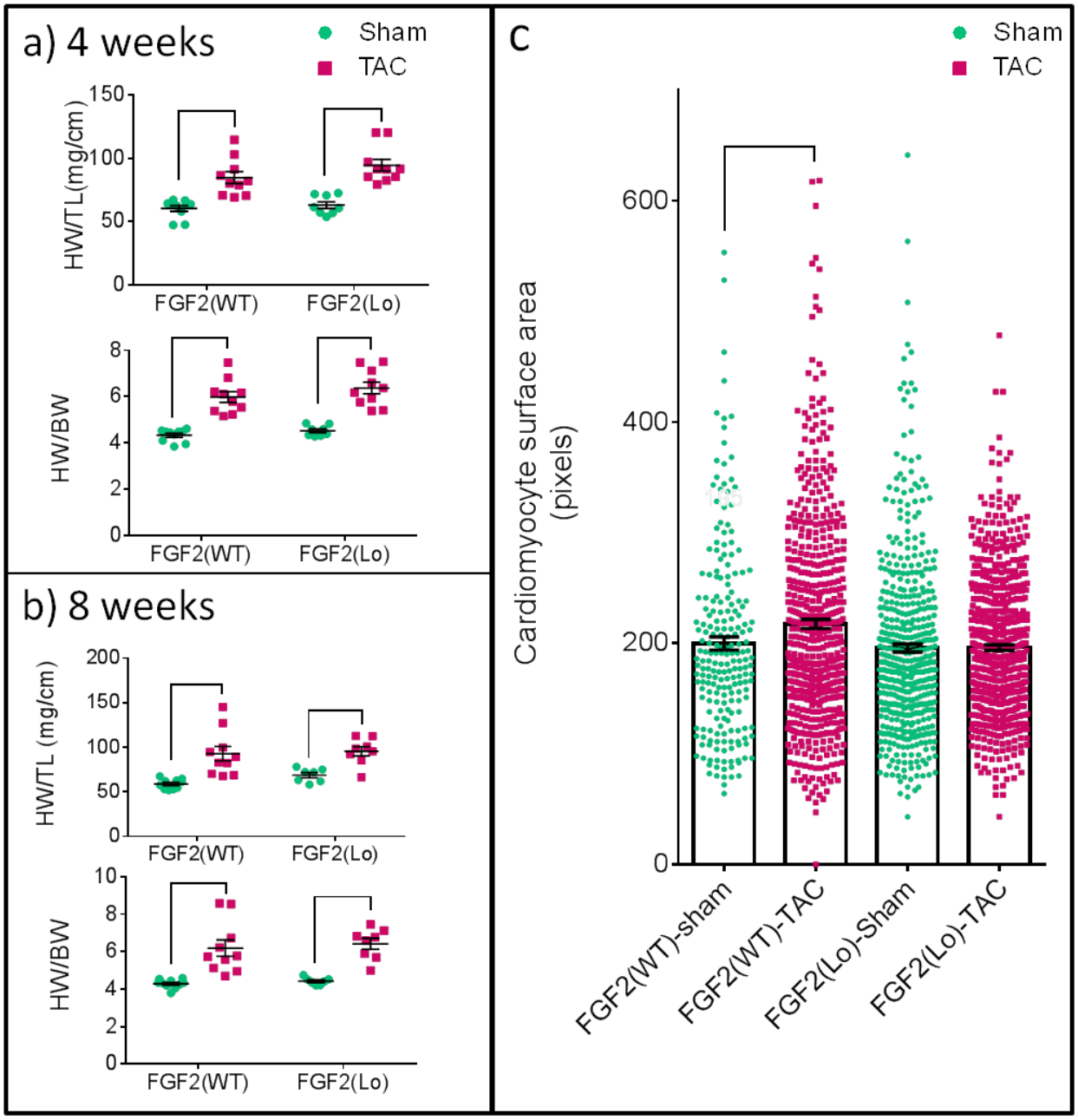

Figure 26. Elimination of Hi-FGF2 does not prevent the increase in cardiac mass post-TAC, but prevents the increase in cardiomyocyte size. Panels a and b show, respectively, heart weight divided by tibial length (HW/TL) and heart weight divided by body weight (HW/BW) at 4- and 8-weeks post- TAC (magenta) or sham (green) surgery, in FGF2 (WT) and FGF2(Lo) mice, as indicated. Brackets point to significant difference between sham and TAC animals ($p<0.05$) by 2-way-ANOVA LSD post-hoc. Sample sizes are n=8-10.

Panel (c) shows measurements of cardiomyocyte cross-sectional area in hearts of mice at 8-weeks post- TAC (magenta) or sham (green) surgery. The bracket points to significant difference between the sham and TAC FGF2(WT) cardiomyocytes, ($p<0.05$) by 2-way-ANOVA LSD post-hoc. N=215, 557, 487, and 625 from, respectively, FGF2(WT)-Sham, FGF2(WT) TAC, FGF2(Lo)-Sham and FGF2(Lo)-TAC.

Figure 27, Elimination of Hi-FGF2 promotes Cyclin D2 upregulation in hearts following pressure overload injury.

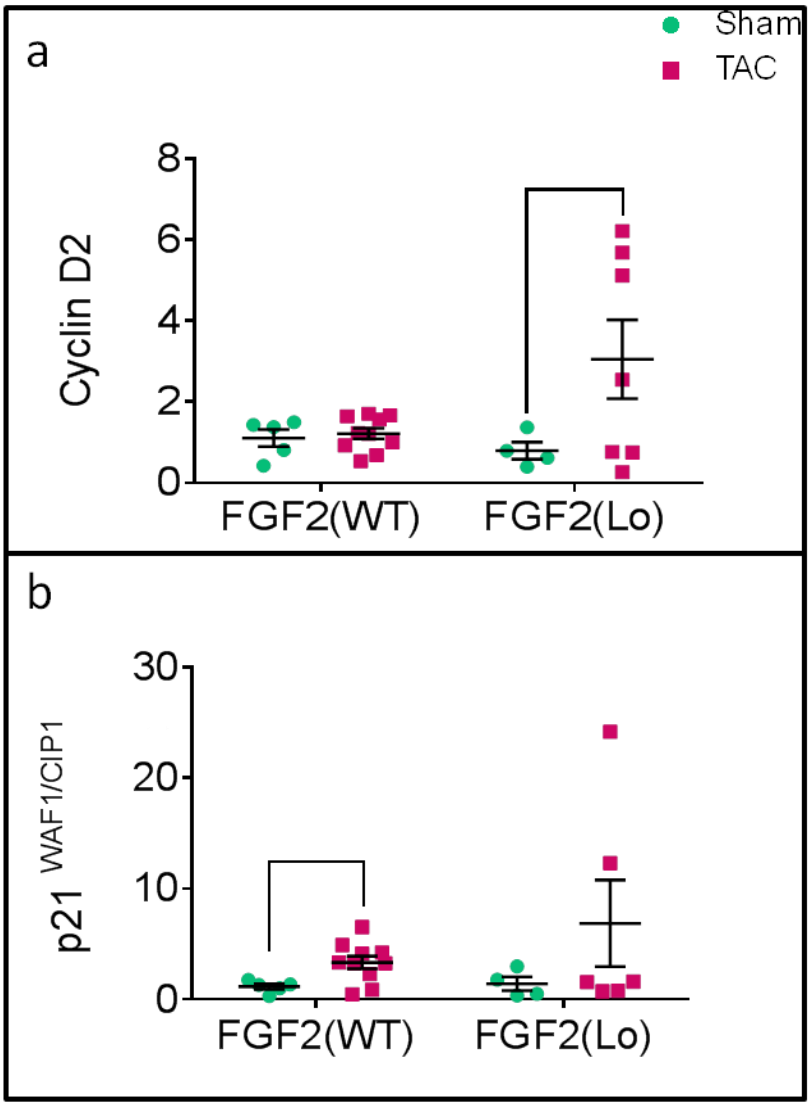

Figure 27. Elimination of Hi-FGF2 promotes Cyclin D2 upregulation in hearts following pressure overload injury. Panels a and b show relative mRNA levels for, respectively, cyclin D2 and p21 $^{WAF1/CIP1}$ in FGF2(WT) and FGF2(Lo) hearts at 8 weeks post-TAC (magenta) or post-sham (green).

The brackets points to significant difference between sham and TAC animals ($p<0.05$) by 2-way-ANOVA LSD post-hoc. Sample sizes are n=5-10.

Figure 28, Elimination of endogenous Hi-FGF2 upregulates cardiac HSP70 and Nur77 and downregulates RAB6B and CXCL9, under non-stressed conditions.

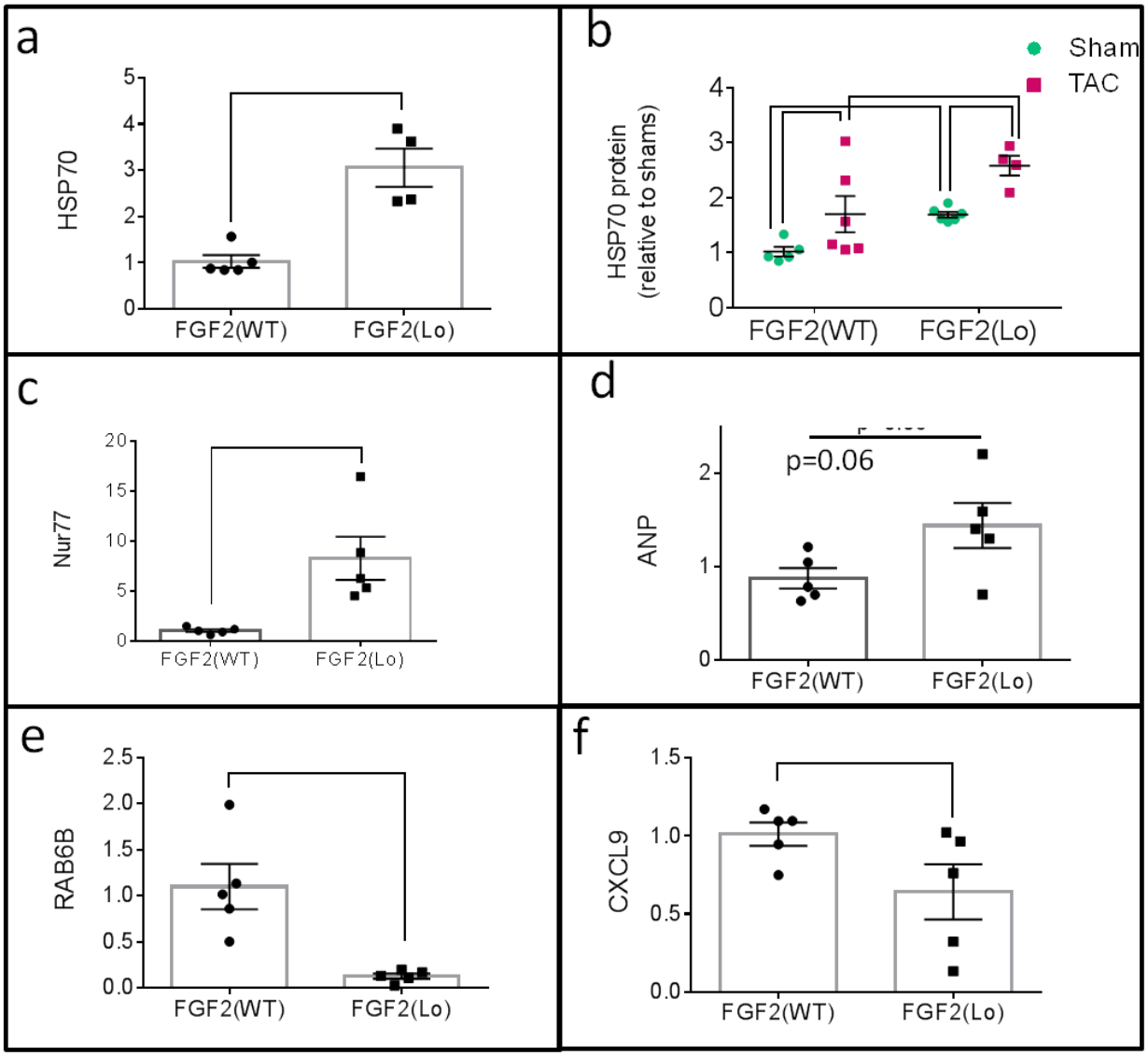

Figure 28. Elimination of endogenous Hi-FGF2 upregulates cardiac *HSP70* and *Nur77* and downregulates *RAB6B* and *CXCL9*, under non-stressed conditions. Panel a shows relative levels of *HSP70* mRNA in FGF2(WT) and FGF2(Lo) mouse hearts at 8 weeks after sham surgery. Panel shows relative levels of *HSP70* protein in FGF2(WT) and FGF2(Lo) hearts, at 8 weeks after sham, or TAC surgery as indicated. The western blot used to estimate relative *HSP70* signal and the corresponding Ponceau S stained membrane can be found in Figure S1. Brackets point to significant difference between groups ($p<0.05$) by student T-test (panel a) or 2-way-ANOVA LSD post-ho, panel b. Sample sizes are n=5-6. Panels c,d,e,and f show relative mRNA levels for, respectively, Nur77, ANP, *RAB6B* and *CXCL9* in the hearts of FGF2(WT) and FGF2(Lo) mice at 8 weeks post-sham surgery. Brackets points to significant difference between groups ($p<0.05$) by student T-test. Sample sizes are n=5-10.

Figure 29, Elimination of endogenous Hi-FGF2 alters expression of circadian rhythm modulators post-TAC.

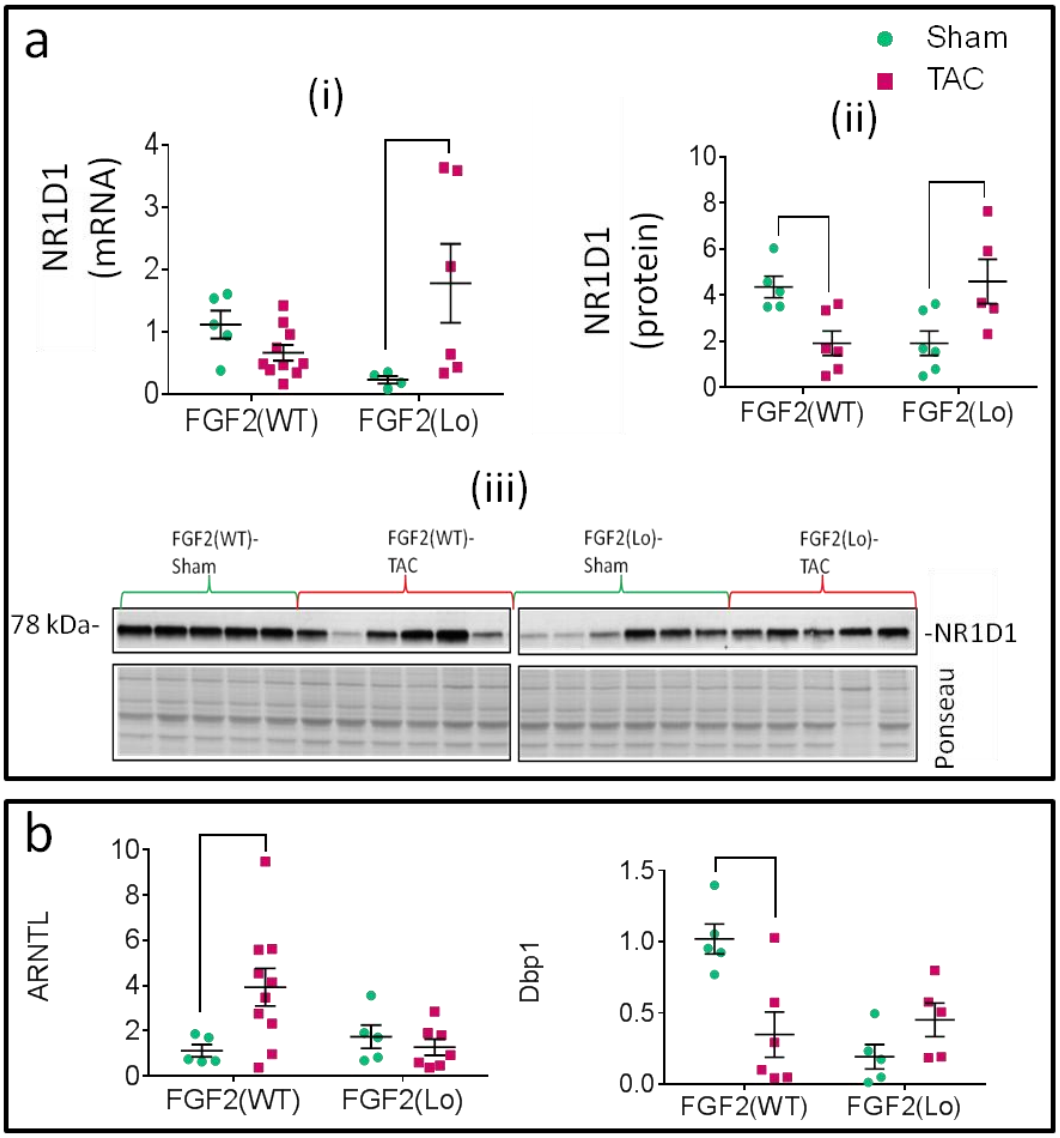

Figure 29. Elimination of endogenous Hi-FGF2 alters expression of circadian rhythm modulators post-TAC. Panel a. The graphs show relative NR1D1 (i) mRNA and (ii) protein levels in FGF2(WT) and FGF2(Lo) mice at 8 weeks post-TAC (magenta) or sham (green) surgery; (iii) shows the western blot used for obtaining the graph in (ii), plus corresponding Ponceau S stained membrane. Panel b shows relative mRNA levels of *ARNTL* and *Dbp1*, in FGF2(WT) and FGF2(Lo) mice, at 8 weeks post-surgery. Brackets point to significant difference between groups($p<0.05$) by 2-way-ANOVA LSD post-hoc. Sample sizes are n=5-10.

Discussion

The purpose of the present study was to investigate the role of Hi-FGF2 in the pathophysiology of pressure overload-induced cardiac dysfunction, structural remodeling, and gene expression using transgenic mice lacking Hi-FGF2. Original findings are that genetic elimination of endogenous Hi-FGF2: (1) prevents TAC-induced decline in systolic function and heart rate; (2) prevents increases in cardiac pathology markers and cardiomyocyte size following pressure overload, and (3) promotes upregulation of HSP70, and post-TAC upregulation of NR1D1, linking these proteins to the mechanism of cardioprotection in FGF2(Lo) mice. Moreover, development of cardiac fibrosis, decline in diastolic function, and increased cardiac mass post-TAC were independent of Hi-FGF2 expression.

Cardiac systolic function was assessed by measuring LVEF and LVESD post-TAC; both these indices were preserved in FGF2(Lo) mice, indicating protection from the adverse changes observed in FGF2(WT) animals. The severity of myocardial pathology post-TAC was reduced in the absence of Hi-FGF2, as indicated by measuring relative levels of *Bnp* (mRNA) and BNIP3 (protein). Overall, our data indicate that endogenous expression of Hi-FGF2 contributes to contractile dysfunction and myocardial damage post-TAC, while expression of only Lo-FGF2 increases cardiac resistance to TAC-induced systolic function decline. These findings reinforce our previous data obtained from a different model of cardiac stress, Doxorubicin cardiotoxicity, indicating that endogenous Hi-FGF2 contributes to cardiac systolic dysfunction in response to different types of injury [13].

Surprisingly, elimination of Hi-FGF2 had no apparent effect on the extent of fibrosis, as estimated by picrosirius red staining of tissue sections. This was supported by microarray data that showed similar upregulation of fibrosis and matrix remodeling markers regardless of Hi-

FGF2 expression. Previous studies based on *in vitro* data had shown that paracrine acting Hi-FGF2 contributes to a pro-fibrotic cardiac phenotype [10], which would predict increased fibrosis in the presence of Hi-FGF2. The effects of endogenous Hi-FGF2 *in vivo*, however, are a combination of intracellular/nuclear and paracrine/autocrine pathways and may not be comparable to the previous *in vitro* studies.

Fibrosis is well known to contribute to diastolic dysfunction, promoting cardiac stiffness, and impaired relaxation. It is likely that the observed similar levels of cardiac diastolic dysfunction seen in FGF2(WT) versus FGF2(Lo) mice are caused by similar levels of fibrosis. Overall our findings indicate that factors other than endogenous Hi-FGF2, for example increased CTGF, contribute to post-TAC surgery fibrosis in our models.

Hypertrophy of the heart and the cardiomyocyte accompany pressure overload remodeling and while initially adaptive, they eventually contribute to heart failure [33].Interestingly, while FGF2(WT) and FGF2(Lo) mice developed similar increases in relative cardiac mass, morphological evidence for cardiomyocyte hypertrophy was only seen in the presence of Hi-FGF2 expression. Cardiomyocyte size, as estimated by measuring cross-sectional surface area in sham versus TAC surgery animals, appeared unchanged in the absence of Hi-FGF2 expression. This is in broad agreement with previous reports that intramyocardial injection of Hi-FGF2 (but not Lo-FGF2) *in vivo*, or fibroblast-secreted Hi-FGF2 *in vitro*, can promote cardiomyocyte hypertrophy [34]. In wild type animals, the neurohormonal changes occurring during pressure overload (such as increased activation of the renin-angiotensin signaling) are known to promote FGF2 protein (consisting mainly of Hi-FGF2) upregulation and secretion from non-myocytes, resulting in paracrine action such as myocyte hypertrophy [10]. Assuming that pressure overload stimulated the renin-angiotensin pathway in FGF2(Lo) mice as well, any

increase in FGF2 protein production would be composed solely of Lo-FGF2, and would not be expected to promote cardiomyocyte hypertrophy [10, 35].

While cardiomyocyte hypertrophy was not detected, there was a measurable increase in cardiac mass seen in the FGF2(Lo) mice. It is possible that endogenous Lo-FGF2 increases cardiac mass post TAC surgery by: (a) promoting cytoprotection, and therefore decreasing cell death and/or (b) stimulating myocyte and non-myocyte (fibroblast, vascular cells, for example) cell cycle entry and proliferation. Regarding (a), protection from systolic dysfunction and from the upregulation of BNP and Bnip3, reported here, is in agreement with unopposed Lo-FGF2 being cytoprotective. An increase in Nurr77 mRNA was detected and is reported to prevent cardiomyocyte apoptotic cell death [25]. There is ample evidence for the cardioprotective role of administered [34], overexpressed [36], as well as endogenous Lo-FGF2 *in vivo* [13]. As discussed later, increased expression of HSP70 would also be expected to raise cardiomyocyte resistance to injurious stimuli and prevent cell death.

Regarding (b), Lo-FGF2 is a mitogen for cardiomyocytes and non-myocytes [37] and thus could stimulate proliferation, or at least cell cycle entry/re-entry under permissive conditions. Hi-FGF2, however, may exert anti-proliferative effects. Overexpression of Hi- or Lo-FGF2 in cardiomyocytes and other cell types indicated that nuclear Hi-FGF2 (but not Lo-FGF2) induces apoptotic cell death [38]. In indirect support of (b), post-TAC hearts from FGF2(Lo) mice were found to express increased cardiac cyclin D2. Mouse cardiomyocyte-specific increase in cyclin D2 expression contributes to preserved cardiac function during chronic pressure overload, and is associated with decreased BNP levels and cardiomyocyte hyperplasia [39]. Our observations support a similar relationship between increased cardiac levels of cyclin D2, decreased BNP, and preserved systolic function post-TAC surgery in the FGF2(Lo) hearts. Thus,

it is possible that a degree of myocyte proliferation//hyperplasia is stimulated in the absence of Hi-FGF2. Our studies however, unlike those in [40], do not discriminate between cell types, and would therefore require further evidence of the proliferative potential, number and status of cardiomyocytes in the FGF2(lo) versus FGF2(WT) hearts.

The absence of endogenous Hi-FGF2 allowed genes associated with cardioprotection (HSP70, Nurr77) to be upregulated in the FGF2 (Lo) mouse hearts. Upregulation of intracellular cardiac HSP70 is well known to be cardioprotective and has been shown to occur during various forms of preconditioning, and post-conditioning [21]. Lo-FGF2 administration to cells and hearts has been shown to exert a preconditioning, and post-conditioning effect [12, 41, 42]. This would be consistent with elevated HSP70 in FGF2(Lo) mice acting as both a preconditioning and postconditioning agent thereby contributing to protection from myocardial damage by pressure overload.

Analysis of the whole-transcriptome profile of the FGF2(WT) and FGF2(Lo) mice as a function of TAC (versus Sham) surgery revealed common changes in several genes associated with cardiac remodeling, but also non-common changes in genes associated with other cellular pathways. Of the non-common changes, NR1D1, which was upregulated in the absence of Hi-FGF2 post-TAC surgery, emerged as an important candidate gene likely to mediate the superior systolic function of FGF2(Lo) mice post-TAC surgery. NR1D1 belongs to a family of nuclear receptors and is considered to be a transcription repressor [43]. It is a heme binding protein [31] that further associates with nuclear corepressor 1 and histone deacetylase 3 to bind to retinoic acid-related orphan receptor response element-binding site and suppresses transcription of target genes [30]. NR1D1 stabilizes circadian rhythmicity by a feedback loop suppressing ARNTL, a major circadian rhythm regulator, and oscillates in various tissues during day/night cycles [30].

NR1D1 is considered as the bridge between circadian rhythm and metabolic pathways [44] as it: inhibits hepatic lipogenesis [45], increases skeletal muscle insulin response and glucose uptake [46], increases mitochondrial biogenesis and respiration in muscles [47], increases exercise capacity by preserving muscle mass [48] and inhibit tissue inflammation [49]. Furthermore, in a mouse model of pressure overload, use of the an NR1D1 agonist resulted in the preservation of systolic function [50], which would support a causative link between NR1D1 upregulation and improved systolic function in the FGF2(Lo) mice reported here. A decrease in NR1D1 one week after myocardial infarction was also reported to coincide with a significant decline in systolic and diastolic function; the NR1D1 agonist preserved systolic function and reduced BNP upregulation after infarction [28]. Nevertheless, the widely used NR1D1 agonist SR9009 was shown to have NR1D1-independent activities [51]. Thus, a critical re-evaluation of studies based solely on the use of NR1D1 agonists is warranted, taking into account that additional factors may have contributed to the protective effects of the agonists. Circadian rhythm modulation is well known to affect cardiac physiology and response to stress in a beneficial or detrimental way, and expression of endogenous Hi-FGF2 in the FGF2(WT) mice appears to contribute to the established interrelationships between genes involved in circadian rhythm and its regulation. It is likely that elimination of Hi-FGF2 exerts NR1D1-mediated changes that contribute to the protected state of FGF2(Lo) mice.

Conclusion. Expression of Lo-FGF2, at endogenous levels and in the absence of endogenous Hi-FGF2, protects from pressure overload-induced decline in systolic dysfunction and myocardial pathology. Our observations indicate a mechanism associated with, and likely mediated by, a ‘cardioprotected’ state, as suggested by increased HSP70 pre-TAC and post-TAC surgery, as well as an upregulation of NR1D1 post-TAC surgery. To further understand the role of Hi-FGF2

in pressure overload pathology it will be important to discriminate between nuclear/intracellular and paracrine/autocrine signaling and determine potential cardiomyocyte cell cycle re-entry in conjunction with cyclin D2 expression at early and late time points post-TAC surgery.

Conflict of interest:

None declared.

Acknowledgements

The authors thank Dr. Ali Maddahi, Colleague of Rehabilitation Sciences, the University of Manitoba, for help in making scattered graphs of microarray data. Funding (EK. PAC, DJ) was provided by the Canadian Institutes for Health Research (FRN-74733) and the Molson Women's Heart Health Foundation, EK. NK is the recipient of a Bank of Montreal studentship award via the St. Boniface Hospital Albrechtsen Research Centre and University of Manitoba funding to PAC.

References:

1. Conrad, N., et al., Temporal trends and patterns in heart failure incidence: a population-based study of 4 million individuals. Lancet, 2018. 391(10120): p. 572-580.

2. Yancy, C.W., et al., 2013 ACCF/AHA guideline for the management of heart failure: executive summary: a report of the American College of Cardiology Foundation/American Heart Association Task Force on practice guidelines. Circulation, 2013. 128(16): p. 1810-52.

3. Jessup, M. and S. Brozena, Heart failure. N Engl J Med, 2003. 348(20): p. 2007-18.

4. Davies, C., et al., Is left ventricular hypertrophy a friend or foe of patients with aortic stenosis? Postepy Kardiol Interwencyjnej, 2018. 14(4): p. 328-337.

5. Tanai, E. and S. Frantz, Pathophysiology of Heart Failure. Compr Physiol, 2015. 6(1): p. 187-214.

6. Lyon, R.C., et al., Mechanotransduction in cardiac hypertrophy and failure. Circ Res, 2015. 116(8): p. 1462-1476.

7. Zhang, Q.J., et al., Histone lysine dimethyl-demethylase KDM3A controls pathological cardiac hypertrophy and fibrosis. Nat Commun, 2018. 9(1): p. 5230.

8. Tillman, F., et al., A comprehensive review of chronic heart failure pharmacotherapy treatment approaches in African Americans. Ther Adv Cardiovasc Dis, 2019. 13: p. 1753944719840192.

9. Kardami, E., et al., Fibroblast growth factor-2 and cardioprotection. Heart Fail Rev, 2007. 12(3-4): p. 267-77.

10. Santiago, J.J., et al., High molecular weight fibroblast growth factor-2 in the human heart is a potential target for prevention of cardiac remodeling. PLoS One, 2014. 9(5): p. e97281.

11. Koleini, N., et al., Non-mitogenic FGF2 protects cardiomyocytes from acute doxorubicin-induced toxicity independently of the protein kinase CK2/heme oxygenase-1 pathway. Cell Tissue Res, 2018. 374(3): p. 607-617.

12. Koleini, N., et al., Fibroblast growth factor-2-mediated protection of cardiomyocytes from the toxic effects of doxorubicin requires the mTOR/Nrf-2/HO-1 pathway. Oncotarget, 2017. 8(50): p. 87415-87430.

13. Koleini, N., et al., Elimination or neutralization of endogenous high-molecular-weight FGF2 mitigates doxorubicin-induced cardiotoxicity. Am J Physiol Heart Circ Physiol, 2019. 316(2): p. H279-h288.

14. Azhar, M., et al., Gene targeted ablation of high molecular weight fibroblast growth factor-2. Dev Dyn, 2009. 238(2): p. 351-7.

15. Bordun, K.A., et al., The utility of cardiac biomarkers and echocardiography for the early detection of bevacizumab- and sunitinib-mediated cardiotoxicity. Am J Physiol Heart Circ Physiol, 2015. 309(4): p. H692-701.

16. Jimenez, S.K., et al., A single bout of exercise promotes sustained left ventricular function improvement after isoproterenol-induced injury in mice. J Physiol Sci, 2011. 61(4): p. 331-6.

17. Khanam, S.S., et al., Prognostic value of short-term follow-up BNP in hospitalized patients with heart failure. BMC Cardiovasc Disord, 2017. 17(1): p. 215.

18. deAlmeida, A.C., R.J. van Oort, and X.H. Wehrens, Transverse aortic constriction in mice. J Vis Exp, 2010(38).

19. Brooks, G., R.A. Poolman, and J.M. Li, Arresting developments in the cardiac myocyte cell cycle: role of cyclin-dependent kinase inhibitors. Cardiovasc Res, 1998. 39(2): p. 301-11.

20. Busk, P.K. and R. Hinrichsen, Cyclin D in left ventricle hypertrophy. Cell Cycle, 2003. 2(2): p. 91-5.

21. Song, Y.J., C.B. Zhong, and X.B. Wang, Heat shock protein 70: A promising therapeutic target for myocardial ischemia-reperfusion injury. J Cell Physiol, 2019. 234(2): p. 1190-1207.

22. Broer, S., The SLC6 orphans are forming a family of amino acid transporters. Neurochem Int, 2006. 48(6-7): p. 559-67.

23. Wu, Y., et al., Reciprocal Regulation between the Circadian Clock and Hypoxia Signaling at the Genome Level in Mammals. Cell Metab, 2017. 25(1): p. 73-85.

24. Song, W., H. Wang, and Q. Wu, Atrial natriuretic peptide in cardiovascular biology and disease (NPPA). Gene, 2015. 569(1): p. 1-6.

25. You, X., et al., Transcriptional up-regulation of relaxin-3 by Nur77 attenuates beta-adrenergic agonist-induced apoptosis in cardiomyocytes. J Biol Chem, 2018. 293(36): p. 14001-14011.

26. Dong, C. and G. Wu, Regulation of anterograde transport of adrenergic and angiotensin II receptors by Rab2 and Rab6 GTPases. Cell Signal, 2007. 19(11): p. 2388-99.

27. Hardison, J.L., et al., The chemokines CXCL9 and CXCL10 promote a protective immune response but do not contribute to cardiac inflammation following infection with Trypanosoma cruzi. Infect Immun, 2006. 74(1): p. 125-34.

28. Stujanna, E.N., et al., Rev-erb agonist improves adverse cardiac remodeling and survival in myocardial infarction through an anti-inflammatory mechanism. PLoS One, 2017. 12(12): p. e0189330.

29. Adams, J.W., et al., Myocardial expression, signaling, and function of GPR22: a protective role for an orphan G protein-coupled receptor. Am J Physiol Heart Circ Physiol, 2008. 295(2): p. H509-21.

30. Everett, L.J. and M.A. Lazar, Nuclear receptor Rev-erbalpha: up, down, and all around. Trends Endocrinol Metab, 2014. 25(11): p. 586-92.

31. Yin, L., N. Wu, and M.A. Lazar, Nuclear receptor Rev-erbalpha: a heme receptor that coordinates circadian rhythm and metabolism. Nucl Recept Signal, 2010. 8: p. e001.

32. Annayev, Y., et al., Gene model 129 (Gm129) encodes a novel transcriptional repressor that modulates circadian gene expression. J Biol Chem, 2014. 289(8): p. 5013-24.

33. Schirone, L., et al., A Review of the Molecular Mechanisms Underlying the Development and Progression of Cardiac Remodeling. Oxid Med Cell Longev, 2017. 2017: p. 3920195.

34. Jiang, Z.S., et al., High- but not low-molecular weight FGF-2 causes cardiac hypertrophy in vivo; possible involvement of cardiotrophin-1. J Mol Cell Cardiol, 2007. 42(1): p. 222-33.

35. Tang, W., et al., Mitogen-activated protein kinases ERK 1/2- and p38-GATA4 pathways mediate the Ang II-induced activation of FGF2 gene in neonatal rat cardiomyocytes. Biochem Pharmacol, 2011. 81(4): p. 518-25.

36. Sheikh, F., et al., Overexpression of FGF-2 increases cardiac myocyte viability after injury in isolated mouse hearts. Am J Physiol Heart Circ Physiol, 2001. 280(3): p. H1039-50.

37. Kardami, E., Stimulation and inhibition of cardiac myocyte proliferation in vitro. Mol Cell Biochem, 1990. 92(2): p. 129-35.

38. Ma, X., et al., Chromatin compaction and cell death by high molecular weight FGF-2 depend on its nuclear localization, intracrine ERK activation, and engagement of mitochondria. J Cell Physiol, 2007. 213(3): p. 690-8.

39. Toischer, K., et al., Cardiomyocyte proliferation prevents failure in pressure overload but not volume overload. J Clin Invest, 2017. 127(12): p. 4285-4296.

40. Tane, S., et al., Repression of cyclin D1 expression is necessary for the maintenance of cell cycle exit in adult mammalian cardiomyocytes. J Biol Chem, 2014. 289(26): p. 18033-44.

41. Jiang, Z.S., et al., High molecular weight FGF-2 promotes postconditioning-like cardioprotection linked to activation of protein kinase C isoforms, as well as Akt and p70 S6 kinases. [corrected]. Can J Physiol Pharmacol, 2009. 87(10): p. 798-804.

42. Srisakuldee, W., et al., Administration of FGF-2 to the heart stimulates connexin-43 phosphorylation at protein kinase C target sites. Cell Commun Adhes, 2006. 13(1-2): p. 13-9.

43. Vaissiere, A., et al., Molecular mechanisms of transcriptional control by Rev-erbalpha: An energetic foundation for reconciling structure and binding with biological function. Protein Sci, 2015. 24(7): p. 1129-46.

44. Fontaine, C. and B. Staels, The orphan nuclear receptor Rev-erbalpha: a transcriptional link between circadian rhythmicity and cardiometabolic disease. Curr Opin Lipidol, 2007. 18(2): p. 141-6.

45. Feng, D., et al., A circadian rhythm orchestrated by histone deacetylase 3 controls hepatic lipid metabolism. Science, 2011. 331(6022): p. 1315-9.

46. Vieira, E., et al., Relationship between AMPK and the transcriptional balance of clock-related genes in skeletal muscle. Am J Physiol Endocrinol Metab, 2008. 295(5): p. E1032-7.

47. Woldt, E., et al., Rev-erb-alpha modulates skeletal muscle oxidative capacity by regulating mitochondrial biogenesis and autophagy. Nat Med, 2013. 19(8): p. 1039-46.

48. Mayeuf-Louchart, A., et al., Rev-erb-alpha regulates atrophy-related genes to control skeletal muscle mass. Sci Rep, 2017. 7(1): p. 14383.

49. Pourcet, B., et al., Nuclear Receptor Subfamily 1 Group D Member 1 Regulates Circadian Activity of NLRP3 Inflammasome to Reduce the Severity of Fulminant Hepatitis in Mice. Gastroenterology, 2018. 154(5): p. 1449-1464.e20.

50. Zhang, L., et al., REV-ERBalpha ameliorates heart failure through transcription repression. JCI Insight, 2017. 2(17).

51. Dierickx, P., et al., SR9009 has REV-ERB-independent effects on cell proliferation and metabolism. Proc Natl Acad Sci U S A, 2019. 116(25): p. 12147-12152.

Chapter IV: General Discussion

Studies presented in this thesis have provided evidence regarding the antithetical involvement of endogenous FGF2 isoforms in regulating cardiac vulnerability to two different and major causes of cardiac injury and dysfunction, such as Doxorubicin administration and pressure-overload as simulated by TAC surgery. Short-term *in vitro* studies, on the other hand, documented the acute cytoprotective effects of administered FGF2 isoforms on cardiomyocyte vulnerability to Doxorubicin toxicity, and the mechanisms involved.

For the first time we have shown that endogenous Hi-FGF2 expression increases cardiac vulnerability to stress-stimuli, *in vivo*: genetic elimination of endogenous Hi-FGF2 in transgenic mice prevented systolic dysfunction induced by Dox administration or TAC surgery. The ability to downregulate Hi-FGF2 expression/accumulation in vivo, through therapeutic interventions, would be expected to attenuate morbidity and mortality in patients at risk for heart failure caused by cancer drug treatments or due to chronic pressure overload.

FGF2 isoforms are localized in the nucleus and cytosol as well as the extracellular space; the isoforms are exported by cells (mainly fibroblasts) and retained by the heparan sulphate proteoglycans at the extracellular matrix and the basement membrane. Both types of FGF2 isoforms are found in biological fluids such as pericardial fluid. Thus, both isoforms are expected to exert intracellular/nuclear as well as extracellular (paracrine/autocrine/systemic) effects.

To better understand the role, and mechanism of action, of FGF2 isoforms in cardiac response to stress, we sought to study separately the effects of: extracellular-acting FGF2, by administering pure recombinant FGF2 isoforms to cardiomyocytes in culture, or by neutralizing the activity of secreted Hi-FGF2 in conditioned media); endogenously expressed FGF2 isoforms

in mice genetically engineered to lack endogenous Hi-(but not Lo-) FGF2 compared to wild type mice.

Extracellular-Acting FGF2. As described in Chapter II (Section 2), pretreatment of cardiomyocytes in culture with Lo- or Hi-FGF2 was equally effective in preventing/attenuating many of the acute adverse effects contributing to Doxorubicin toxicity and cell death such as oxidative stress, mitochondrial damage and loss of ATP. Importantly, the protective effect of both isoforms required the activity of the mTOR/Nrf2/HO-1 pathway. Since mTOR is activated downstream of tyrosine kinase receptors such as FGFR1 (the main FGF2 receptor in cardiomyocytes) it is likely that both Lo- and Hi-FGF2 acute protection against Dox was mediated through FGFR1 activation. In agreement, Kole and colleagues have shown that all human FGF2 isoforms activate FGFR1-IIIb followed by ERK phosphorylation in human dermal fibroblasts [166]. Cheng et al. have also shown that both isoforms protected hippocampal neurons against amyloid beta toxicity where specific inhibitors of FGFR1 abrogated protection by Hi- or Lo-FGF2 [52].

In agreement with the in vitro studies presented here, previous in vivo studies [91] have reported that exogenous administration of Hi-FGF2 by intracardiac injection in the ischemic myocardium in rats in vivo was protective against myocardial damage and loss of systolic function in the short-term; the injected Hi-FGF2 protection in vivo was not sustained at the later time points, as the animals developed hypertrophy and deterioration of contractile function; in contract, sustained cardioprotection was seen in Lo-FGF2 injected hearts [91]. These earlier in vivo studies pointed to a dichotomous effect of administered Hi-FGF, such as acute cardioprotection but deleterious effects at later stages. The in vivo studies presented here, using

the Hi-FGF2-knockout mice, showed that endogenous Hi-FGF2 expression has a broadly similar effect to that of exogenously added Hi-FGF2, being detrimental in the setting of chronic injury.

Since both Lo- and Hi-FGF2 isoforms appear to bind and activate the same cell surface FGFR receptor, differences in their long-term effects suggest the existence of additional, isoform-selective signaling pathways, with opposing end-points. It is possible that the FGF2 isoforms can engage different co-receptor(s), acting in concert with FGFR1. The Levin group [167-169] has shown that neuropilin-1 acts a co-receptor for Hi-FGF2, preventing angiogenesis. While Lo-FGF2 has been widely recognized as an angiogenic factor stimulating formation of new blood vessels (capillaries, arterioles), Hi-FGF2 appears to be antagonistic to that action [169]. Lack of new vessel formation near the infarct area subsequent to the injection of Hi-FGF2 (unlike the case with Lo-FGF2 injection) in the ischemic heart is likely to contribute to loss of acute protection and eventual functional deterioration [91]. Whether lack of endogenous Hi-FGF2 in the mouse models used here promoted changes in vascular/capillary density is under further investigation.

Intracellular-acting FGF2. FGF2 isoforms exert intracellular effects that can be distinguished from those of extracellular-acting [1]. Previous work has identified distinct intracellular (cytosolic/nuclear) activities between the isoforms [87]. These include increased incidence of bi-nucleation, and apoptotic cell death by overexpressed, intracellular and nuclear-acting, Hi-FGF2, but not Lo-FGF2 in cardiomyocytes [87]. Although both isoforms can localize to the nucleus, the patterns of intranuclear localization appear to be distinct, suggesting different nuclear activities [170]. It is possible that the isoforms may bind to distinct DNA sequences, histones, transcription factors, or other entities involved in transcriptional regulation, thus, influencing gene transcription. Han et, al. reported that overexpressed, intracellular Hi-FGF2 in

osteoblasts stimulated FGF23 promoter activity; this was achieved "through a cAMP-dependent binding of FGFR1 and cAMP-response element binding protein (CREB) to a conserved cAMP response element (CRE) contiguous with the NFAT binding site in the FGF-23 promoter" [171]. This report is of importance as it suggests that nuclear Hi-FGF2 can directly influence transcription. A similar mechanism involving nuclear Hi-FGF2 may be responsible for some of the differences observed in cardiac gene expression brought about by the absence or presence of endogenous Hi-FGF2. Nuclear Lo-FGF2 may also exert distinct effects, at least in the context of prostate cancer cells: internalized Lo-FGF2 (in complex with FGFR1) interacts with the centrosomal protein 57 (CEP57), which promotes the translocation of the complex to the nucleus, resulting in centriole overduplication and mitotic instability [172].

There is also evidence that Lo-FGF2 or Hi-FGF2 have opposing direct effects on isolated cardiac mitochondria; Hi-FGF2 is toxic, promoting opening of permeability transition pore (PTP) and release of cytochrome C to the extra-mitochondrial environment (a process that would lead to cell death if realized in the cytosolic environment), while Lo-FGF2 is protective, preventing the calcium-overload-induced opening of PTP [173]. Thus, it is possible that endogenous, cytosolic/nuclear and even internalized, Hi-FGF in the FGF2(WT) mice renders cardiomyocyte mitochondria more vulnerable to Dox- or pressure overload stress.

FGF2 as a therapy against cardiac injury. The in vitro and in vivo studies presented here documented and validated the cardioprotective effect of administered or endogenous Lo-FGF2. Exogenously given Lo-FGF2 is well established to be cytoprotective in cardiac, neural, renal, hepatic, and dermal injuries [52, 56, 174, 175]. Harnessing the protective effect of Lo-FGF2 might be beneficial in the context of Dox-induced cardiac damage in patients. On the other hand, Lo-FGF2 is a potent angiogenic and mitogenic factor which may trigger further tumor

growth and resistance to chemotherapy drugs. Since, however, the cardioprotective effect of Lo-FGF2 can be dissociated from its mitogenic and angiogenic properties by a single mutation, in recombinant S117A-FGF2, one can consider such a mutated version of Lo-FGF2 (or other mutations that may have similar outcomes) worthy of consideration to protect patients from at least the acute cardiotoxic effects of Dox.

What about the potential of Hi-FGF2 in treating hearts vulnerable to stress stimuli? Our findings from the in vivo models suggest that strategies aimed at eliminating or reducing endogenous Hi-FGF2 would be beneficial against cardiac injury from Dox or pressure overload (Chapters II and III). An in-depth understanding of the regulation of FGF2 mRNA translation is currently lacking and would be required to design reagents/drugs to selectively prevent translation of the FGF2 mRNA from the CUG start sites producing Hi-FGF2. To our knowledge there are no drugs currently available to block translation/production of Hi-FGF2.

On the other hand, our in vitro studies demonstrated that fibroblast secreted, paracrine-acting Hi-FGF2, renders cardiomyocytes more vulnerable to Dox-toxicity. Cardiomyocytes co-cultured with fibroblasts lacking Hi-FGF2 expression were more resistant to Dox-injury, compared to those co-cultured with wild type fibroblasts. Furthermore, selective neutralization of human fibroblast-secreted Hi-FGF2 with specific antibodies attenuated Dox-induced injury of cardiomyocytes. Therefore, neutralizing extracellular, paracrine Hi-FGF2 provides a means to raise cardiac myocyte resistance to injury, by allowing the unopposed protective action of extracellular Lo-FGF2. Were we to identify that a co-receptor is required for the chronic effects of Hi-FGF2, designing an antibody-based approach to inactivate the co-receptor may provide another means to selectively interfere with Hi-FGF2-specific signaling. Antibody-based

approaches to inactivate or neutralize accessible antigens (extracellular matrix, extracellular ligand domains of receptors) are now widely used in many therapeutic applications.

Knockout of endogenous Hi-FGF2 alters cardiac transcriptome profile. As presented and discussed in Chapter III, transcription of several genes was significantly altered depending on the presence of Hi-FGF2. While extensive studies will be needed to address the significance of all the changes observed, it is of note that the absence of endogenous Hi FGF2 led to the upregulation of the cardioprotective HSP70 and Nur77 genes in the sham-operated (non-stressed) animals. In addition, elevated HSP70 upregulation in the FGF2(Lo) hearts persisted after TAC. Based on the well-established cardioprotective function of HSP70 [176] it is highly likely that it conferred protection from pressure-overload, or Doxorubicin cardiac systolic dysfunction and damage. Nur77 has been shown to exert an anti-apoptotic effect during pressure-overload conditions [177], and therefore would expected to decrease incidence of cardiomyocyte cell death and damage post-TAC in our model.

The RAB6B gene, coding for the Ras-related protein RAB6B was the most downregulated in the absence of Hi-FGF2, in non-stressed hearts: by qPCR, expression of RAB6B gene was 10-fold higher in the FGF2(WT) hearts or MEFs compared to those from FGF2(lo) mice. Such a dramatic change suggests the possibility of an important functional role, but what that role might be is as yet unclear. Very little is known about RAB6B, and there are no antibodies available to validate its expression at the protein level. RAB6B is involved in vesicle transportation within cells and there is a report showing that its overexpression stimulates internalization of the β-adrenergic receptors [178]. If this were established to be the case in cardiomyocytes, one can speculate that modulation in RAB6B expression brought about by Hi-FGF2 would affect adrenergic signaling, and contractile function in the heart.

Comparative analysis identified NR1D1 as the most differentially regulated gene following TAC between the FGF2(WT) and FGF2(Lo) mice, implicating this protein in the protected phenotype of FGF2(Lo) mice. NR1D1 as discussed in Chapter III is involved in multiple cellular pathways including modulation of circadian rhythm, metabolism, and inflammatory responses; further studies are required to address the direct consequences of upregulated NR1D1 expression in the absence of Hi-FGF2 during TAC on cardiac metabolism and circadian rhythm modulation.

Chapter V: Limitations and future directions

We addressed our research questions using rodent *in vitro* and *in vivo* models of human pathology. Rat neonatal cardiomyocyte were used for our in vitro studies, and, in general, findings from these cultures, representing acute responses, were in agreement with the *in vivo* studies. On the other hand, validating the signal transduction pathways mediating acute FGF2 protection by additional studies on isolated adult cardiomyocytes would increase the impact of our findings. Use of human cardiomyocytes (derived from pluripotent stem cells) could also increase impact and help us better understand the role of FGF2 isoforms in the human context.

We have used a global Hi-FGF2 knockout mouse model. A more precise understanding of the role of endogenous Hi-FGF2 would require eliminating this isoform in a cell-type specific (fibroblast, as the main producer). In addition, chronic lack of Hi-FGF2 in the mouse model we used could result in a chronic adaptation causing a mitigated response to stimuli. Therefore, conditional knockout models can be a used in the future to study the effects of this isoform. The Kardami group is currently collaborating in the design of this mouse model. The inhibitors used in the current thesis were chosen to show the maximum specificity, however, unwanted targets might be affected with the inhibitors. Dox cardiotoxicity was modeled using a single injection (20 mg/kg) in mice, however, using multiple divided doses could have better recapitulate the Dox cardiotoxicity in humans. In addition, the long term effects of Dox in animals could have been studied by keeping the mice for a longer time.

In the pressure overload model, the animals were sacrificed at 4- and 8-weeks post-TAC. Examination of post-TAC surgery heart structure function at later time points should be considered in future experiments, to allow us to determine sustainability of protection in the

FGF2(Lo) mice; it would also have exacerbated the cardiac phenotype of the FGF2(WT) mice, and perhaps revealed further differences in post-TAC surgery responses.

Differentiating between paracrine and intracellular FGF-2 actions (of Hi- or Lo-FGF2) would also be important in interpreting findings and identifying therapeutic targets. For example, the use of **specific antibodies neutralizing extracellular acting (human) Hi-FGF2** should next be applied in an in vivo model, to examine if it would be capable to increase cardiac resistance to injury. Since the neutralizing antibodies also recognize porcine Hi-FGF2 (the sequence of which is identical to that of human Hi-FGF2), they could be tested in a porcine model to examine if they can mitigate systolic dysfunction due to deleterious stimuli.

Investigating the nuclear functions of Hi- and Lo-FGF2 is also paramount in order to determine how they may affect differential gene expression, in cardiomyocytes and non-myocytes.

Hi-FGF2 has been reported to contribute in or be associated with various pathologies and conditions including: cardiac hypertrophy and remodeling, cardiac arrhythmias, gastric cancer aggravation and cancer metastasis, and osteoarthritis. Further research is required in this field to find out whether such neutralizing antibodies can prevent deleterious effects of Hi-FGF2 and the benefits outweigh the risks regarding their use.

Importantly, we have shown using a wide-screening approach that Hi-FGF2 knockout results in differential regulation of the genes involved in the circadian regulation. We know that the circadian regulation has a broad range of effects, including metabolism, inflammation, and cell cycle regulation. The studies we presented in the current thesis provided the first step toward understanding the complex biology of Hi-FGF2 in disease progression which merits future

studies to identify how Hi-FGF2 alters circadian regulation and how these changes could reflect the effects of Hi-FGF2.

Chapter VI: References

References listed here are cited in the Chapter I (Introduction) and Chapter IV (Discussion).

1. Kardami, E., et al., *Fibroblast growth factor-2 and cardioprotection.* Heart Fail Rev, 2007. **12**(3-4): p. 267-77.
2. Gospodarowicz, D., *Purification of a fibroblast growth factor from bovine pituitary.* J Biol Chem, 1975. **250**(7): p. 2515-20.
3. Kardami, E. and R.R. Fandrich, *Basic fibroblast growth factor in atria and ventricles of the vertebrate heart.* J Cell Biol, 1989. **109**(4 Pt 1): p. 1865-75.
4. Shibata, F., A. Baird, and R.Z. Florkiewicz, *Functional characterization of the human basic fibroblast growth factor gene promoter.* Growth Factors, 1991. **4**(4): p. 277-87.
5. Jimenez, S.K., et al., *Transcriptional regulation of FGF-2 gene expression in cardiac myocytes.* Cardiovasc Res, 2004. **62**(3): p. 548-57.
6. Lee, J.G. and E.P. Kay, *NF-kappaB is the transcription factor for FGF-2 that causes endothelial mesenchymal transformation in cornea.* Invest Ophthalmol Vis Sci, 2012. **53**(3): p. 1530-8.
7. Sun, L., et al., *NUDT6, the FGF-2's antisense gene, showed associations with fat deposition related traits in pigs.* Mol Biol Rep, 2012. **39**(4): p. 4119-26.
8. Li, A.W., C.K. Too, and P.R. Murphy, *The basic fibroblast growth factor (FGF-2) antisense RNA (GFG) is translated into a MutT-related protein in vivo.* Biochem Biophys Res Commun, 1996. **223**(1): p. 19-23.
9. Santiago, J.J., et al., *High molecular weight fibroblast growth factor-2 in the human heart is a potential target for prevention of cardiac remodeling.* PLoS One, 2014. **9**(5): p. e97281.

10. Arnaud, E., et al., *A new 34-kilodalton isoform of human fibroblast growth factor 2 is cap dependently synthesized by using a non-AUG start codon and behaves as a survival factor.* Mol Cell Biol, 1999. **19**(1): p. 505-14.

11. Holcik, M. and N. Sonenberg, *Translational control in stress and apoptosis.* Nat Rev Mol Cell Biol, 2005. **6**(4): p. 318-27.

12. Gonzalez-Herrera, I.G., et al., *IRES-dependent regulation of FGF-2 mRNA translation in pathophysiological conditions in the mouse.* Biochem Soc Trans, 2006. **34**(Pt 1): p. 17-21.

13. Creancier, L., et al., *Fibroblast growth factor 2 internal ribosome entry site (IRES) activity ex vivo and in transgenic mice reveals a stringent tissue-specific regulation.* J Cell Biol, 2000. **150**(1): p. 275-81.

14. Galy, B., et al., *p53 directs conformational change and translation initiation blockade of human fibroblast growth factor 2 mRNA.* Oncogene, 2001. **20**(34): p. 4613-20.

15. Bonnal, S., et al., *Heterogeneous nuclear ribonucleoprotein A1 is a novel internal ribosome entry site trans-acting factor that modulates alternative initiation of translation of the fibroblast growth factor 2 mRNA.* J Biol Chem, 2005. **280**(6): p. 4144-53.

16. Vagner, S., et al., *Translation of CUG- but not AUG-initiated forms of human fibroblast growth factor 2 is activated in transformed and stressed cells.* J Cell Biol, 1996. **135**(5): p. 1391-402.

17. Touriol, C., et al., *Alternative translation initiation of human fibroblast growth factor 2 mRNA controlled by its 3'-untranslated region involves a Poly(A) switch and a translational enhancer.* J Biol Chem, 2000. **275**(25): p. 19361-7.

18. Ebert, A.D., et al., *Tec-kinase-mediated phosphorylation of fibroblast growth factor 2 is essential for unconventional secretion.* Traffic, 2010. **11**(6): p. 813-26.

19. Pintucci, G., N. Quarto, and D.B. Rifkin, *Methylation of high molecular weight fibroblast growth factor-2 determines post-translational increases in molecular weight and affects its intracellular distribution.* Mol Biol Cell, 1996. **7**(8): p. 1249-58.

20. Klein, S., et al., *Biochemical analysis of the arginine methylation of high molecular weight fibroblast growth factor-2.* J Biol Chem, 2000. **275**(5): p. 3150-7.

21. Doble, B.W., et al., *Calcium protects pituitary basic fibroblast growth factors from limited proteolysis by co-purifying proteases.* Biochem Biophys Res Commun, 1990. **173**(3): p. 1116-22.

22. Yu, P.J., et al., *Thrombin cleaves the high molecular weight forms of basic fibroblast growth factor (FGF-2): a novel mechanism for the control of FGF-2 and thrombin activity.* Oncogene, 2008. **27**(18): p. 2594-601.

23. Rizvi, F., et al., *Chamber-specific differences in human cardiac fibroblast proliferation and responsiveness toward simvastatin.* Am J Physiol Cell Physiol, 2016. **311**(2): p. C330-9.

24. Przybylski, M., *A review of the current research on the role of bFGF and VEGF in angiogenesis.* J Wound Care, 2009. **18**(12): p. 516-9.

25. Santiago, J.J., et al., *Preferential accumulation and export of high molecular weight FGF-2 by rat cardiac non-myocytes.* Cardiovasc Res, 2011. **89**(1): p. 139-47.

26. Okada-Ban, M., J.P. Thiery, and J. Jouanneau, *Fibroblast growth factor-2.* Int J Biochem Cell Biol, 2000. **32**(3): p. 263-7.

27. Sheng, Z., J.A. Lewis, and W.J. Chirico, *Nuclear and nucleolar localization of 18-kDa fibroblast growth factor-2 is controlled by C-terminal signals.* J Biol Chem, 2004. **279**(38): p. 40153-60.

28. Bugler, B., F. Amalric, and H. Prats, *Alternative initiation of translation determines cytoplasmic or nuclear localization of basic fibroblast growth factor.* Mol Cell Biol, 1991. **11**(1): p. 573-7.

29. Quarto, N., F.P. Finger, and D.B. Rifkin, *The NH2-terminal extension of high molecular weight bFGF is a nuclear targeting signal.* J Cell Physiol, 1991. **147**(2): p. 311-8.

30. Wang, F., et al., *Nuclear translocation of fibroblast growth factor-2 (FGF2) is regulated by Karyopherin-beta2 and Ran GTPase in human glioblastoma cells.* Oncotarget, 2015. **6**(25): p. 21468-78.

31. Dahl, J.P., et al., *Participation of Na,K-ATPase in FGF-2 secretion: rescue of ouabain-inhibitable FGF-2 secretion by ouabain-resistant Na,K-ATPase alpha subunits.* Biochemistry, 2000. **39**(48): p. 14877-83.

32. La Venuta, G., et al., *The Startling Properties of Fibroblast Growth Factor 2: How to Exit Mammalian Cells without a Signal Peptide at Hand.* J Biol Chem, 2015. **290**(45): p. 27015-20.

33. Steringer, J.P. and W. Nickel, *A direct gateway into the extracellular space: Unconventional secretion of FGF2 through self-sustained plasma membrane pores.* Semin Cell Dev Biol, 2018. **83**: p. 3-7.

34. Steringer, J.P., et al., *Key steps in unconventional secretion of fibroblast growth factor 2 reconstituted with purified components.* Elife, 2017. **6**.

35. Keller, M., et al., *Active caspase-1 is a regulator of unconventional protein secretion.* Cell, 2008. **132**(5): p. 818-31.

36. Martin-Sanchez, F., et al., *Inflammasome-dependent IL-1beta release depends upon membrane permeabilisation.* Cell Death Differ, 2016. **23**(7): p. 1219-31.

37. Javidi-Sharifi, N., et al., *FGF2-FGFR1 signaling regulates release of Leukemia-Protective exosomes from bone marrow stromal cells.* Elife, 2019. **8**.

38. Itoh, N. and H. Ohta, *Pathophysiological roles of FGF signaling in the heart.* Front Physiol, 2013. **4**: p. 247.

39. Ornitz, D.M. and N. Itoh, *The Fibroblast Growth Factor signaling pathway.* Wiley Interdiscip Rev Dev Biol, 2015. **4**(3): p. 215-66.

40. Iwai-Kanai, E., et al., *Basic fibroblast growth factor protects cardiac myocytes from iNOS-mediated apoptosis.* J Cell Physiol, 2002. **190**(1): p. 54-62.

41. House, S.L., et al., *Fibroblast Growth Factor 2 Mediates Isoproterenol-induced Cardiac Hypertrophy through Activation of the Extracellular Regulated Kinase.* Mol Cell Pharmacol, 2010. **2**(4): p. 143-154.

42. House, S.L., et al., *Cardioprotection induced by cardiac-specific overexpression of fibroblast growth factor-2 is mediated by the MAPK cascade.* Am J Physiol Heart Circ Physiol, 2005. **289**(5): p. H2167-75.

43. Ma, X., et al., *Chromatin compaction and cell death by high molecular weight FGF-2 depend on its nuclear localization, intracrine ERK activation, and engagement of mitochondria.* J Cell Physiol, 2007. **213**(3): p. 690-8.

44. Brand, C.S., J.K. Lighthouse, and M.A. Trembley, *Protective transcriptional mechanisms in cardiomyocytes and cardiac fibroblasts.* J Mol Cell Cardiol, 2019. **132**: p. 1-12.

45. Ong, S.H., et al., *Stimulation of phosphatidylinositol 3-kinase by fibroblast growth factor receptors is mediated by coordinated recruitment of multiple docking proteins.* Proc Natl Acad Sci U S A, 2001. **98**(11): p. 6074-9.

46. Ediriweera, M.K., K.H. Tennekoon, and S.R. Samarakoon, *Role of the PI3K/AKT/mTOR signaling pathway in ovarian cancer: Biological and therapeutic significance.* Semin Cancer Biol, 2019.

47. Mortenson, M.M., et al., *BCL-2 functions as an activator of the AKT signaling pathway in pancreatic cancer.* J Cell Biochem, 2007. **102**(5): p. 1171-9.

48. Ye, G., et al., *Vascular smooth muscle cells activate PI3K/Akt pathway to attenuate myocardial ischemia/reperfusion-induced apoptosis and autophagy by secreting bFGF.* Biomed Pharmacother, 2018. **107**: p. 1779-1785.

49. Ling, L., et al., *bFGF promotes Sca1+ cardiac stem cell migration through activation of the PI3K/Akt pathway.* Mol Med Rep, 2018. **17**(2): p. 2349-2356.

50. Chen, Q., et al., *FGF-2 Transcriptionally Down-Regulates the Expression of BNIP3L via PI3K/Akt/FoxO3a Signaling and Inhibits Necrosis and Mitochondrial Dysfunction Induced by High Concentrations of Hydrogen Peroxide in H9c2 Cells.* Cell Physiol Biochem, 2016. **40**(6): p. 1678-1691.

51. Liu, M.H., et al., *PI3K/Akt/FoxO3a signaling mediates cardioprotection of FGF-2 against hydrogen peroxide-induced apoptosis in H9c2 cells.* Mol Cell Biochem, 2016. **414**(1-2): p. 57-66.

52. Cheng, Y., et al., *Neuroprotective effects of LMW and HMW FGF2 against amyloid beta toxicity in primary cultured hippocampal neurons.* Neurosci Lett, 2016. **632**: p. 109-13.

53. Wang, Z., et al., *bFGF attenuates endoplasmic reticulum stress and mitochondrial injury on myocardial ischaemia/reperfusion via activation of PI3K/Akt/ERK1/2 pathway.* J Cell Mol Med, 2015. **19**(3): p. 595-607.

54. Jhanwar-Uniyal, M., et al., *Discrete signaling mechanisms of mTORC1 and mTORC2: Connected yet apart in cellular and molecular aspects.* Adv Biol Regul, 2017. **64**: p. 39-48.

55. Sciarretta, S., M. Volpe, and J. Sadoshima, *Mammalian target of rapamycin signaling in cardiac physiology and disease.* Circ Res, 2014. **114**(3): p. 549-64.

56. Koleini, N., et al., *Fibroblast growth factor-2-mediated protection of cardiomyocytes from the toxic effects of doxorubicin requires the mTOR/Nrf-2/HO-1 pathway.* Oncotarget, 2017. **8**(50): p. 87415-87430.

57. Wang, Z.G., et al., *bFGF regulates autophagy and ubiquitinated protein accumulation induced by myocardial ischemia/reperfusion via the activation of the PI3K/Akt/mTOR pathway.* Sci Rep, 2015. **5**: p. 9287.

58. Tappia, P.S., et al., *Fibroblast growth factor-2 stimulates phospholipase Cbeta in adult cardiomyocytes.* Biochem Cell Biol, 1999. **77**(6): p. 569-75.

59. Padua, R.R., et al., *FGF-2-induced negative inotropism and cardioprotection are inhibited by chelerythrine: involvement of sarcolemmal calcium-independent protein kinase C.* J Mol Cell Cardiol, 1998. **30**(12): p. 2695-709.

60. Jiang, Z.S., et al., *Acute protection of ischemic heart by FGF-2: involvement of FGF-2 receptors and protein kinase C.* Am J Physiol Heart Circ Physiol, 2002. **282**(3): p. H1071-80.

61. Doble, B.W., et al., *Phosphorylation of serine 262 in the gap junction protein connexin-43 regulates DNA synthesis in cell-cell contact forming cardiomyocytes.* J Cell Sci, 2004. **117**(Pt 3): p. 507-14.

62. Srisakuldee, W., et al., *Administration of FGF-2 to the heart stimulates connexin-43 phosphorylation at protein kinase C target sites.* Cell Commun Adhes, 2006. **13**(1-2): p. 13-9.

63. Jiang, Z.S., et al., *High molecular weight FGF-2 promotes postconditioning-like cardioprotection linked to activation of protein kinase C isoforms, as well as Akt and p70 S6 kinases. [corrected]*. Can J Physiol Pharmacol, 2009. **87**(10): p. 798-804.

64. Wang, J., et al., *FGF-2 protects cardiomyocytes from doxorubicin damage via protein kinase C-dependent effects on efflux transporters.* Cardiovasc Res, 2013. **98**(1): p. 56-63.

65. Zhou, M., et al., *Fibroblast growth factor 2 control of vascular tone.* Nat Med, 1998. **4**(2): p. 201-7.

66. Dono, R., et al., *Impaired cerebral cortex development and blood pressure regulation in FGF-2-deficient mice.* Embo j, 1998. **17**(15): p. 4213-25.

67. Ortega, S., et al., *Neuronal defects and delayed wound healing in mice lacking fibroblast growth factor 2.* Proc Natl Acad Sci U S A, 1998. **95**(10): p. 5672-7.

68. Schultz, J.E., et al., *Fibroblast growth factor-2 mediates pressure-induced hypertrophic response.* J Clin Invest, 1999. **104**(6): p. 709-19.

69. Pellieux, C., et al., *Dilated cardiomyopathy and impaired cardiac hypertrophic response to angiotensin II in mice lacking FGF-2.* J Clin Invest, 2001. **108**(12): p. 1843-51.

70. Virag, J.A., et al., *Fibroblast growth factor-2 regulates myocardial infarct repair: effects on cell proliferation, scar contraction, and ventricular function.* Am J Pathol, 2007. **171**(5): p. 1431-40.

71. House, S.L., et al., *Fibroblast growth factor 2 is an essential cardioprotective factor in a closed-chest model of cardiac ischemia-reperfusion injury.* Physiol Rep, 2015. **3**(1).

72. Bush, M.A., et al., *Pharmacokinetics and pharmacodynamics of recombinant FGF-2 in a phase I trial in coronary artery disease.* J Clin Pharmacol, 2001. **41**(4): p. 378-85.

73. Garmy-Susini, B., et al., *Role of fibroblast growth factor-2 isoforms in the effect of estradiol on endothelial cell migration and proliferation.* Circ Res, 2004. **94**(10): p. 1301-9.

74. Azhar, M., et al., *Gene targeted ablation of high molecular weight fibroblast growth factor-2.* Dev Dyn, 2009. **238**(2): p. 351-7.

75. Nusayr, E. and T. Doetschman, *Cardiac development and physiology are modulated by FGF2 in an isoform- and sex-specific manner.* Physiol Rep, 2013. **1**(4).

76. Homer-Bouthiette, C., et al., *Knockout of nuclear high molecular weight FGF2 isoforms in mice modulates bone and phosphate homeostasis.* J Biol Chem, 2014. **289**(52): p. 36303-14.

77. Du, E., L. Xiao, and M.M. Hurley, *FGFR Inhibitor Ameliorates Hypophosphatemia and Impaired Engrailed-1/Wnt Signaling in FGF2 High Molecular Weight Isoform Transgenic Mice.* J Cell Biochem, 2016. **117**(9): p. 1991-2000.

78. Meo Burt, P., et al., *FGF2 High Molecular Weight Isoforms Contribute to Osteoarthropathy in Male Mice.* Endocrinology, 2016. **157**(12): p. 4602-4614.

79. Du, E., L. Xiao, and M.M. Hurley, *FGF23 Neutralizing Antibody Ameliorates Hypophosphatemia and Impaired FGF Receptor Signaling in Kidneys of HMWFGF2 Transgenic Mice.* J Cell Physiol, 2017. **232**(3): p. 610-616.

80. Florkiewicz, R.Z., et al., *Gastric mucosal injury activates bFGF gene expression and triggers preferential translation of high molecular weight bFGF isoforms through CUG-initiated, non-canonical codons.* Biochem Biophys Res Commun, 2011. **409**(3): p. 494-9.

81. Sahores, A., et al., *Increased High Molecular Weight FGF2 in Endocrine-Resistant Breast Cancer.* Horm Cancer, 2018. **9**(5): p. 338-348.

82. Padua, R.R., et al., *Basic fibroblast growth factor is cardioprotective in ischemia-reperfusion injury.* Mol Cell Biochem, 1995. **143**(2): p. 129-35.

83. Cuevas, P., et al., *Fibroblast growth factor cardioprotection against ischemia-reperfusion injury may involve K+ ATP channels.* Eur J Med Res, 2000. **5**(4): p. 145-9.

84. Unger, E.F., et al., *Basic fibroblast growth factor enhances myocardial collateral flow in a canine model.* Am J Physiol, 1994. **266**(4 Pt 2): p. H1588-95.

85. Sontag, D.P., et al., *FGF-2 and FGF-16 protect isolated perfused mouse hearts from acute doxorubicin-induced contractile dysfunction.* Cardiovasc Toxicol, 2013. **13**(3): p. 244-53.

86. Pasumarthi, K.B., et al., *Over-expression of CUG- or AUG-initiated forms of basic fibroblast growth factor in cardiac myocytes results in similar effects on mitosis and protein synthesis but distinct nuclear morphologies.* J Mol Cell Cardiol, 1994. **26**(8): p. 1045-60.

87. Pasumarthi, K.B., E. Kardami, and P.A. Cattini, *High and low molecular weight fibroblast growth factor-2 increase proliferation of neonatal rat cardiac myocytes but*

have differential effects on binucleation and nuclear morphology. Evidence for both paracrine and intracrine actions of fibroblast growth factor-2. Circ Res, 1996. **78**(1): p. 126-36.

88. Hirst, C.J., et al., *High levels of CUG-initiated FGF-2 expression cause chromatin compaction, decreased cardiomyocyte mitosis, and cell death.* Mol Cell Biochem, 2003. **246**(1-2): p. 111-6.

89. Chlebova, K., et al., *High molecular weight FGF2: the biology of a nuclear growth factor.* Cell Mol Life Sci, 2009. **66**(2): p. 225-35.

90. Wang, Q., et al., *Cajal bodies are linked to genome conformation.* Nat Commun, 2016. **7**: p. 10966.

91. Jiang, Z.S., et al., *High- but not low-molecular weight FGF-2 causes cardiac hypertrophy in vivo; possible involvement of cardiotrophin-1.* J Mol Cell Cardiol, 2007. **42**(1): p. 222-33.

92. Liao, S., et al., *The influence of FGF2 high molecular weight (HMW) isoforms in the development of cardiac ischemia-reperfusion injury.* J Mol Cell Cardiol, 2010. **48**(6): p. 1245-54.

93. Sun, L.Y., et al., *High molecular weight fibroblast growth factor-2 as a promising prognostic biomarker to predict the occurrence of heart failure in atrial fibrillation patients.* Heart Vessels, 2017. **32**(12): p. 1506-1512.

94. Braunwald, E., *Heart failure.* JACC Heart Fail, 2013. **1**(1): p. 1-20.

95. Felker, G.M., et al., *Underlying causes and long-term survival in patients with initially unexplained cardiomyopathy.* N Engl J Med, 2000. **342**(15): p. 1077-84.

96. Ponikowski, P., et al., *2016 ESC Guidelines for the diagnosis and treatment of acute and chronic heart failure: The Task Force for the diagnosis and treatment of acute and chronic heart failure of the European Society of Cardiology (ESC). Developed with the special contribution of the Heart Failure Association (HFA) of the ESC.* Eur J Heart Fail, 2016. **18**(8): p. 891-975.

97. Lipshultz, S.E., et al., *Continuous Versus Bolus Infusion of Doxorubicin in Children With ALL: Long-term Cardiac Outcomes.* Pediatrics, 2012. **130**(6): p. 1003-11.

98. Lipshultz, S.E., et al., *Assessment of dexrazoxane as a cardioprotectant in doxorubicin-treated children with high-risk acute lymphoblastic leukaemia: long-term follow-up of a prospective, randomised, multicentre trial.* Lancet Oncol, 2010. **11**(10): p. 950-61.

99. Lipshultz, S.E., et al., *Changes in cardiac biomarkers during doxorubicin treatment of pediatric patients with high-risk acute lymphoblastic leukemia: associations with long-term echocardiographic outcomes.* J Clin Oncol, 2012. **30**(10): p. 1042-9.

100. Colombo, A., et al., *Cardiac toxicity of anticancer agents.* Curr Cardiol Rep, 2013. **15**(5): p. 362.

101. Wang, E.Y., et al., *Autophagy in the heart: too much of a good thing?* J Cardiovasc Pharmacol, 2012. **60**(2): p. 110-7.

102. Zamorano, J.L., et al., *2016 ESC Position Paper on cancer treatments and cardiovascular toxicity developed under the auspices of the ESC Committee for Practice Guidelines: The Task Force for cancer treatments and cardiovascular toxicity of the European Society of Cardiology (ESC).* Eur J Heart Fail, 2017. **19**(1): p. 9-42.

103. Desai, V.G., et al., *Development of doxorubicin-induced chronic cardiotoxicity in the B6C3F1 mouse model.* Toxicol Appl Pharmacol, 2013. **266**(1): p. 109-21.

104. Zhang, Y.W., et al., *Cardiomyocyte death in doxorubicin-induced cardiotoxicity.* Arch Immunol Ther Exp (Warsz), 2009. **57**(6): p. 435-45.

105. Ichikawa, Y., et al., *Cardiotoxicity of doxorubicin is mediated through mitochondrial iron accumulation.* J Clin Invest, 2014. **124**(2): p. 617-30.

106. Tacar, O., P. Sriamornsak, and C.R. Dass, *Doxorubicin: an update on anticancer molecular action, toxicity and novel drug delivery systems.* J Pharm Pharmacol, 2013. **65**(2): p. 157-70.

107. Wang, X., et al., *Ghrelin inhibits doxorubicin cardiotoxicity by inhibiting excessive autophagy through AMPK and p38-MAPK.* Biochem Pharmacol, 2014. **88**(3): p. 334-50.

108. Guo, R., et al., *Hydrogen sulfide attenuates doxorubicin-induced cardiotoxicity by inhibition of the p38 MAPK pathway in H9c2 cells.* Int J Mol Med, 2013. **31**(3): p. 644-50.

109. Simunek, T., et al., *Anthracycline-induced cardiotoxicity: overview of studies examining the roles of oxidative stress and free cellular iron.* Pharmacol Rep, 2009. **61**(1): p. 154-71.

110. Angsutararux, P., S. Luanpitpong, and S. Issaragrisil, *Chemotherapy-Induced Cardiotoxicity: Overview of the Roles of Oxidative Stress.* Oxid Med Cell Longev, 2015. **2015**: p. 795602.

111. Damiani, R.M., et al., *Pathways of cardiac toxicity: comparison between chemotherapeutic drugs doxorubicin and mitoxantrone.* Arch Toxicol, 2016. **90**(9): p. 2063-76.

112. Octavia, Y., et al., *Doxorubicin-induced cardiomyopathy: from molecular mechanisms to therapeutic strategies.* J Mol Cell Cardiol, 2012. **52**(6): p. 1213-25.

113. Neilan, T.G., et al., *Disruption of nitric oxide synthase 3 protects against the cardiac injury, dysfunction, and mortality induced by doxorubicin.* Circulation, 2007. **116**(5): p. 506-14.

114. Mukhopadhyay, P., et al., *Role of superoxide, nitric oxide, and peroxynitrite in doxorubicin-induced cell death in vivo and in vitro.* Am J Physiol Heart Circ Physiol, 2009. **296**(5): p. H1466-83.

115. Miura, T., S. Muraoka, and T. Ogiso, *Adriamycin-Fe3+-induced mitochondrial protein damage with lipid peroxidation.* Biol Pharm Bull, 1995. **18**(4): p. 514-7.

116. Nohl, H., *Identification of the site of adriamycin-activation in the heart cell.* Biochem Pharmacol, 1988. **37**(13): p. 2633-7.

117. de Wolf, F.A., *Binding of doxorubicin to cardiolipin as compared to other anionic phospholipids--an evaluation of electrostatic effects.* Biosci Rep, 1991. **11**(5): p. 275-84.

118. Robinson, N.C., *Functional binding of cardiolipin to cytochrome c oxidase.* J Bioenerg Biomembr, 1993. **25**(2): p. 153-63.

119. Parker, M.A., V. King, and K.P. Howard, *Nuclear magnetic resonance study of doxorubicin binding to cardiolipin containing magnetically oriented phospholipid bilayers.* Biochim Biophys Acta, 2001. **1514**(2): p. 206-16.

120. Cheung, K.G., et al., *Sirtuin-3 (SIRT3) Protein Attenuates Doxorubicin-induced Oxidative Stress and Improves Mitochondrial Respiration in H9c2 Cardiomyocytes.* J Biol Chem, 2015. **290**(17): p. 10981-93.

121. Galluzzi, L., et al., *Mitochondrial control of cellular life, stress, and death.* Circ Res, 2012. **111**(9): p. 1198-207.

122. Unverferth, D.V., et al., *Attempt to prevent doxorubicin-induced acute human myocardial morphologic damage with acetylcysteine.* J Natl Cancer Inst, 1983. **71**(5): p. 917-20.

123. Broeyer, F.J., et al., *Evaluation of lecithinized human recombinant super oxide dismutase as cardioprotectant in anthracycline-treated breast cancer patients.* Br J Clin Pharmacol, 2014. **78**(5): p. 950-60.

124. Vincent, D.T., et al., *The role of antioxidants in the era of cardiooncology.* Cancer Chemother Pharmacol, 2013. **72**(6): p. 1157-68.

125. Green, H., et al., *Pegylated liposomal doxorubicin as first-line monotherapy in elderly women with locally advanced or metastatic breast cancer: novel treatment predictive factors identified.* Cancer Lett, 2011. **313**(2): p. 145-53.

126. Jones, S.E., et al., *Adjuvant docetaxel and cyclophosphamide plus trastuzumab in patients with HER2-amplified early stage breast cancer: a single-group, open-label, phase 2 study.* Lancet Oncol, 2013. **14**(11): p. 1121-8.

127. Press, M.F., et al., *Alteration of topoisomerase II-alpha gene in human breast cancer: association with responsiveness to anthracycline-based chemotherapy.* J Clin Oncol, 2011. **29**(7): p. 859-67.

128. O'Malley, F.P., et al., *Topoisomerase II alpha protein and responsiveness of breast cancer to adjuvant chemotherapy with CEF compared to CMF in the NCIC CTG randomized MA.5 adjuvant trial.* Breast Cancer Res Treat, 2011. **128**(2): p. 401-9.

129. Burgess, D.J., et al., *Topoisomerase levels determine chemotherapy response in vitro and in vivo.* Proc Natl Acad Sci U S A, 2008. **105**(26): p. 9053-8.

130. Lyu, Y.L., et al., *Topoisomerase IIbeta mediated DNA double-strand breaks: implications in doxorubicin cardiotoxicity and prevention by dexrazoxane.* Cancer Res, 2007. **67**(18): p. 8839-46.

131. Deng, S., et al., *Dexrazoxane may prevent doxorubicin-induced DNA damage via depleting both topoisomerase II isoforms.* BMC Cancer, 2014. **14**: p. 842.

132. Tokarska-Schlattner, M., et al., *Early effects of doxorubicin in perfused heart: transcriptional profiling reveals inhibition of cellular stress response genes.* Am J Physiol Regul Integr Comp Physiol, 2010. **298**(4): p. R1075-88.

133. Zhang, S., et al., *Identification of the molecular basis of doxorubicin-induced cardiotoxicity.* Nat Med, 2012. **18**(11): p. 1639-42.

134. Hasinoff, B.B., et al., *Chemical, biological and clinical aspects of dexrazoxane and other bisdioxopiperazines.* Curr Med Chem, 1998. **5**(1): p. 1-28.

135. Vavrova, A., et al., *Catalytic inhibitors of topoisomerase II differently modulate the toxicity of anthracyclines in cardiac and cancer cells.* PLoS One, 2013. **8**(10): p. e76676.

136. Yoshida, M., et al., *Chronic doxorubicin cardiotoxicity is mediated by oxidative DNA damage-ATM-p53-apoptosis pathway and attenuated by pitavastatin through the inhibition of Rac1 activity.* J Mol Cell Cardiol, 2009. **47**(5): p. 698-705.

137. Chang, Y.L., et al., *Different roles of p53 in the regulation of DNA damage caused by 1,2-heteroannelated anthraquinones and doxorubicin.* Int J Biochem Cell Biol, 2011. **43**(12): p. 1720-8.

138. Velez, J.M., et al., *p53 Regulates oxidative stress-mediated retrograde signaling: a novel mechanism for chemotherapy-induced cardiac injury.* PLoS One, 2011. **6**(3): p. e18005.

139. Wang, E.Y., et al., *p53 mediates autophagy and cell death by a mechanism contingent on Bnip3.* Hypertension, 2013. **62**(1): p. 70-7.

140. Park, A.M., et al., *Mechanism of anthracycline-mediated down-regulation of GATA4 in the heart.* Cardiovasc Res, 2011. **90**(1): p. 97-104.

141. Feridooni, T., et al., *Cardiomyocyte specific ablation of p53 is not sufficient to block doxorubicin induced cardiac fibrosis and associated cytoskeletal changes.* PLoS One, 2011. **6**(7): p. e22801.

142. Zhu, W., et al., *P53 inhibition exacerbates late-stage anthracycline cardiotoxicity.* Cardiovasc Res, 2014. **103**(1): p. 81-9.

143. Dhingra, R., et al., *Bnip3 mediates doxorubicin-induced cardiac myocyte necrosis and mortality through changes in mitochondrial signaling.* Proc Natl Acad Sci U S A, 2014. **111**(51): p. E5537-44.

144. Roca-Alonso, L., et al., *Myocardial MiR-30 downregulation triggered by doxorubicin drives alterations in beta-adrenergic signaling and enhances apoptosis.* Cell Death Dis, 2015. **6**: p. e1754.

145. Maejima, Y., et al., *Induction of premature senescence in cardiomyocytes by doxorubicin as a novel mechanism of myocardial damage.* Aging Cell, 2008. **7**(2): p. 125-36.

146. Xu, X., et al., *Macrophage Migration Inhibitory Factor (MIF) Deficiency Exacerbates Aging-Induced Cardiac Remodeling and Dysfunction Despite Improved Inflammation: Role of Autophagy Regulation.* Sci Rep, 2016. **6**: p. 22488.

147. Shirakabe, A., et al., *Aging and Autophagy in the Heart.* Circ Res, 2016. **118**(10): p. 1563-76.

148. Hoshino, A., et al., *Cytosolic p53 inhibits Parkin-mediated mitophagy and promotes mitochondrial dysfunction in the mouse heart.* Nat Commun, 2013. **4**: p. 2308.

149. Rader, F., et al., *Left ventricular hypertrophy in valvular aortic stenosis: mechanisms and clinical implications.* Am J Med, 2015. **128**(4): p. 344-52.

150. Tanai, E. and S. Frantz, *Pathophysiology of Heart Failure.* Compr Physiol, 2015. **6**(1): p. 187-214.

151. Lyon, R.C., et al., *Mechanotransduction in cardiac hypertrophy and failure.* Circ Res, 2015. **116**(8): p. 1462-1476.

152. Ruwhof, C. and A. van der Laarse, *Mechanical stress-induced cardiac hypertrophy: mechanisms and signal transduction pathways.* Cardiovasc Res, 2000. **47**(1): p. 23-37.

153. Spadari, R.C., et al., *Role of Beta-adrenergic Receptors and Sirtuin Signaling in the Heart During Aging, Heart Failure, and Adaptation to Stress.* Cell Mol Neurobiol, 2018. **38**(1): p. 109-120.

154. Khamssi, M. and O.E. Brodde, *The role of cardiac beta1- and beta2-adrenoceptor stimulation in heart failure.* J Cardiovasc Pharmacol, 1990. **16 Suppl 5**: p. S133-7.

155. Tse, J., et al., *Down regulation of myocardial beta1-adrenoceptor signal transduction system in pacing-induced failure in dogs with aortic stenosis-induced left ventricular hypertrophy.* Mol Cell Biochem, 2000. **205**(1-2): p. 67-73.

156. Anthonio, R.L., et al., *Beta-adrenoceptor density in chronic infarcted myocardium: a subtype specific decrease of beta1-adrenoceptor density.* Int J Cardiol, 2000. **72**(2): p. 137-41.

157. Chesley, A., et al., *The beta(2)-adrenergic receptor delivers an antiapoptotic signal to cardiac myocytes through G(i)-dependent coupling to phosphatidylinositol 3'-kinase.* Circ Res, 2000. **87**(12): p. 1172-9.

158. Amin, P., M. Singh, and K. Singh, *beta-Adrenergic Receptor-Stimulated Cardiac Myocyte Apoptosis: Role of beta1 Integrins.* J Signal Transduct, 2011. **2011**: p. 179057.

159. Gorre, F. and H. Vandekerckhove, *Beta-blockers: focus on mechanism of action. Which beta-blocker, when and why?* Acta Cardiol, 2010. **65**(5): p. 565-70.

160. He, Y.M., et al., *beta-Blockers in heart failure: benefits of beta-blockers according to varying male proportions of study patients.* Clin Cardiol, 2012. **35**(8): p. 505-11.

161. Bayes-Genis, A., *Highlights of the 2016 European Society of Cardiology Guidelines on Heart Failure.* Eur Cardiol, 2017. **12**(2): p. 76-77.

162. Takezako, T., et al., *Current topics in angiotensin II type 1 receptor research: Focus on inverse agonism, receptor dimerization and biased agonism.* Pharmacol Res, 2017. **123**: p. 40-50.

163. Li, Y., X.H. Li, and H. Yuan, *Angiotensin II type-2 receptor-specific effects on the cardiovascular system.* Cardiovasc Diagn Ther, 2012. **2**(1): p. 56-62.

164. Falcon, B.L., et al., *Angiotensin II type 2 receptor gene transfer elicits cardioprotective effects in an angiotensin II infusion rat model of hypertension.* Physiol Genomics, 2004. **19**(3): p. 255-61.

165. Rosca, M.G., B. Tandler, and C.L. Hoppel, *Mitochondria in cardiac hypertrophy and heart failure.* J Mol Cell Cardiol, 2013. **55**: p. 31-41.

166. Kole, D., et al., *High molecular weight FGF2 isoforms demonstrate canonical receptor-mediated activity and support human embryonic stem cell self-renewal.* Stem Cell Res, 2017. **21**: p. 106-116.

167. Zhang, L., G.C. Parry, and E.G. Levin, *Inhibition of tumor cell migration by LD22-4, an N-terminal fragment of 24-kDa FGF2, is mediated by Neuropilin 1.* Cancer Res, 2013. **73**(11): p. 3316-25.

168. Levin, E.G., et al., *Suppression of tumor growth and angiogenesis in vivo by a truncated form of 24-kd fibroblast growth factor (FGF)-2.* Am J Pathol, 2004. **164**(4): p. 1183-90.

169. Ding, L., et al., *Inhibition of cell migration and angiogenesis by the amino-terminal fragment of 24kD basic fibroblast growth factor.* J Biol Chem, 2002. **277**(34): p. 31056-61.

170. Claus, P., et al., *Differential intranuclear localization of fibroblast growth factor-2 isoforms and specific interaction with the survival of motoneuron protein.* J Biol Chem, 2003. **278**(1): p. 479-85.

171. Han, X., Z. Xiao, and L.D. Quarles, *Membrane and integrative nuclear fibroblastic growth factor receptor (FGFR) regulation of FGF-23.* J Biol Chem, 2015. **290**(16): p. 10447-59.

172. Cuevas, R., et al., *FGF-2 disrupts mitotic stability in prostate cancer through the intracellular trafficking protein CEP57.* Cancer Res, 2013. **73**(4): p. 1400-10.

173. Srisakuldee, W., *Studies on the role of connexin 43 phosphorylation in the injury - resistant heart*. 2014, The University of Manitoba.

174. Tan, X.H., et al., *Fibroblast growth factor 2 protects against renal ischaemia/reperfusion injury by attenuating mitochondrial damage and proinflammatory signalling.* J Cell Mol Med, 2017. **21**(11): p. 2909-2925.

175. Pan, R.L., et al., *Low-molecular-weight fibroblast growth factor 2 attenuates hepatic fibrosis by epigenetic down-regulation of Delta-like1.* Hepatology, 2015. **61**(5): p. 1708-20.

176. Song, Y.J., C.B. Zhong, and X.B. Wang, *Heat shock protein 70: A promising therapeutic target for myocardial ischemia-reperfusion injury.* J Cell Physiol, 2019. **234**(2): p. 1190-1207.

177. You, X., et al., *Transcriptional up-regulation of relaxin-3 by Nur77 attenuates beta-adrenergic agonist-induced apoptosis in cardiomyocytes.* J Biol Chem, 2018. **293**(36): p. 14001-14011.

178. Dong, C. and G. Wu, *Regulation of anterograde transport of adrenergic and angiotensin II receptors by Rab2 and Rab6 GTPases.* Cell Signal, 2007. **19**(11): p. 2388-99.

Appendices:

Appendix 1, FGF-2 isoforms prevent the dox-induced mitochondrial permeability transition pore, mPTP.

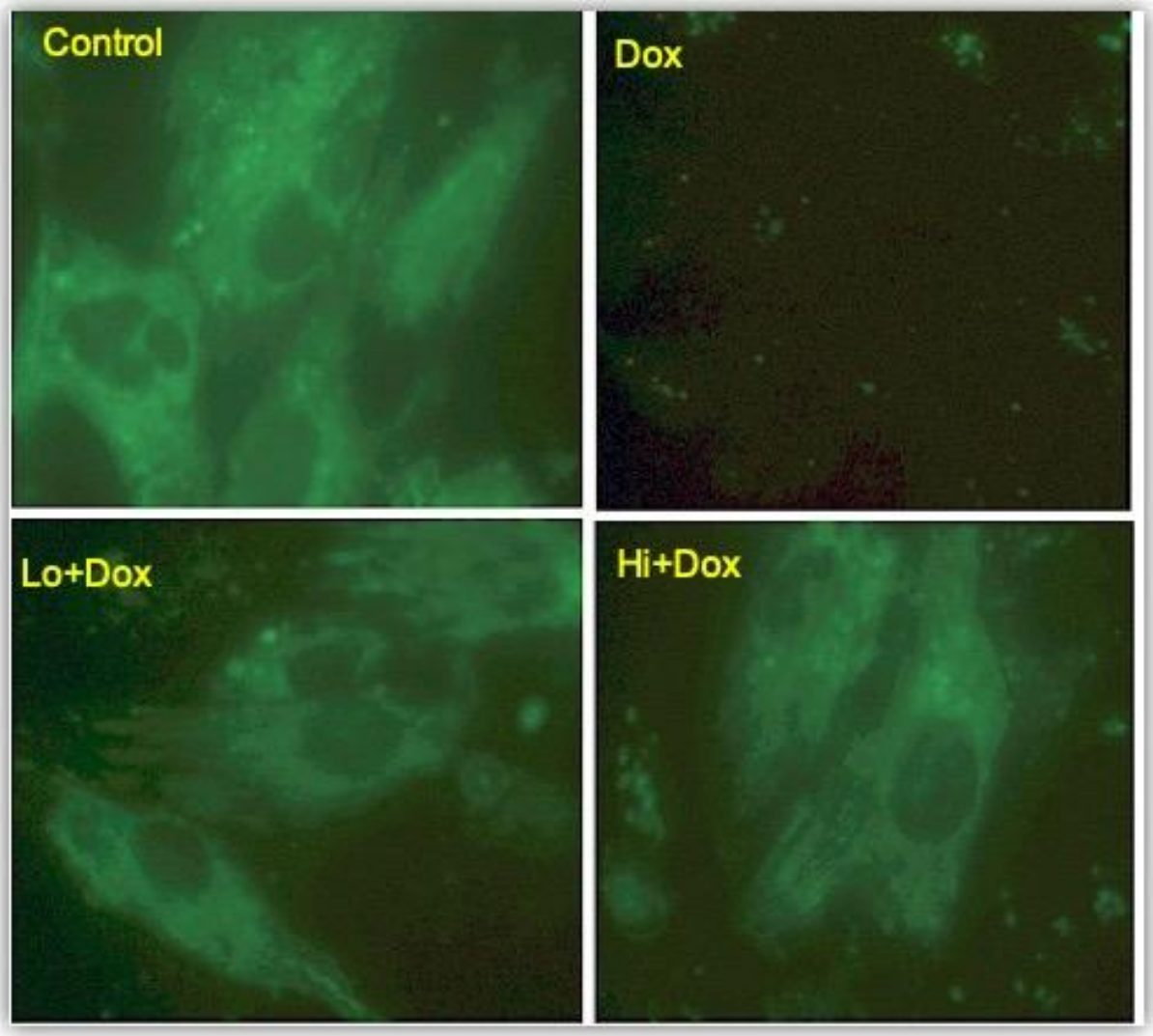

FGF-2 isoforms prevent the Dox-induced mitochondrial permeability transition pore, mPTP.

Representative images of cardiomyocytes, in the absence or presence of Dox and FGF-2 isoforms, as indicated, stained with Calcein-Cobalt, where healthy mitochondria display green color. Cardiomyocytes were exposed to 0.5μM of Dox for 24 hours in the presence and absence of Lo- or Hi-FGF-2 pre-incubation.

Appendix 2, FGF-2 isoforms do not protect MCF-7 cell from dox-induced death.

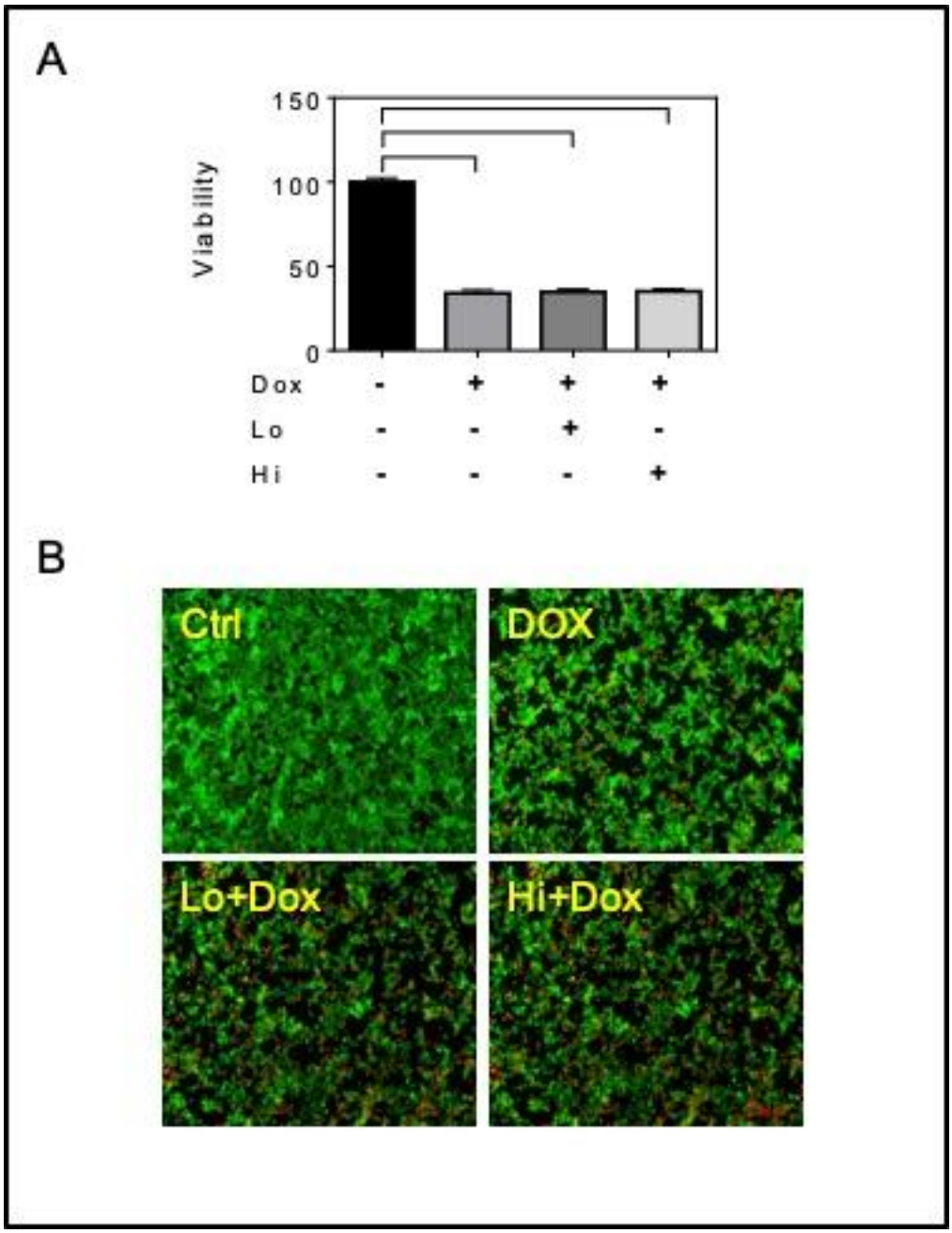

FGF-2 isoforms do not protect MCF-7 cell from Dox-induced death.

A. Viability of MCF-7 cells, measured by the Calcein-AM fluorescence intensity assay. Cells were insulted with Dox 0.5 μM for 24 hours in the presence and absence of FGF-2 isoform pre-incubation for 30 min. **B**. Representative images of Calcein-AM (green, live cells)/Ethidium homodimer (red, dead cells) assay are shown in the lower section. Data is plotted as mean ± SEM and statistical differences are shown by brackets where significant $P<0.05$. The scale bar shown in the figure corresponds to 200 μm.

Appendix 3, FGF-2 isoforms do not change Nrf-2 and HO-1 protein levels in the absence of Doxorubicin.

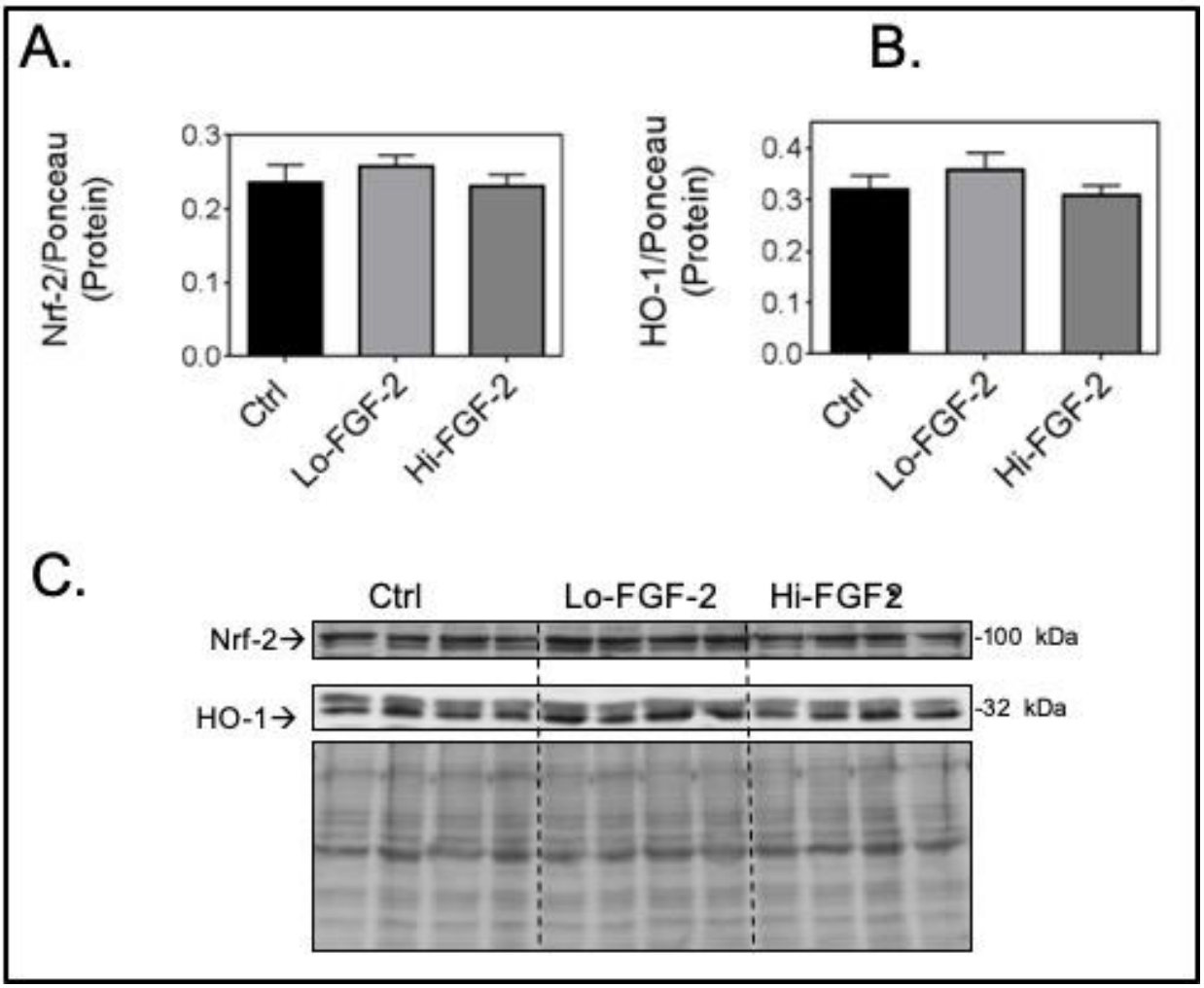

FGF-2 isoforms do not change Nrf-2 and HO-1 protein levels in the absence of Doxorubicin. (A) and (B) show, respectively, relative protein levels of Nrf-2 and HO-1 in cardiomyocytes stimulated with Lo- or Hi-FGF-2 (10 ng/ml) for 24 hours. The corresponding western blots are shown in (**C)**. Ponceau S staining of the total transferred proteins was used for normalization. There are no significant differences between the groups.

Appendix 4, Representative western blots.

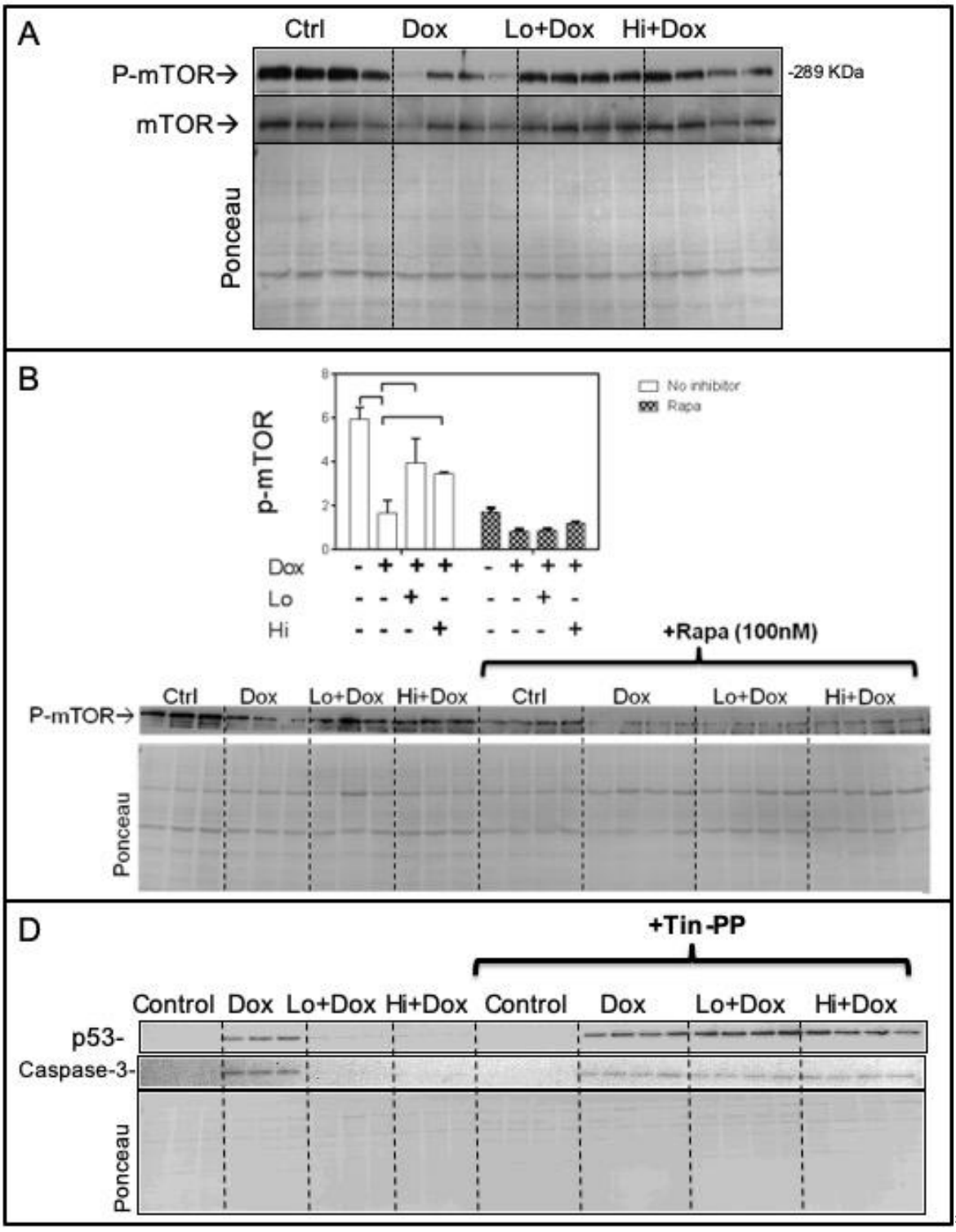

Western blots of cardiomyocytes insulted with Dox for 24 hours, with and without Lo- or Hi-FGF-2 (10ng/ml) 30-min pre-incubation, in the presence and absence of Rapamycin or Tin-PP. [raw data for figures 5 & 6]

Appendix 5, Torin-1 prevents cardioprotection and upregulation of HO-1 by FGF-2 isoforms.

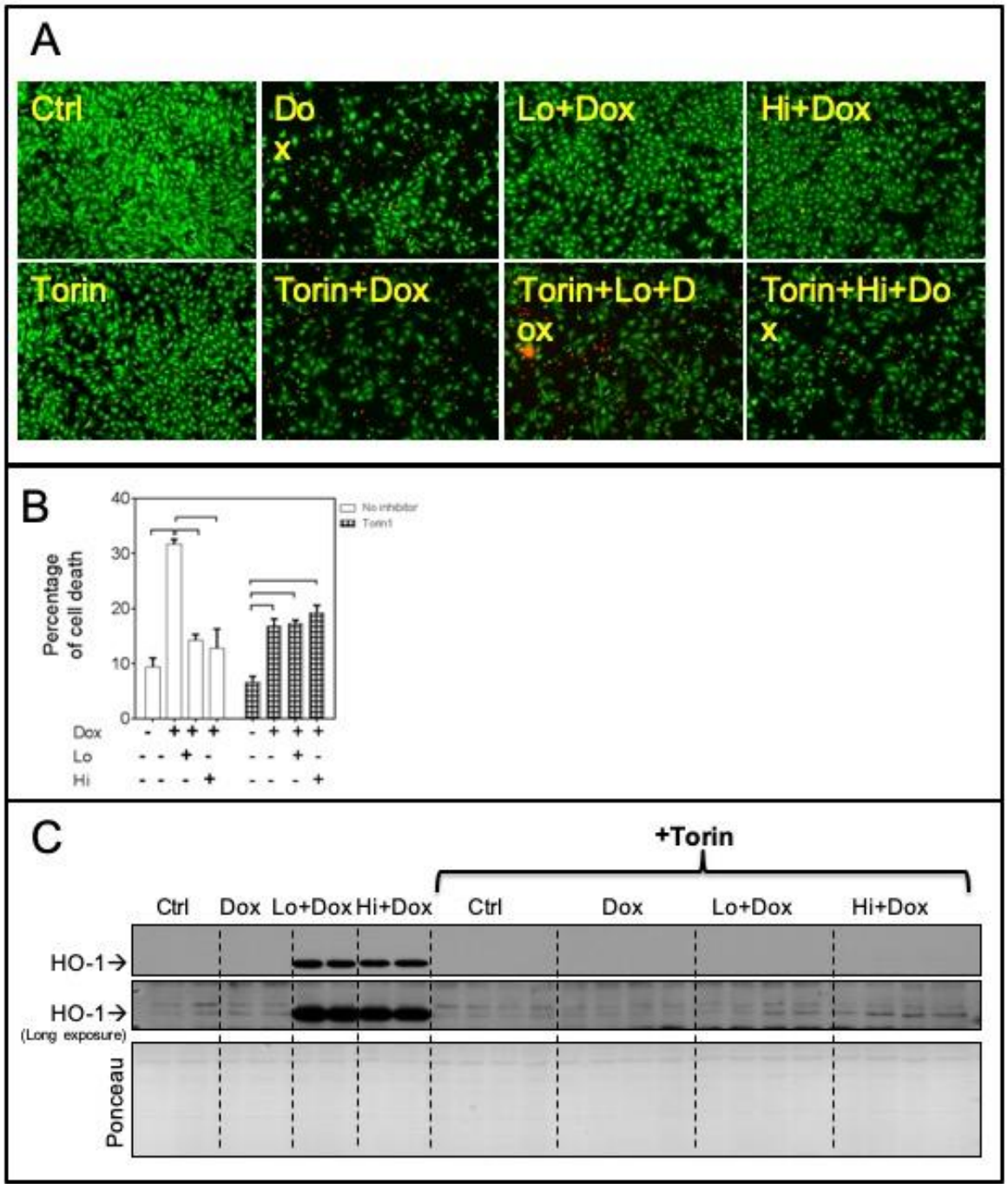

Torin-1 prevents cardioprotection and upregulation of HO-1 by FGF-2 isoforms. (A) Representative fluorescence images from cardiomyocytes exposed or not to Dox, FGF-2 isoforms, and Torin-1, as indicated, stained with the Live/Dead assay. **(B)** Corresponding quantitative data (percent cell death on attached cells), n=4. **(C)** shows a western blot illustrating the effect of Torin on the FGF-2-induced upregulation of HO-1. Both short and long exposed immunoblot images are shown, and demonstrate that Torin abolished the FGF-2 isoform-induced HO-1 upregulation in the presence of Doxorubicin.

Appendix 6, S117A-FGF2 does not protect MCF-7 cells against Dox.

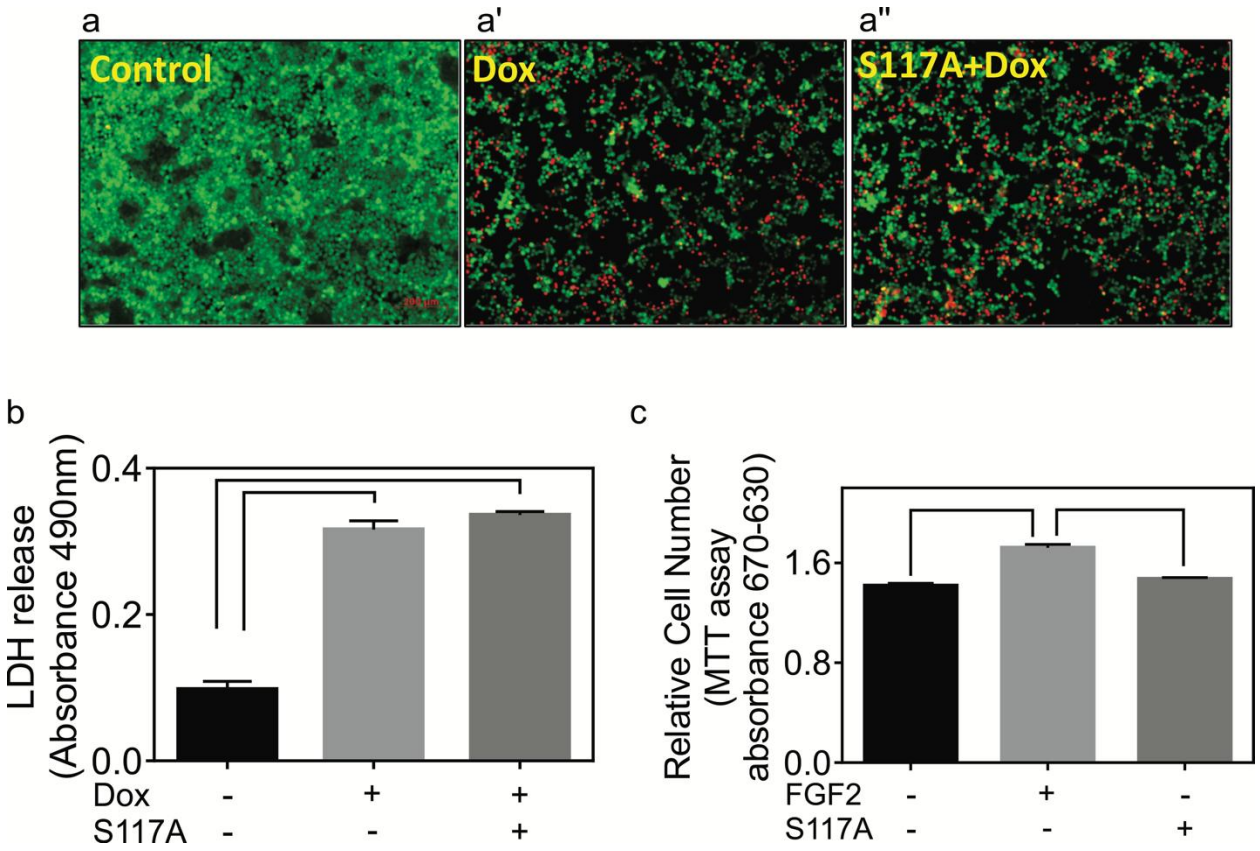

S117A-FGF2 does not protect MCF-7 cells from Dox-induced cell death or damage (LDH release), and does not stimulate MCF-7 cell proliferation. Panel a-a" shows representative images of MCF-7 cells subjected to Dox, in the abcence or presence of S117A-FGF2 pre-treatment, stained based on the live/dead, Calcein-AM/Ethidium homodimer assay. A similar abundance of red (dead) cells can be seen rehardless of S117A-FGF2 in Dox-treated cells. Panel b shows the absence of an effect of S117A-FGF2 on Dox-induced LDH release. Panel c shows the effect of S117A-FGF2, and FGF2, on MCF-7 cell proliferation, as estimated by the MTT assay. In al lpanels, bracket mark groups that are significantly different from each other.

Appendix 7, S117A-FGF2 activates AKT, P38, and ERK.

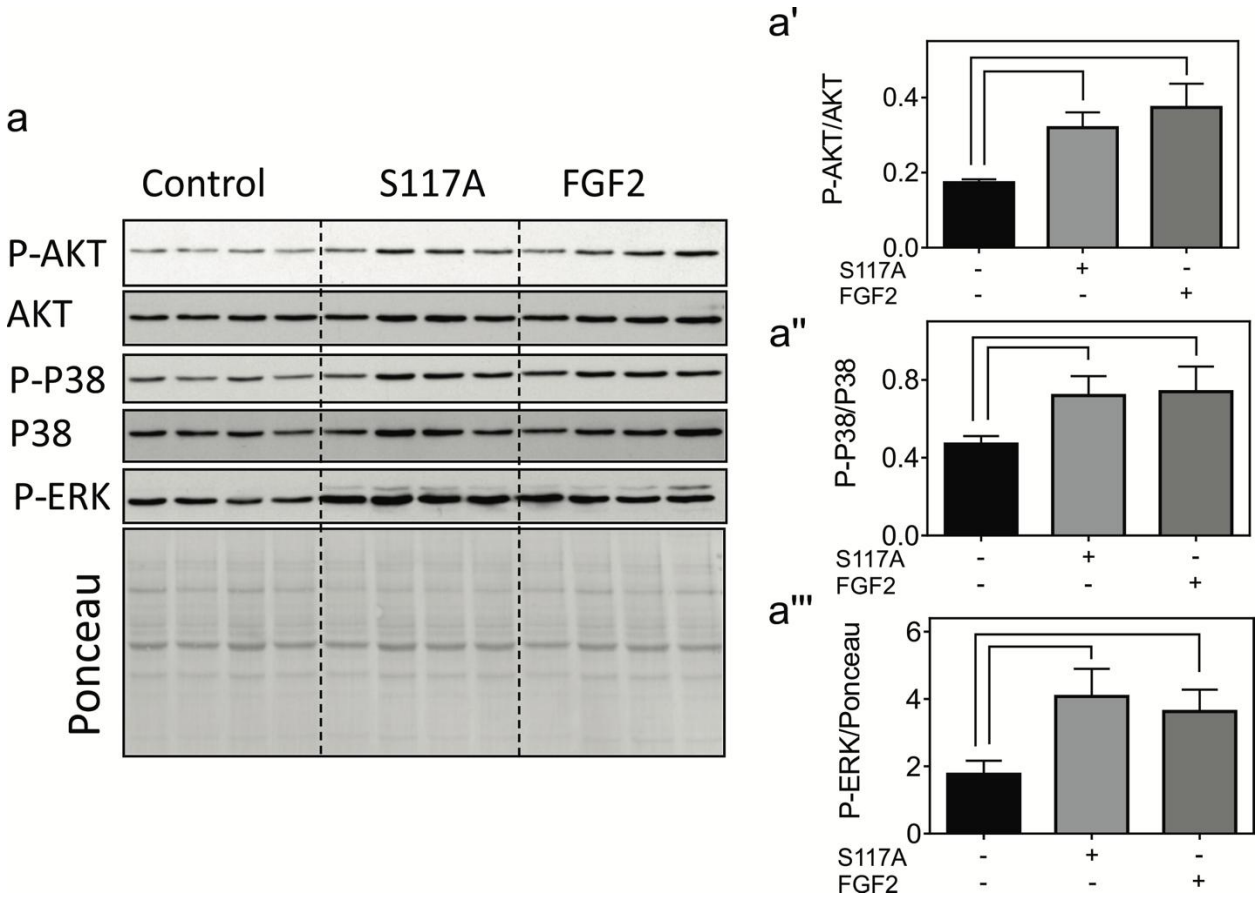

Neonatal rat cardiomyocytes were stimulated with S117A-FGF2 or FGF2 (10ng/ml) for 60 min. Both S117A-FGF2 and FGF2 were able to increase phosphorylation of AKT (tyrosine 473) and P38 (panels a-a'''). Phospho-ERK was also upregulated at this time point, included for comparisons. The experiment was done with n=4 and the brackets in the corresponding graph show significant differences between the groups.

Appendix 8, Levels of various oxidized phospholipids.

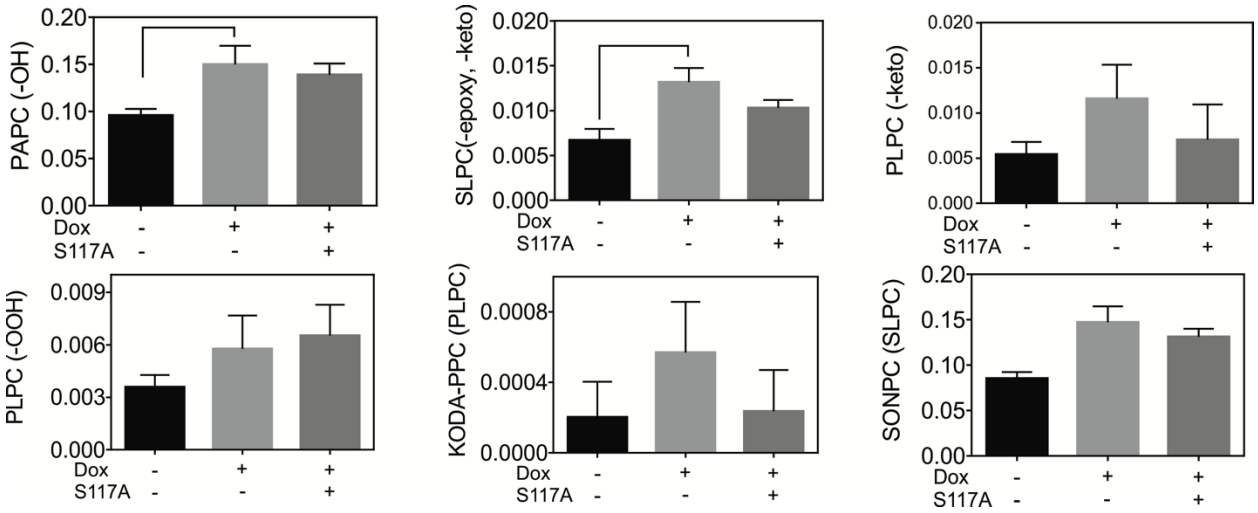

The graphs show the effect of Dox, in the absence or presence of S117A-FGF2, on the oxidation of additional phosphatidylcholine species, not included in Figure 5. Brackets point to groups that are significantly different from each other (n=3). The Y axis shows the amount (ng) of OxPC per μg cardiomyocyte protein.

Appendix 9, List of specific primers used for amplification

Target	**Forward 5`---3`**	**Reverse 5`---3`**
Bnp	CAGCTCTTGAAGGACCAAGG	ACTTCAGTGCGTTACAGCCC
Mhy7	CTGTTTCCTTACTTGCTACCCTC	GCTGAGCCTTGGATTCTCAAAC
Cyclin D2	AAGGACCGGTGCGAGTCA	GGGAGTGCTTCCCTTACCTC
P21	ATCCAGACATTCAGAGCCACAG	CAAAGTTCCACCGTTCTCGG
GPCR22	CACCTTTTGGTGCAGATCCC	CTCCCACCACTGCTTTGTGA
Nppa	GCTTCGGGGGTAGGATTGAC	CACACCACAAGGGCTTAGGA
ARNTL	TCAAGACGACATAGGACACCT	GGACATTGGCTAAAACAACAGTG
RAB6B #2	GGGGAGATTTTGGGAACCCG	CCGATGGTTGCCTGGTAGG
CXCL9	GTTACACACCAGGCATTGGC	TGGTAAGCAAGCAAGGAGGC
DBP1	GAAAAGGAGCGCAAGGCAAC	CGTATTCCACGTCCCCGAAA
CTGF	GCCTACCGACTGGAAGACAC	GTAACTCGGGTGGAGATGCC
Nur77	GGGAGTGTGCTAGAAGGACTG	GGTAGGCTTGCCGAACTCA
HSP70	ACAAGTCGGAGAACGTGCAGGA	GTTGTCCGAGTAGGTGGTGAAG
NR1D1	CCCTGGACTCCAATAACAACAC	GCCATTGGAGCTGTCACTGTAG
HPRT	CTCATGGACTGATTATGGACAG GAC	GCAGGTCAGCAAAGAACTTATAGC C

Appendix 10, Western blot for HSP70 used to obtain data for Fig.28b

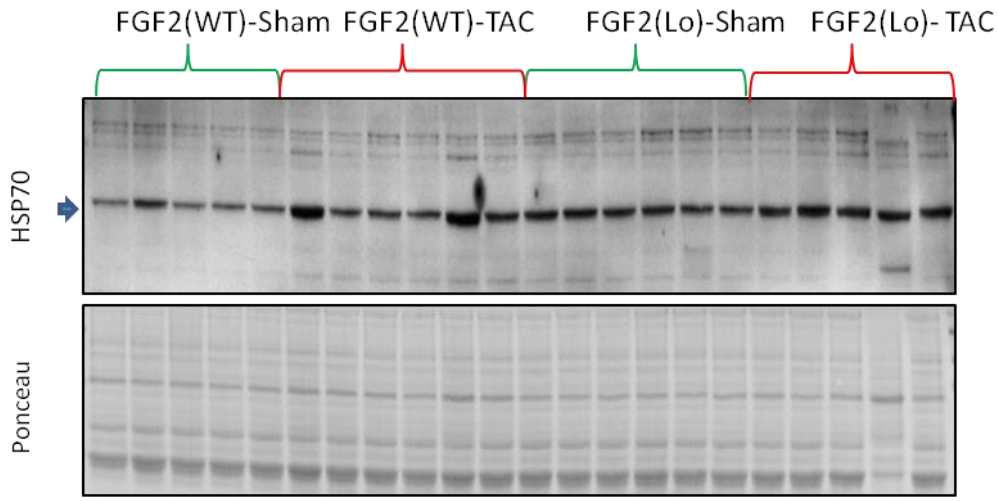

Original western blotting showing the protein levels of HSP70 in the cardiac tissue used for obtaining data for Fi.28b.

Appendix11, mRNA levels of NR1D1 and RAB6B in MEFs

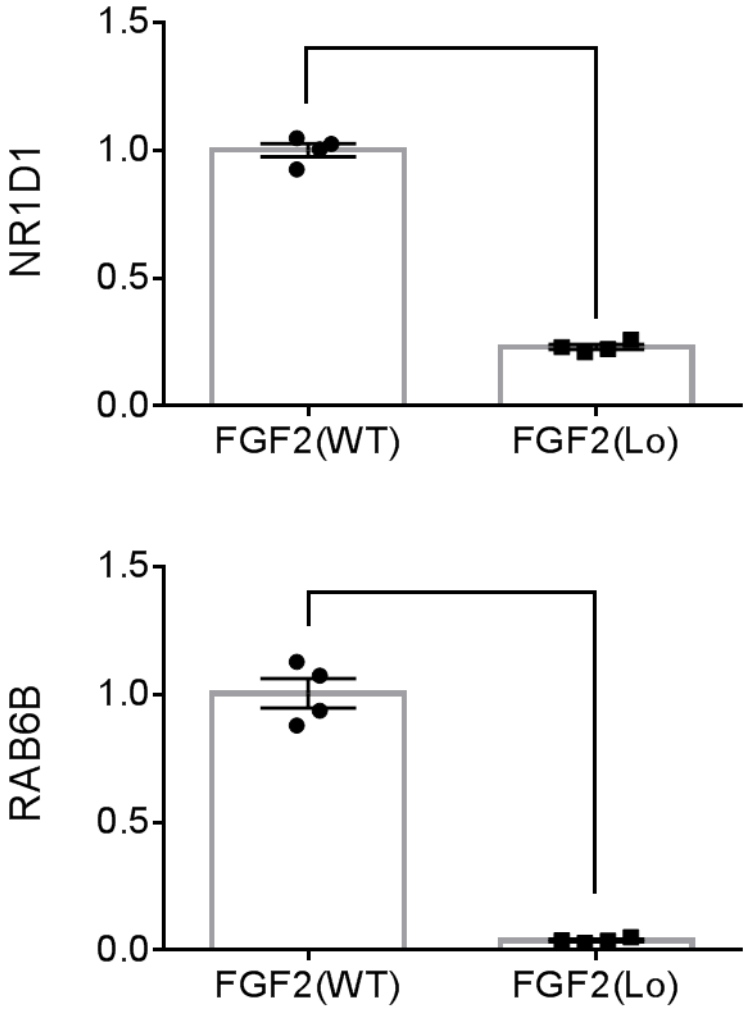

Relative mRNA levels of NR1D1 and RAB6B in mouse embryonic fibroblasts from FGF2(WT) or FGF2(Lo) mice, as indicated. Brackets point to significant difference between the groups ($p<0.05$) by student T-test.

Appendix 12, TAC-induced changes in common genes involved in cardiac remodeling.

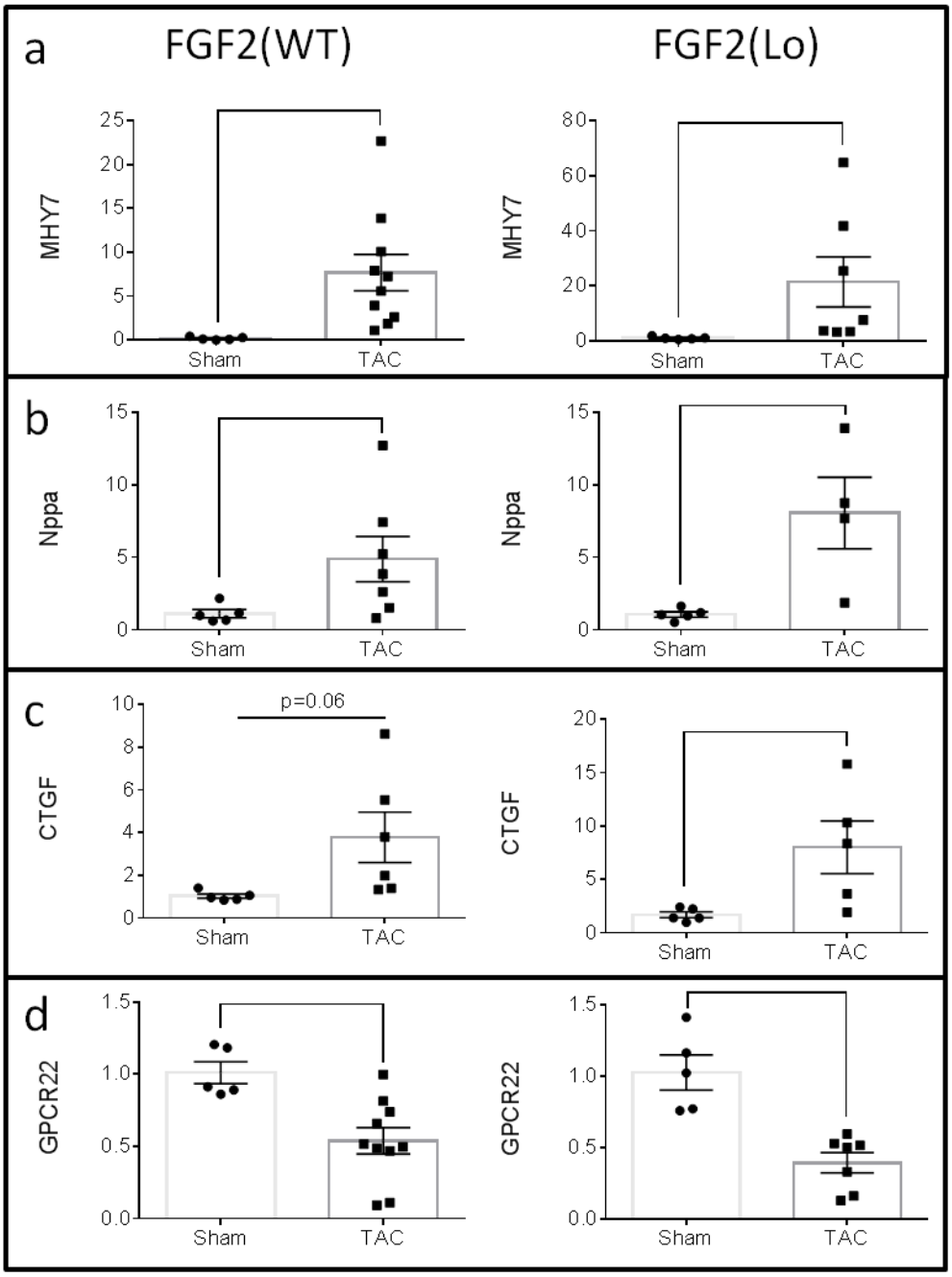

TAC-induced changes in common genes involved in cardiac remodeling.

Panels a-d represent qPCR results for MHY7, Nppa, CTGF, and GPCR22 in mice hearts underwent TAC or sham surgeries. The graphs on the represent changes in FGF2(WT), while the graphs on the right demonstrates changes in FGF2(Lo) mice. The brackets points to significant difference between the groups ($p<0.05$) by student T-test. Sample sizes are n=5-6.

Appendix 13, Circadian related genes were differentially regulated following TAC between FGF2(WT) and FGF2(Lo).

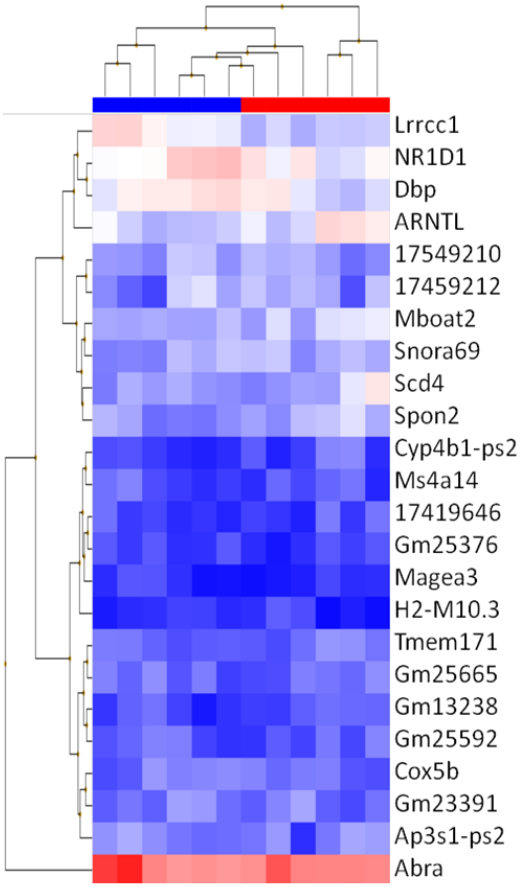

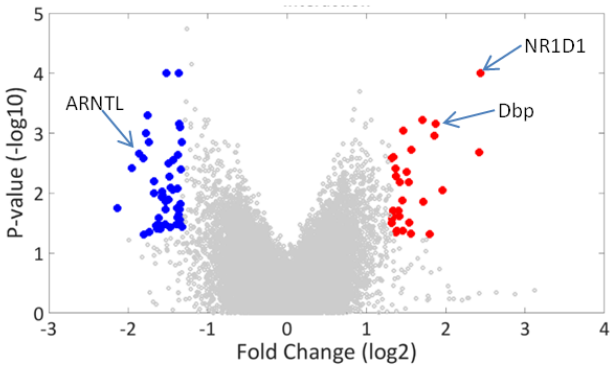

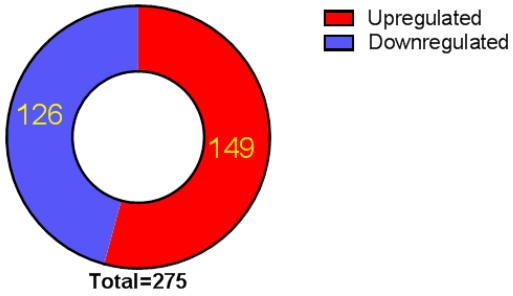

Circadian related genes were differentially regulated following TAC between FGF2(WT) and FGF2(Lo).

The hierarchical and scatter graphs of the transcription of genes differentially changed between FGF2(Lo) and FGF2(WT) following TAC (fold change(±) >3, $p<0.05$) are shown in panels (a) and (b), respectively. The number of genes differentially upregulated or downregulated between the mice strains following TAC are shown in the bar chart, panel (c).